The neutral photochemistry of nitriles, amines and imines in the atmosphere of Titan

J.C. Loison[c,d], E. Hébrard[a,b], M. Dobrijevic[a,b,*], K.M. Hickson[c,d], F. Caralp[c,d], V. Hue[a,b], G. Gronoff[e], O. Venot[f], Y. Benilan[g]

[a] *Université de Bordeaux, Laboratoire d'Astrophysique de Bordeaux, UMR 5804, F-33270 Floirac, France*
[b] *CNRS, Laboratoire d'Astrophysique de Bordeaux, UMR 5804, F-33270, Floirac, France*
[c] *Université de Bordeaux, Institut des Sciences Moléculaires, UMR 5255, F-33400 Talence, France*
[d] *CNRS, Institut des Sciences Moléculaires, UMR 5255, F-33400 Talence, France*
[e] *SSAI/NASA LaRC, Hampton, Va, USA*
[f] *Katholieke Univ Leuven, Inst Sterrenkunde, B-3001 Louvain, Belgium*
[g] *Laboratoire Interuniversitaire des Systèmes Atmosphériques, UMR CNRS 7583, Universités Paris Est Créteil (UPEC) et Paris Diderot (UPD), Créteil, France*

Abstract

The photochemistry of N_2 and CH_4 in the atmosphere of Titan leads to a very rich chemistry which is not well understood. The aim of our study is to improve our understanding of the production of nitrogen compounds and to predict the abundances of those with high molar mass with better accuracy. We have made a careful investigation of the neutral nitrogen photochemistry to improve current chemical schemes including the most abundant species and the most efficient reactions. We also studied the propagation of uncertainties on rate constants in our model and determined the key reactions from a global sensitivity analysis. Our photochemical model contains 124 species, 60 of which are nitrogen containing compounds, and 1141 reactions. Our results are in reasonable agreement with Cassini/INMS data in the higher atmosphere but our model overestimates the mole fractions of several nitriles in the lower stratosphere. New species such as CH_3C_3N and C_3H_7CN could be relatively abundant in Titan's atmosphere. Uncertainties on some nitrogen compounds are important and further studies of the key reactions that we have identified are needed to improve the predictivity of photochemical models. Meridional transport is expected to be an efficient process to govern the abundances of several nitriles in the lower stratosphere.

Keywords: Titan, Photochemistry, Atmospheres, Nitrogen compounds

*Tel: +33-5-5777-6124
Email address: Michel.Dobrijevic@obs.u-bordeaux1.fr (M. Dobrijevic)

1. Introduction

The atmosphere of Titan can be regarded as chemical reactor on the planetary scale. It produces a variety of molecules through the coupled chemistry occurring between hydrocarbons, oxygen and nitrogen containing species. The various chemical processes taking place at different atmospheric levels are so efficient that they ultimately produce aerosols, which then sink down to the surface. Several simple molecules found in Titan's atmosphere have been followed over a period of many years, allowing us to study their spatial and temporal variations. One of the dominant processes driving the production of these chemical species is neutral photochemistry starting with the photolysis of methane (CH_4) and molecular nitrogen (N_2) in the upper atmosphere. To a lesser extent, the photochemistry of water (H_2O) resulting from the injection of oxygen into the upper atmosphere (in the form of O^+, OH and/or H_2O) also participates to this complexification (Hörst et al., 2008; Dobrijevic et al., 2014). Many photochemical models have been developed to explain the presence of detected compounds and to predict the abundance of as yet undetected ones. Several recent studies have improved the chemical scheme of photochemical models of Titan's atmosphere by introducing new reactions and new compounds. Vuitton et al. (2012) introduced several association reactions in their model showing that the mole fractions of certain species could change locally by as much as an order of magnitude. Hébrard et al. (2012) introduced several new reactions in their model to explain the presence of HNC, a newly detected nitrile (Moreno et al., 2011), which was not previously present in photochemical models. Hébrard et al. (2013) carefully examined the photochemistry of C_3H_p compounds in the atmosphere of Titan (including both photolysis and neutral-neutral thermal reactions), improving and updating the existing network for hydrocarbon chemistry. They demonstrated the noticeable impact that such an improvement could have on the calculated abundances of many hydrocarbons (for C_3- and C_2-hydrocarbons alike) whilst predicting that as yet undetected compounds such as the carbon trimer (C_3), cyclopropenylidene (c-C_3H_2) and the propargyl radical (C_3H_3) could be abundant enough to be contribute to Cassini/INMS data. Dobrijevic et al. (2014) improved the photochemistry of oxygen species, introducing in particular a coupling between the chemistries of hydrocarbons, oxygen and nitrogen containing species. They predicted the presence of new and as yet undetected compounds such as NO (nitric oxide), HNO (nitrosyl hydride), HNCO (isocyanic acid) and N_2O (nitrous oxide) and showed that the abundance profiles of these compounds depend on the nature and the source of oxygen compounds in the atmosphere. All of these recent models have shown that the improvement of neutral chemical schemes used in photochemical models is necessary for several reasons: it allows us to better understand which processes drive the chemistry of Titan's atmosphere, it improves the chemistry of coupled neutral-ion models, it allows us to predict the presence of undetected compounds, and it places additional constraints on different physical parameters such as transport and external inputs. In the present paper, we extend these previous studies, updating and improving the photochemical scheme for

nitrogen containing compounds with a particular focus on nitriles that have already been detected. Several nitrile compounds (HCN, HNC, HC_3N, CH_3CN and C_2N_2) have been firmly detected in Titan's atmosphere and their altitude profiles have been determined by spectroscopic observations. Other nitrogen containing compounds have been detected by (or tentatively suggested by) the Ion and Neutral Mass Spectrometer (INMS) instrument aboard the Cassini orbiter and their abundances have been inferred from analysis of the spectra and the use of photochemical models that include ion and neutral chemistry (references are given below). Among these compounds, we can highlight certain nitriles (C_2H_3CN, C_2H_5CN, HC_5N and probably CH_3C_3N), one amine (NH_3) and one imine (CH_2NH). Three other compounds have been found to be present in INMS spectra (C_5H_5N, C_6H_3N, C_6H_7N) but many isomers are possible for these molecules. Upper limits for a few compounds have also been inferred from the INMS data (two amines: CH_3NH_2, N_2H_4 and one nitrile: C_4H_5N). C_4N_2 has been detected only as C_4N_2 ice in Titan's North polar stratosphere.

Our methodology to improve the chemical scheme, which includes new calculations as well as an extensive literature review, is presented in section 2. The photochemical model is briefly presented in section 3, highlighting only those parts which are different from our previous model. In section 4, we use the recent determination of the altitude profiles of six hydrocarbons in the equatorial region (including the new detection of propene) by Nixon et al. (2013) and the water profile determined by Moreno et al. (2012) to constrain the eddy diffusion coefficient before presenting the main reaction pathways for the production of nitriles, amines and imines. A review of available observations for all the nitrogen compounds detected so far is given. For each compound, the model results with their associated uncertainties, due to uncertainties on chemical rate constants are presented. Some as yet undetected nitrogen compounds are also highlighted. In section 5, we pinpoint the reactions that require further investigation to improve the predictivity of photochemical models. In section 6, several important aspects of the nitrogen photochemistry in Titan's atmosphere are discussed before presenting our conclusions in section 7.

2. Chemical scheme

Several recent modeling studies of Titan's atmosphere (Vuitton et al., 2012; Hébrard et al., 2012; Hébrard et al., 2013; Dobrijevic et al., 2014), have shown that current chemical schemes used in photochemical models are far from complete. Previous work (Hébrard et al., 2006, 2007; Hébrard et al., 2009; Dobrijevic et al., 2008) has also underlined the importance of uncertainties on reaction rates. Indeed, the propagation of these uncertainties in such highly non-linear systems is responsible for important deviations of the model results, weakening the possibility to constrain some physical parameters. As a consequence, we consider that the improvement of chemical schemes is an important prerequisite (1) to increase the accuracy and precision of 1D photochemical models (for a better interpretation and preparation of observations) and (2) to construct basic chemical schemes that could be introduced into 2D or 3D models. Indeed, the

development of a reduced scheme that could be used in such complex models should be based on a nominal chemical scheme for which we are confident of its completeness and predictivity.

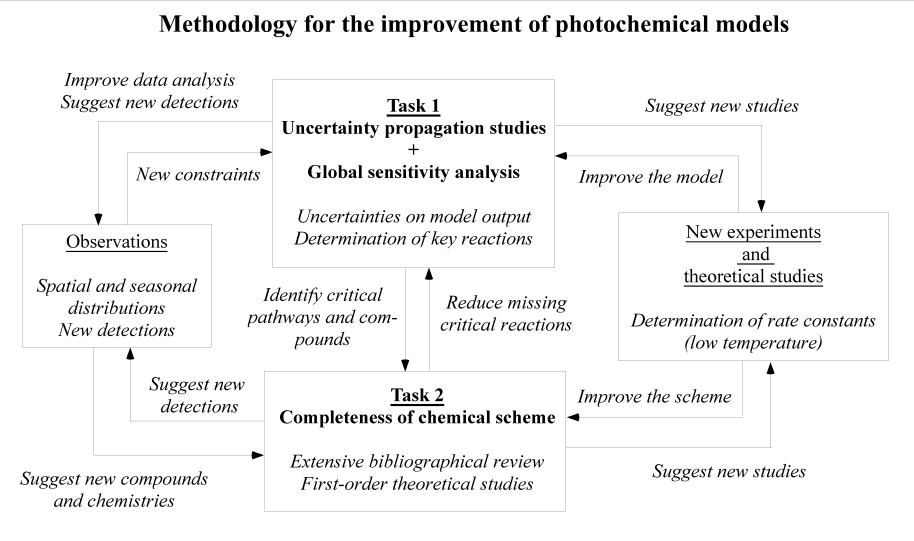

Figure 1: Methodology based on two tasks to improve the chemical networks of photochemical models. These two tasks serve as an efficient basis for new studies focused on selected reactions, which in return can improve significantly the chemical scheme used in models. Improvement of models favor new detection attempts and put better constraints on physical parameters.

The methodology we have developed during the last few years to improve chemical schemes is based on two complementary tasks (see Figure 1): (1) the determination of key reactions through uncertainty propagation studies and global sensitivity analyses, (2) the completeness of the chemical scheme. Key reactions are reactions which have a noticeable effect on model results because their uncertainty factors are relatively important and/or because they are strongly coupled with the main compounds. Determining these key reactions is an important aspect of this approach since it promotes new theoretical and/or experimental studies to provide better estimation of the reaction rates and product branching ratios at low temperature. These new data can then quantitatively improve photochemical models (see Hébrard et al. (2009) as an example). Many reactions included in current networks remain to be studied by theoretical or experimental means. For many others, very few data are available under physical conditions that are directly relevant to the atmosphere of Titan. However, by considering the abundance and reactivity of some species, it is quite clear that many missing reactions are likely to be important and should not be neglected in photochemical models. By introducing these new reactions with an estimation of their rate constant and the associated uncertainty factor, it is possible - thanks to uncertainty propagation studies and global sensitivity

analyses (task 1) - to conclude whether these reactions are important or not. For the reactions that are considered to be important, further in depth theoretical and experimental studies will be necessary (see Hébrard et al. (2013) and Dobrijevic et al. (2014) as examples).

The methodology we propose is iterative, when task (2) is performed, task (1) should be repeated to determine a new list of key reactions. Moreover, following the publication of new rate constants and their uncertainty factors, both tasks (1) and (2) should also be repeated. The improvement of chemical schemes for low mass compounds should be realized first to obtain a firm chemical scheme which could then allow its extension to higher mass species.

In the present paper, we follow this methodology to improve the neutral photochemistry of nitrogen compounds in Titan's atmosphere. To get a nitrogen chemical scheme as complete as possible we reformulate the chemical reaction scheme leading to complex nitrile formation. This scheme, which is initiated by the photodissociation of N_2 and CH_4 is presented in Appendix C (main processes are summarized in Figure 8), and is based in part on the reaction networks of previous models (Wilson and Atreya, 2004; Hébrard et al., 2006; Lavvas et al., 2008; Krasnopolsky, 2009; Vuitton et al., 2006, 2007). At each step we consider all the main reactions (determined from the calculations of production and loss rates) for the various species produced from the previous step, as well as some secondary reactions. For atoms and radicals we consider systematically the reactions with N_2 (almost negligible), CH_4, C_2H_2, C_2H_4, HCN, HNC, H, CH_3 and N. For closed-shell molecules with double or triple CC bond (HC_3N, CH_2NCH, C_2H_3CN, CH_3C_3N, C_4N_2) we consider photodissociations and reactions with H atoms through three body associations. For saturated nitriles (HCN, CH_3CN, C_2H_5CN, C_3H_7CN), which react slowly with H atoms, we consider photodissociations and reactions with highly reactive atoms and radicals produced in Titan's atmosphere (thus mainly involving $N(^2D)$ atoms but also CH, CN and C_2H radicals but neglecting the reactions with $^1CH_2$, C, C_2N, C_3N, C_4H as they play only a minor role). We consider also the reactivity of saturated nitriles with C_2H_3 for which the rates deduced from the studies of Monks et al. (1993) and Petrie (2002) are likely to be overestimated and are the subject of theoretical calculations performed in that work. For each important reaction we perform an extensive bibliographic review including chemical databases such as the KIDA database, Wakelam et al. (2012). When no information exists, we calculate the presence and the value of the entrance barrier using Density Functional Theory (DFT) calculations with the hybrid M06-2X functional developed by Zhao and Truhlar (2008), which is well suited for calculations involving molecules and radicals with C, N, H and O atoms, associated with aug-cc-pVTZ basis sets (Dunning Jr, 1989) using Gaussian09. 23 reactions were studied using DFT calculations; these reactions concern mainly H + nitriles and C_2H_3 reactions with H_2, CH_4, C_2H_6, C_3H_6, C_4H_2, HCN, HNC, HC_3N. For barrierless reactions, the rate constants $k(T)$ are calculated using capture rate theory, which leads to an upper limit value of the rate constant (Georgievskii and Klippenstein, 2005). For reactions with a barrier, the rate constants are calculated using conventional Transition State Theory. For mi-

nor secondary reactions, the rate constants are generally deduced from similar reactions. Particular attention should be paid to photodissociation processes. Indeed, the branching ratios for nitrile photolysis are poorly known, except for HCN, leading to large uncertainties. Moreover, the nitriles present a low energy triplet state which may be responsible for non-negligible absorption in the 200-350 nm range (Rianda et al., 1984) and may lead to photodissociation. In that case, such a process will strongly increase the overall photodissociation efficiency. In this study we neglect the reactivity of metastable N_2^{**}. Since N_2 in its ground state is very unreactive, almost all nitrogen chemistry arises from N_2 dissociation (photodissociation and dissociation by collision with high kinetic energy electrons) (Lavvas et al., 2011). In this study we do not describe ionic chemistry. However, N_2 dissociation results mainly in the formation of N^+ and N_2^+ (Lavvas et al., 2011). Fortunately, the main reactions involving these ions are limited in Titan's atmosphere. N^+ reacts mainly with CH_4 leading to CH_3^+ + NH, $HCNH^+$ + H_2 and HCN^+ + H_2 + H (Anicich, 2003). CH_3^+ reacts with CH_4, C_2H_2 and C_2H_4 leading only to hydrocarbons, and HCN^+ reacts mainly with CH_4 and H_2 leading to $HCNH^+$ (Anicich, 2003). As a result, N^+ chemistry leads mainly to two nitrogen products: NH and $HCNH^+$. As $HCNH^+$ mostly gives back HCN (through dissociative electronic recombination and reaction with other neutral nitrile species) and NH reacts mainly with CH_3 leading ultimately to HCN, we consider that N^+ behaves as $N(^4S)$ in our model. It is even more simple for N_2^+ (the main dissociation product) as it reacts mainly with CH_4 leading to CH_2^+ and CH_3^+ (and N_2), and with H_2 leading to N_2H^+. So as CH_2^+ and CH_3^+ will lead only to hydrocarbon formation and N_2H^+ reacts with CH_4 to give CH_5^+ + N_2, N_2^+ reactions do not lead to the formation of nitrogen compounds but give back N_2 instead. We consider that N_2 dissociation through VUV photons and cosmic rays produces 50% ground-state $N(^4S)$ atoms and 50% long-lived and metastable-state $N(^2D)$ and $N(^2P)$ atoms (Dutuit et al., 2013). As $N(^2P)$ state is much less reactive than the $N(^2D)$ state, with rate constants lower by several orders of magnitude, we consider that $N(^2P)$ mainly relaxes toward $N(^2D)$ and that N_2 photodissociation produces 50% ground-state $N(^4S)$ atoms and 50% long-lived $N(^2D)$ atoms.

The present chemical scheme contains 124 species, 969 reactions, 171 photolysis processes and 1 dissociation by galactic cosmic rays. The list of species is given in Table 1 for the different families of compounds and divided into 4 main groups: H-C, H-C-O, H-N-O and H-C-N. The complete list of reactions is given in Appendix C with references or information regarding the estimation of rate constants and their uncertainty factors.

3. Photochemical model

We present in the following section the various modifications that we have performed compared to the model presented in Dobrijevic et al. (2014).

Table 1: Complete list of species considered in the present model.

Family	Number	Species
	3	H, H_2, Ar
H-C	45	C CH $^1CH_2$ $^3CH_2$ CH_3 CH_4 C_2 C_2H C_2H_2 C_2H_3 C_2H_4 C_2H_5 C_2H_6 C_3 c-C_3H l-C_3H c-C_3H_2 t-C_3H_2 l-C_3H_2 C_3H_3 CH_2CCH_2 CH_3C_2H C_3H_5 C_3H_6 C_3H_7 C_3H_8 C_4 C_4H C_4H_2 $C_4H_2^*$ C_4H_3 C_4H_4 C_4H_5 C_4H_6 C_4H_7 C_4H_8 C_4H_9 C_4H_{10} C_6H C_6H_2 C_6H_3 C_6H_4 C_6H_5 C_6H_6 C_8H_2
H-C-O	16	O^3P O^1D OH H_2O CO HCO H_2CO CH_3O CH_3OH HCCO CH_2CO CH_3CO C_2H_2OH CO_2 CH_3CHO C_2H_4OH
H-N-O	6	NO HNO NCO HNCO N_2O CH_3NO
H-C-N	54	N(^{4}S) N(^{2}D) NH NH_2 NH_3 CN HCN HNC N_2 H_2CN N_2H CH_2NH N_2H_2 CH_3NH N_2H_3 CH_3NH_2 N_2H_4 C_2N CHCN CN_2 CH_2CN HCNN CH_3CN CH_2NCH c-CH_2NCH H_2CNN HNCNH CH_2NCH_3 CH_3NHCH_3 C_3N HC_3N C_2N_2 H_2C_3N HC_2N_2 C_2H_3CN C_2H_4CN C_2H_5CN C_4N HC_4N CH_2C_3N CH_3C_3N H_4C_4N C_3H_5CN C_3H_6CN C_3H_7CN C_5N HC_5N C_4N_2 H_2C_5N HC_4N_2 C_4H_3CN C_4H_4CN $C_2H_5C_3N$ $C_3H_7C_3N$
Total	124	

3.1. Atmospheric profile

In the present study, we use the recommended atmospheric profile of the engineering model of Waite et al. (2013). In our previous studies (i.e. Hébrard et al. (2013); Dobrijevic et al. (2014)), we used the atmospheric profile of Moreno et al. (2012). The present modification has no noticeable effect on the model results.

3.2. Boundary conditions

We use a model similar to scenario IM1 of Dobrijevic et al. (2014) for oxygen compounds as the nominal model, i.e. a fixed value for the mole fraction of CO at the lower boundary ($y_{CO} = 5.1 \times 10^5$), an external flux of O(^{3}P) (at the top of the atmosphere) and OH (from micrometeoritic ablation) equal respectively to 1.6×10^6 and 5.2×10^5 cm^{-2} s^{-1} (values referred to the surface). The OH flux has been slightly modified to obtain a water mole fraction profile in good agreement with Moreno et al. (2012). This difference with Dobrijevic et al. (2014) is due to modifications of the chemical scheme.

Krasnopolsky (2009) stated that H_2 could be produced photochemically in the atmosphere and that it was not necessary to fix its mole fraction at the lower boundary. We confirm this statement, H_2 being efficiently produced through CH_4 and C_2H_4 photodissociations and through H + CH_2 and H + C_2H_3 reactions. Considering that there is no hydrodynamical escape of CH_4 (or for higher mass species) in the current model, the mole fraction of H_2 reaches a steady state of 1.7×10^{-3} after 10^{16} s, in agreement with the minimal value of 1.0×10^{-3} derived by Waite et al. (2013). For simplicity, when considering the propagation of uncertainties, we have fixed the mole fraction of H_2 at the lower boundary with the recommended value of 3.0×10^{-3} (Waite et al., 2013). This has no effect on the abundances of other species.

The mole fractions of CH_4 and Ar are fixed at the lower boundary following the recommended model of Waite et al. (2013) ($y_{CH4} = 1.48 \times 10^{-2}$ and $y_{Ar} = 3.39 \times 10^{-5}$). The mole fraction of N_2 is simply given by: $y_{N_2} = 1 - (y_{CO} + y_{H_2} + y_{CH_4} + y_{Ar})$.

We assumed a zero flux as an upper boundary condition for all species, except for atomic hydrogen (H) and molecular hydrogen H_2, which were allowed to escape with velocities following Jean's thermal escape mechanism (and except for OH and $O(^3P)$, see above).

3.3. Condensation

Some nitrogen compounds may condense in the lower stratosphere of Titan. The expressions we use to obtain the saturated vapor pressure of various species are given in Table 2. For CH_2NH, CH_3C_3N and HC_5N, we were unable to find any experimental data in the literature regarding their saturated vapor pressure profile as a function of temperature. We have thus estimated that CH_2NH has the same saturated vapor pressure as CH_3OH and that CH_3C_3N and HC_5N have the same saturated vapor pressure as HC_3N. We have also considered that the HNC saturated vapor pressure is the same than HCN.

Table 2: Expressions of saturated vapor pressure over ice or liquid (depending on the triple point temperature) for nitrogen compounds.

species	Saturated vapor pressure	Comments and References
NH_3	$\log(P) = 15.96 - \frac{3.537\times10^3}{T} - \frac{3.310\times10^4}{T^2} + \frac{1.742\times10^6}{T^3} - \frac{2.995\times10^7}{T^4}$	P in bar, $T \in [15, 195.41]$ K (Fray and Schmitt, 2009)
CH_3NH_2	$\log(P) = 19.413 - \frac{3333.325}{T}$	P in mbar, $T \in [196.45 - 266.55]$ K (Lide and Kehiaian (1994); fit)
N_2O	$\log(P) = 16.22 - \frac{2.971\times10^3}{T}$	P in bar, $T < 182.3$ K (Fray and Schmitt, 2009)
HCN	$\log(P) = 23.055 - \frac{4522.242}{T}$	P in mbar, $T \in [196.15 - 298.55]$ K (Lide and Kehiaian (1994); Clausius-Clapeyron formula)
HC_3N	$\log(P) = 23.72 - \frac{5087.52}{T}$	P in mbar, $T \in [214.45 - 315.15]$ K (Lide and Kehiaian (1994); Clausius-Clapeyron formula)
CH_3CN	$\log(P) = 18.2432 - \frac{4017.098}{T}$	P in mbar, $T \in [294.55 - 354.35]$ K (Lide and Kehiaian (1994); Clausius-Clapeyron formula)
C_2H_3CN	$\log_{10}(P) = 21.058 - \frac{2371.0}{T} - 1.560 \times \log(T)$	P in Pa, $T \in [290.85 - 350.15]$ K (Lide and Kehiaian, 1994)
C_2H_5CN	$\log(P) = 18.7211 - \frac{4352.66}{T}$	P in mbar, $T \in [203.75 - 370.55]$ K (Lide and Kehiaian (1994), Clausius-Clapeyron formula)
C_3H_5CN	$\log_{10}(P) = 4.38253 - \frac{1526.272}{T-43.316}$	P in bar, $T \in [282.45 - 391.55]$ K (Lide and Kehiaian (1994), Antoine formula)
C_3H_7CN	$\log_{10}(P) = 19.169 - \frac{4739.935}{T}$	P in mbar, $T \in [325.45 - 390.35]$ K (Lide and Kehiaian (1994); Clausius-Clapeyron formula)
C_2N_2	$\log_{10}(P) = 21.381 - \frac{2031.0}{T} - 1.502 \times \log(T)$	P in Pa, $T \in [146.15 - 251.75]$ K (Lide and Kehiaian, 1994)
C_4N_2	$\log_{10}(P) = 8.269 - \frac{2155.0}{T}$	P in mmHg, $T \in [147 - 162]$ K (Lara et al. (1996))
CH_3NHCH_3	$\log(P) = 20.633 - \frac{3781.856}{T}$	P in mbar, $T \in [196.45 - 266.55]$ K (Lide and Kehiaian (1994); fit)

3.4. Galactic Cosmic Rays

The production of N atoms ($N(^2D)$ and $N(^4S)$) by Galactic Cosmic Rays (GCR) comes from Gronoff et al. (2011) and from Gronoff et al. (2012) for cross sections. The products from the interaction of GCR with N_2 and their yields are taken from Lellouch et al. (1994): 65% for ion production and 35% for $N(^2D)$ and $N(^4S)$. Considering the large uncertainty of cosmic ray effects we do not consider cosmic ray ion formation in this study. The total loss rate of N_2 by UV and GCR is presented in Figure 2. We do not consider Saturn's magnetospheric

protons and electrons in the model. According to Krasnopolsky (2009), this contributes only a few percent to the total N atom production.

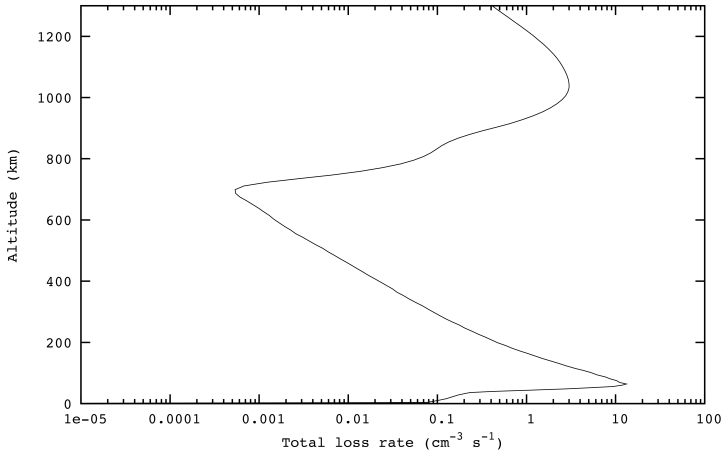

Figure 2: Total N_2 loss rate as a function of altitude. The photodissociation of N_2 contributes exclusively at high altitude where as the dissociation by cosmic rays is the dominant process in the lower atmosphere. Each mechanism produces 50% of N(^{4}S) and 50% of N(^{2}D).

3.5. Actinic flux

We use a 3D radiative transfer model to compute the actinic flux as a function of altitude and latitude in the atmosphere of Titan. The code accounts for absorption by gases and aerosols (see section below) as well as multiple Rayleigh scattering based on a Monte-Carlo procedure. We assume that the atmosphere is homogeneous and that its composition is given by the results of our photochemical model. Three iterations are performed between the radiative transfer code and the photochemical code to yield consistent results. In the following, we use the recent analysis of hydrocarbon observations by Nixon et al. (2013) to constrain the eddy diffusion coefficient profile. Nixon et al. (2013) based their analysis on observations restricted to latitudes between 30°S and 10°N at times from July 1st 2004 and July 1st 2010. They used these observations to have good homogeneity within the sample since low latitudes show the least seasonal variation. Between these two dates, the subsolar point on Titan moved from 24°S to 5°N and the season moved from the end of winter in the northern hemisphere to the equinox. We calculated the actinic flux in a region located 10° around the subsolar point located at the equator. To account for the day and night side alternance, we calculated the mean actinic flux between the atmospheric column at the subsolar point and the one at the anti-subsolar point. As a consequence, results presented in the following correspond to daily averaged conditions at the equator and at the equinox. The normalized actinic flux profile

(ratio between the solar flux at the top of the atmosphere and the actinic flux at a given altitude) is presented in Figure 3 for several wavelengths.

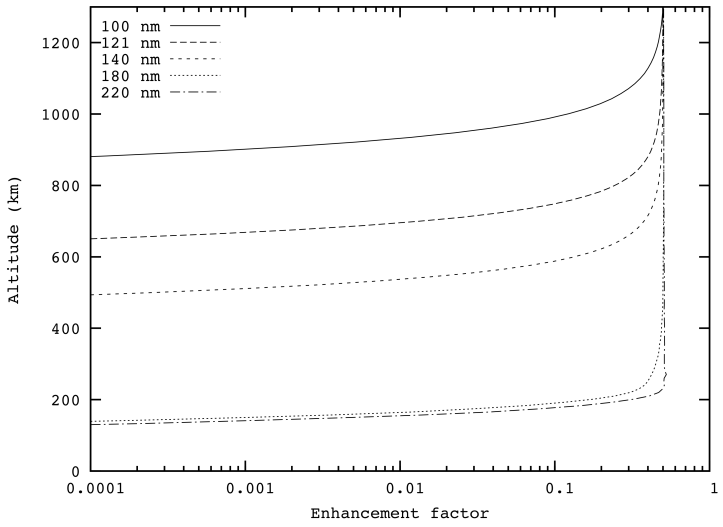

Figure 3: Normalized actinic flux as a function of altitude for several wavelengths in the atmosphere of Titan corresponding to daily average conditions at the equator and at the equinox. The normalized actinic flux is the ratio of the actinic flux at a given altitude and the solar flux at the top of the atmosphere.

3.6. Attenuation by aerosols

In addition to the extinction of solar radiation by gases due to absorption and Rayleigh scattering, we included the absorption due to aerosols using an optical depth given by:

$$\tau(z,\lambda) = \begin{cases} \frac{(z-250)^2}{7500} & \text{if } z \in [60,250] \text{ km and } \lambda < 500 \text{ nm;} \\ \frac{(z-250)^2}{7500} \times \exp\left(-\frac{\lambda-500}{320}\right) & \text{if } z \in [60,250] \text{ km and } \lambda \geq 500 \text{ nm.} \end{cases} \quad (1)$$

This expression is in agreement with the optical depth inferred by Toon et al. (1992) and Barth and Toon (2003) above 60 km of altitude. They obtained an optical depth around 5 between 200 and 500 nm and an exponential decrease beyond with a value around 0.7-1.5 at 1000 nm.

3.7. Propagation of uncertainties

It has been demonstrated in several previous studies (see Hébrard et al. (2012); Hébrard et al. (2013) and Dobrijevic et al. (2014) for the most recent ones) that uncertainties on rate constants have noticeable effects on some photochemical model outputs. We study the propagation of uncertainties on the

chemical rate constants according to the methodology presented in those papers. We performed 500 Monte-Carlo runs to obtain statistically significant results and the integration time for each run was set to 10^{12} s for simplicity and to limit the computation time. This time allows steady state to be attained for most of the compounds with a very good accuracy. As a result, we obtain for each compound a statistical set of mole fraction profiles as a function of altitude. Since the distributions of these profiles are not always normal or lognormal for a given altitude, we use the 5th and 15th 20-quantiles and the 1st and 19th 20-quantiles (which represent the intervals containing respectively 50% and 90% of the mole fraction profiles) to represent the results in a simple way. We also depict the mean value of the distribution. The nominal profile corresponds to the result of the model using the unperturbed rate constants. For some compounds, the mean profile can be different from the nominal profile because their distributions are bimodal (or multimodal) (see below).

4. Results

4.1. Eddy diffusion coefficient profile

Our one dimensional photochemical model computes the abundance of various compounds as a function of altitude, under daily-averaged conditions at the equator and at the equinox. Dynamical processes in the homosphere are parameterized by a vertical eddy diffusion at similar conditions. The eddy diffusion coefficient profile $K(z)$ is fitted as a function of altitude in order to reproduce the observations gathered under similar conditions. Several earlier studies (see for example Lavvas et al. (2008)) have already faced the difficulty to simulate the HCN, HC_3N and $C_2H_{x=2,4,6}$ abundances with a unique mixing profile. This may be due to meridional circulation, dominated by global Hadley cells, responsible for an intense stratospheric zonal flow, as computed in the multidimensional treatment by Hourdin et al. (2004), Rannou et al. (2005) and Crespin et al. (2008). Subsidence of stratospheric air, where photochemical production processes occur, lead to the enrichment of air in the North winter polar region. Rising air from the troposphere at low latitudes is depleted of condensable species as the temperature at the tropopause is close to 70 K (see Teanby et al. (2006, 2009), Vinatier et al. (2010), ...). In this paper we have then constrained $K(z)$ using species which present low polar enrichment values, namely C_2H_2, C_2H_6, C_3H_4, C_3H_6, C_3H_8 and H_2O in the lower atmosphere and Ar and CH_4 in the upper atmosphere. The use of water in particular has the added advantage that the chemistry is relatively well known (Hörst et al. (2008), Dobrijevic et al. (2014)).

Nixon et al. (2013) recently reported the detection of propene (C_3H_6) in Titan's stratosphere using spectra from the Composite Infrared Spectrometer (CIRS) on Cassini. Until then, propyne (CH_3C_2H) and propane (C_3H_8) were the only C_3-hydrocarbons to have been identified in the stratosphere. The detection of a new C_3-hydrocarbon gives valuable new constraints for photochemical models, allowing us to better understand which chemical processes drive hydrocarbon production in Titan's atmosphere. In addition to C_3H_6, Nixon et al.

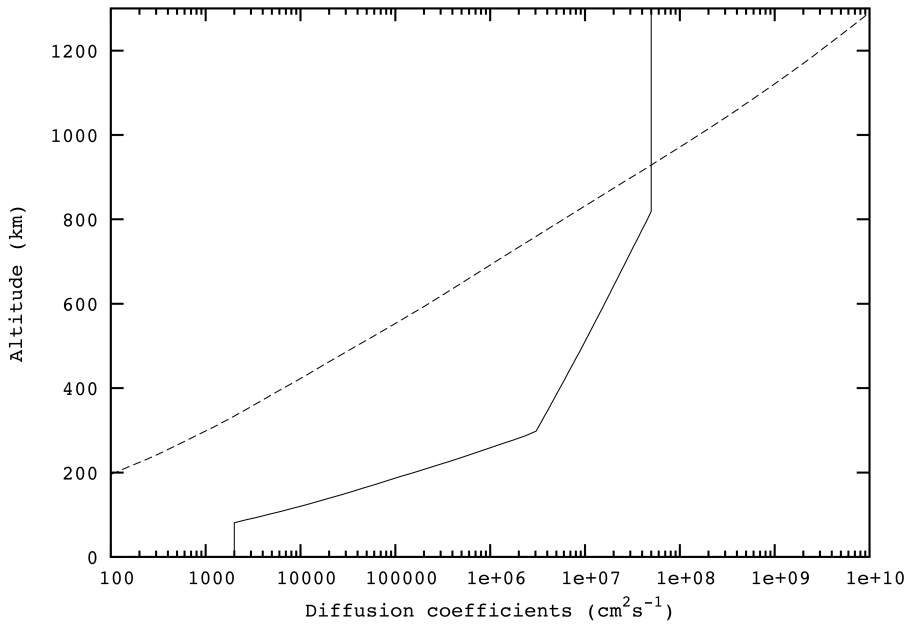

Figure 4: . Eddy (solid line) and CH_4 (dashed line) diffusion coefficient profiles as a function of altitude. This eddy diffusion coefficient has been constrained by the abundances of H_2O and hydrocarbons (like C_2H_6) in the lower atmosphere and CH_4 and Ar in the higher atmosphere.

(2013) retrieved the abundance profiles of 5 other hydrocarbon species previously detected in Titan's stratosphere from the same Cassini/CIRS dataset: acetylene (C_2H_2), ethylene (C_2H_4), ethane (C_2H_6), CH_3C_2H and C_3H_8. We take advantage of the averaged abundance profiles as a function of altitude for these 6 hydrocarbons using a single instrument, as such observations are more suitable for comparison with photochemical models than individual observations gathered from various instruments at different times and locations. We also used the recent water observation derived by the Herschel telescope (Moreno et al., 2012) to constrain eddy diffusion in the lower atmosphere. The water observations of Moreno et al. (2012) are preferred to the results derived by Cottini et al. (2012) because the former should be in principle more representative of a global average abundance. However, it is interesting to note that the CO_2 mole fraction we obtain is in a better agreement with CO_2 observations when we use a higher OH influx in agreement with the Cottini et al. (2012) water profile (see Dobrijevic et al. (2014) for a detailed discussion of this point). As argon is a chemically inert species, it is a good tracer of diffusive processes in the atmosphere. In particular, the abundance profile of argon in the upper atmosphere depends on the location of the homopause. We obtain a satisfactory argon profile compared to Waite et al. (2013), using an argon homopause located around 915 km. At this level, the eddy diffusion is 5.0×10^7 cm^{2}s^{-1}. Our methane profile is then also in agreement with Waite et al. (2013). It is possible to obtain a better profile introducing a hydrodynamic escape of methane equal to 1.2×10^9 cm^{-2}s^{-1} at 1300 km (about two times lower than the value inferred by Yelle et al. (2008)). The introduction of methane escape at the upper boundary has no effect on neutral atmospheric chemistry since the peak of methane photodissociation, located around 800 km, is unchanged. Our nominal $K(z)$ is presented in Figure 4 and results for the main species are presented in Figures 5, 6 and 7.

4.2. Nitrogen chemistry

In this section, we present a simple overview of neutral nitrogen chemistry in Titan which is developed in detail in Appendix A and is presented as a flow graph in Figure 8. Neutral nitrogen chemistry is mostly initiated by nitrogen atoms in the ground N(^{4}S) state and in the excited N(^{2}D) state produced by N_2 photodissociation and dissociation by cosmic rays. In Titan's atmosphere, N(^{4}S) reacts mainly with CH_3 radicals leading ultimately to HCN. N(^{2}D) atoms react mainly with CH_4, C_2H_2, C_2H_4 and with HCN. The reaction of N(^{2}D) with CH_4 also mainly leads to HCN formation (with low CH_2NH steady state concentrations). The N(^{2}D) + C_2H_4 reaction does not give H + CH_3CN products, yielding H + CH_2NCH and H + c-CH_2(N)CH (cyclic compound) (Balucani et al., 2012; Lee et al., 2011), CH_2NCH and c-CH_2(N)CH leading quickly to HCN in Titan's atmosphere conditions. The reaction of N(^{2}D) with C_2H_2 produces HCCN (Takayanagi et al., 1998; Herron, 1999) which is quickly transformed into CCN through reaction with H atoms (Osamura and Petrie, 2004; Takayanagi et al., 1998), initiating the formation of complex nitriles in Titan's upper atmosphere. The reaction of N(^{2}D) atoms with HCN should lead to CH

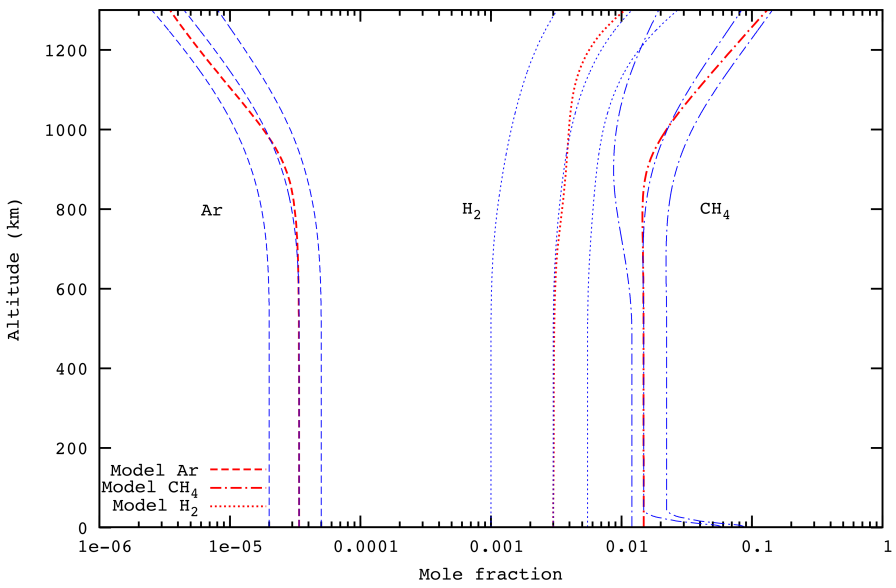

Figure 5: Mole fraction profiles of Ar, H_2 and CH_4 from our nominal model (red) and comparison with the engineering model of Waite et al. (2013) (blue) showing the recommended, minimal and maximal profiles. Model uncertainties on our nominal profiles are low and are not presented.

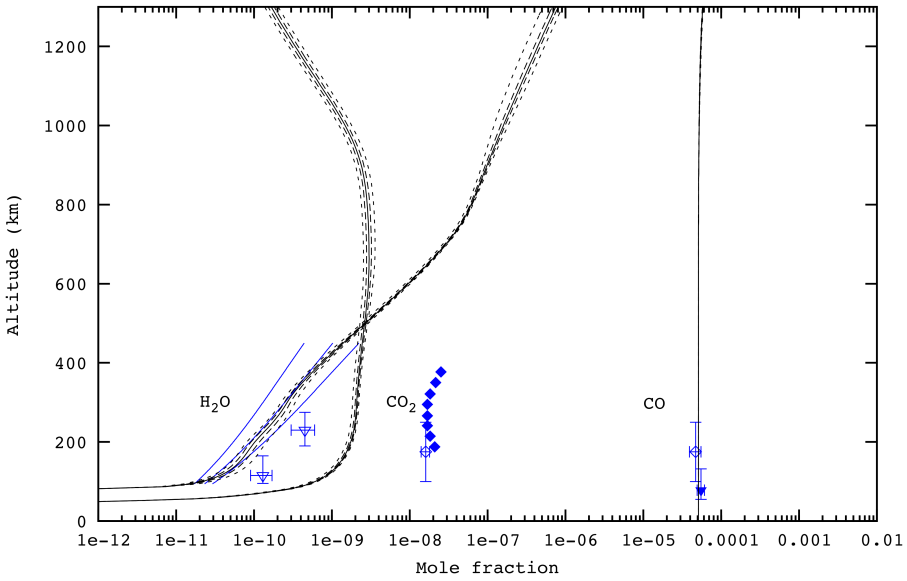

Figure 6: Mole fraction profiles of H_2O, CO_2 and CO and comparison with some observations. The eddy diffusion coefficient has been constrained in the lower atmosphere to fit the H_2O observations of Moreno et al. (2012) (see text). Dashed lines and dotted lines give the intervals containing respectively 50% and 90% of the abundance profiles. Observations (in blue) of Moreno et al. (2012) (solid lines for mean and 1-σ uncertainty), Cottini et al. (2012) (open triangles) for H_2O, observations of CO and CO_2 from de Kok et al. (2007) (open diamonds), CO_2 observations from Vinatier et al. (2010) (filled diamonds) and the CO observation of Teanby et al. (2010) (star) are shown for comparison.

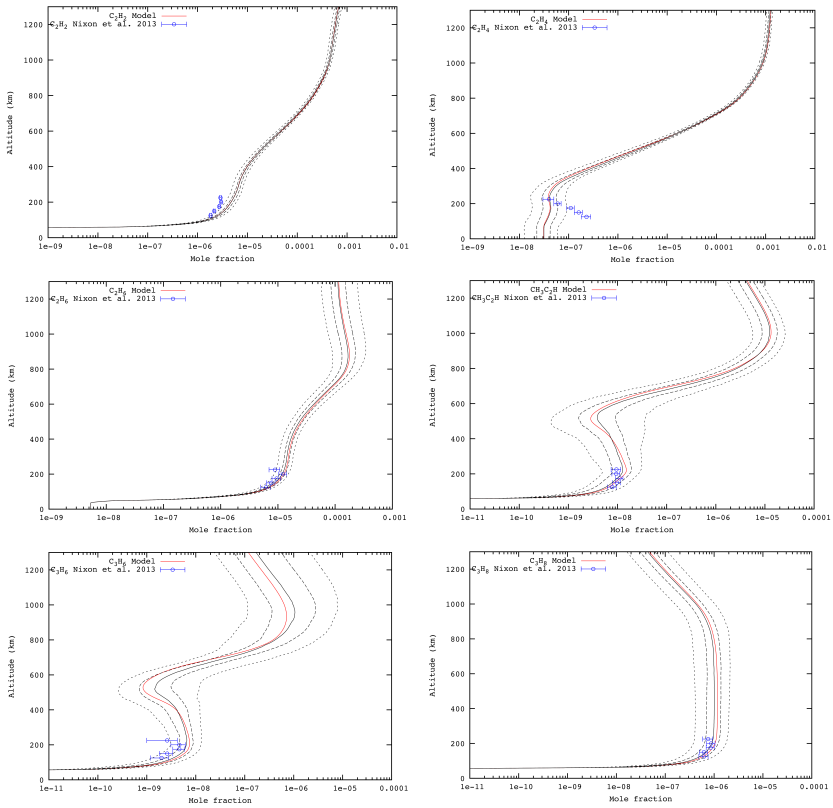

Figure 7: Mole fraction profiles of the main C_2 and C_3 hydrocarbons and comparison with the recent observations of Nixon et al. (2013) (in blue). Red solid line: Nominal profile. Black solid line: Mean profile. Dashed lines and dotted lines give the intervals containing respectively 50% and 90% of the abundance profiles.

+ N_2 (Hébrard et al., 2012) and is therefore a net loss of nitrile species. The photodissociation of HCN, which is the main nitrogen containing compound in Titan's atmosphere, leads to the formation of HC_3N and C_2H_3CN. HC_3N photodissociates to H + C_3N and as C_3N reacts quickly with CH_4 (Fournier et al., 2014) gives back HC_3N. Therefore, HC_3N photodissociation is not an efficient destruction pathway of HC_3N and does not lead to substantial new chemistry. C_2H_3CN is easily photodissociated in the UV producing ultimately HCN, CH_3CN and C_2H_5CN. The neutral nitrogen chemistry in Titan's atmosphere leads mainly to nitriles because once formed, the triple CN bond is not easily broken by photodissociation and is not very sensitive to chemical attack except from $N(^2D)$ which leads to relatively low loss rates. Even if $N(^2D)$ atom reactions lead to imine formation, the steady state concentrations of imines are low as they absorb and photodissociate in the UV (Teslja et al., 2004). Moreover, in contrast to the ion chemistry of Titan's atmosphere (Yelle et al., 2010), the neutral nitrogen chemistry does not result in significant amine formation.

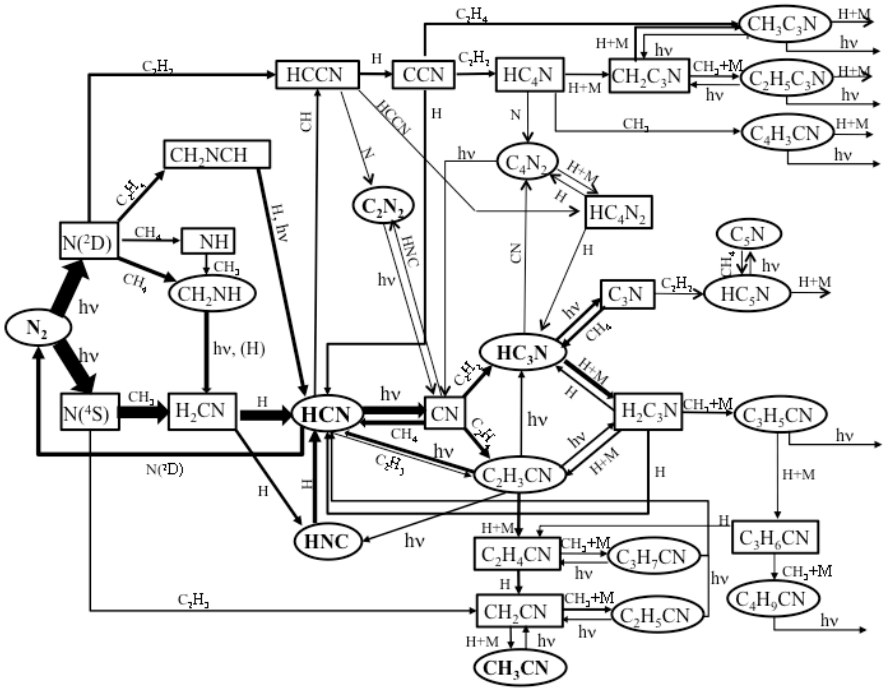

Figure 8: Schematic diagram highlighting the important neutral reaction pathways for the production of the main nitriles and imines. The thickness of each arrow is proportional to the integral of the total production rate over the atmosphere. The reactions of $N(^2D)$ with C_2H_2 and C_2H_4 are mainly localized in the upper atmosphere (corresponding roughly to the top part of the figure) whereas association reactions involving H and CH_3 are mainly localized in the stratosphere. For each pathway, the main reactant is given. Compounds that have been detected are highlighted in bold. Radicals are shown in boxes, whereas stable compounds are shown in circles.

4.3. Main nitrogen species profiles

In this section, we present the results of our model for the main nitrogen species in Titan's atmosphere. For each species, we give the nominal mole fraction profiles (with unperturbed rate constants) and the Monte-Carlo profiles generated by our uncertainty propagation procedure. We also summarize for each species the different observations that have been published so far, allowing us to present our current knowledge of the atmospheric composition as well as to highlight the various discrepancies. Our 1D photochemical model is best suited to reproduce averaged profiles located near the equator. Consequently, we emphasize in particular the comparison of our model results with observations which correspond to global average abundances or equatorial profiles. Additionally, we give some details about the main reactions for the production and loss of each species and emphasize the differences with earlier models. A critical review of the rate constants and branching ratios for the different products is presented and the importance of ionic chemistry is discussed when it is considered as important.

4.3.1. Hydrogen cyanide (HCN)

Coustenis et al. (1991) inferred from Voyager 1 infrared spectra the vertical distribution of HCN in Titan's North polar region (70°N). They obtained a mixing ratio of $(2.3^{+1.8}_{-1.4}) \times 10^{-6}$ at 0.1 mbar (around 300 km) and $(4.0^{+2.8}_{-2.2}) \times 10^{-7}$ at 1.5 mbar (around 170 km). High-resolution submillimetric observations performed with the SPIRE instrument on the Herschel satellite allowed Courtin et al. (2011) to derive the HCN stratospheric profile. Their analysis confirms the profile inferred by Marten et al. (2002) from whole-disk millimetric observations. The disk integrated SPIRE observations are mostly sensitive to the equatorial and mid-latitude regions. Analysis of Cassini-CIRS mid infrared limb spectra corresponding to 15°S latitude (Vinatier et al., 2007) are also in good agreement with these profiles. Gurwell (2004) conducted interferometric observations of the atmosphere of Titan with the Submillimeter Array to investigate the global average vertical distributions of HCN above the tropopause. The vertical profile of HCN increases from 30 parts per billion at the condensation altitude ($\sim$ 83 km) to 5 ppm at $\sim$ 300 km, in quite close agreement with Marten et al. (2002) in that part of the atmosphere. Koskinen et al. (2011) used stellar occultations observed by the Cassini/UVIS instrument to probe the mesosphere and thermosphere of Titan at altitudes between 400 and 1000 km. They analyzed data obtained between flybys Tb in December 2004 and T58 in July 2009. In particular, they derived the mole fraction of HCN (from small absorption peaks near 142-145 nm) for T41 I flyby which correspond to a latitude of 6°S. The mole fraction of HCN decreases with altitude in the mesosphere from around 5.5×10^{-4} at 900 km to 2.0×10^{-5} at 55 km. The latter value is one order of magnitude greater than the value obtained by CIRS data at 400 km. The neutral composition of Titan's upper atmosphere between 1000 and 1100 km has been inferred from the interpretation of Cassini Ion and Neutral Mass Spectrometer (INMS) measurements by Magee et al. (2009). In particular, the

global average mixing ratio of HCN at 1050 km is $(2.44 \pm 0.10) \times 10^{-4}$. Previous interpretation of INMS data from Vuitton et al. (2007) gave a similar abundance of HCN of 2.0×10^{-4} at 1100 km, with an uncertainty factor of 2-3. Geballe et al. (2003) detected HCN emission features in a high resolution spectrum near 3 μm acquired at the Keck II telescope. These data were re-analyzed by Yelle and Griffith (2003) with a model for fluorescence in the $\nu 3$ band of HCN and by Kim et al. (2005) with an updated model. Their results were in agreement in the upper atmosphere. The HCN mixing ratio is from $(1 - 3) \times 10^{-3}$ around 1000 km. The density of HCN between 600 and 1000 km has been also inferred by Shemansky et al. (2005) from observations of stellar occultations by the atmosphere of Titan using the Cassini Ultraviolet Imaging Spectrometer (UVIS). The HCN mixing ratio at 1000 km is about 4×10^{-3}. Recently, Adriani et al. (2011) used the limb observations of the Visual and Infrared Mapping Spectrometer (VIMS) onboard the Cassini spacecraft to retrieve vertical profiles of HCN from its 3 μm non-LTE emission in the region from 600 to 1100 km altitude during the daytime. The mixing ratio of HCN is about $(5.5 \pm 1.5) \times 10^{-3}$ at 1050 km. This result is in agreement with the upper value of the HCN profile derived by Yelle and Griffith (2003) and Kim et al. (2005). HCN has been also detected in Titan's upper atmosphere in the ultraviolet by the UltraViolet Spectrometer (UVS) instrument aboard *Voyager 1* (Vervack et al., 2004). The mixing ratio of HCN is around 10^{-4} at 500 km (about 20 times higher than other observations) and then increases with altitude leading to a value in agreement with all the other observations (but with large uncertainties).

The HCN molecule is the main nitrile in Titan's atmosphere and there is a relatively wide consensus for its main formation and loss pathways (Lavvas et al., 2008a,b; Krasnopolsky, 2009, 2012; Vuitton et al., 2006; Wilson and Atreya, 2004; Hébrard et al., 2012) despite the fact that uni-dimensional models tend to overestimate its abundance. It is efficiently produced through the neutral $N + CH_3 \rightarrow H_2CN + H$ reaction followed by the $H_2CN + H$ reaction but also from important secondary reactions such as HNC + H, CCN + H, H_2C_3N + H, photodissociations such as $C_2H_3CN + h\nu$ and CH_2NCH + H and less importantly through ionic reactions (Krasnopolsky, 2009) leading to $HCNH^+$ followed by the dissociative electronic recombination reaction $HCNH^+ + e^-$ and proton transfer ($HCNH^+ + CH_2NH \rightarrow HCN + CH_2NH^+$, ...). Most of the N_2 photodissociation products lead to HCN formation. As N_2 is photolysed in the upper atmosphere, HCN is mainly produced in the upper atmosphere. The main HCN loss reaction is photodissociation leading to H + CN. CN reacts mostly with CH_4 and C_2H_6 leading back to HCN, acting to recycle back to HCN and producing CH_3 and C_2H_5, whilst a small fraction of the CN radicals react with C_2H_2 and C_2H_4 leading to HC_3N and C_2H_3CN production. In our previous study of the HNC molecule (Hébrard et al., 2012) we introduced the $N(^2D) + HCN \rightarrow CH + N_2$ reaction which is indeed the main HCN loss process as CN reactions mainly give back HCN, either directly through reaction with CH_4 and C_2H_6, or indirectly through the photodissociation of complex nitriles such as $C_2H_3CN + h\nu \rightarrow HCN + C_2H_2$. One important difference with other recent models is the C_2H_3 + HCN reaction which has been considered to be

an important source of C_2H_3CN. The rate constant for the C_2H_3 + HCN → C_2H_3CN + H reaction is generally taken from Monks et al. (1993). However the data of Monks et al. (1993), at room temperature only, are very imprecise and their rate constant for the C_2H_3 + HCN reaction is notably higher than the rate constant of reactions of C_2H_3 with unsaturated hydrocarbons (Wang and Frenklach, 1994; Knyazev et al., 1996a; Callear and Smith, 1986; Ismail et al., 2007) which is a surprising result as several other atoms and radicals (C_2, C_2H, CN, OH, F, Cl) are significantly less reactive with HCN (Frost et al., 1986; Hoobler and Leone, 1997; Fukuzawa and Osamura, 1997; Sander et al., 2011) than with unsaturated hydrocarbons (Nesbitt et al., 1994; Li et al., 2006a,b; Paramo et al., 2008; Daugey et al., 2008; Canosa et al., 2007; Lee et al., 2000; Vakhtin et al., 2001c; Sims et al., 1993; Gannon et al., 2007; Atkinson et al., 2004; McKee et al., 2007; Nesbitt et al., 1999; Gu et al., 2006; Mebel et al., 2006; Bouwman et al., 2012; Golden, 2012). We performed theoretical calculations for this reaction finding a barrier in the entrance valley equal to 18.0 kJ/mol at the DFT level (M06-2X/cc-pVTZ), in good agreement with Petrie (2002), and classical transition state theory leads to a rate constant equal to $k(C_2H_3+HCN) = 1.0 \times 10^{-12} \exp(-2300/T)$ cm^3 molecule^{-1} s^{-1}, a much lower value than Monks et al. (1993). It should be noted also that in their work, Monks et al. (1993) determined a branching ratio for the CN + C_2H_4 → C_2H_3CN + H equal to 20 ± 10 % in poor agreement with the recent reliable result of Gannon et al. (2007) leading to 100 ± 4 %.

The use of the new N_2 dissociation efficiency derived from Lavvas et al. (2011) gives a simulated HCN abundance in relatively good agreement with Cassini and microwave observations in the lower atmosphere as well as with the value from INMS (Magee et al., 2009) and with the one derived from $HCNH^+$ modeling (Vuitton et al., 2007), but it is smaller than the abundance derived from UV absorption in the upper atmosphere. However, it should be noted that the HCN contribution to UV absorption is low which gives rise to substantial uncertainties. An earlier study (Krasnopolsky, 2009) estimated that the total HCN production by the N^+ + CH_4 reaction represents approximately 25% of the total integrated HCN production in Titan's atmosphere. The inclusion of N^+ in the form of N(^{4}S) in the present work takes into account most of this HCN production. Precise quantification of the role of ionic chemistry requires a fully coupled neutral and ionic chemistry model, but the difference between the simulated and observed abundances in the upper atmosphere is unlikely to originate from ionic chemistry itself. Another possibility is the effect of the meridional circulation. Titan's atmosphere is dominated by global Hadley cells, responsible for an intense stratospheric zonal flow, as computed in the multidimensional treatments by Hourdin et al. (2004) and Rannou et al. (2005). The subsidence of stratospheric air, from altitudes where photochemical production processes are important, leads to the enrichment of the North winter polar region. In contrast, rising air from the troposphere at low latitudes is depleted of condensable species as the temperature at the tropopause is close to 70 K (see Teanby et al. (2006, 2009); Vinatier et al. (2010)). If meridional circulation and/or depletion are molecule dependent, the use of a unique eddy

coefficient for all the species may explain the relative disagreement between observations and models for HCN compared to hydrocarbon molecules. It should be noted however that this argument does not seem convincing considering the good agreement between observations and models for C_2H_2, C_2H_4, C_2H_6, C_3H_4, C_3H_6, C_3H_8, CO_2 and H_2O.

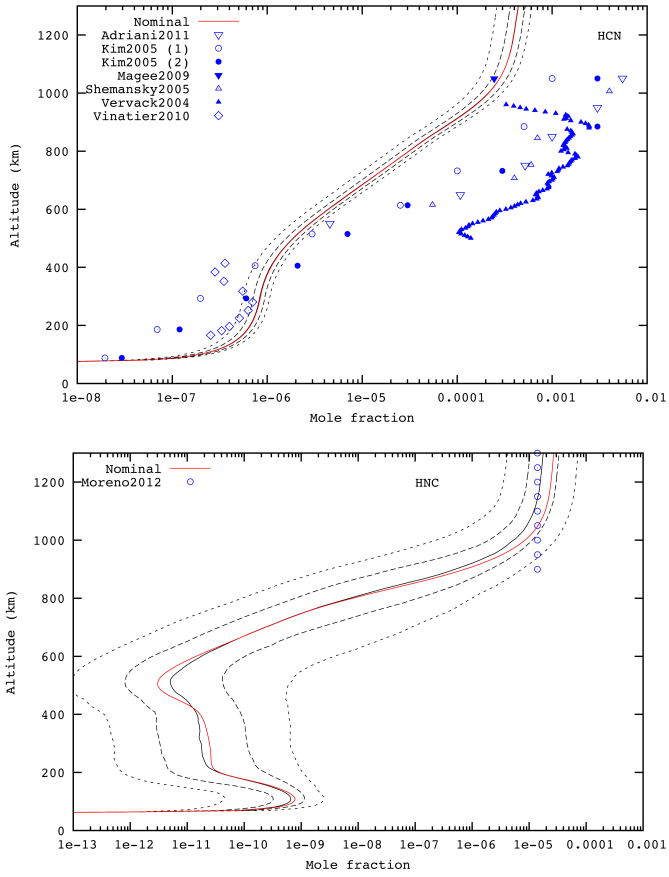

Figure 9: Top: Mole fraction profiles of HCN and comparison with some observations. Error bars for observations are not depicted for clarity. Bottom: Mole fraction profiles of HNC and comparison with an example of one profile retrieved from Moreno et al. (2011) observations (see also Hébrard et al. (2012)). Dashed lines and dotted lines give the intervals containing respectively 50% and 90% of the abundance profiles. See text for references and complementary observations.

4.3.2. Hydrogen isocyanide (HNC)

Moreno et al. (2011) reported the first identification of HNC in Titan's atmosphere from observations using the HIFI instrument on the Herschel Space

Observatory. The column density of HNC inferred from these observations is in the range $(0.6 - 1.5) \times 10^{13}$ cm^{-2} for altitudes between 400 and 1000 km. It was not possible to constrain the vertical profile of HNC from these data since several constant profiles of HNC give a satisfactory agreement with the observations depending on the mixing ratio and the altitude cut-off. As an example, possible profiles are constant mixing ratios of 6.0×10^{-5} above 1000 km or 1.4×10^{-5} above 900 km (see Figure 9).

The chemistry of HNC, an isomer of HCN, has been described in detail in a previous study (Hébrard et al., 2012). It is mainly produced by the H_2CN + H reaction, as a minor product, the main products being HCN + H_2. Its main loss reaction is thought to be isomerization toward HCN through its reaction with H atoms (Talbi and Ellinger, 1996; Sumathi and Nguyen, 1998; Petrie, 2002). There is likely to be another efficient neutral HNC production mechanism: C_2H_3CN photodissociation. Indeed, Wilhelm et al. (2009) detected unambiguously HNC IR emission in their C_2H_3CN photodissociation experiment at 193 nm with a HCN/HNC ratio equal to 3.34 in good agreement with theoretical calculations from Homayoon et al. (2011) as well as direct HNC absorption by the Chirped-Pulse millimetre-Wave study of C_2H_3CN photodissociation (Prozument et al., 2013). The dissociative recombination reaction of $HCNH^+$ is an efficient source of HNC as $HCNH^+$ is the main ion in Titan's upper atmosphere and the branching ratio for HNC production is estimated to be close to 30% (Semaniak et al., 2001; Mendes et al., 2012; Barger et al., 2003). However, the situation is more complicated. Indeed, in Titan's upper atmosphere, the $HCNH^+$ ion is abundant so that HNC will react with $HCNH^+$ leading to HCN + $HCNH^+$ products (Cotton et al., 2013). Then, net production of HNC from this ionic reaction is reduced. Cosmic ray induced nitrogen chemistry is important in the lower stratosphere where the H atom abundance falls. Then in our model HNC reaches a non negligible concentration around 100-150 km and as HNC absorbs strongly in the IR in the Cassini window (464 cm^{-1}, Maki and Mellau (2001)), it could be interesting to evaluate the upper limits for this species from Cassini observations.

4.3.3. Cyanoacetylene (HC_3N)

Coustenis et al. (1991) inferred from Voyager 1 infrared spectra the vertical distribution of HC_3N in Titan's north polar region (70°N). They obtained a mixing ratio of $(2.5^{+1.1}_{-1.0}) \times 10^{-7}$ at 0.1 mbar (around 300 km) and $(8.4^{+3.0}_{-3.5}) \times 10^{-8}$ at 1.5 mbar (around 170 km). Five individual lines of HC_3N were measured with the IRAM 30-m telescope by Marten et al. (2002), allowing them to retrieve disk-averaged vertical profiles for HC_3N up to 500 km. The mole fraction of HC_3N is about 6.0×10^{-8} at 500 km and 3.0×10^{-13} at the condensation level (around 70 km). Using the Submillimeter Array, Gurwell (2004) performed interferometric observations of the atmosphere of Titan. The HC_3N transitions they observed were consistent with the Marten et al. (2002) profile for all the model temperature profiles. Early Cassini infrared observations of Titan from Flasar et al. (2005) confirmed the enhancement of HC_3N in northern latitudes. They obtained a mole fraction around 1.0×10^{-9} between 30°S and 30°N and

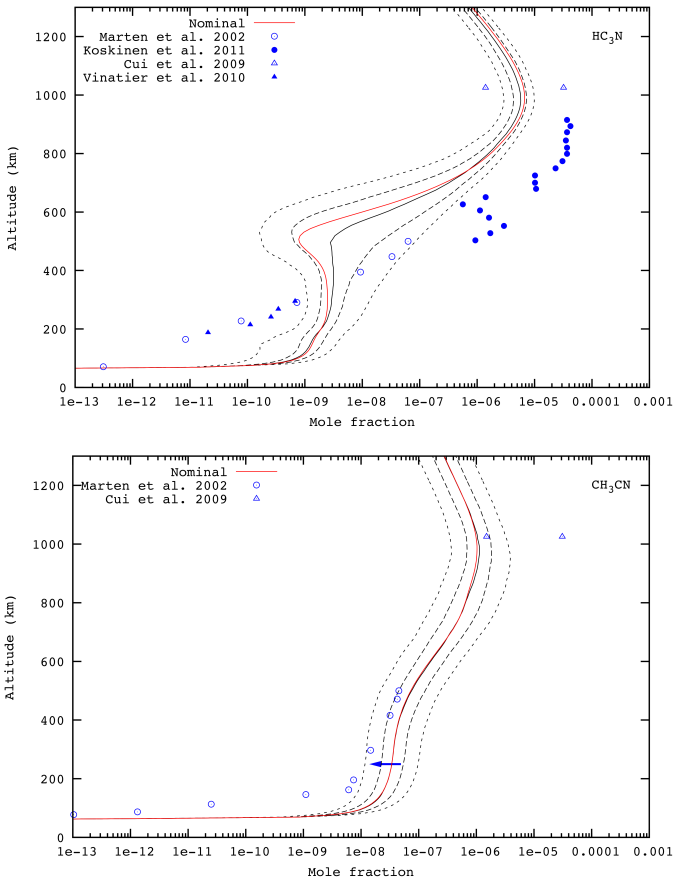

Figure 10: Top: Mole fraction profiles of HC_3N and comparison with some observations. Bottom: Mole fraction profiles of CH_3CN and comparison with some observations. The upper limit of Nixon et al. (2013) at 25°S is also given. Both corrected and uncorrected data of Cui et al. (2009) are presented. Dashed lines and dotted lines give the intervals containing respectively 50% and 90% of the abundance profiles. See text for references and complementary observations.

4.5×10^{-9} at 60°N. Teanby et al. (2006) used mid- and far-infrared spectra from Cassini/CIRS covering three different flybys to infer the vertical profiles of HC_3N at different latitudes. They showed that HC_3N displays a very sharp increase towards the North Pole, where it has a mixing ratio of around 4.0×10^{-8} at 60°N at the 0.1 mbar level. Teanby et al. (2007) used mid-infrared limb spectra in the range 600-1400 cm^{-1} taken with Cassini/CIRS to determine new vertical profiles of HC_3N at different latitudes. The profile retrieved from observations at 15°S was in agreement with the ground based disc-average profile of Marten et al. (2002). They also observed a large increase in HC_3N northward of 60°N which was attributed to a subsidence of nitrile rich air from high altitude where it is produced in the mesosphere and thermosphere by photochemical reactions. Vinatier et al. (2010) analysed limb data of Cassini/CIRS acquired during nine different flybys to derive the latitudinal distribution of the HC_3N vertical profile in the pressure range 5-0.001 mbar (130-500 km). They confirmed that HC_3N has a very steep vertical profile, particularly in the southern hemisphere, and an important enrichment toward the North Pole. HC_3N has also been detected in the higher atmosphere by UV Voyager data analysis (Vervack et al., 2004) and by Cassini/INMS (Vuitton et al., 2007; Cui et al., 2009; Magee et al., 2009). From INMS/Cassini ion spectra obtained during the T5 flyby, Vuitton et al. (2007) derived a mole fraction of 4.0×10^{-5} at 1100 km. Cui et al. (2009) obtained $(1.96 \pm 0.08) \times 10^{-6}$ at 981 km and $(1.43 \pm 0.06) \times 10^{-6}$ at 1025 km (or $(3.2 \pm 0.7) \times 10^{-5}$ at 1025 km correcting for potential wall adsorption/desorption effects). Magee et al. (2009) obtained a value of $(1.48 \pm 0.09) \times 10^{-6}$ at 1050 km in agreement with the uncorrected value of Cui et al. (2009). UV data allowed Vervack et al. (2004) to study intermediate altitudes between those probed by the Cassini/INMS and Cassini/CIRS instruments. Large error bars were reported by Vervack et al. (2004). They obtained HC_3N mole fractions of about 6.0×10^{-6} at 850 km and 4.5×10^{-7} at 500 km. Koskinen et al. (2011) used stellar occultations observed by the Cassini/UVIS instrument to probe the mesosphere and thermosphere of Titan at altitudes between 400 and 1000 km. They derived the mole fractions of HC_3N from absorption between 142 and 148 nm. The mole fraction of HC_3N decreases from 4.0×10^{-5} at 900 km (in agreement with corrected INMS data) to 1.0×10^{-6} at 500 km (about 15 times greater than the value derived by Marten et al. (2002)) .

The main source of the HC_3N molecule in our model is the CN + C_2H_2 $\rightarrow$ HC_3N + H reaction, which presents no barrier in the entrance valley (Sims et al., 1993) with a 100% yield of atomic hydrogen (Gannon et al., 2007). We performed RRKM calculations showing that even at 150 K the three body association is negligible below 5 Torr in good agreement with the results of Gannon et al. (2007) so that the steep decrease of the HC_3N abundance below 200 km cannot be attributed to the lower relative yield of bimolecular products at higher pressures. As the HCN concentration is large in the stratosphere and it is not fully shielded by CH_4 and C_2H_2, HCN photolysis is an efficient HC_3N production mechanism preventing any decrease at low altitude due to the absence of any new loss processes. C_2H_3CN photodissociation is a secondary source of HC_3N although as the HCN + C_2H_3 reaction has a small rate

constant, the C_2H_3CN abundance is lower than in earlier photochemical models so that HC_3N production by C_2H_3CN photodissociation is correspondingly small. The photodissociation of HC_3N in Titan's atmosphere leads mainly to H + C_3N (Seki et al., 1996; Luo et al., 2008; Silva et al., 2009), although the photodissociation is thought to be a minor pathway with respect to absorption, leading to metastable HC_3N^{**} formation (Clarke and Ferris, 1995; Seki et al., 1996; Halpern et al., 1988). A new experiment, using the CRESU method, has shown that the experimental rate constant for the $C_3N + CH_4 \rightarrow HC_3N + CH_3$ reaction increases at low temperature (Fournier et al., 2014). As a result, photodissociation does not lead to HC_3N loss. HC_3N reacts without a barrier with C_2H and CN (Cheikh Sid Ely et al., 2013) and very likely also with $N(^2D)$ but the main HC_3N loss process is though the addition of an H atom followed by the reaction of the H_2C_3N adduct with another H atom leading to HCN + C_2H_2 and C_2H_3CN. For the H + HC_3N reaction we use the k_∞ value from Parker et al. (2004). We performed preliminary DFT/RRKM calculations showing a much smaller k_0 for H + HC_3N than for H + C_4H_2. We use $k_0 = 0.002 \times k_0$(H + C_4H_2) (equivalent to $k_0(300K) = 500 \times k_0$(H + C_2H_2)), and k_0(H + C_2H_2, C_4H_2) taken from Vuitton et al. (2012). Even if the reaction of H atoms with HC_3N is an efficient pathway for HC_3N loss, it leads partly back to $HC_3N + H_2$ (by comparison with H + C_2H_3) and partly back to HCN and C_2H_3CN which both give back some HC_3N. Polymerization cannot be invoked to explain the sharp decrease of HC_3N below 400 km as reactions with radicals are already included in the model and reactions with molecules such as HCN and C_2H_2 involve high energy transition states (Smith et al., 2001) considering HC_3N in its ground state. Moreover, the low temperature associated with the low density of HC_3N lead to a very improbable concerted trimerization (or polymerization), which has been observed for CH_3CHO in the gas phase leading to paraldehyde (Busfield et al., 1973; Zhu et al., 2008). It should be noted however that, as for C_4H_2 (Zwier and Allen, 1996), the reactivity may be enhanced for HC_3N in excited electronic or vibrational states, which should be the main products of the interaction of HC_3N with photons (Clarke and Ferris, 1995; Seki et al., 1996; Halpern et al., 1988). Another possible explanation for the decrease of HC_3N below 400 km is the effect of the meridional circulation if the depletion of the rising air coming from the tropopause is molecule dependent as suggested by Hourdin et al. (2004) who found that the altitude level at which species are removed by condensation controls a large fraction of the magnitude of equatorial stratospheric depletion. However, this behaviour should also apply to other easily condensable species. Another possibility may be the sticking of HC_3N on aerosols (Liang et al., 2007) but in this case the sticking should also apply to polar (like HCN, H_2O) or easily polarizable molecules.

4.3.4. Acetonitrile (CH_3CN)

The CH_3CN(12-11) rotational line has been detected in 1999 by Marten et al. (2002) using the IRAM 30-m telescope. They obtained a disk-averaged vertical profile of CH_3CN from the condensation level up to 500 km (mostly representative of the equatorial region of Titan). The mixing ratio of CH_3CN

reaches 4.0×10^{-8} at 450 km for instance, comparable to HC_3N but 10 times lower than HCN (two compounds also detected by Marten et al. (2002)). Nixon et al. (2013) reported the search for CH_3CN using the CIRS/Cassini instrument for 3 different flybys between May 2009 and September 2010. They obtained the following mole fraction upper limits: 49 ppb at 25°S and 0.27 mbar (∼250 km), 660 ppb at 76°N and 0.018 mbar (∼385 km), 53 ppb at 76°N and 0.3 mbar (∼240 km). Interpretation of INMS/Cassini spectra performed by Vuitton et al. (2007) allowed the detection of CH_3CN in the ionosphere. From an ionospheric model, they obtained a mole fraction at 1100 km equal to 3.0×10^{-6} (with an estimated uncertainty factor of 3). Cui et al. (2009) proposed an average value of 3.0×10^{-5} around 1100 km from the INMS/Cassini analysis of 15 flybys, arguing that some important reactions were probably missing in Vuitton et al. (2007). On the other hand, Magee et al. (2009) did not include CH_3CN in their analysis of INMS data.

The CH_3CN molecule is not produced in our model by the $N(^2D) + C_2H_4$ reaction but through the association reaction $H + CH_2CN$ (Balucani et al., 2012; Lee et al., 2011). We calculated the rate constant from our semi-empirical model for association reactions (Hébrard et al., 2013), the CH_2CN radical being produced by the $H + C_2H_4CN$ reaction (this work, C_2H_4CN itself being the product of the $H + C_2H_3CN$ association) and the $N + C_2H_3$ reaction (Payne et al., 1996). The main loss reactions are photodissociation (we consider a similar low reactivity with C_2H_3 as for HCN and the reaction between C_2H and CH_3CN presents a notable barrier (Nizamov and Leone, 2004a,b)). The simulated CH_3CN abundance is slightly higher than the one obtained by microwave observations and is less than the upper atmospheric observations, although most of the observations fall within the uncertainty range of the simulations. As outlined above this small difference could originate from the same low latitude stratospheric depletion of condensable species as for HCN and HC_3N.

4.3.5. Propionitrile (C_2H_5CN)

Marten et al. (2002) proposed an upper limit of 2.0×10^{-9} from millimeter heterodyne observations obtained with the IRAM 30-m telescope for altitudes between 100 and 300 km and de Kok et al. (2008) estimated an upper limit of 8.0×10^{-9} for latitudes above 70°N. The detection of $C_2H_5CNH^+$ at 74°N and 1100 km was reported by Vuitton et al. (2007) from the Cassini/INMS ions spectrum obtained during the Cassini T5 flyby. From the analysis of the mass spectrum, they inferred a mole fraction of C_2H_5CN equal to 5.0×10^{-7}. C_2H_5CN was excluded from the spectral analysis of Cui et al. (2009). In contrast, Magee et al. (2009) reported a mixing ratio of $(1.54 \pm 0.48) \times 10^{-7}$ at 1050 km.

Our model clearly overestimates the production of C_2H_5CN in the lower atmosphere, as well as in the upper atmosphere although it is in agreement with the value derived from ionic spectra by Vuitton et al. (2007). We ignore ionic chemistry which likely acts as a sink for this compound. The most probable reactions are the following: $C_2H_5CN + HCNH^+ \rightarrow C_2H_5CNH^+ + HCN$ followed by $C_2H_5CNH^+ + e^-$ which is unlikely to give 100% of $C_2H_5CN + H$ products. However ionic chemistry is unlikely to explain the large overestimation in the

lower atmosphere. The main source of C_2H_5CN is the association reaction between CH_2CN and CH_3, and is then directly correlated to CH_3CN production. The main loss processes are photodissociation and reaction with C_2H. The rate constant for the $C_2H + C_2H_5CN$ reaction is estimated to be similar to the one for the $C_2H + C_2H_6$ reaction. The $C_2H + CH_3CN$ rate constant (Nizamov and Leone, 2004a,b) is similar to the $C_2H + CH_4$ rate constant (Paramo et al., 2008; Richardson and Francisco, 1994; Matsugi et al., 2010; Canosa et al., 2007; Horner et al., 1995) indicating little effect of the -CN group. We consider a similar low reactivity with C_2H_3 as for HCN. The calculated C_2H_5CN abundance is two orders of magnitude higher than the upper limit derived from microwave observations. There is little doubt regarding the relative $CH_2CN + H + M \rightarrow CH_3CN + M$ and $CH_2CN + CH_3 + M \rightarrow C_2H_5CN + M$ rate constants leading to similar CH_3CN and C_2H_5CN production fluxes. However, the absorption cross section of C_2H_5CN is not well known (we use Kanda et al. (1999)) and may be larger for C_2H_5CN than for CH_3CN as indicated by EOM-CCSD(T) calculations. There is a clear need for measurements of the cross section for C_2H_5CN to get a reliable modeled abundance. Moreover, in a similar manner to CH_3CN and HC_3N, the low latitude stratospheric depletion of condensable species may also play a role. in this case, C_2H_5CN could show a large enrichment near the North pole (although this has not yet been observed with an upper limit estimated to 8.0×10^{-9} for latitudes above 70°N (de Kok et al., 2008)). Khanna (2005) proposed that C_2H_5CN could be one of the main components of the Haze B layer (the definition of the Haze B layer can be found in de Kok et al. (2007)). Despite the good agreement between the laboratory infrared band of C_2H_5CN ice and the 221 cm^{-1} band of Haze B, C_2H_5CN cannot be the only component of Haze B as the 100 cm^{-1} infrared band of C_2H_5CN ice, corresponding to a lattice vibration, is not present in Cassini observations (de Kok et al., 2008). However, this lattice vibration of pure C_2H_5CN ice will be strongly affected in the case of mixed ices (C_2H_5CN, HC_3N, HCN, C_4N_2 being most probable candidates).

4.3.6. Acrylonitrile (C_2H_3CN)

Marten et al. (2002) proposed an upper limit of 2.0×10^{-9} from millimeter heterodyne observations obtained with the IRAM 30-m telescope for altitudes between 100 and 300 km. Analysis of Cassini/INMS spectra acquired during several different flybys allowed Cui et al. (2009) to derive an upper limit of 4.0×10^{-7} at 1025 km (or a corrected value of 1.8×10^{-5} at 1077 km). Magee et al. (2009) obtained a mixing ratio of $(3.46 \pm 0.51) \times 10^{-7}$ at 1050 km. It should be noted than the value derived from ionic spectra by Vuitton et al. (2007) is 1.0×10^{-5} at 1100 km.

In the middle atmosphere, we obtain a great diversity of profiles from our uncertainty propagation procedure. This result shows that many chemical pathways are possible due to the current uncertainties in rate constants. The main source of the C_2H_3CN molecule in our nominal model is the $CN + C_2H_4 \rightarrow C_2H_3CN + H$ reaction which shows no barrier in the entrance valley (Sims et al., 1993) with 100% of H production (Gannon et al., 2007). There are also

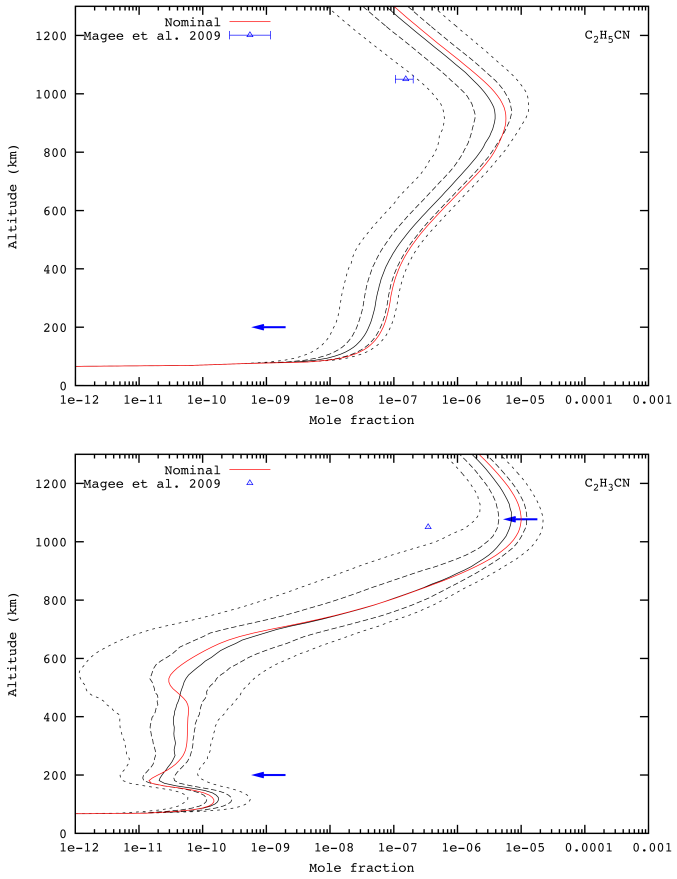

Figure 11: Top: Mole fraction profiles of C_2H_5CN and comparison with INMS observations. The upper limit of Marten et al. (2002) in the lower atmosphere is presented. Bottom: Mole fraction profiles of C_2H_3CN and comparison with INMS observations. Upper limit of Cui et al. (2009) in the higher atmosphere and Marten et al. (2002) in the lower atmosphere are presented. Dashed lines and dotted lines give the intervals containing respectively 50% and 90% of the abundance profiles. See text for references and complementary observations.

two secondary sources, the reactions H + HC_3N + M → H_2C_3N + M followed by H + H_2C_3N + M → C_2H_3CN + M, which are efficient in the stratosphere, and the C_2H_3 + HCN reaction (relatively minor considering the newly reduced rate constant calculated by a classical TST calculation in compared with the previous estimation from Monks et al. (1993)). The main loss process is photodissociation leading to HCN + C_2H_2, HNC + C_2H_2, HC_3N + H_2 and H_2C_3N + H (see Appendix B) and also reaction with H atoms leading to C_2H_4CN adduct formation. The rate constants for H atom addition are taken to be equal to $k_\infty = k_\infty$(H + C_2H_4) and $k_0 = 10 \times k_0$(H + C_2H_4) (Vuitton et al., 2012) considering the height of the entrance barrier calculated at the M06-2X/cc-pVTZ level and the size of the system. As C_2H_4CN should react quickly with H atoms leading to CH_3 + CH_2CN, the H + C_2H_3CN reaction is a net C_2H_3CN loss.

4.3.7. Cyanogen (C_2N_2)

Coustenis et al. (1991) inferred from Voyager 1 infrared spectra the vertical distribution of C_2N_2 in Titan's North polar region (70°N). They obtained a mixing ratio of $(1.6^{+2.6}_{-1.0})\times10^{-8}$ at 0.1 mbar (around 300 km) and $(5.5^{+5.0}_{-2.2})\times10^{-9}$ at 1.5 mbar (around 170 km). Analysing several Voyager 1 infrared spectral averages covering Titan's disk from 53°S to 70°N, Coustenis and Bezard (1995) detected C_2N_2 near the North Pole but not at latitudes southward of 50°N. These observations suggest at least a tenfold enhancement in the C_2N_2 mole fraction. They inferred a mole fraction upper limit of about 1.5×10^{-9} near the equator around 18 mbar (80 km of altitude) and a mole fraction of $(1.5 \pm 0.2) \times 10^{-8}$ and $(2.2 \pm 0.3) \times 10^{-8}$ at 50°N and 70°N respectively. Teanby et al. (2006) detected C_2N_2 from Cassini/CIRS data. They obtained a value of around 9.0×10^{-10} at 48°N at the 3 mbar level (145 km of altitude) and 1-σ upper limits of 5.0×10^{-10} at 30°S and 30°N. Teanby et al. (2009) used four years of far-IR data from Cassini/CIRS to provide measurements of C_2N_2 in Titan's atmosphere. The C_2N_2 mole fraction reaches a maximum value of 3.5×10^{-9} in Titan's northern hemisphere around a pressure level of 10 mbar (100 km of altitude). At southern and equatorial latitudes they find average mole fractions of $(5.5\pm1.4)\times10^{-11}$ from limb data and $(6\pm3)\times10^{-11}$ from nadir data (with a 3-σ upper limit of $< 17\times10^{-11}$ from nadir data). From Cassini/INMS data, Cui et al. (2009) inferred a C_2N_2 mixing ratio of $(1.70\pm0.07)\times10^{-6}$ at 1025 km (or $(4.8\pm0.8)\times10^{-5}$ at 1077 km correcting for possible wall adsorption/desorption effects) and Magee et al. (2009) obtained a value of $(2.14\pm0.12)\times10^{-6}$ at 1050 km.

The model slightly overestimate the C_2N_2 abundance at low altitude with a strong influence of cosmic rays, and underestimate the C_2N_2 abundance at high altitude. The measured C_2N_2 abundances in the upper atmosphere are uncertain although no error bars were associated with these observations. The C_2N_2 molecule is mainly produced in our model by the reactions N + HCCN and CN + HNC. There is no experimental or theoretical information for the N + HCCN reaction which should not show any barrier as a radical-radical reaction, forming in first step the NC(H)CN adduct which should lead to HCN + CN and H + C_2N_2 products, a part of HCN will likely isomerize into HNC due to

the large amount of internal HCN energy. We estimated the rate constant using capture theory (rate constant similar to the N + CH_2 reaction which is also a quadruplet + triplet reaction), the branching ratio being in favor of C_2N_2 due to the larger exothermicity. For the CN + HNC reaction we also considered a rate constant given by capture rate theory as Petrie and Osamura (2004) found no barrier in the entrance valley. It should be noted that the CN + HCN reaction is not an efficient way to produce C_2N_2 due to the low rate constant (Zabarnick, 1989; Yang et al., 1992a,b). The main losses of C_2N_2 are through photodissociation. The reaction with H atoms needs to be considered. Basiuk and Kobayashi (2004) found a barrier equal to 14 kJ/mol for H atom addition but DFT calculations (M06-2X/cc-pVTZ) lead to a barrier equal to 30 kJ/mol. There is one experimental measurement at 300K (Phillips, 1978) leading to $0.01 \times k(\mathrm{H} + \mathrm{C_2H_2})$ but at 150K the reaction occurs mostly by tunneling. We propose k_0 and $k_\infty = 0.1 \times k_\infty(\mathrm{H} + \mathrm{C_2H_2})$ from Vuitton et al. (2012), taking into account the higher TS in the entrance valley and the smaller ΔH_r. There are large uncertainties associated with this rate constant but H + C_2N_2 is likely to be a minor loss process.

4.3.8. Dicyanoacetylene (C_4N_2)

Samuelson et al. (1997) detected C_4N_2 ice from IRIS/Voyager observations. The non-detection of gaseous C_4N_2 allowed them to determine an upper limit of 4.0×10^{-10} for the vapour mole fraction above the cloud top located at 90 km. Khlifi et al. (1997) obtained also from IRIS/Voyager data an upper limit of 5.6×10^{-9}. More recently, using CIRS/Cassini observations, de Kok et al. (2008) obtained an upper limit of 9.0×10^{-9}.

The mean profile and the nominal profile do not overlap at some altitudes because the distributions of the logarithm of the mole fractions at these altitudes are not symmetric with the existence of a kind of a bimodal distribution. The C_4N_2 molecule is mainly produced by the N + HC_4N and CN + HC_3N reactions as well as by the reactions HCCN + HCCN $\rightarrow$ H + HC_4N_2 followed by H + $HC_4N_2 \rightarrow H_2 + C_4N_2$. The CN + HC_3N reaction has been recently studied at low temperature (Cheikh Sid Ely et al., 2013) leading to a high value of the rate constant at low temperature. There is no information for the N + HC_4N and HCCN + HCCN reactions but as they are radical-radical reactions (similar to like N + CH_2 and N + HCCN reactions, all being quadruplet + triplet reactions) they should not show any barrier in the entrance valley. The rate of the HCCN + HCCN reaction includes a steric hindrance factor by comparison with alkyl + alkyl reactions (Klippenstein et al., 2006). As the HC_4N + H reaction has no exothermic bimolecular exit channel, HC_4N, produced through the quick CCN + C_2H_2 reaction (Zhu et al., 2003a; Wang et al., 2006), reaches a non-negligible concentration in the upper atmosphere so that the N + HC_4N reaction is an important source of C_4N_2. C_4N_2 is mainly lost by photodissociation and through reaction with H atoms. Due to the large size of C_4N_2 compared to C_2N_2 and to the fact that H addition on the CC triple bond shows a smaller barrier than H addition on the CN triple bond, the rate for H addition should be larger for H + C_4N_2 than for H + C_2N_2. We use $k_\infty = 0.2 \times k_\infty(\mathrm{H} + \mathrm{C_2H_2})$ as the

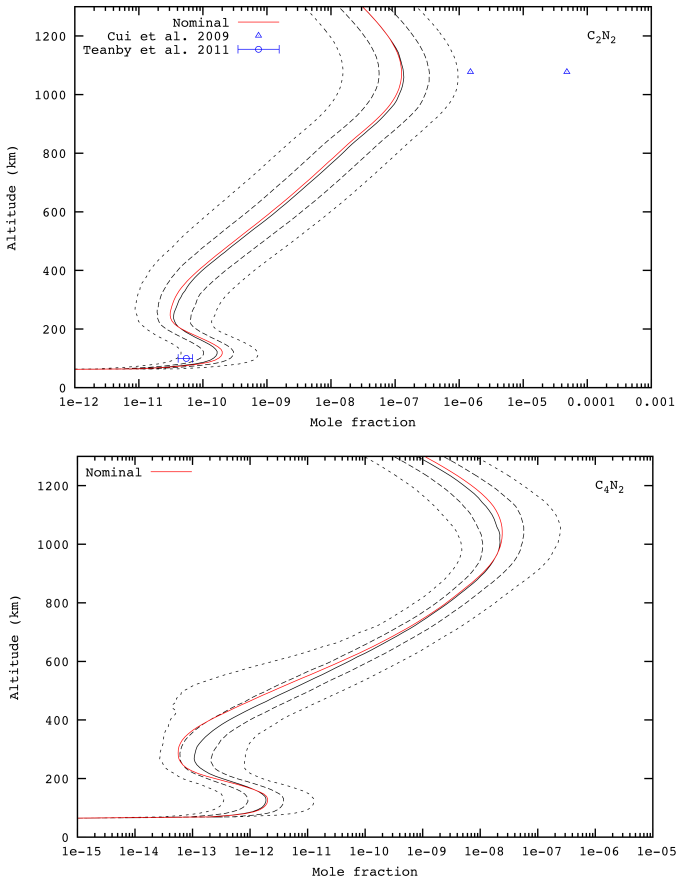

Figure 12: Top: Mole fraction profiles of C_2N_2 and comparison with some observations. Both corrected and uncorrected data of Cui et al. (2009) are presented. Bottom: Mole fraction profiles of C_4N_2. Dashed lines and dotted lines give the intervals containing respectively 50% and 90% of the abundance profiles. See text for references and complementary observations.

entrance barrier is higher for H + C_4N_2 at the DFT level (M06-2X/cc-pVTZ) and $k_0 = 10 \times k_0$(H + C_2H_4) considering the relative sizes of the systems. As k_0(H + C_4N_2) is much larger than k_0(H + C_2N_2), the reaction H + C_4N_2 → HC_4N_2 followed by the reaction H + HC_4N_2 → HCN + C_3N is an important sink for C_4N_2 in the lower atmosphere, leading to C_4N_2 abundances which are much lower than the C_2N_2 ones. However, the rate constant for the critical H + C_4N_2 reaction is only poorly known and may be considerably smaller, leading to larger C_4N_2 abundances. As for the other large nitriles, C_4N_2 should condense in the lower stratosphere, leading to a depletion at mid-latitudes and an enrichment in the North polar region. If C_4N_2 condenses very efficiently, it should form C_4N_2 ice when reaching the polar troposphere, potentially explaining the detection of C_4N_2 ice. The condensation of C_4N_2 thereby leads to very low C_4N_2 abundances near the lower equatorial stratosphere preventing its detection in the infrared region. Nevertheless, a recent modeling study by de Kok et al. (2008) could not explain the low gas phase C_4N_2 abundances through C_4N_2 ice formation.

4.3.9. Ammonia (NH_3)

Ammonia has not been detected yet in the lower atmosphere and has not yet been detected spectroscopically. Using the SPIRE/Herschel spectrometer, Teanby et al. (2013) obtained a 3-σ upper limit on the NH_3 abundance of 0.19 ppb for altitudes 65-110 km (with a peak of sensitivity at 75 km) considering a constant mole fraction with altitude. Data from CIRS/Cassini limb observations obtained during two flybys of Titan (T55 at 25°S and T64 at 75°N) gave upper limits on the abundances of NH_3 (Nixon et al., 2013). The upper limit is 0.59 ppb at 7.6 mbar (∼ 110 km, T55 flyby) and 2.0 ppb at 0.26 mbar (∼ 250 km, T64 flyby). Data from INMS/Cassini ion spectra obtained during the T5 flyby of Titan by the Cassini spacecraft suggested the presence of NH_3 in the ionosphere of Titan (Vuitton et al., 2007) with a model dependent mole fraction at 1100 km equal to 7.0×10^{-6} (required to match the density of NH_4^+). Cui et al. (2009) claimed a firm detection of NH_3 in the ionosphere from an in-depth study of the distributions of various neutral species in Titan's upper atmosphere, between 950 and 1200 km. These analyses were based on a large sample of Cassini/INMS measurements in the Closed Source Neutral (CSN) mode, obtained during 15 close flybys of Titan. They obtained a global average mixing ratio of $(3-4)\times10^{-5}$ below 1100 km, one order of magnitude greater than the value derived by Vuitton et al. (2007). Cui et al. (2009) stated that claims of NH_3 detection in Titan's upper atmosphere should be taken cautiously, since a significant fraction of the observed NH_3 molecules might have been formed on the chamber walls from N and H radicals in the ambient atmosphere. Magee et al. (2009) stated that the source of NH_3 seen by INMS was a topic of debate and noticed that it is conceivable that small amounts of NH_3 may reach the INMS antechamber from spent hydrazine fuel.

We obtain large uncertainties on the NH_3 mole fraction profile and our model underestimates the production of NH_3 compared to the potentially erroneous value derived by Cui et al. (2009) (see above). Our model is in agreement with upper limits obtained in the lower atmosphere (Teanby et al. (2013) for instance)

although some Monte-Carlo profiles are greater than these upper limits. Neutral chemistry is not an efficient process to produce ammonia (see also Appendix A) because it systematically involves the NH_2 radical which is inefficiently produced through neutral chemistry as NH reacts mainly in Titan's atmosphere with the CH_3 radical to form CH_2NH. However, as shown by Yelle et al. (2010), CH_2NH is an important NH_2 source in the upper atmosphere through ionic reactions. Indeed, the high proton affinity value of CH_2NH leads to its easy protonation through reactions with the major ions in Titan's upper atmosphere ($HCNH^+$, CH_5^+, $C_2H_5^+$, HC_3NH^+). The dissociative electronic recombination reaction of $CH_2NH_2^+$, which has never been studied, should then lead to CH_2 + NH_2 products acting as a sink for CH_2NH and an important source of NH_2. The absence of ion reactions in our model leads to an overestimation of CH_2NH and an underestimation of NH_3 in the upper atmosphere.

4.4. Other nitrogen species profiles

In addition to the compounds previously presented, several nitrogen compounds were suspected to be present and their densities have been inferred from the analysis of the Cassini/INMS data by Vuitton et al. (2007). These compounds (CH_2NH, C_4H_3N, HC_5N, C_5H_5N, C_6H_3N and C_6H_7N) were not reported in latter analyses of INMS spectra.

4.4.1. (CH_2NH)

CH_2NH is mainly produced by the $N(^2D)$ + CH_4 reaction (Herron, 1999) (there is a typographical error in the Herron paper: we should read $A = 4.8 \times 10^{-11}$ instead of 4.8×10^{-12} in Table 3) (see also Ouk et al. (2011); Takayanagi and Kurosaki (1999); Takayanagi et al. (1999); Balucani et al. (2009)) and by the NH + CH_3 reaction (Redondo et al., 2006), with a secondary contribution from the $N(^2D)$ + C_2H_6 reaction (Herron, 1999; Balucani et al., 2010). CH_2NH is mainly lost through photodissociation. The photodissociation cross section has been calculated at the EOM-CCSD(T)/aug-cc-pV5Z level (as well as at the MRCI+Q/aug-ccpVTZ level) and has been scaled to the experimental spectrum between 235 and 260 nm (Teslja et al., 2004). The branching ratios in Hébrard et al. (2012) were deduced from theoretical calculations (Zhou and Schlegel, 2009; Nguyen et al., 1996; Hébrard et al., 2012), the main products being H + H_2CN (the UV absorption dominates the photodissociation). The reaction of CH_2NH with H atoms was suspected to be an important CH_2NH loss process (Lavvas et al., 2008a,b). The H + CH_2NH reaction can lead to association (CH_2NH_2 and CH_3NH) or to abstraction. There is one theoretical calculation for the association Blitz et al. (2012) leading to a barrier equal to 20 kJ/mol and one estimation of the abstraction rate constant for combustion (Tomeczek and Gradon, 2003) leading to a relatively small activation barrier. The addition channel is of minor importance here as CH_2NH is mainly produced in upper atmosphere where the pressure is low. We use the rate constant for H + C_2H_4 from Vuitton et al. (2012) considering only one isomer for the adduct. For the abstraction pathway we calculate the barrier at the M06-2X/cc-pVTZ level

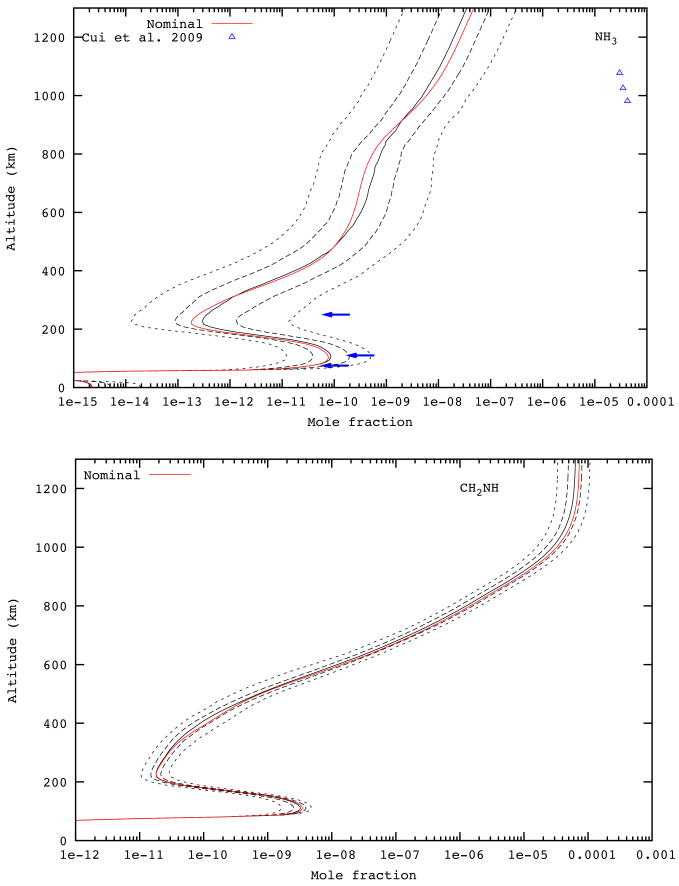

Figure 13: Top: Mole fraction profiles of NH_3 and comparison with some observations. Only upper limits are available in the lower atmosphere. Bottom: Mole fraction profiles of CH_2NH. Dashed lines and dotted lines give the intervals containing respectively 50% and 90% of the abundance profiles. See text for references and complementary observations.

and the rate using classical TST, leading to a smaller rate constant value than the previous estimation by Tomeczek and Gradon (2003). The loss of CH_2NH by reaction with H atoms is significantly smaller than its loss by photodissociation in our model. CH_2NH is mainly formed in upper atmosphere with a contribution from cosmic rays induced dissociation of N_2 in the stratosphere. The simulations overestimate CH_2NH mole fractions compared to the values obtained by Vuitton et al. (2007) and this may be attributed to ionic reactions which should play an important role for CH_2NH due to its high Protonic Affinity (Yelle et al., 2010) as explained above, leading eventually to CH_2 + NH_2 products. The mole fraction of CH_2NH between 100 and 200 km (induced by cosmic rays (CR) photochemistry) is around 10^{-9} and it will be interesting to have upper limit value from Cassini measurements (CH_2NH absorbs in the 1040-1150 cm^{-1} range (Halonen et al., 1986)) to estimate the importance of CR induced photochemistry (even if ionic chemistry is likely to be very different in the stratosphere than in upper atmosphere as most of the electrons should stick to aerosols, the loss of CH_2NH through protonation followed by $CH_2NH_2^+$ sticking to negatively charged aerosols should lead to similar loss rates to the DR reaction but without producing ammonia).

4.4.2. (HC_5N)

Marten et al. (2002) proposed an upper limit for the HC_5N mole fraction of 4.0×10^{-10} from millimeter heterodyne observations obtained with the IRAM 30-m telescope assuming a uniform distribution of this compound in the lower stratosphere. The calculated mole fraction profile of HC_5N is uniform with altitude in the stratosphere, with a similar shape to the calculated HC_3N mole fraction. Our model is in agreement with this upper limit. There are three equivalent HC_5N production pathways: $CN + C_4H_2 \rightarrow HC_5N + H$, $C_3N + C_2H_2 \rightarrow HC_5N + H$, $C_2H + HC_3N \rightarrow HC_5N + H$. In addition to a secondary one in the upper atmosphere: $C_2H + CH_3C_3N \rightarrow HC_5N + CH_3$. However, all these reactions (without barriers in the entrance valley) lead to relatively small production rates and consequently to a relatively low HC_5N concentration. The main difference compared to previous models is the fact that C_3N reacts quickly with CH_4 (Fournier et al., 2014) leading to a small steady state C_3N concentration and a low production rate from the $C_3N + C_2H_2$ reaction. The main HC_5N losses are unlikely to be photodissociation by comparison with HC_3N (HC_5N photodissociation leads mainly to C_5N which should react quickly with CH_4 leading back to HC_5N) but rather by association with H atoms followed by the H_2C_5N adduct reaction with another H atom leading to $HCN + C_4H_2$, $HC_3N + C_2H_2$ and $C_2H_3C_3N$.

4.4.3. (CH_3C_3N)

Detection of $C_4H_3NH^+$ isomers, likely to be $CH_3C_3NH^+$, at 74°N and 1100 km were reported by Vuitton et al. (2007) from the Cassini/INMS data obtained on the Cassini T5 flyby. From the analysis of the mass spectrum, they inferred a mole fraction of C_4H_3N (CH_3C_3N) equal to 4.0×10^{-6}. Our model is in agreement with this value.

In the middle atmosphere, we obtain for CH_3C_3N a huge diversity of profiles from our uncertainty propagation procedure illustrated by the remarkable difference between the mean profile and the nominal profile. This result shows that many chemical pathways are possible due to the current uncertainties on several rate constants. There are two CH_3C_3N production pathways in our nominal model, both arising from CCN radical reactions (formed by the H + HCCN reaction (Osamura and Petrie, 2004; Takayanagi et al., 1998)) and therefore localized in the upper atmosphere. CH_3C_3N is directly produced by the CCN + C_2H_4 reaction (Zhu et al., 2003a) and is also formed by the reactions CCN + C_2H_2 → HC_4N + H (Zhu et al., 2003a; Wang et al., 2006) followed by HC_4N + H + M → CH_2C_3N + M and CH_2C_3N + H + M → CH_3C_3N + M (this work). As there is no bimolecular exit channel for the H + HC_4N reaction in contrast to the H + HCCN reaction, both ways to produce CH_3C_3N are efficient. The photodissociation of CH_3C_3N has never been studied. The absorption cross section should be similar to HC_3N, but the products which are likely to be mainly CH_2C_3N + H and CH_3 + C_3N, do not react quickly with CH_4 to give back CH_3C_3N so photodissociation becomes a sink, in contrast to HC_3N. As our model is limited to neutral reactions, it cannot describe correctly nitriles in the upper atmosphere where ionic reactions are important. The proton affinity of CH_3C_3N is calculated to be equal to 788 kJ/mol at the M06-2X/cc-pVTZ level so CH_3C_3N will react quickly with $C_2H_5^+$, $HCNH^+$ and HC_3NH^+ leading to $CH_3C_3NH^+$ (the $CH_3C_3NH^+$ ion could be the "$C_4H_3NH^+$" identified in INMS spectra). Further evolution of $CH_3C_3NH^+$ will be controlled by the competition between H^+ exchange with CH_2NH and NH_3, the two main species having proton affinities larger than CH_3C_3N, and DR reactions. The branching ratio giving back CH_3C_3N for the DR reaction of $CH_3C_3NH^+$ is unknown but it is almost certainly less than 1 so that ionic reactions act mainly as loss processes for CH_3C_3N. It should be noted that a large part of the rich nitrile chemistry in the upper atmosphere (concerning CH_3C_3N as well as $C_2H_5C_3N$ and $C_4H_3C_3N$) is directly dependent on the HCCN + H reaction which is not well known despite the theoretical studies of Osamura and Petrie (2004) and Takayanagi et al. (1998). It should also be noted that various isomers can be synthesized in the CCN + C_2H_4 and CCN + C_2H_2 reactions.

4.4.4. (C_3H_7CN)

$C_3H_7CNH^+$ ion is found to be 700 less abundant than CH_3CNH^+ and 50 times less abundant than $C_2H_5CNH^+$, in INMS ions spectra reported by Vuitton et al. (2007) from Cassini/INMS measurements obtained on the Cassini T5 flyby. Our model leads to elevated abundances of C_3H_7CN in both the lower and upper atmosphere. The $CH_3CN/C_2H_5CN/C_3H_7CN$ abundances given by our model are in relatively good agreement with the INMS data deduced from the protonated form, particularly considering that ionic chemistry acts as sinks for these compounds (R-CN + $HCNH^+$ → $RCNH^+$ + HCN followed by R-CNH^+ + e^- which do not give 100% RCNH + H). The main production of C_3H_7CN molecule is through the association reaction between C_2H_4CN and CH_3, so this species is then directly correlated to CH_3CN and C_2H_5CN. The main losses are

photodissociation and reaction with C_2H, the rate constant being taken to be similar to the $C_2H + C_2H_6$ reaction. The calculated C_3H_7CN abundance is very likely to be overestimated by comparison with CH_3CN and C_2H_5CN. Firstly, the association rate constant for the $C_2H_4CN + CH_3 + M \rightarrow C_2H_5CN + M$ reaction is unknown and has been estimated using our semi-empirical model. Secondly, the photodissociation cross section of C_3H_7CN is unknown so we use the same value as for C_2H_5CN. Moreover, as C_3H_7CN condenses in the lower stratosphere, its mole fraction should be very low at mid latitudes as discussed for other nitriles like HCN. This effect may be very strong for C_3H_7CN as it should condense at higher altitudes. Then, C_3H_7CN should also show a large enrichment near the North pole and might be a component of the Haze B layer.

4.5. Chemical and dynamical lifetimes

Chemical and dynamical lifetimes are useful characteristics of the model, in particular to determine whether transport (vertical or horizontal) could be the dominant process at a given altitude in the atmosphere. Figure 15 shows the chemical and dynamical lifetimes of major nitrogen compounds as a function of altitude. The chemical lifetime is defined as $\tau_{chem}(z) = 1/L(z)$ where $L(z)$ is the total loss rate (in s^{-1}) at altitude z. The dynamical lifetime $\tau_{dyn_i}(z)$ for species i at altitude z takes both eddy diffusion and molecular diffusion processes into account and is expressed as : $1/\tau_{dyn_i}(z) = 1/\tau_{D_i(z)} + 1/\tau_{K(z)}$ for each species i, with $\tau_{K(z)} = H(z)^2/K(z)$ and $\tau_{D_i(z)} = H(z)^2/D_i(z)$. $H(z)$ is the atmospheric scale height, $K(z)$ the eddy diffusion coefficient and $D_i(z)$ the molecular diffusion coefficient in N_2 for species i. We see that some species are very stable from a chemical point of view, like HCN, CH_3CN, C_2H_5CN and C_2N_2 throughout the whole atmosphere. For other species, there is an alternate between regions dominated by photochemical equilibrium and those dominated by dynamical equilibrium with altitude. We note also that the chemical lifetimes of all the species depicted in Figure 15 have a strong dependance with altitude below 200 km since this quantity increases by 4 orders of magnitude (at least). Wilson and Atreya (2004) published the chemical lifetimes of several nitrogen species at 300 km (HCN, CH_3CN, C_2N_2, HC_3N, C_2H_3CN and C_4N_2). Our results (at least at this altitude) are somewhat different since we obtain nominal values which differ by factors of roughly 1.5 (for HCN, CH_3CN, C_4N_2), 2.5 (C_2H_3CN), 4 (HC_3N) and 6 (C_2N_2).

5. Key reactions

From an uncertainty propagation study and a global sensitivity analysis (see Hébrard et al. (2009) for instance), we have determined a list of the key reactions for the main nitrogen species of our model. These key reactions (which can be different from reactions that give the main production rates), are the ones which are responsible for the uncertainties on the mole fraction profiles calculated from our model. They are consequently the reactions that should be studied in priority to improve photochemical models of Titan's atmosphere. The key

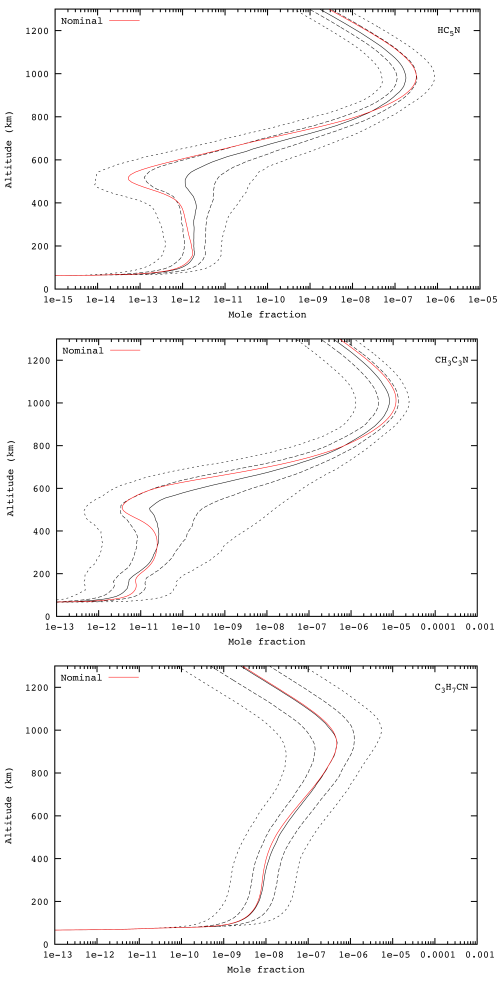

Figure 14: Top: Mole fraction profiles of HC_5N. Middle: Mole fraction profiles of CH_3C_3N. Bottom: Mole fraction profiles of C_3H_7CN. Dashed lines and dotted lines give the intervals containing respectively 50% and 90% of the abundance profiles.

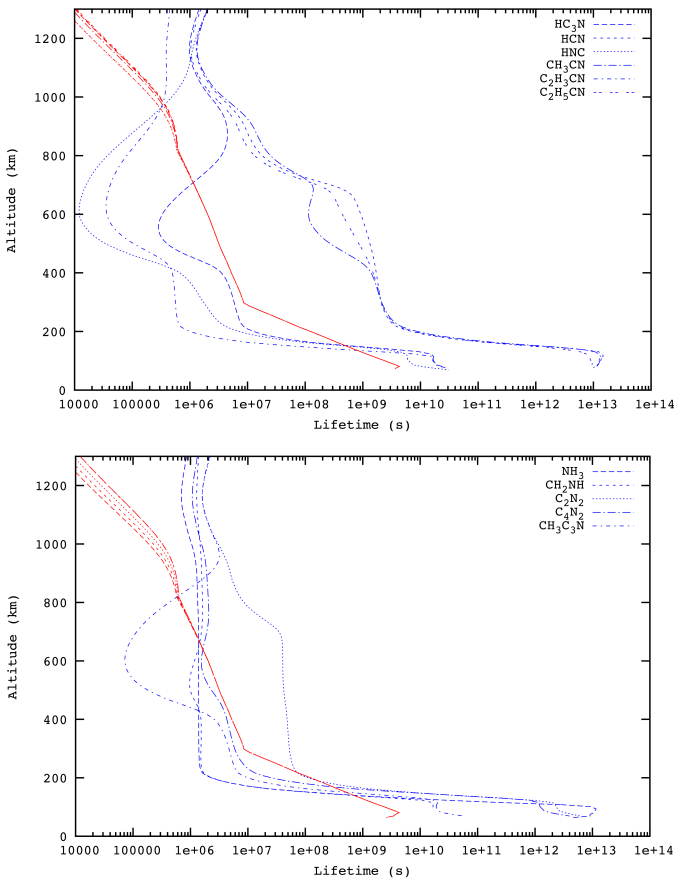

Figure 15: Chemical and dynamical lifetimes of HC_3N, HCN, HNC, CH_3CN, C_2H_3CN and C_2H_5CN (top) and NH_3, CH_2NH, C_2N_2, C_4N_2, CH_3C_3N (bottom) as a function of altitude for the nominal model. The cut-off in the lower atmosphere corresponds to the condensation altitude of the corresponding compounds. The dynamical lifetime takes both eddy diffusion and molecular diffusion into account. The homopause is localized around 900 km (see Figure 4).

reactions for the main nitrogen compounds are given in Table 3 and Table 4 for 3 different altitudes. Many reactions which are important for the production of these species and discussed in Appendix A are also reactions that are not well known. As a consequence, they appear as key reactions. In particular, this is the case for numerous association reactions with H. Some other reactions are critical: $N(^2D)$ + HCN, H + HNC and reactions with C_2N which is a key species in the production of several nitriles.

Table 3: Key reactions responsible for uncertainties on major nitrogen compounds at altitude of 900, 500 and 100 km. Only reactions with an absolute RCC (Rank Correlation Coefficient) value greater than 0.2 are given. A blank means that the absolute value of the RCC is lower than 0.2 and it is not given for clarity. Some compounds are just considered as products and are not included in our model.

NH_3			
Reaction	RCC		
	at 900 km	at 500 km	at 100 km
$N(^4S) + NH_2 \rightarrow N_2 + H + H$	-0.21		-0.30
$NH + H_2CN \rightarrow NH_2 + HCN$			0.29
$NH_2 + H_2CN \rightarrow HCN + NH_3$	0.35		0.36
$CH_2NH + H \rightarrow CH_3NH$	0.61	0.48	
$NH_2 + C_2H_3 \rightarrow NH_3 + C_2H_2$	0.34	0.61	0.36
$NH_2 + C_2H_5 \rightarrow NH_3 + C_2H_4$		0.34	
$NH + C_2H_5 \rightarrow NH_2 + C_2H_4$			0.22
$NH + C_2H_3 \rightarrow NH_2 + C_2H_2$			0.23
HCN			
$N(^2D) + C_2H_4 \rightarrow CH_2NCH + H$	0.31	0.24	0.23
$N(^2D) + HCN \rightarrow CH + N_2$	-0.83	-0.84	-0.83
$C_2H_3CN + H \rightarrow C_2H_4CN$		-0.20	
HNC			
$HNC + H \rightarrow HCN + H$	-0.94	-0.89	-0.74
$N(^4S) + {}^3CH_2 \rightarrow HNC + H$			0.22
$NH + C_2H_3 \rightarrow HNC + CH_3$			0.22
HC_3N			
$N(^2D) + HCN \rightarrow CH \text{ v } N_2$	-0.43		
$CN + C_2H_2 \rightarrow HC_3N + H$	0.30		
$CN + C_2H_4 \rightarrow C_2H_3CN + H$	-0.33		
$HC_3N + H \rightarrow H_2C_3N$	-0.36	-0.83	-0.38
$C_2H_3CN + H \rightarrow C_2H_4CN$	-0.34		
$HC_4N + H \rightarrow CH_2C_3N$	-0.22		
$H + C_2H_4 \rightarrow C_2H_5$		0.20	
$N(^4S) + CH_2CN \rightarrow H_2CN + CN$			0.23
$HC_3N + C_2H_3 \rightarrow C_2H_3C_3N$ (product) + H			-0.44
$H + C_2H_2 \rightarrow C_2H_3$			0.21
CH_3CN			
$N(^2D) + C_2H_4 \rightarrow c\text{-}CH_2NCH + H$	0.36	0.35	0.27
$CH_2NH + CH \rightarrow CH_3CN + H$	0.25		
$c\text{-}CH_2NCH + H \rightarrow CH_3CN + H$	0.27		
$CH_2CN + H \rightarrow CH_3CN$	0.52	0.62	
$CH_2CN + CH_3 \rightarrow C_2H_5CN$	-0.28	-0.25	-0.20
$NH + C_2H_3 \rightarrow CH_3CN + H$			0.26
C_2H_3CN			
$CHCN + H \rightarrow C_2N + H_2$	-0.22		
$C_2H_3CN + H \rightarrow C_2H_4CN$	-0.89	-0.71	
$H_2C_3N + H \rightarrow C_2H_3CN$		0.40	
$H_2C_3N + H \rightarrow HCN + C_2H_2$		-0.21	
$H_2C_3N + H \rightarrow HC_3N + H_2$		-0.21	
$N(^4S) + C_3H_5 \rightarrow C_2H_3CN + H_2$			0.48
$HCN + C_2H_3 \rightarrow C_2H_3CN + H$			0.30
C_2H_5CN			
$CH_2CN + H \rightarrow CH_3CN$	-0.21	-0.39	
$CH_2CN + CH_3 \rightarrow C_2H_5CN$	0.28		
$C_2H_3CN + H \rightarrow C_2H_4CN$	0.72	0.49	
$N(^2D) + HCN \rightarrow CH + N_2$		-0.24	-0.23

Table 4: Continued.

CH_2NH			
$N(^2D) + N_2 \rightarrow N(^4S) + N_2$	-0.22		-0.70
$N(^2D) + CH_4 \rightarrow NH + CH_3$	0.24		
$N(^2D) + CH_4 \rightarrow CH_2NH + H$	0.51	0.33	0.50
$N(^2D) + C_2H_4 \rightarrow CH_2NCH + H$	-0.43	-0.29	
$N(^2D) + C_2H_6 \rightarrow CH_2NH + CH_3$	0.25		
$N(^2D) + HCN \rightarrow CH + N_2$	-0.38	-0.30	
$H + C_2H_4 \rightarrow C_2H_5$		0.31	
$CH_2NH + H \rightarrow CH_3NH$		-0.32	-0.26
CH_3C_3N			
$^1CH_2 + CH_4 \rightarrow CH_3 + CH_3$	-0.26		
$C_2N + H \rightarrow HCN + C$	-0.51		
$C_2N + C_2H_4 \rightarrow CH_3C_3N + H$	0.39		
$CHCN + H \rightarrow C_2N + H_2$	0.30		
$CHCN + CH_3 \rightarrow C_2H_3CN + H$	-0.20		
$CH_3C_3N + H \rightarrow H_4C_4N$	-0.25	-0.84	-0.46
$C_2H + C_2H_2 \rightarrow C_4H_2 + H$			0.20
$N(^4S) + C_4H_3 \rightarrow CH_2C_3N + H$			0.31
$CH_2C_3N + H \rightarrow CH_3C_3N$			0.47
C_2N_2			
$^1CH_2 + CH_4 \rightarrow CH_3 + CH_3$	-0.28	-0.28	
$^1CH_2 + N_2 \rightarrow {}^3CH_2 + N_2$	0.25	0.24	
$N(^4S) + CHCN \rightarrow C_2N_2 + H$	0.37	0.36	0.23
$CN + HNC \rightarrow C_2N_2 + H$	0.37	0.37	
$HNC + H \rightarrow HCN + H$	-0.25	-0.27	
$CHCN + H \rightarrow C_2N + H_2$	-0.25	-0.24	
$N(^4S) + CH_2CN \rightarrow H_2CN + CN$			-0.21
$N(^4S) + CH_2CN \rightarrow HC_2N_2 + H$			0.56
$HC_2N_2 + H \rightarrow C_2N_2 + H_2$			0.28
$HC_2N_2 + H \rightarrow HCN + HNC$			-0.43
C_4N_2			
$^1CH_2 + CH_4 \rightarrow CH_3 + CH_3$	-0.36	-0.20	
$^1CH_2 + N_2 \rightarrow {}^3CH_2 + N_2$	0.25		
$N(^4S) + HC_4N \rightarrow C_4N_2 + H$	0.23		0.35
$N(^2D) + HCN \rightarrow CH + N_2$	-0.34	-0.27	
$HCN + C_3N \rightarrow C_4N_2 + H$	0.26	0.25	
$CHCN + CH_3 \rightarrow C_2H_3CN + H$	-0.33		
$HC_4N + H \rightarrow CH_2C_3N$	-0.20		
$C_4N_2 + H \rightarrow HC_4N_2$		-0.58	
$N(^4S) + CHCN \rightarrow C_2N_2 + H$			-0.37
$N(^2D) + N_2 \rightarrow N(^4S) + N_2$			-0.31
$CHCN + H \rightarrow C_2N + H_2$			0.33

6. Discussion

6.1. Sensitivity to Galactic Cosmic Rays

The production of nitrogen atoms in the lower stratosphere by GCR increases the production of many nitrogen compounds. We show in Figure 16 the mole fractions of the most abundant species which are affected by this process. The contribution of GCR in the production of amines like NH_3, CH_3NH_2 and CH_3NHCH_3 or imines like CH_2NH is particularly remarkable since their mole fractions decrease by about 3 orders of magnitude when turning off the production of N atoms by GCR. Some nitriles like HNC, C_2N_2, C_4N_2 and C_2H_3CN are also efficiently produced by chemical processes following the interaction of GCR with N_2. The effect for other species is much less pronounced or negligible. It is also important to pinpoint that the GCR precipitation spectrum in the atmosphere of Titan depends on the solar activity. The production of N atoms by GCR considered in the present study corresponds to a low solar activity (high GCR production rate). For a high solar activity, the GCR production rate can be 30% lower (Gronoff et al., 2011). The nitrogen chemistry induced by GCR is very similar to the nitrogen chemistry induced by N_2 photodissociation as GCR lead to the formation of $N(^4S)$ and $N(^2D)$ (considering the large uncertainty of cosmic ray effects we do not consider cosmic ray ion formation in this study). The chemistry induced by GCR is mainly localized in the lower stratosphere. The N_2 dissociation flux induced by GCR is smaller than the N_2 photodissociation flux. For very stable species, such HCN which is formed efficiently in the upper atmosphere and transported to lower altitudes by diffusion, the supplementary lower atmosphere production by GCR does not drastically change the abundance profile. However, for photo-sensible species (amines and imines) and for reactive species (HNC, C_2H_3CN) which do not have time to diffuse, lower atmospheric production by GCR leads to a notable increase of their abundance in the lower stratosphere. C_2N_2 is a special case, the production from N + HCCN in the lower stratosphere is comparable to transport as the H atom concentration decreases in the lower stratosphere due to the H + C_2H_2 reaction so that the main HCCN loss process, the H + HCCN reaction, is less efficient.

6.2. Epistemic bimodalities

More or less pronounced epistemic bimodalities are present in the distribution of Monte-Carlo profiles generated by our uncertainty propagation study for some compounds (like HC_3N and C_2H_5CN) at some altitudes. These bimodalities are called epistemic because they are due to the uncertainties on certain key reaction rates. Bimodalities were observed in Dobrijevic et al. (2008) for C_2H_2 and C_2H_4 but subsequent improvements of the chemical scheme have removed these effects. In the present study, the introduction of new compounds and reactions to improve the chemical scheme of nitrogen compounds cause the appearance of some new bimodalities for some nitrogen compounds. The key reactions that are responsible of this behaviour are given in Tables 3 and 4. These reactions need to be investigated to lower the current uncertainties in our model.

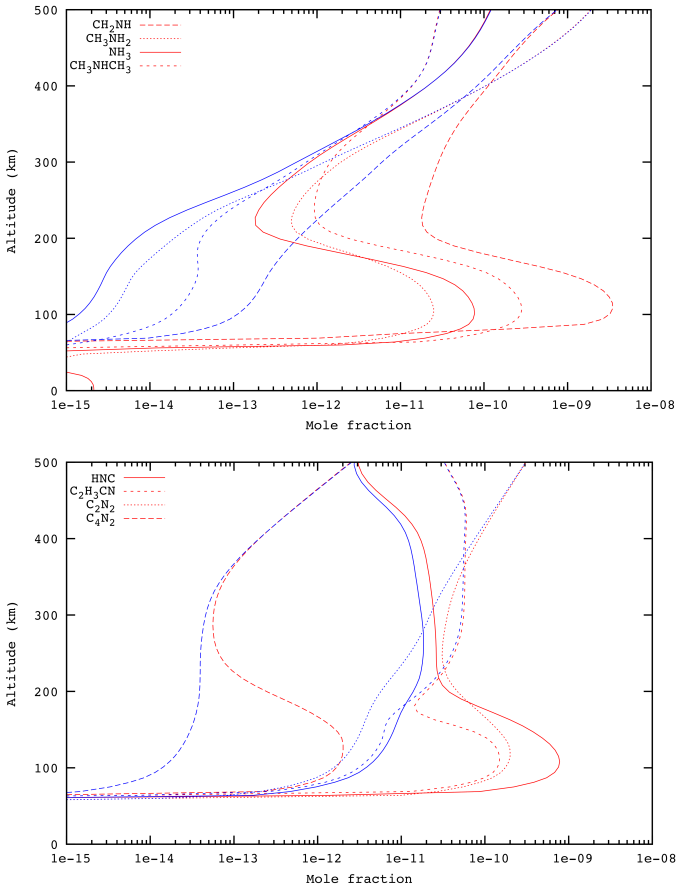

Figure 16: Effect of Galactic Cosmic Rays (GCR) on the production of several nitrogen compounds in the lower atmosphere of Titan. Red: nominal model with N atoms produced by GCR. Blue: model with no GCR.

6.3. Towards higher complexity

A large fraction of the nitriles formed in Titan's atmosphere are unsaturated nitriles (C_2H_3CN, HC_3N, CH_3C_3N, HC_5N, C_4H_3CN, C_4H_5CN) which then react relatively quickly with H atoms leading to adducts. These adducts will react quickly with H atoms and CH_3 radicals, but also with hydrocarbon radicals C_2H_3, C_2H_5, C_3H_7, leading either to HCN and hydrocarbons or to larger nitriles. Moreover, unsaturated nitriles photodissociate in the 190-230 nm range for which the solar flux is strong down to low altitudes forming some HCN and hydrocarbon radicals. H atoms (or CH_3 radicals) are also lost with a nitrile radical species as the coproduct which can go on to form larger nitriles through reaction with hydrocarbon radicals. It is difficult to describe this full network in detail but there is no doubt that a large variety of nitriles are synthesized in Titan's atmosphere. Nevertheless, only the saturated ones (HCN, CH_3CN and probably C_2H_5CN and C_3H_7CN) can reach high abundances because they are not easily photodissociated and do not react with H atoms.

6.4. Hot topics and new insights

- In our model C_2H_3CN, HC_5N and C_4N_2 do not reach large concentrations in the gas-phase, in agreement with the non-detection of these compounds: C_2H_3CN is easily photodissociated and the rate constant of the C_2H_3 + HCN reaction is much slower than in previous models; for HC_5N, the $C_3N + C_2H_2$ reaction involves low rates as C_3N reacts quickly with CH_4; C_4N_2 reacts quickly with H atoms leading to HCN + HC_3N (the high reactivity of C_4N_2 with H atoms is questionable and should be confirmed by experimental and additional theoretical studies). The low abundance of HC_5N and C_2H_3CN in the stratosphere has a low uncertainty which is not the case for C_4N_2.

- CH_3C_3N, formed through the CCN + C_2H_2 and CCN + C_2H_4 reactions, reaches a high concentration in the upper atmosphere. The HCCN + H reaction is critical and further experimental and theoretical studies are needed.

- C_2H_5CN and C_3H_7CN reach high concentrations in the stratosphere but their photodissociation cross sections are poorly known and should be studied. These compounds could give an interesting constraint for the model of Hourdin et al. (2004), since they should present a high polar enrichment.

- Nitriles present a low energy triplet state, which may be responsible for non negligible absorption in the 200-350 nm range. In particular, cross sections of CH_3CN, C_2H_5CN and C_3H_7CN at ambient and low temperature are needed. The quantum yields of C_2H_3CN photolysis are not well-known. It is important in particular to evaluate the yield for HNC production. Also, the quantum yields for CH_4 and C_2H_2 in the full wavelength range where they are dissociated is required to better compute the abundances of hydrocarbons and H atoms.

- The excited state chemistry of some molecules is required, in particular for $C_2H_2^{**}$.
- The abundances of all nitriles are directly dependent on the photodissociation of N_2 which is not well known and depends on the variation of the solar flux.
- The large decrease of the HC_3N abundance below 400 km is not well described by our 1D photochemical model and seems not to be related to chemical processes.
- Cosmic rays induce a relatively active nitrogen chemistry in the stratosphere leading to notable CH_2NH and non-negligible NH_3 and CH_3NH_2 concentrations. Ionic chemistry is likely to be very different in this region than in the upper atmosphere as most of the electrons should stick to aerosols. Due to their high proton affinity, CH_2NH, NH_3 and CH_3NH_2 should easily be protonated. Nevertheless, the main $CH_2NH_2^+$, NH_4^+ and $CH_3NH_3^+$ reactions will not be dissociative electronic recombination but rather sticking to negatively charged aerosols leading to a net loss. In particular, CH_2NH will probably not lead to NH_3 formation in the lower atmosphere.

7. Conclusion

We have made a careful investigation of the neutral chemistry of nitrogen compounds in the atmosphere of Titan. Our model includes 60 species containing nitrogen atoms with the heaviest molecule reaching a molar mass of 93 amu. We have built a consistent chemical scheme based on the abundances of the main species and their reactivity. Many rate constants and their uncertainty factors have been calculated or estimated based on theoretical considerations. Based on this new scheme, we have computed the mole fraction profiles for all of these compounds and we have studied how associated rate constant uncertainties affect these profiles. For some species like HCN, uncertainties on model results are reasonable. For other nitrogen containing species (like HC_3N, C_2H_3CN, CH_3C_3N), uncertainties are very large. We carried out a global sensitivity analysis to determine the key reactions that are responsible for these uncertainties. Most of the key reactions are reactions that have yet to be studied at low temperature, many of these involve reactions with H atoms. Several species newly introduced into our photochemical model have not been detected yet and are relatively abundant (like CH_3C_3N and C_3H_7CN). Our study shows that the photolysis of several compounds plays a crucial role in the chemistry of nitriles and should be studied in depth, with particular reference to CH_3CN, C_2H_5CN, C_3H_7CN and C_2H_2. Compared to observations, our model overestimates the abundances of several species in the lower stratosphere for equatorial and equinoxial conditions. This is particularly marked for HC_3N and C_2H_5CN. Since our 1D photochemical model gives satisfactory results for many compounds (C_2- and C_3-hydrocarbons, water), this discrepancy is thought not to

be brought about by a poor description of the chemistry but could rather be explained by meridional transport and condensation in the polar region as proposed for instance by Hourdin et al. (2004). If we consider that this model is correct and following our own results, we predict that C_2H_5CN and C_3H_7CN should also present high polar enrichment factors. For most of the species, good agreement is obtained between our 1D photochemical model and INMS data in the higher atmosphere despite the fact that we do not take ionic reactions into account. For all the main nitrogen compounds, we have identified the main production and loss pathways. We find that nitrile photolysis is important in the overall nitrogen chemistry. However, the absorption cross sections for many compounds are not well known. In particular, the cross section for wavelengths greater than 150 nm for CH_3CN, C_2H_5CN and C_3H_7CN and the absorption of CH_3C_3N are unknown. Quantum yields as a function of wavelength for almost all the species are not determined. We have identified two main chemical pathways in the complexification of nitrogen compounds. Most of the nitrogen atoms produced by the dissociation of N_2 lead to the production of HCN. Its photolysis leads to the production of CN radicals which are the precursors for numerous nitriles (including HC_3N, C_2H_3CN, CH_3CN...), which are produced along the pathways to more complex nitrogen containing compounds. Another distinct pathway for the complexification of nitrogen compounds goes through C_2N, which is also a precursor for many other complex nitriles (like CH_3C_3N...). The next step for these neutral photochemical modeling studies should be the coupling with a ionospheric model. Many nitrogen species would be affected by this coupling in the higher atmosphere. As shown by Plessis et al. (2012); Krasnopolsky (2009); Vuitton et al. (2006), ionic chemistry contributes significantly to the production of neutral compounds, despite only a minor production of HCN initiated by N^+ reactions. Moreover, as ionic chemistry is driven mainly by H^+ transfer between ions and neutrals with large protonic affinity, ionic chemistry act as a sink for large nitriles and CH_2NH as the corresponding protonated form reacts mainly with electrons leading back to the neutral form at levels less than 100%. Secondly, negative ion chemistry involves nitrogen containing anions (CN^- and C_3N^-, Vuitton et al. (2009)) so it will be interesting to couple our coherent neutral scheme with anion chemistry too.

8. Acknowledgement

We thank the Programme National de Plantologie (PNP) of the Institut National des Sciences de l'Univers (INSU) for funding a part of this work. O.V. acknowledges support from the KU Leuven IDO project IDO/10/2013 and from the FWO Postdoctoral Fellowship program.

Appendix A. Nitrogen chemistry overview

In this section, we highlight the main chemical pathways leading to the production of the most abundant nitrogen species in Titan's atmosphere.

Appendix A.1. Primary nitrogen chemistry

Nitrogen chemistry is mostly initiated by nitrogen atoms in the ground state $N(^4S)$ and excited state $N(^2D)$ produced by N_2 photodissociation and dissociation by cosmic rays. In Titan's upper atmosphere, $N(^4S)$ reacts mainly with CH_3 radicals leading to H_2CN + H and HCN + H + H (Hébrard et al., 2012; Dutuit et al., 2013). H_2CN then reacts quickly with atomic hydrogen (and CH_3 radicals) leading mainly to HCN and some HNC, which is efficiently converted to HCN through reaction with H atoms (Talbi and Ellinger, 1996; Sumathi and Nguyen, 1998; Petrie, 2002). At this point, HCN can only be lost through photodissociation or through minor reactions with $N(^2D)$ and CH radicals (Hébrard et al., 2012). HCN is therefore stable in Titan's upper atmosphere and its steady state concentration is relatively high. Below 200 km the situation is more complex: $N(^4S)$ (produced in the lower atmosphere by N_2 dissociation by cosmic rays) reacts not only with CH_3 radicals but also with the numerous alkyl radicals that are efficiently produced through three body association reactions with H atoms. For $N(^2D)$, the situation is almost the opposite in complexity. In Titan's upper atmosphere, $N(^2D)$ atoms react mainly with HCN (albeit with a large associated uncertainty (Hébrard et al., 2012)), with CH_4, C_2H_2 and C_2H_4 (Herron, 1999) and are also partly relaxed to $N(^4S)$ (Herron, 1999). Below 200 km however, $N(^2D)$ reacts almost exclusively with CH_4. The reaction of $N(^2D)$ atoms with HCN should lead to CH + N_2 (Hébrard et al., 2012) and is therefore a net loss of nitriles. The reaction of $N(^2D)$ with CH_4 leads to CH_2NH + H and CH_3 + NH (Herron, 1999; Ouk et al., 2011; Takayanagi and Kurosaki, 1999; Takayanagi et al., 1999; Balucani et al., 2009). NH radicals mainly react with CH_3 leading to CH_2NH + H (Redondo et al., 2006) with a minor contribution from the $N(^4S)$ + NH reaction leading to N_2 + H (Hack et al., 1994; Caridade et al., 2005; Frankcombe and Nyman, 2007). CH_2NH is easily photodissociated in the UV (Teslja et al., 2004) leading to H_2CN + H, HCN + H + H and HNC + H_2 (Zhou and Schlegel, 2009; Nguyen et al., 1996) or reacts with H atoms leading to H_2CN + H_2 (Tomeczek and Gradon, 2003). As already noted, H_2CN reacts mainly with H atoms leading mainly to HCN and some HNC, which is efficiently converted into HCN through reaction with H atoms. As a result, reaction of $N(^2D)$ with CH_4 leads mainly to HCN with only low HNC and CH_2NH steady state abundances. The $N(^2D)$ + C_2H_4 reaction has been studied experimentally and theoretically (Sato et al., 1999; Takayanagi et al., 1998; Lee et al., 2011; Balucani et al., 2000b, 2012). Contrary to what is considered in usual models of Titan's atmosphere (Lebonnois et al., 2001; Wilson and Atreya, 2004; Lavvas et al., 2008; Krasnopolsky, 2009), the products are not H + CH_3CN, but rather H + CH_2NCH and H + c-CH_2(N)CH (cyclic compound) (Balucani et al., 2012; Lee et al., 2011). This non-production of CH_3CN is of crucial importance as it was thought to be the main (if not only) source of CH_3CN. In this study we use the RRKM results of Balucani et al. (2012) leading to 74% of CH_2NCH production and 26% of c-CH_2(N)CH production. We then introduced these new compounds and developed their chemical networks relevant for Titan chemistry. CH_2NCH is a diradical with a singlet ground state ($H_2C^{\cdot}$-N=$C^{\cdot}$H $\leftrightarrow$ H_2C=N-$C^{\cdot\cdot}$H) and should react quickly with atoms and rad-

icals, particularly with H atoms as shown by theoretical calculations (Balucani et al., 2012; Lee et al., 2011) probably leading to CH_3 + HCN. As there is likely to be no barrier in the entrance valley for the CH_2NCH + H reaction we consider a rate constant deduced from capture rate theory. We also consider the $CH_2NCH + CH_3 \rightarrow C_2H_5$ + HCN reaction with a rate constant of 2.0×10^{-11} cm^3 $molecule^{-1}$ s^{-1}. c-CH_2(N)CH is a closed-shell molecule and much less reactive than CH_2NCH. Balucani et al. (2012); Lee et al. (2011) found a barrier close to 14 kJ mol^{-1} for H addition leading to c-CH_2(N)CH_2 or c-CH_2(NH)CH. The c-CH_2(N)CH_2 production channel seems to have no bimolecular exit channel and as c-CH_2(N)CH is formed at high altitude where the pressure is low and stabilization is weak then we neglect this channel as c-CH_2(N)CH_2 will backdissociate into c-CH_2(N)CH + H. The other adduct, c-CH_2(NH)CH, is described in the theoretical calculations of Balucani et al. (2012) and should isomerize toward CH_2CHNH and then lead to CH_2CNH + H through a loose barrier or isomerize toward CH_3CNH and then CH_3CN + H. CH_2CNH formation will be favored due to loose transition state. Considering the theoretical calculations we propose a global rate constant equal to $1.0 \times 10^{-10} \exp(-1600/T)$, close to the rate of the H + C_2H_4 reaction, with 70% of CH_2CNH + H production and 30% CH_3CN + H production. As c-CH_2(N)CH reacts relatively slowly with H atoms we need to consider c-CH_2(N)CH photodissociation, the absorption spectrum being calculated at the EOM-CCSD/cc-pVTZ level using Gaussian 2009; the photodissociation products being c-$^1CH_2$(N)CH + $h\nu \rightarrow {}^1CH_2 + {}^1$HCN. We also consider the reactions of c-CH_2(N)CH with highly reactive radicals N(^{2}D), CH, C_2H, CN estimating rate constants equal to the rate constants for the corresponding reactions with C_2H_4. The main reactions of c-CH_2(N)CH are photodissociation and reaction with H atoms. CH_2NCH and c-CH_2(N)CH have low steady state concentrations because they are efficiently converted into HCN. The reaction of N(^{2}D) with C_2H_2 leads to HCCN formation (Takayanagi et al., 1998; Herron, 1999). HCCN, a di-radical with a triplet ground state, should have low reactivity with closed-shell molecules (Adamson et al., 1997) so it will react in Titan's atmosphere mainly with H atoms leading to CCN + H_2 (Osamura and Petrie, 2004; Takayanagi et al., 1998). CCN is a very reactive radical (Wang et al., 2006) but not with CH_4 (Zhu et al., 2003a,b). As a result, in Titan's atmosphere CCN radicals will react mainly with C_2H_2 (leading to HC_4N (Wang et al., 2006)), with C_2H_4 (leading to CH_3C_3N (Wang et al., 2006)) and with H atoms (leading to HCN + C (Mebel and Kaiser, 2002; Takahashi and Takayanagi, 2006)). HC_4N is a strongly bound radical and is likely to be unreactive with closed-shell molecules by comparison with HCCN and without bimolecular exit channels for reaction with H atoms. Then in the low pressures of Titan's upper atmosphere where it is formed, HC_4N will slowly react, through addition, with H atoms leading to CH_2C_3N, with CH_3 (leading likely to C_4H_3CN + H atom) and with N(^{4}S) (leading likely mainly to C_4N_2 + H). The reactions of N(^{4}S) with HCCN and HC_4N are the main C_2N_2 and C_4N_2 production pathways in the present model . As there is no exothermic bimolecular exit channel for the H + HC_4N reaction, in contrast to H + HCCN, HC_4N should reach a non-negligible steady state abundance leading to relatively large

C_4N_2 abundance. In the upper atmosphere, the production of CN and CCN radicals leads to a rich nitrile chemistry (HC_3N, $C_2H_3C_3N$ CH_3C_3N, C_4H_3CN, $C_2H_5C_3N$) which is enhanced by the addition of H atoms to double and triple CC bonds (H + CH_3C_3N → $CH_3CH{=}C^{\cdot}$-CN, followed by H + $CH_3CH{=}C^{\cdot}$-CN → $CH_3CH{=}CH$-CN and CH_3 + $CH_3CH{=}C^{\cdot}$-CN → $CH_3CH{=}C(CH_3)$-CN) as their barriers are relatively low and the size of the molecules leads to relatively high rate constant at the low pressure limit k_0. The chemistry of N atoms thus leads mainly to HCN formation with some CH_2NH, HNC, CH_3C_3N (also C_4H_3CN, $C_2H_5C_3N$, ...), CH_2NCH (or CH_3CN), C_2N_2 and C_4N_2 formation.

Appendix A.2. Secondary nitrogen chemistry

Secondary nitrogen chemistry is driven by HCN photodissociation (leading to H + CN (Herzberg, 1957; Lee, 1980; Guo et al., 2000; West and Berry, 1974)). CN radicals react mainly with C_2H_2 (leading to H + HC_3N) and C_2H_4 (leading to H + C_2H_3CN) in the upper atmosphere and with C_2H_2 (leading to H + HC_3N) and with CH_4 and C_2H_6 (leading back to HCN) at low altitude. CN radicals also react quickly with HNC and HC_3N leading to additional secondary sources of C_2N_2 and C_4N_2. Therefore, secondary nitrogen chemistry, induced by HCN photodissociation, leads to HC_3N and C_2H_3CN formation. It should be noted that as HCN has a long chemical lifetime, it diffuses to low altitude. Since it is not shielded by CH_4 the photodissociation flux of HCN is larger in the stratosphere than in the upper atmosphere leading to efficient CN chemistry at low altitude. HC_3N is photodissociated in the UV leading mainly to H + C_3N with a low fraction of C_2H + CN products. As C_3N reacts quickly with CH_4 (Fournier et al., 2014), its steady state abundance is very low, and the C_3N + C_2H_2 → HC_5N + H and C_3N + C_2H_4 → $C_2H_3C_3N$ + H reactions have low fluxes. Therefore, HC_3N photodissociation does not lead to substantial new chemistry and the CN + HC_3N pathway is only an additional minor C_4N_2 source. HC_3N is lost mainly through reaction with H atoms in the lower atmosphere leading to H_2C_3N. H_2C_3N radicals react mainly with H atom to form excited $C_2H_3CN^{**}$ which can either stabilize or form HCN + C_2H_2 or HC_3N + H_2 products. C_2H_3CN is a key molecule for nitriles chemistry. C_2H_3CN is produced by the CN + C_2H_4 reaction (and in a minor way by the C_2H_3 + HCN reaction). C_2H_3CN is easily photodissociated in the UV leading to H + H_2C_4N (also produced by H + HC_3N reaction), H_2 + HC_3N, C_2H_2 + HCN and C_2H_2 + HNC. Apart from photodissociation, C_2H_3CN is mostly lost through its association with H atoms leading to C_2H_4CN. C_2H_4CN reacts mainly with H atoms producing CH_2CN + CH_3 and C_2H_5CN at low altitude. C_2H_4CN reacts also with CH_3 leading to C_3H_7CN. The H + C_2H_4CN reaction is the main source of CH_2CN (with a contribution of $N(^4S)$ + C_2H_3 between 100 km and 200 km) and the CH_2CN radical lead to CH_3CN production through reaction with H and to C_2H_5CN through reaction with CH_3. As there are no bimolecular exit channels for these two reactions, they are efficient CH_3CN and C_2H_5CN production pathways. The C_2H_3CN + H reaction is indeed the source of CH_3CN in the present model as CH_3CN is not produced by the $N(^2D)$ + C_2H_4 reaction, and it is also the source of C_2H_5CN and C_3H_7CN. As CH_3CN photodissociation

leads to CH_2CN + H (Eden et al., 2003; McElcheran et al., 1958; Moriyama et al., 1998) and C_2H_5CN photodissociation leads to C_2H_4CN + H and CH_2CN + CH_3 and eventually to C_2H_4 + HCN, CH_3CN and C_2H_5CN do not lead to the formation of new species, the ratio between CH_3CN and C_2H_5CN depending on their losses by photodissociation and on the efficiency of H and CH_3 addition reactions. It should be noted that there is a high level of correlation between HC_3N, C_2H_3CN, C_2H_5CN, C_3H_7CN and CH_3CN. The third step of nitrogen chemistry leads to CH_3CN, C_2H_5CN and C_3H_7CN formation (and little C_3H_5CN, HC_5N and $C_2H_3C_3N$).

The neutral nitrogen chemistry in Titan's atmosphere leads mainly to nitriles because once formed, the triple CN bond is not easily broken by photodissociation and it is not very sensitive to chemical attack except from $N(^2D)$ which leads to relatively low loss rates. There are also minor production routes for imine and amine formation.

Appendix A.3. The production of imines and amines

The reactions of $N(^2D)$ with alkanes leads to imine formation (Herron, 1999; Balucani et al., 2009, 2010). However, except for CH_2NH, which is the main product of the $N(^2D)$ + CH_4 and $N(^2D)$ + C_2H_6 reactions, the formation of other imines is weak ($N(^2D)$ + $C_2H_6 \rightarrow CH_3CHNH$ + H has a branching ratio of 12% only (Balucani et al., 2010)) and as imines absorb and photodissociate in the UV (Teslja et al., 2004) the steady state abundances are low. In the stratosphere, the three body association reaction H_2CN + $CH_3 \rightarrow H_2CNCH_3$ has a non-negligible flux but H_2CNCH_3 should absorb in the UV by comparison with CH_2NH (Teslja et al., 2004), probably leading to H_2CN + CH_3 products rather than to H_2CNCH_2 + H (58 kJ/mol more endothermic) and also eventually to HCN/HNC + CH_4. As a result, the steady state abundance of this compound is also low.

In contrast to the ion chemistry of Titan's atmosphere, the neutral nitrogen chemistry leads to low amine abundances. Firstly, amines are very sensitive to photodissociation as they absorb in the 180-220 nm range (Edvardsson et al., 1999; Hubin-Franskin et al., 2002). They lead mainly to N_2 formation through the N + $NH_2 \rightarrow N_2$ + H + H reaction at least in Titan's upper atmosphere. Secondly, amine formation systematically involves NH_2 radicals (NH_2 + H_2CN, C_2H_5, C_2H_3 to form ammonia NH_3 or NH_2 + CH_3 to form methylamine CH_3NH_2). NH_2 is formed, through neutral chemistry, from NH radicals (NH + H_2CN, C_2H_5, C_2H_3) which involves low fluxes as NH reacts mainly in Titan's atmosphere with CH_3 radicals to form CH_2NH. However, as shown by Yelle et al. (2010), CH_2NH is an important source of NH_2 in the upper atmosphere through ionic reactions. Indeed, due to the very high value of its proton affinity (Hunter and Lias, 1998), CH_2NH is easily protonated through reaction with the major cations in Titan's upper atmosphere ($HCNH^+$, CH_5^+, $C_2H_5^+$, HC_3NH^+) (Vuitton et al., 2007; Yelle et al., 2010)). Then electronic recombination of $CH_2NH_2^+$ may lead to CH_2 + NH_2 despite the lack of any information (Yelle et al., 2010). This process therefore also acts as a sink for CH_2NH. The absence of ionic reactions in our model leads to an overestimation of CH_2NH

and an underestimation of NH_3 in upper atmosphere. In the lower atmosphere, cosmic rays are thought to induce a relatively rich nitrogen chemistry with the formation of NH through the $N(^2D)$ + CH_4, $N(^2D,^4S)$ + C_2H_3, N + C_2H_5 and $N(^2D,^4S)$ + H_2CN reactions, and with the formation of NH_2 through the NH + C_2H_3, NH + C_2H_5 and NH + H_2CN reactions, as well as through the reactions CH_2NH + H → CH_3NH/CH_2NH_2 followed by CH_3NH/CH_2NH_2 + H → CH_3 + NH_2. Although the NH and NH_2 production rates increase, their loss rates also increase through the $N(^2D,^4S)$ + NH and $N(^2D,^4S)$ + NH_2 reactions, and through the reactions of NH and NH_2 with alkyls radicals (C_2H_3, C_2H_5, ... abundant in the stratosphere) which should lead to adduct formation at high pressures. The various complex amines and imines are all sensitive to photodissociation, so ultimately, HCN/HNC or N_2 formation occurs.

Appendix A.4. Importance of H atoms reactions

H atom reactions play a critical role in Titan's atmosphere, either for bimolecular reactions (H + CH_2, H + H_2CN, ...) or through three body reactions (H + C_2H_2, C_2H_4, HC_3N, ...) as these represent the main loss processes for most unsaturated hydrocarbons. In particular, the concentration of H atoms is critical for many nitrogen compounds like HNC, HC_3N, CH_2NH, C_4N_2, C_2H_3CN. It is then crucial to determine precisely the H atom concentration throughout the atmosphere of Titan. Its concentration is controlled by its production (mainly through CH_4 and C_2H_2 photodissociation) and loss (mainly from H + C_2H_2 and H + CH_2 reactions with minor contributions from H + C_2H_3, C_2H_4, C_4H_2). Despite the significant body of work for CH_4 and C_2H_2 photodissociations, there are still large uncertainties on their branching ratios. CH_4 photodissociation at Lyman-α (L_α) and 118.2 nm has been recently revisited (Gans et al., 2011) leading to a total production of H atoms at L_α equal to $(55 \pm 17)\%$. Even if methane is mainly photodissociated at L_α, the L_α-140 nm photodissociation range accounts for about 30% of the photolysis rate. There is no measurement of branching ratio for photodissociation above L_α, but considering theoretical works (Mebel et al., 1997) we consider a branching ratio of $(50 \pm 30)\%$ for CH_3 + H production and $(50 \pm 30)\%$ for $^1CH_2$ + H_2 production in the L_α-140 nm range. H atom production from CH_4 is then equal to $(53 \pm 20)\%$ of the total. The case of C_2H_2 photodissociation is even more critical. C_2H_2 photodissociation has been studied since the early 1960's (Stief et al., 1965), leading to a total production of H atoms varying from 6% (Okabe, 1983) to 100% (Läuter et al., 2002; Kovacs et al., 2010). There is definitively no consensus even at 193.3 nm which is the most studied photodissociation wavelength but not the most important one for Titan's atmosphere. In Hébrard et al. (2013), C_2H_2 photodissociation was reconsidered using the latest measurements, which lead exclusively to the formation of C_2H + H at L_α and 193 nm (Läuter et al., 2002; Kovacs et al., 2010). In our present nominal model, we use instead Satyapal and Bersohn (1991); Shin and Michael (1991); Seki and Okabe (1993) to derive photodissociation branching ratios of 30% for C_2H + H and 70% for metastable $C_2H_2^{**}$.

$C_2H_2 + h\nu \rightarrow C_2H + H$, $q_1 = 0.3$

$C_2H_2 + h\nu \rightarrow C_2H_2^{**} \rightarrow C_2H_2$, $q_2 = 0.7$

In the model, $C_2H_2^{**}$ gives back C_2H_2 even if $C_2H_2^{**}$ (supposed to be a triplet state) may react with C_2H_2 (Laufer, 1983; Seki et al., 1986; Seki and Okabe, 1993). There are no obvious reasons to choose one particular branching ratio as there are potential experimental bias in all experiments. Production of C_4H_2 from $C_2H_2^{**} + C_2H_2 \rightarrow C_4H_2 + H_2$ reactions with a rate constant estimated around 3.0×10^{-13} to 5.0×10^{-13} (Laufer, 1983; Seki et al., 1986; Seki and Okabe, 1993) seems established and may explain the C_4H_2 "tongue distribution" observed near Titan's North pole by Teanby et al. (2008). However this reaction is likely to be not very efficient as $C_2H_2^{**}$ will be efficiently quenched by N_2 (Seki and Okabe, 1993). Nevertheless, we have tested the influence of the photolysis of C_2H_2 using $q_1 = 1.0$ and $q_2 = 0.0$. The mole fractions of the main C_2H_x and C_3H_x compounds do not differ significantly from the nominal results since their abundance profiles lie within the error bars of the models, but the general agreement is rather less good. In particular, a 100% yield for H production from C_2H_2 photodissociation increases notably the CH_3 abundance due to the following cycle

$C_2H_2 + h\nu \rightarrow C_2H + H$

$C_2H + CH_4 \rightarrow C_2H_2 + CH_3$

leading to an overproduction of C_2H_6 and C_3H_8 in the lower atmosphere through addition reactions with CH_3. For uncertainty propagation we consider an uncertainty of 20% for all photodissociations, a specific study of the large uncertainties on this branching ratio is beyond the scope of this work but should be performed in the future to pinpoint the key photolysis processes.

Among the main H atom loss processes, the $H + CH_2$ reaction is relatively well known despite being an atom + radical reaction (Fulle and Hippler, 1997; Böhland et al., 1987; Boullart and Peeters, 1992) and we consider an uncertainty of 50% on the rate constant at low temperature. The other main H loss is the $H + C_2H_2 \rightarrow C_2H_3$ reaction which has been the subject of various theoretical and experimental studies. As already noted by Moses et al. (2005) the Baulch et al. (2005, 1994) expressions are not valid at low temperature, so that other modeling studies (Lavvas et al., 2008a,b; Krasnopolsky, 2009, 2012) have tended to underestimate the rate of this reaction. Recently, Vuitton et al. (2012) extended previous theoretical work of Miller and Klippenstein (2004) to the low temperatures relevant to Titan leading to rate constants valid down to 50 K. We use this latter work with slightly modified k_0 and F_c factors to fit the experimental data from Payne and Stief (1976) and Keil et al. (1976). Our expressions for k_0 and k_∞ are indeed very close to the Model C of Moses et al. (2005) and notably larger than Lavvas et al. (2008a,b) and Krasnopolsky (2009, 2012) leading to smaller H atom abundances in the stratosphere. The H atom heterogeneous recombination scheme proposed by Sekine et al. (2008a,b) was not included in our model but may substantially reduce the H atom concentration.

Appendix B. Photolysis processes of some selected nitrile compounds

In this section, we present a short review of the available data concerning the photolysis of several nitriles (see Table B.5). References for the cross sections and quantum yields we use in the present model are given and we discuss how we have completed the missing data when needed.

Appendix B.1. CH_3CN

The absorption spectrum has been recorded by Eden et al. (2003) between 115 nm and 320 nm, the low absorption above 190 nm, attributed to the first triplet excited states (Rianda et al., 1984), is ambiguous and is neglected here. McElcheran et al. (1958) found indirect evidence for both CH_2CN + H and CH_3 + CN formation in the 184.9 nm photodissociation of CH_3CN. Moriyama et al. (1998) studied the CH_3CN photodissociation at 121.56 nm showing that both H atoms and $CN(B^2\Sigma^+)$ were produced and also that the Rydberg state formed by the photoabsorption was converted to the vibrationally excited molecule by a fast intramolecular process prior to the statistical elimination of the H atom. The isotope effect on this channel is consistent with statistical dissociation. Considering that photodissociation occurs on a vibrationally excited ground state, both H + CH_2CN and CH_3 + CN channels will compete, although the H atom production channel may be favored (more exothermic channel) as noted by Schwell et al. (2008).

Appendix B.2. HC_3N

The HC_3N photodissociation has been studied between 185 and 254 nm, with the main channel suspected to be metastable HC_3N^{**} (Clarke and Ferris, 1995; Seki et al., 1996; Halpern et al., 1988) with a quantum yield equal to 70% at 193 nm (Seki et al., 1996). At 193 nm, H + C_3N products represent the other 30% quantum yield, with the C_2H + CN products being very minor (Seki et al., 1996). Using theoretical work (Luo et al., 2008; Silva et al., 2009) we can assume that H + C_3N is always the main bimolecular exit channel, although the C_2H + CN channel may not be negligible at high energy (below 160 nm).

Appendix B.3. C_2H_3CN

C_2H_3CN exhibits a strong absorption in the UV range (Eden et al., 2003) so it should be easily photodissociated in Titan's atmosphere. There have been various branching ratio measurements, mostly at 193 nm (Fahr and Laufer, 1992; North and Hall, 1996; Blank et al., 1998; Wilhelm et al., 2009), with an early study at 213.9 nm (Gandini and Hackett, 1978). Among the various products, CN production is always very minor and is neglected here. The various studies lead only to qualitative results, except for CN and for the work of (Gandini and Hackett, 1978) which leads to quantitative branching ratios, equal to 50% for C_2H_4 + HCN and 31% for HC_3N + H_2 after photodissociation at 213.9 nm. In the same study the authors also performed preliminary measurement at 206.5 nm showing a drop in the HC_3N + H_2 quantum yield

suggesting the onset of a competitive radical dissociation channel that may attributed to H_2C_3N + H from theoretical calculations (Derecskei-Kovacs and North, 1999; Homayoon et al., 2011). Wilhelm et al. (2009) performed spectral modeling of the IR emission from the products of C_2H_3CN photodissociation at 193 nm detecting HCN, HNC, C_2H_2 and probably H_2C_3N but not HC_3N. The ratio HCN/HNC was found to be equal to 3.34 in good agreement with the theoretical calculations of Homayoon et al. (2011), but not with the calculated value of 126 from Rice-Ramsperger-Kassel-Marcus analysis by Derecskei-Kovacs and North (1999). The lack of cyanoacetylene detection is either because it is formed relatively cold (no IR emission) or it is produced at only a minor level with respect to acetylene, hydrogen cyanide, and hydrogen isocyanide products. Nevertheless, the study of Blank et al. (1998) has clearly shown the presence of cyanoacetylene as a photofragment so that it is more likely that a four-center transition state dominates the cyanoacetylene elimination channel, in contrast to the observation that a three-center transition state dominates the acetylene elimination channel. A recent study of C_2H_3CN photodissociation at 193 nm using Chirped-Pulse millimetre-Wave (Prozument et al., 2013) absorption spectroscopy clearly shows the production of HCN and HNC but without quantifying the relative yields of these two species. The branching ratios used in the present work are estimated, taking into account the various experimental studies. It should be noted that C_2H_3CN photodissociation may contribute to a non-negligible production of HNC.

Appendix B.4. C_2H_5CN

The absorption spectrum of C_2H_5CN has been recorded between 115 nm and 150 nm (Kanda et al., 1999). The absorption above 190 nm, attributed to the first triplet excited state (Rianda et al., 1984) is neglected here but may play a crucial role. The branching ratios are highly speculative; the CH_3 + CH_2CN channel may be favored.

Table B.5: Quantum yields (in %) for photolysis of CH_3CN, HC_3N, C_2H_3CN, C_2H_5CN as a function of wavelength.

$CH_3CN + h\nu \rightarrow$	CH_3 + CN		308-235 nm 0	< 235 nm 20
	CH_2CN + H		100	80
	CH_2 + HCN		0	0
		220-185 nm	185-160 nm	< 160 nm
$HC_3N + h\nu \rightarrow$	H + C_3N	30	30	30
	C_2H + CN	0	25	25
	C_2 + HCN	0	0	10
	HC_3N**	70	45	35
$C_2H_3CN + h\nu \rightarrow$	$HC_3N + H_2$		261-240 nm 0	< 240 nm 20
	$HCN + C_2H_2$		0	60
	$HNC + C_2H_2$		0	10
	$H_2C_3N + H + H$		100	10
	C_2H_3 + CN		0	0
$C_2H_5CN + h\nu \rightarrow$	C_2H_5 + CN		347-280 nm 0	< 280 nm 0
	$CH_3 + CH_2CN$		100	20
	C_2H_4CN		0	0
	C_2H_4 + HCN		0	40
	$C_2H_3CN + H_2$		0	40

Appendix C. List of reactions

Table C.6: Neutral-neutral reactions.
$k = \alpha \times (T/300)^{\beta} \times \exp(-\gamma/T)$ in cm^3 $molecule^{-1}$ s^{-1} or cm^6 $molecule^{-2}$ s^{-1}, k comprised between $k \times [F(300\ K) \times \exp(g \times |1/T - 1/300|)]$ and $k/[F(300\ K) \times \exp(g \times |1/T - 1/300|)]$. $k_{\rm adduct} = (k_0[M]F + k_r)k_\infty/k_0[M] + k_\infty$ with $\log(F) = \log(F_c)/1 + \left[\log(k_0[M] + k_{capture})/N\right]^2$, $F_c = 0.60$ and $N = 1$. Please refer to Hébrard et al. [2013] for details about our semi-empirical model.

Reactions		Rate coefficients	$F(300\ K)$	g	References
H + H	$\rightarrow H_2$	$k_0 = 9.14 \times 10^{-33} \times (T/300)^{-0.6}$	3.16	100	k_0 from Tsang and Hampson [1986],
		$k_\infty = 1.0 \times 10^{-10}$	2	100	k_∞ from capture rate theory
		$k_r = 0$	30	0	
H + CH	$\rightarrow C + H_2$	$1.24 \times 10^{-10} \times (T/300)^{0.26}$	3	14	KIDA
H + $^1CH_2$	$\rightarrow CH + H_2$	$2.2 \times 10^{-10} \times (T/300)^{0.32}$	1.5	7	Taken equal to H + $^3CH_2$
H + $^3CH_2$	$\rightarrow CH + H_2$	$2.2 \times 10^{-10} \times (T/300)^{0.32}$	1.5	7	Fulle and Hippler [1997], Böhland et al. [1987]
H + $^3CH_2$	$\rightarrow CH_3$	$k_0 = 3.1 \times 10^{-30} \times \exp(457/T)$	2	100	Gladstone [1996]
		$k_\infty = 1.5 \times 10^{-10}$	2	100	
		$k_r = 0$	30	0	
H + CH_3	$\rightarrow {}^3CH_2 + H_2$	$1.0 \times 10^{-10} \times \exp(-7600/T)$	10	100	Baulch et al. [1992]
H + CH_3	$\rightarrow CH_4$	$k_0 = 8.9 \times 10^{-29} \times (T/300)^{-1.8} \times \exp(-31.8/T)$	2	0	Brouard et al. [1989], Smith [2003], Vuitton et
		$k_\infty = 3.2 \times 10^{-10} \times (T/300)^{0.133} \times \exp(-2.54/T)$	1.4	0	al. [2012], Hébrard et al. [2013]
		$k_r = 1.31 \times 10^{-16} \times (T/300)^{-1.29} \times \exp(-19.6/T)$	10	0	
H + CH_4	$\rightarrow CH_3 + H_2$	$5.89 \times 10^{-13} \times (T/300)^3 \times \exp(-4040/T)$	1.58	100	Baulch et al. [1992]
H + C_2H	$\rightarrow C_2H_2$	$k_0 = 2.4 \times 10^{-28} \times (T/300)^{-1.8}$	10	0	k_∞ from Harding et al. [2005], Hébrard et al.
		$k_\infty = 2.3 \times 10^{-10} \times (T/300)^{0.32}$	2	0	[2013]
		$k_r = 2.1 \times 10^{-16} \times (T/300)^{-1.5}$	30	0	
H + C_2H_2	$\rightarrow C_2H + H_2$	$1.0 \times 10^{-10} \times \exp(-11200/T)$	5	100	Tsang and Hampson [1986]
H + C_2H_2	$\rightarrow C_2H_3$	$k_0 = 2.0 \times 10^{-30} \times (T/300)^{-1.07} \times \exp(-83.8/T)$	3	0	Vuitton et al. [2012] with smaller k_0 to fit the experimental data from Payne and Stief [1976] and Keil et al. [1976]. $Fc = 0.24$
		$k_\infty = 1.17 \times 10^{-13} \times (T/300)^{8.41} \times \exp(359/T)$	1.6	0	
		$k_r = 0$	10	0	
H + C_2H_3	$\rightarrow C_2H_2 + H_2$	6.0×10^{-11}	1.6	0	Heinemann et al. [1988], Monks et al. [1995]
H + C_2H_3	$\rightarrow C_2H_4$	$k_0 = 3.47 \times 10^{-27} \times (T/300)^{-1.3}$	4	0	Monks et al. [1995],
		$k_\infty = 1.0 \times 10^{-10}$	2	0	Klippenstein and Harding [1999]
		$k_r = 0$	30	0	
H + C_2H_4	$\rightarrow C_2H_5$	$k_0 = 1.0 \times 10^{-29} \times (T/300)^{-1.51} \times \exp(-72.9/T)$	3	0	Vuitton et al. [2012], Michael et al. [1973] with k_0 scaled for $F_c = 0.64$
		$k_\infty = 6.07 \times 10^{-13} \times (T/300)^{5.31} \times \exp(174/T)$	1.6	0	
		$k_r = 0$	10	0	
H + C_2H_5	$\rightarrow C_2H_4 + H_2$	3.0×10^{-12}	2	0	Camilleri et al. [1974]
H + C_2H_5	$\rightarrow C_2H_6$	$k_0 = 2.0 \times 10^{-28} \times (T/300)^{-1.5}$	10	0	Harding et al. [2005], Baulch et al. [2005],
		$k_\infty = 1.07 \times 10^{-10}$	1.6	0	Pimentel et al. [2004]
		$k_r = 0$	1	0	
H + C_2H_5	$\rightarrow CH_3 + CH_3$	$k = k_\infty - k_{\rm adduct}$	0	0	
H + C_2H_6	$\rightarrow C_2H_5 + H_2$	$1.22 \times 10^{-11} \times (T/300)^{1.5} \times \exp(-3720/T)$	2	100	Baulch et al. [1992]
H + C_3	$\rightarrow c\text{-}C_3H$	$k_0 = 5.0 \times 10^{-29} \times (T/300)^{-1.8}$	10	0	Hébrard et al. [2013]
		$k_\infty = 3.0 \times 10^{-11}$	3	0	
		$k_r = 5.0 \times 10^{-17} \times (T/300)^{-1.5}$	30	0	
H + C_3	$\rightarrow l\text{-}C_3H$	$k_0 = 5.0 \times 10^{-29} \times (T/300)^{-1.8}$	10	0	Hébrard et al. [2013]
		$k_\infty = 3.0 \times 10^{-11}$	3	0	
		$k_r = 5.0 \times 10^{-17} \times (T/300)^{-1.5}$	30	0	
H + $l\text{-}C_3H$	$\rightarrow c\text{-}C_3H_2$	$k_0 = 1.0 \times 10^{-28} \times (T/300)^{-1.8}$	30	0	Hébrard et al. [2013]
		$k_\infty = 2.0 \times 10^{-10}$	3	0	
		$k_r = 1.0 \times 10^{-16} \times (T/300)^{-1.5}$	100	0	
H + $l\text{-}C_3H$	$\rightarrow C_3 + H_2$	$k = 0.8 \times (k_\infty - k_{\rm adduct})$	0	0	Hébrard et al. [2013]
H + $l\text{-}C_3H$	$\rightarrow c\text{-}C_3H + H$	$k = 0.2 \times (k_\infty - k_{\rm adduct})$	0	0	Hébrard et al. [2013]
H + $c\text{-}C_3H$	$\rightarrow c\text{-}C_3H_2$	$k_0 = 1.0 \times 10^{-28} \times (T/300)^{-1.8}$	30	0	Hébrard et al. [2013]
		$k_\infty = 2.0 \times 10^{-10}$	3	0	
		$k_r = 1.0 \times 10^{-16} \times (T/300)^{-1.5}$	100	0	
H + $c\text{-}C_3H$	$\rightarrow C_3 + H_2$	$k = k_\infty - k_{\rm adduct}$	0	0	Hébrard et al. [2013]
H + $c\text{-}C_3H_2$	$\rightarrow C_3H_3$	$k_0 = 8.1 \times 10^{-26} \times (T/300)^{-1.8}$	10	0	Hébrard et al. [2013]
		$k_\infty = 2.0 \times 10^{-10}$	3	0	
		$k_r = 1.5 \times 10^{-14} \times (T/300)^{-1.5}$	30	0	
H + $l\text{-}C_3H_2$	$\rightarrow C_3H_3$	$k_0 = 1.0 \times 10^{-28} \times (T/300)^{-1.8}$	30	0	Hébrard et al. [2013]
		$k_\infty = 4.0 \times 10^{-10} \times (T/300)^{0.17}$	3	0	
		$k_r = 1.0 \times 10^{-16} \times (T/300)^{-1.5}$	100	0	
H + $l\text{-}C_3H_2$	$\rightarrow c\text{-}C_3H_2 + H$	$k = k_\infty - k_{\rm adduct}$	0	0	Hébrard et al. [2013]
H + $t\text{-}C_3H_2$	$\rightarrow C_3H_3$	$k_0 = 1.0 \times 10^{-28} \times (T/300)^{-1.8}$	30	0	Hébrard et al. [2013]
		$k_\infty = 4.42 \times 10^{-10} \times (T/300)^{0.22} \times \exp(-43.7/T)$	2	0	
		$k_r = 1.0 \times 10^{-16} \times (T/300)^{-1.5}$	100	0	
H + $t\text{-}C_3H_2$	$\rightarrow c\text{-}C_3H_2 + H$	$k = k_\infty - k_{\rm adduct}$	0	0	Hébrard et al. [2013]
H + C_3H_3	$\rightarrow CH_3C_2H$	$k_0 = 3.2 \times 10^{-25} \times (T/300)^{-1.8}$	10	0	Hébrard et al. [2013]

Reactions		Rate coefficients	$F(300\ K)$	g	References
		$k_\infty = 2.3 \times 10^{-10} \times (T/300)^{0.15} \times \exp(46.3/T)$	2	0	
		$k_r = 4 \times 10^{-14} \times (T/300)^{-1.5}$	30	0	
$H + C_3H_3$	$\rightarrow CH_2CCH_2$	$k_0 = 8 \times 10^{-26} \times (T/300)^{-1.8}$	10	0	Hébrard et al. [2013]
		$k_\infty = 6.0 \times 10^{-11} \times (T/300)^{0.15} \times \exp(46.3/T)$	2	0	
		$k_r = 1.0 \times 10^{-14} \times (T/300)^{-1.5}$	30	0	
$H + CH_3C_2H$	$\rightarrow C_3H_5$	$k_0 = 1.0 \times 10^{-25} \times (T/300)^{-2.48} \times \exp(-191/T)$	4	0	Whytock et al. [1976], Faravelli et al. [2000],
		$k_\infty = 6.0 \times 10^{-11} \times \exp(-1233/T)$	1.4	50	Miller et al. [2008], Vuitton et al. [2012],
		$k_r = 3.9 \times 10^{-15} \times (T/300)^{2.63} \times \exp(-63/T)$	10	0	Hébrard et al. [2013]
$H + CH_2CCH_2$	$\rightarrow C_3H_5$	$k_0 = 1.0 \times 10^{-25} \times (T/300)^{-2.48} \times \exp(-191/T)$	4	0	Wagner and Zellner [1972], Aleksandrov et al. [1980], Miller et al. [2008], Vuitton et al.
		$k_\infty = 1.4 \times 10^{-11} \times \exp(-1010/T)$	2	100	[2012], Hébrard et al. [2013]
		$k_r = 3.9 \times 10^{-15} \times (T/300)^{2.63} \times \exp(-63/T)$	10	0	
$H + C_3H_5$	$\rightarrow CH_2CCH_2 + H_2$	1.5×10^{-11}	3	0	Hanning-Lee and Pilling [1992], Harding et al. [2007], Hébrard et al. [2013]
$H + C_3H_5$	$\rightarrow CH_3C_2H + H_2$	1.5×10^{-11}	3	0	Hanning-Lee and Pilling [1992], Harding et al. [2007], Hébrard et al. [2013]
$H + C_3H_5$	$\rightarrow C_3H_6$	$k_0 = 2.2 \times 10^{-23} \times (T/300)^{-1.8}$	10	0	Hanning-Lee and Pilling [1992], Harding et al.
		$k_\infty = 2.3 \times 10^{-10} \times (T/300)^{0.18} \times \exp(63/T)$	1.6	0	[2007], Hébrard et al. [2013]
		$k_r = 9.2 \times 10^{-13} \times (T/300)^{-1.5}$	30	0	
$H + C_3H_6$	$\rightarrow CH_3 + C_2H_4$	$2.19 \times 10^{-11} \times \exp(-1640/T)$	2	21	Tsang [1991], Seakins et al. [1993], Hébrard et al. [2013]
$H + C_3H_6$	$\rightarrow C_3H_5 + H_2$	$4.33 \times 10^{-13} \times (T/300)^{2.5} \times \exp(-1250/T)$	1.8	21	Tsang [1991], Seakins et al. [1993], Hébrard et al. [2013]
$H + C_3H_6$	$\rightarrow C_3H_7$	$k_0 = 3.0 \times 10^{-25} \times (T/300)^{-2.48} \times \exp(-191/T)$	10	100	Tsang [1991], Seakins et al. [1993],
		$k_\infty = 7.02 \times 10^{-12} \times (T/300)^{1.16} \times \exp(-440/T)$	1.6	0	Hébrard et al. [2013]
		$k_r = 0$	30	0	
$H + C_3H_7$	$\rightarrow C_3H_6 + H_2$	3.0×10^{-12}	3	0	Hébrard et al. [2013]
$H + C_3H_7$	$\rightarrow C_3H_8$	$k_0 = 6.11 \times 10^{-28} \times (T/300)^{-2} \times \exp(-1040/T)$	10	21	Hébrard et al. [2013]
		$k_\infty = 9.68 \times 10^{-11} \times (T/300)^{0.22}$	2	0	
		$k_r = 0$	1	0	
$H + C_3H_7$	$\rightarrow C_2H_5 + CH_3$	$k = k_\infty - k_{\text{adduct}}$	0	0	Hébrard et al. [2013]
$H + C_3H_8$	$\rightarrow C_3H_7 + H_2$	$4.31 \times 10^{-12} \times (T/300)^{2.54} \times \exp(-3400/T)$	3	100	Tsang [1988]
$H + C_4H$	$\rightarrow C_4H_2$	$k_0 = 1.1 \times 10^{-22} \times (T/300)^{-1.8}$	10	0	Harding et al. [2005],
		$k_\infty = 2.3 \times 10^{-10} \times (T/300)^{0.32}$	2	0	Hébrard et al. [2013]
		$k_r = 3.0 \times 10^{-12} \times (T/300)^{-1.5}$	30	0	
$H + C_4H_2$	$\rightarrow C_4H_3$	$k_0 = 3.0 \times 10^{-25} \times (T/300)^{-2.93} \times \exp(-176/T)$	10	0	k_0 from Vuitton et al. [2012], k_∞ in
		$k_\infty = 1.6 \times 10^{-12} \times (T/300)^{5.55} \times \exp(153/T)$	2	0	agreement with Nava et al. [1986]
		$k_r = 0$	30	0	
$H + C_4H_3$	$\rightarrow C_4H_2 + H_2$	3.0×10^{-11}	3	0	By comparison with $H + C_2H_3$
$H + C_4H_3$	$\rightarrow C_4H_4$	$k_0 = 1.0 \times 10^{-25} \times (T/300)^{-3.97}$	10	0	Ghibaudi and Colussi [1988], Kiefer and
		$k_\infty = 1.3 \times 10^{-10} \times \exp(14/T)$	2	0	Mitchell [1988], Cremer et al. [2006], Vuitton
		$k_r = 0$	1	0	et al. [2012] taking into account the bimolecular exit channel
$H + C_4H_3$	$\rightarrow C_2H_2 + C_2H_2$	$k = 0.1 \times (k_\infty - k_{\text{adduct}})$	0	0	Ghibaudi and Colussi [1988], Kiefer and Mitchell [1988], Cremer et al. [2006]
$H + C_4H_4$	$\rightarrow C_4H_5$	$k_0 = 3.0 \times 10^{-25} \times (T/300)^{-2.93} \times \exp(-176/T)$	10	0	Schwanebeck and Warnatz [1975]
		$k_\infty = 3.3 \times 10^{-12}$	2	100	
		$k_r = 0$	30	0	
$H + C_4H_5$	$\rightarrow C_4H_4 + H_2$	3.0×10^{-11}	3	0	By comparison with $H + C_2H_3$
$H + C_4H_5$	$\rightarrow C_4H_6$	$k_0 = 1.0 \times 10^{-26} \times (T/300)^{-4}$	10	0	Mu et al. [2004], Newby et al. [2007], Lee et
		$k_\infty = 1.3 \times 10^{-10}$	2	0	al. [2003], relatively low k_0 due to bimolecular
		$k_r = 0$	1	0	exit channels
$H + C_4H_5$	$\rightarrow CH_3 + C_3H_3$	$k = 0.8 \times (k_\infty - k_{\text{adduct}})$	0	0	
$H + C_4H_5$	$\rightarrow C_2H_2 + C_2H_4$	$k = 0.2 \times (k_\infty - k_{\text{adduct}})$	0	0	
$H + C_4H_6$	$\rightarrow C_4H_5 + H_2$	$5.69 \times 10^{-12} \times (T/300)^{0.7} \times \exp(-3020/T)$	2	100	Weissman and Benson [1988]
$H + C_4H_6$	$\rightarrow C_4H_7$	$k_0 = 1.4 \times 10^{-24} \times (T/300)^{2.48} \times \exp(-191/T)$	4	100	$k_0 = 10 \times k_0(H + C_3H_4)$
		$k_\infty = 7.9 \times 10^{-12}$	1.4	100	k_∞ from Oka and Cvetanovic [1979]
		$k_r = 0$	30	0	
$H + C_4H_7$	$\rightarrow C_4H_6 + H_2$	1.0×10^{-11}	3	0	$k(H + C_3H_5)/3$ considering the steric hindrance
$H + C_4H_7$	$\rightarrow C_4H_8$	$k_0 = 1.0 \times 10^{-26}$	10	0	Harding et al. [2005], [2007], relatively low k_0
		$k_\infty = 1.0 \times 10^{-10}$	3	0	due to bimolecular exit channel
		$k_r = 0$	1	0	
$H + C_4H_7$	$\rightarrow CH_3 + C_3H_5$	$k = k_\infty - k_{\text{adduct}}$	0	0	
$H + C_4H_8$	$\rightarrow C_4H_9$	$k_0 = 1.4 \times 10^{-25} \times (T/300)^{2.48} \times \exp(-191/T)$	10	100	Harris and Pitts [1982], Kyogoku et al. [1983],
		$k_\infty = 3.97 \times 10^{-11} \times \exp(-1060/T)$	1.4	100	This work
		$k_r = 0$	30	0	
$H + C_4H_9$	$\rightarrow C_4H_8 + H_2$	3.0×10^{-12}	3	0	Tsang [1990]
$H + C_4H_9$	$\rightarrow C_4H_{10}$	$k_0 = 1.0 \times 10^{-25}$	10	0	Harding et al. [2005], relatively low k_0 due to
		$k_\infty = 1.0 \times 10^{-10}$	1.4	0	bimolecular exit channels
		$k_r = 0$	1	0	
$H + C_4H_9$	$\rightarrow CH_3 + C_3H_7$	$k = 0.5 \times (k_\infty - k_{\text{adduct}})$	0	0	
$H + C_4H_9$	$\rightarrow C_2H_5 + C_2H_5$	$k = 0.5 \times (k_\infty - k_{\text{adduct}})$	0	0	

Reactions		Rate coefficients	$F(300\ K)$	g	References
$H + C_6H$	$\rightarrow C_6H_2$	$k_0 = 2.64\times10^{-26}\times(T/300)^{-3.1}\times\exp(-721/T)$	2	100	Kiefer and von Drasek [1990]
		$k_\infty = 3.0\times10^{-10}$	2	100	
		$k_r = 0$	30	0	
$H + C_6H_2$	$\rightarrow C_6H_3$	$k_0 = 3.0\times10^{-24}\times(T/300)^{-2.93}\times\exp(-176/T)$	10	0	$k_0 = 10\times k_0(H + C_4H_2)$
		$k_\infty = 1.6\times10^{-12}\times(T/300)^{5.55}\times\exp(153/T)$	2	0	$k_\infty = k_\infty(H + C_4H_2)$
		$k_r = 5.6\times10^{-12}\times(T/300)^{2.75}\times\exp(-50.3/T)$	30	0	
$H + C_6H_3$	$\rightarrow C_6H_2 + H_2$	1.0×10^{-12}	10	0	We consider mostly addition rather than H abstraction considering the size of the species.
$H + C_6H_3$	$\rightarrow C_6H_4$	$k_0 = 1.0\times10^{-23}$	3	0	k_0 from Hébrard et al. [2013], k_∞ from
		$k_\infty = 1.4\times10^{-10}$	3	0	capture rate theory, see also Moskaleva et al.
		$k_r = 1.2\times10^{-12}$	10	0	[1999], Deng et al. [1998]
$H + C_6H_3$	$\rightarrow C_2H_2 + C_4H_2$	$k = k_\infty - k_{adduct}$	0	0	
$H + C_6H_4$	$\rightarrow C_6H_5$	$k_0 = 1.0\times10^{-25}$	100	0	Estimated using Madden et al. [1997]
		$k_\infty = 1.0\times10^{-11}$	10	0	
		$k_r = 0$	30	0	
$H + C_6H_5$	$\rightarrow C_6H_6$	$k_0 = 4\times10^{-18}\times(T/300)^{-2.54}\times\exp(-122/T)$	10	0	Vuitton et al. [2012]
		$k_\infty = 1.4\times10^{-10}\times\exp(14/T)$	2	0	
		$k_r = 1.4\times10^{-10}\times\exp(14/T)$	30	0	
$H + C_6H_6$	$\rightarrow C_6H_5 + H_2$	$4.15\times10^{-10}\times\exp(-8050/T)$	2	100	Wang and Frenklach [1997]
$H + C_6H_6$	$\rightarrow C_6H_7$	$k_0 = 3.3\times10^{-30}\times\exp(-740/T)$	10	100	By comparison with $H + C_2H_2$
		$k_\infty = 5.27\times10^{-11}\times\exp(-1600/T)$	2	100	Mebel et al. [1997]
		$k_r = 0$	30	0	
$C + H_2$	$\rightarrow {}^3CH_2$	$k_0 = 7.0\times10^{-32}\times(T/300)^{-1.5}$	2	100	Husain and Young [1975], Harding et al. [1993]
		$k_\infty = 2.06\times10^{-11}\times\exp(-57/T)$	3	100	
		$k_r = 0$	30	0	
$C + C$	$\rightarrow C_2$	$k_0 = 5.3\times10^{-31}\times(T/300)^{-1.6}$	2	100	Slack et al. [1976], Martinotti et al. [1968]
		$k_\infty = 2.16\times10^{-11}$	2	100	
		$k_r = 0$	30	0	
$C + C_2H_2$	$\rightarrow C_3 + H_2$	$2.6\times10^{-10}\times(T/300)^{-0.07}$	1.2	0.9	Bergeat and Loison [2001], Costes et al. [2009], Mebel et al. [2007]
$C + C_2H_2$	$\rightarrow c\text{-}C_3H + H$	$4.1\times10^{-11}\times(T/300)^{-0.39}\times\exp(-2/T)$	1.4	0.8	Bergeat and Loison [2001], Costes et al. [2009], Mebel et al. [2007]
$C + C_2H_2$	$\rightarrow l\text{-}C_3H + H$	$7.8\times10^{-12}\times(T/300)^{1.08}$	1.8	2	Bergeat and Loison [2001], Costes et al. [2009], Mebel et al. [2007]
$C + C_2H_3$	$\rightarrow c\text{-}C_3H_2 + H$	4.0×10^{-11}	3	0	Nguyen et al. [2001a], Nguyen et al. [2001b], Crider et al. [2009], Wilson et al. [2012]
$C + C_2H_3$	$\rightarrow l\text{-}C_3H_2 + H$	2.0×10^{-11}	3	0	Nguyen et al. [2001a], Nguyen et al. [2001b], Crider et al. [2009], Wilson et al. [2012]
$C + C_2H_3$	$\rightarrow t\text{-}C_3H_2 + H$	3.0×10^{-11}	3	0	Nguyen et al. [2001a], Nguyen et al. [2001b], Crider et al. [2009], Wilson et al. [2012]
$C + C_2H_3$	$\rightarrow c\text{-}C_3H + H_2$	1.0×10^{-11}	3	0	Nguyen et al. [2001a], Nguyen et al. [2001b], Crider et al. [2009], Wilson et al. [2012]
$C + C_2H_3$	$\rightarrow l\text{-}C_3H + H_2$	1.0×10^{-11}	3	0	Nguyen et al. [2001a], Nguyen et al. [2001b], Crider et al. [2009], Wilson et al. [2012]
$C + C_2H_4$	$\rightarrow C_3H_3 + H$	$2.1\times10^{-10}\times(T/300)^{-0.11}$	1.4	0	Chastaing et al. [1999], Chastaing et al. [2001], Bergeat and Loison [2001], Haider and Husain [1993a], Haider and Husain [1993b]
$C + C_2H_4$	$\rightarrow C_2H_2 + {}^3CH_2$	$2.0\times10^{-11}\times(T/300)^{-0.11}$	2	0	Chastaing et al. [1999], Chastaing et al. [2001], Bergeat and Loison [2001], Haider and Husain [1993a], Haider and Husain [1993b]
$C + c\text{-}C_3H_2$	$\rightarrow C_4H + H$	2.0×10^{-10}	3	0	Georgievskii and Klippenstein [2005] considering no barrier
$C + t\text{-}C_3H_2$	$\rightarrow C_4H + H$	$2.0\times10^{-11}\times(T/300)^{-0.54}$	3	0	Georgievskii and Klippenstein [2005] considering no barrier
$C + l\text{-}C_3H_2$	$\rightarrow C_4H + H$	2.0×10^{-10}	3	0	Georgievskii and Klippenstein [2005] considering no barrier
$C + CH_3C_2H$	$\rightarrow C_4H_3 + H$	$2.67\times10^{-10}\times(T/300)^{-0.11}$	1.4	0	Chastaing et al. [2000], Loison et al. [2004]
$C + CH_2CCH_2$	$\rightarrow C_4H_3 + H$	$3.5\times10^{-10}\times(T/300)^{-0.01}$	1.4	0	Chastaing et al. [2000], Loison et al. [2004]
$C + C_3H_6$	$\rightarrow C_4H_5 + H$	$1.4\times10^{-10}\times(T/300)^{-0.08}$	1.6	0	Chastaing et al. [1999], Loison and Bergeat [2004]
$C + C_3H_6$	$\rightarrow C_3H_3 + CH_3$	$1.4\times10^{-10}\times(T/300)^{-0.08}$	1.6	0	Chastaing et al. [1999], Loison and Bergeat [2004]
$C + C_4H_2$	$\rightarrow C_5H + H$	3.0×10^{-10}	2	0	Loison et al. [2014]
$C + C_4H_4$	$\rightarrow C_5H_3 + H$	3.0×10^{-10}	2	0	Loison et al. [2014]
$C + C_4H_6$	$\rightarrow C_5H_5 + H$	3.0×10^{-10}	1.4	21	Husain and Ioannou [1997], Chastaing et al. [2001]
$C + C_4H_8$	$\rightarrow C_5H_7 + H$	3.0×10^{-10}	1.4	21	Loison et al. [2014]
$C + C_6H_4$	$\rightarrow C_7H_3 + H$	3.0×10^{-10}	3	0	Loison et al. [2014]
$C + C_6H_6$	$\rightarrow C_7H_5 + H$	3.0×10^{-10}	3	0	Bergeat and Loison [2001], Bettinger et al. [2000]
$CH + H_2$	$\rightarrow {}^3CH_2 + H$	$3.1\times10^{-10}\times\exp(-1650/T)$	1.3	100	Brownsword et al. [1997]
$CH + H_2$	$\rightarrow CH_3$	$k_0 = 6.2\times10^{-30}\times(T/300)^{-1.6}$	1.4	100	Brownsword et al. [1997], Fulle and Hippler [1997]
		$k_\infty = 1.6\times10^{-10}\times(T/300)^{-0.08}$	1.4	21	
		$k_r = 0$	30	0	

Reactions		Rate coefficients	$F(300\ K)$	g	References
CH + CH	$\rightarrow C_2H + H$	2.0×10^{-10}	2	0	Shen and Pritchard [1991], Dean and Hanson [1992], Bergeat et al. [1999]
CH + CH	$\rightarrow {}^3CH_2 + C$	2.0×10^{-11}	3	0	Shen and Pritchard [1991], Dean and Hanson [1992], Bergeat et al. [1999]
CH + $^3CH_2$	$\rightarrow C_2H_2 + H$	2.0×10^{-10}	3	0	Georgievskii and Klippenstein [2005] considering no barrier
CH + CH_3	$\rightarrow C_2H_3 + H$	1.0×10^{-11}	3	0	Satyapal et al. [1990], Chang et al. [1998b], Georgievskii and Klippenstein [2005]
CH + CH_3	$\rightarrow C_2H_2 + H + H$	1.0×10^{-10}	3	0	Satyapal et al. [1990], Chang et al. [1998b], Georgievskii and Klippenstein [2005]
CH + CH_4	$\rightarrow C_2H_4 + H$	$1.05 \times 10^{-10} \times (T/300)^{-1.04} \times \exp(-36.1/T)$	1.3	4.45	KIDA
CH + C_2H_2	$\rightarrow c{-}C_3H_2 + H$	$1.3 \times 10^{-10} \times (T/300)^{-0.233} \times \exp(-16/T)$	1.6	7	Butler et al. [1981], Berman et al. [1982], Canosa et al. [1997], Thiesemann et al. [1997], Boullart et al. [1996], McKee et al. [2003], Loison and Bergeat [2009], Maksyutenko et al. [2010], Goulay et al. [2009]
CH + C_2H_2	$\rightarrow t{-}C_3H_2 + H$	$2.5 \times 10^{-10} \times (T/300)^{-0.233} \times \exp(-16/T)$	1.6	7	Butler et al. [1981], Berman et al. [1982], Canosa et al. [1997], Thiesemann et al. [1997], Boullart et al. [1996], McKee et al. [2003], Loison and Bergeat [2009], Maksyutenko et al. [2010], Goulay et al. [2009]
CH + C_2H_2	$\rightarrow l{-}C_3H + H_2$	$3.71 \times 10^{-11} \times (T/300)^{-0.233} \times \exp(-16/T)$	1.6	7	Butler et al. [1981], Berman et al. [1982], Canosa et al. [1997], Thiesemann et al. [1997], Boullart et al. [1996], McKee et al. [2003], Loison and Bergeat [2009], Maksyutenko et al. [2010], Goulay et al. [2009]
CH + C_2H_4	$\rightarrow CH_3C_2H + H$	$1.0 \times 10^{-10} \times (T/300)^{-0.546} \times \exp(-29.6/T)$	1.6	7	Butler et al. [1981], Berman et al. [1982], Thiesemann et al. [1997], Thiesemann et al. [2001], Canosa et al. [1997], McKee et al. [2003], Loison and Bergeat [2009], Goulay et al. [2009], Gosavi et al. [1985], Wang and Huang [1998], Davis et al. [1999], Stranges et al. [2008]
CH + C_2H_4	$\rightarrow CH_2CCH_2 + H$	$2.4 \times 10^{-10} \times (T/300)^{-0.546} \times \exp(-29.6/T)$	1.6	7	Butler et al. [1981], Berman et al. [1982], Thiesemann et al. [1997], Thiesemann et al. [2001], Canosa et al. [1997], McKee et al. [2003], Loison and Bergeat [2009], Goulay et al. [2009], Gosavi et al. [1985], Wang and Huang [1998], Davis et al. [1999], Stranges et al. [2008]
CH + C_2H_6	$\rightarrow C_3H_6 + H$	$5.0 \times 10^{-12} \times (T/300)^{-0.648} \times \exp(-43.6/T)$	1.6	7	Butler et al. [1980], Butler et al. [1981], Berman and Lin [1983], Canosa et al. [1997], McKee et al. [2003], Galland et al. [2003]
CH + C_2H_6	$\rightarrow C_2H_4 + CH_3$	$2.8 \times 10^{-11} \times (T/300)^{-0.648} \times \exp(-43.6/T)$	1.6	7	Butler et al. [1980], Butler et al. [1981], Berman and Lin [1983], Canosa et al. [1997], McKee et al. [2003], Galland et al. [2003]
CH + C_3	$\rightarrow C_4 + H$	2.0×10^{-10}	3	0	Estimated by comparison with CH + unsaturated hydrocarbons (Butler et al. [1980], Berman et al. [1982], Thiesemann et al. [1997], Canosa et al. [1997], Thiesemann et al. [2001], Daugey et al. [2005])
CH + $c{-}C_3H_2$	$\rightarrow C_4H_2 + H$	2.0×10^{-10}	3	0	Hébrard et al. [2013]
CH + $t{-}C_3H_2$	$\rightarrow C_4H_2 + H$	2.0×10^{-10}	3	0	Hébrard et al. [2013]
CH + $l{-}C_3H_2$	$\rightarrow C_4H_2 + H$	2.0×10^{-10}	3	0	Hébrard et al. [2013]
CH + CH_3C_2H	$\rightarrow C_4H_4 + H$	4.0×10^{-10}	2	14	Fleming et al. [1980], Butler et al. [1981], Daugey et al. [2005], Loison and Bergeat [2009], Goulay et al. [2009]
CH + CH_2CCH_2	$\rightarrow C_4H_4 + H$	4.2×10^{-10}	2	14	Daugey et al. [2005], Loison and Bergeat [2009], Goulay et al. [2009]
CH + C_3H_6	$\rightarrow C_4H_6 + H$	3.3×10^{-10}	1.4	7	Daugey et al. [2005], Loison and Bergeat [2009]
CH + C_3H_6	$\rightarrow CH_2CCH_2 + CH_3$	9×10^{-11}	1.4	7	Daugey et al. [2005], Loison and Bergeat [2009]
CH + C_3H_8	$\rightarrow C_4H_8 + H$	5.0×10^{-11}	1.8	7	Loison et al. [2006]
CH + C_3H_8	$\rightarrow C_3H_6 + CH_3$	1.4×10^{-10}	1.8	7	Loison et al. [2006]
CH + C_3H_8	$\rightarrow C_2H_5 + C_2H_4$	8.0×10^{-11}	1.8	7	Loison et al. [2006]
CH + C_4H_2	$\rightarrow C_5H_2 + H$	$4.21 \times 10^{-10} \times (T/300)^{-0.233} \times \exp(-16/T)$	10	100	By comparison with CH + C_2H_2
CH + C_4H_4	$\rightarrow C_5H_4 + H$	2.0×10^{-10}	2	0	By comparison with CH + alkenes and alkynes (Butler et al. [1980], Berman et al. [1982], Thiesemann et al. [1997], Canosa et al. [1997], Thiesemann et al. [2001], Daugey et al. [2005], Loison and Bergeat [2009])
CH + C_4H_6	$\rightarrow C_5H_6 + H$	1.0×10^{-10}	2	100	By comparison with CH + alkenes and alkynes (Butler et al. [1980], Berman et al. [1982], Thiesemann et al. [1997], Canosa et al. [1997], Thiesemann et al. [2001], Daugey et al. [2005], Loison and Bergeat [2009])
CH + C_4H_6	$\rightarrow C_4H_4 + CH_3$	1.0×10^{-10}	2	100	By comparison with CH + alkenes and alkynes (Butler et al. [1980], Berman et al. [1982], Thiesemann et al. [1997], Canosa et al. [1997], Thiesemann et al. [2001], Daugey et al. [2005], Loison and Bergeat [2009])

Reactions		Rate coefficients	$F(300\ K)$	g	References
$CH + C_4H_8$	$\rightarrow C_5H_8 + H$	2.6×10^{-10}	1.8	7	Canosa et al. [1997], Loison and Bergeat [2009]
$CH + C_4H_8$	$\rightarrow C_4H_6 + CH_3$	1.1×10^{-10}	1.8	7	Canosa et al. [1997], Loison and Bergeat [2009]
$CH + C_4H_{10}$	$\rightarrow C_5H_{10} + H$	5.0×10^{-11}	1.8	7	Loison et al. [2006]
$CH + C_4H_{10}$	$\rightarrow C_4H_8 + CH_3$	3.0×10^{-10}	1.8	7	Loison et al. [2006]
$CH + C_6H_6$	$\rightarrow C_7H_6 + H$	4.3×10^{-10}	3	0	Berman et al. [1982]
$^1CH_2 + H_2$	$\rightarrow {}^3CH_2 + H_2$	$1.6 \times 10^{-11} \times (T/300)^{-0.9}$	1.6	7	Gannon et al. [2008]
$^1CH_2 + H_2$	$\rightarrow CH_3 + H$	$8.8 \times 10^{-11} \times (T/300)^{0.35}$	1.4	7	Gannon et al. [2008]
$^1CH_2 + {}^3CH_2$	$\rightarrow C_2H_2 + H + H$	3.0×10^{-11}	2	100	Tsang and Hampson [1986]
$^1CH_2 + {}^1CH_2$	$\rightarrow C_2H_2 + H + H$	5.0×10^{-11}	2	100	Tsang and Hampson [1986]
$^1CH_2 + CH_3$	$\rightarrow C_2H_4 + H$	3.0×10^{-11}	2	100	Tsang and Hampson [1986]
$^1CH_2 + CH_4$	$\rightarrow {}^3CH_2 + CH_4$	$3.1 \times 10^{-12} \times \exp(250/T)$	1.4	100	Böhland et al. [1985]
$^1CH_2 + CH_4$	$\rightarrow CH_3 + CH_3$	$2.79 \times 10^{-11} \times \exp(250/T)$	1.4	100	Ashfold et al. [1981], Langford et al. [1983], Irle and Morokuma [2000]
$^1CH_2 + C_2H$	$\rightarrow c\text{-}C_3H_2 + H$	1.0×10^{-10}	3	0	Deduced from C_3H_3 dissociation, Nguyen [2001]
$^1CH_2 + C_2H$	$\rightarrow t\text{-}C_3H_2 + H$	2.0×10^{-10}	3	0	Deduced from C_3H_3 dissociation, Nguyen [2001]
$^1CH_2 + C_2H$	$\rightarrow l\text{-}C_3H_2 + H$	5.0×10^{-11}	3	0	Deduced from C_3H_3 dissociation, Nguyen [2001]
$^1CH_2 + C_2H_2$	$\rightarrow {}^3CH_2 + C_2H_2$	2.3×10^{-10}	1.8	21	Gannon et al. [2010b], Gannon et al. [2010c], Hébrard et al. [2013]
$^1CH_2 + C_2H_2$	$\rightarrow C_3H_3 + H$	$7.6 \times 10^{-11} \times (T/300)^{-0.3}$	1.8	21	Gannon et al. [2010b], Gannon et al. [2010c], Hébrard et al. [2013]
$^1CH_2 + C_2H_3$	$\rightarrow C_2H_2 + CH_3$	3.0×10^{-11}	3	100	Tsang and Hampson [1986]
$^1CH_2 + C_2H_4$	$\rightarrow {}^3CH_2 + C_2H_4$	1.4×10^{-10}	1.8	21	Gannon et al. [2010b], Gannon et al. [2010c], Hébrard et al. [2013]
$^1CH_2 + C_2H_4$	$\rightarrow C_3H_5 + H$	6.3×10^{-11}	1.8	21	Gannon et al. [2010b], Gannon et al. [2010c], Hébrard et al. [2013]
$^1CH_2 + C_2H_5$	$\rightarrow C_2H_4 + CH_3$	1.5×10^{-11}	3	100	Tsang and Hampson [1986]
$^1CH_2 + C_2H_5$	$\rightarrow C_3H_6 + H$	1.5×10^{-11}	3	100	Tsang and Hampson [1986]
$^1CH_2 + C_2H_6$	$\rightarrow {}^3CH_2 + C_2H_6$	3.6×10^{-11}	2	100	Baulch et al. [1992]
$^1CH_2 + C_2H_6$	$\rightarrow C_2H_5 + CH_3$	1.9×10^{-10}	2	100	Tsang and Hampson [1986]
$^1CH_2 + C_3$	$\rightarrow C_4H + H$	2.0×10^{-10}	3	0	By comparison with $^1CH_2 + C_2H_4$ (C_3 is a pseudo alkene)
$^1CH_2 + CH_3C_2H$	$\rightarrow C_4H_5 + H$	9.62×10^{-11}	10	100	By comparison with $^1CH_2 + C_2H_2$
$^1CH_2 + CH_2CCH_2$	$\rightarrow C_4H_5 + H$	9.62×10^{-11}	10	100	By comparison with $^1CH_2 + C_2H_4$
$^1CH_2 + C_3H_5$	$\rightarrow C_4H_6 + H$	3.33×10^{-10}	2.5	100	Tsang [1991]
$^1CH_2 + C_3H_5$	$\rightarrow C_2H_4 + C_2H_3$	6.7×10^{-11}	2	100	Tsang [1991]
$^1CH_2 + C_3H_7$	$\rightarrow C_2H_5 + C_2H_4$	3.0×10^{-11}	3	100	Tsang [1988]
$^1CH_2 + C_3H_7$	$\rightarrow C_3H_6 + CH_3$	3.0×10^{-12}	3	100	Tsang [1988]
$^1CH_2 + C_3H_8$	$\rightarrow C_2H_5 + C_2H_5$	1.6×10^{-10}	2	100	Tsang [1988]
$^1CH_2 + C_4H$	$\rightarrow C_4H_2 + CH$	3.0×10^{-11}	10	100	By comparison with $^1CH_2 + C_2H$ from Tsang [1986]
$^1CH_2 + C_4H_2$	$\rightarrow C_5H_3 + H$	9.62×10^{-11}	10	100	By comparison with $^1CH_2 + C_2H_2$
$^1CH_2 + N_2$	$\rightarrow {}^3CH_2 + N_2$	$1.1 \times 10^{-11} \times (T/300)^{0.81}$	1.6	0	Gannon et al. [2010a]
$^1CH_2 + c\text{-}C_3H_2$	$\rightarrow C_4H_3 + H$	3.0×10^{-10}	3	0	Capture rate constant considering no barrier in the entrance valley
$^1CH_2 + t\text{-}C_3H_2$	$\rightarrow C_4H_3 + H$	3.0×10^{-10}	3	0	Capture rate constant considering no barrier in the entrance valley
$^1CH_2 + l\text{-}C_3H_2$	$\rightarrow C_4H_3 + H$	3.0×10^{-10}	3	0	Capture rate constant considering no barrier in the entrance valley
$^3CH_2 + H_2$	$\rightarrow CH_3 + H$	$8.0 \times 10^{-12} \times \exp(-4500/T)$	10	1000	Tsang and Hampson [1986] - Upper limit
$^3CH_2 + {}^3CH_2$	$\rightarrow C_2H_2 + H + H$	7.0×10^{-11}	3	0	Estimated by comparison with the photodissociation of C_2H_4 (Satyapal et al. [1990], Chang et al. [1998a], Chang et al. [1998b], Lee et al. [2004])
$^3CH_2 + {}^3CH_2$	$\rightarrow C_2H_2 + H_2$	3.0×10^{-11}	3	0	Estimated by comparison with the photodissociation of C_2H_4 (Satyapal et al. [1990], Chang et al. [1998a], Chang et al. [1998b], Lee et al. [2004])
$^3CH_2 + {}^3CH_2$	$\rightarrow C_2H_3 + H$	5.0×10^{-12}	4	0	Estimated by comparison with the photodissociation of C_2H_4 (Satyapal et al. [1990], Chang et al. [1998a], Chang et al. [1998b], Lee et al. [2004])
$^3CH_2 + CH_3$	$\rightarrow C_2H_4 + H$	1.0×10^{-10}	2	0	Wang and Fockenberg [2001], Georgievskii and Klippenstein [2005]
$^3CH_2 + CH_4$	$\rightarrow CH_3 + CH_3$	$7.13 \times 10^{-12} \times \exp(-5050/T)$	3	100	Böhland et al. [1985a] - Upper limit
$^3CH_2 + C_2H$	$\rightarrow c\text{-}C_3H_2 + H$	4.0×10^{-11}	3	0	Estimated by comparison with the photodissociation of C_3H_3 (Crider et al. [2009], Nguyen et al. [2001b])
$^3CH_2 + C_2H$	$\rightarrow t\text{-}C_3H_2 + H$	2.0×10^{-11}	3	0	Estimated by comparison with the photodissociation of C_3H_3 (Crider et al. [2009], Nguyen et al. [2001b])

Reactions		Rate coefficients	$F(300\ K)$	g	References
$^3CH_2 + C_2H$	$\rightarrow l\text{-}C_3H_2 + H$	3.0×10^{-11}	3	0	Estimated by comparison with the photodissociation of C_3H_3 (Crider et al. [2009], Nguyen et al. [2001b])
$^3CH_2 + C_2H$	$\rightarrow c\text{-}C_3H + H_2$	1.0×10^{-11}	3	0	Estimated by comparison with the photodissociation of C_3H_3 (Crider et al. [2009], Nguyen et al. [2001b])
$^3CH_2 + C_2H$	$\rightarrow l\text{-}C_3H + H_2$	1.0×10^{-11}	3	0	Estimated by comparison with the photodissociation of C_3H_3 (Crider et al. [2009], Nguyen et al. [2001b])
$^3CH_2 + C_2H_3$	$\rightarrow C_2H_2 + CH_3$	3.0×10^{-11}	3	100	Tsang and Hampson [1986]
$^3CH_2 + C_2H_5$	$\rightarrow C_2H_4 + CH_3$	3.0×10^{-11}	3	100	Tsang and Hampson [1986]
$^3CH_2 + c\text{-}C_3H$	$\rightarrow C_4H_2 + H$	1.0×10^{-10}	3	0	by comparison with $CH_2 + CH_3$ (Wang and Fockenberg [2001], Georgievskii and Klippenstein [2005])
$^3CH_2 + l\text{-}C_3H$	$\rightarrow C_4H_2 + H$	1.0×10^{-10}	3	0	by comparison with $CH_2 + CH_3$ (Wang and Fockenberg [2001], Georgievskii and Klippenstein [2005])
$^3CH_2 + c\text{-}C_3H_2$	$\rightarrow C_4H_3 + H$	1.0×10^{-13}	10	100	value at 150-190K considering a small barrier
$^3CH_2 + c\text{-}C_3H_2$	$\rightarrow C_2H_2 + C_2H_2$	1.0×10^{-13}	10	100	value at 150-190K considering a small barrier
$^3CH_2 + C_3H_3$	$\rightarrow C_4H_4 + H$	1.0×10^{-10}	3	0	Estimated by comparison with $^3CH_2 + CH_3 + CH_3$ (Wang and Fockenberg [2001], Georgievskii and Klippenstein [2005])
$^3CH_2 + C_3H_5$	$\rightarrow C_4H_6 + H$	5.0×10^{-11}	2	100	Tsang [1991], Miller [2004]
$^3CH_2 + C_3H_5$	$\rightarrow C_2H_3 + C_2H_4$	1.2×10^{-11}	2	100	Tsang [1991], Miller [2004]
$^3CH_2 + C_3H_7$	$\rightarrow C_2H_4 + C_2H_5$	3.01×10^{-11}	3	100	Tsang [1988]
$^3CH_2 + C_3H_7$	$\rightarrow C_3H_6 + CH_3$	3.0×10^{-12}	3	100	Tsang [1988]
$^3CH_2 + C_4H$	$\rightarrow C_4H_2 + CH$	3.0×10^{-11}	10	100	By comparison with $^1CH_2 + C_2H$ from Tsang [1986]
$^3CH_2 + C_4H_2$	$\rightarrow C_4H + CH_3$	$2.16 \times 10^{-11} \times \exp(-2160/T)$	1.25	100	Böhland et al. [1988]
$^3CH_2 + C_4H_3$	$\rightarrow C_4H_2 + CH_3$	3.0×10^{-11}	10	100	By comparison with $CH_2 + C_2H_3$
$CH_3 + H_2$	$\rightarrow CH_4 + H$	$2.45 \times 10^{-14} \times (T/300)^{2.88} \times \exp(-4600/T)$	1.12	0	Baulch et al. [2005]
$CH_3 + CH_3$	$\rightarrow C_2H_5 + H$	$1.46 \times 10^{-11} \times (T/300)^{0.1} \times \exp(-5340/T)$	2	100	Stewart et al. [1989]
$CH_3 + CH_3$	$\rightarrow C_2H_6$	$k_0 = 1.8 \times 10^{-26} \times (T/300)^{-3.77} \times \exp(-61.6/T)$	2	0	Vuitton et al. [2012] with some modifications to fit the experimental data from Slagle et al.
		$k_\infty = 6.8 \times 10^{-11} \times (T/300)^{-0.359} \times \exp(-30.2/T)$	1.4	0	[1988], Cody et al. [2002], Cody et al. [2003].
		$k_r = 0$	100	0	Very similar to Moses et al. [2005] but with $F_c = 0.64$
$CH_3 + C_2H$	$\rightarrow C_3H_3 + H$	1.0×10^{-10}	3	0	Tsang [1986], Georgievskii and Klippenstein [2005]
$CH_3 + C_2H_2$	$\rightarrow C_3H_5$	$k_0 = 3.3 \times 10^{-30} \times \exp(-740/T)$	10	100	k_0 by comparison with $H + C_2H_2$, k_∞ from
		$k_\infty = 1.0 \times 10^{-12} \times \exp(-3900/T)$	3.16	100	Baulch [2005]
		$k_r = 0$	30	0	
$CH_3 + C_2H_3$	$\rightarrow C_2H_2 + CH_4$	3.3×10^{-11}	1.4	0	Hébrard et al. [2013]
$CH_3 + C_2H_3$	$\rightarrow C_3H_6$	$k_0 = 2.4 \times 10^{-27} \times (T/300)^{-3.77} \times \exp(-61.6/T)$	10	0	Fahr et al. [1999], Thorn et al. [2000], Stoliarov et al. [2000],
		$k_\infty = 1.0 \times 10^{-10}$	1.4	0	$k_0 = 0.1 \times k_0(CH_3 + CH_3)$ considering the
		$k_r = 0$	1	0	bimolecular exit channel
$CH_3 + C_2H_3$	$\rightarrow C_3H_5 + H$	$k = k_\infty - k_{\text{adduct}}$	0	0	
$CH_3 + C_2H_4$	$\rightarrow C_2H_3 + CH_4$	$1.61 \times 10^{-14} \times (T/300)^{3.7} \times \exp(-4780/T)$	2	100	Tsang and Hampson [1986]
$CH_3 + C_2H_4$	$\rightarrow C_3H_7$	$k_0 = 1.39 \times 10^{-29} \times \exp(-562/T)$	10	100	k_0 by comparison with $H + C_2H_4$,k_∞ from
		$k_\infty = 3.5 \times 10^{-13} \times \exp(-3700/T)$	2	100	Baulch [2005]
		$k_r = 0$	30	0	
$CH_3 + C_2H_5$	$\rightarrow C_2H_4 + CH_4$	1.91×10^{-12}	2.5	100	Hébrard et al. [2013]
$CH_3 + C_2H_5$	$\rightarrow C_3H_8$	$k_0 = 1.0 \times 10^{-24} \times (T/300)^{-4.47} \times \exp(-95/T)$	4	0	Vuitton et al. [2012], Hébrard et al. [2013]
		$k_\infty = 8.8 \times 10^{-11} \times (T/300)^{-0.61} \times \exp(-44.8/T)$	2	0	
		$k_r = 0$	10	0	
$CH_3 + C_2H_6$	$\rightarrow C_2H_5 + CH_4$	$1.82 \times 10^{-16} \times (T/300)^6 \times \exp(-3040/T)$	1.58	100	Baulch et al. [1992]
$CH_3 + c\text{-}C_3H$	$\rightarrow C_4H_3 + H$	1.0×10^{-10}	3	0	By comparison with $CH_3 + C_2H_3$
$CH_3 + l\text{-}C_3H$	$\rightarrow C_4H_3 + H$	1.0×10^{-10}	3	0	By comparison with $CH_3 + C_2H_3$
$CH_3 + c\text{-}C_3H_2$	$\rightarrow C_4H_4 + H$	$1.0 \times 10^{-11} \times \exp(-700/T)$	4	0	Estimated considering a small barrier in the entrance valley
$CH_3 + c\text{-}C_3H_2$	$\rightarrow C_2H_3 + C_2H_2$	$1.0 \times 10^{-11} \times \exp(-700/T)$	4	0	Estimated considering a small barrier in the entrance valley
$CH_3 + t\text{-}C_3H_2$	$\rightarrow C_4H_4 + H$	4.0×10^{-11}	10	0	By comparison with $CH_3 + {}^3CH_2$
$CH_3 + t\text{-}C_3H_2$	$\rightarrow C_2H_3 + C_2H_2$	4.0×10^{-11}	10	0	By comparison with $CH_3 + {}^3CH_2$
$CH_3 + l\text{-}C_3H_2$	$\rightarrow C_4H_4 + H$	4.0×10^{-11}	10	0	Estimated considering no barrier in the entrance valley
$CH_3 + l\text{-}C_3H_2$	$\rightarrow C_2H_3 + C_2H_2$	4.0×10^{-11}	10	0	Estimated considering no barrier in the entrance valley

Reactions		Rate coefficients	$F(300\ K)$	g	References
$CH_3 + C_3H_3$	$\rightarrow C_4H_6$	$k_0 = 8.0 \times 10^{-26} \times (T/300)^{-3.5}$	10	0	k_0 from our semi empirical model
+		$k_\infty = 6.8 \times 10^{-11} \times \exp(130/T)$	1.6	21	Hébrard et al. [2013] taking into account the
		$k_r = 1.0 \times 10^{-12} \times (T/300)^{-1.5}$	30	0	bimolecular exit channel, k_∞ from Knyazev and Slagle [2001], Fahr and Nayak [2000]
$CH_3 + C_3H_3$	$\rightarrow C_2H_2 + C_2H_4$	$= k_\infty - k_{\text{adduct}}$	0	0	
$CH_3 + CH_3C_2H$	$\rightarrow C_2H_6 + C_2H$	$8.32 \times 10^{-13} \times \exp(-4430/T)$	2	100	Kerr and Parsonage [1972]
$CH_3 + CH_2CCH_2$	$\rightarrow C_2H_5 + C_2H_2$	$3.32 \times 10^{-13} \times \exp(-4080/T)$	2	100	Kerr and Parsonage [1972]
$CH_3 + C_3H_5$	$\rightarrow CH_3C_2H + CH_4$	$4.03 \times 10^{-13} \times (T/300)^{-0.32} \times \exp(66/T)$	3	100	Tsang [1991]
$CH_3 + C_3H_5$	$\rightarrow CH_2CCH_2 + CH_4$	$4.03 \times 10^{-13} \times (T/300)^{-0.32} \times \exp(66/T)$	3	100	Tsang [1991]
$CH_3 + C_3H_5$	$\rightarrow C_4H_8$	$k_0 = 1.1 \times 10^{-22} \times (T/300)^{-3.5}$	10	0	Hébrard et al. [2013], Knyazev and Slagle
		$k_\infty = 7.1 \times 10^{-11} \times (T/300)^{-0.54} \times \exp(117/T)$	1.6	21	[2001], Hébrard et al. [2013]
		$k_r = 3.4 \times 10^{-11} \times (T/300)^{-1.5}$	30	0	
$CH_3 + C_3H_6$	$\rightarrow C_3H_5 + CH_4$	$2.32 \times 10^{-13} \times \exp(-4390/T)$	2	100	Kinsman and Roscoe [1994]
$CH_3 + C_3H_6$	$\rightarrow C_4H_9$	$k_0 = 1.39 \times 10^{-29} \times \exp(-562/T)$	10	100	k_0 by comparison with $H + C_2H_4$, k_∞ from
		$k_\infty = 1.34 \times 10^{-13} \times \exp(-3330/T)$	2	100	Tsang [1991]
		$k_r = 0$	30	0	
$CH_3 + C_3H_7$	$\rightarrow C_3H_6 + CH_4$	$7.52 \times 10^{-12} \times (T/300)^{0.68}$	3	0	Tsang [1991]
$CH_3 + C_3H_7$	$\rightarrow C_4H_{10}$	$k_0 = 2.7 \times 10^{-21} \times (T/300)^{-3.5}$	10	0	By comparison with $CH_3 + C_2H_5$
		$k_\infty = 8.9 \times 10^{-11} \times (T/300)^{-0.61} \times \exp(-44.8/T)$	3	0	
		$k_r = 8.9 \times 10^{-11} \times (T/300)^{-0.61} \times \exp(-44.8/T)$	3	0	
$CH_3 + C_3H_8$	$\rightarrow C_3H_7 + CH_4$	$1.65 \times 10^{-15} \times (T/300)^{3.65} \times \exp(-3600/T)$	1.5	100	Tsang [1988]
$CH_3 + C_4H$	$\rightarrow C_5H_3 + H$	4.0×10^{-11}	10	100	By comparison with $CH_3 + C_2H$
$CH_3 + C_4H_2$	$\rightarrow C_5H_5$	$k_0 = 3.3 \times 10^{-30} \times \exp(-740/T)$	10	100	k_0 by comparison with $H + C_2H_2$
		$k_\infty = 1.0 \times 10^{-12} \times \exp(-3900/T)$	10	100	
		$k_r = 0$	30	0	
$CH_3 + C_4H_3$	$\rightarrow C_4H_2 + CH_4$	1.0×10^{-11}	3	0	By comparison with $CH_3 + C_2H_3$
$CH_3 + C_4H_3$	$\rightarrow C_5H_6$	$k_0 = 2.2 \times 10^{-21} \times (T/300)^{-3.5}$	10	0	Using our semi empirical model Hébrard [2012]
		$k_\infty = 8 \times 10^{-11}$	2	0	
		$k_r = 0$	30	0	
$CH_3 + C_4H_4$	$\rightarrow C_4H_3 + CH_4$	$6.61 \times 10^{-13} \times \exp(-2500/T)$	2	100	Scherzer et al. [1985]
$CH_3 + C_4H_5$	$\rightarrow C_4H_4 + CH_4$	3.0×10^{-11}	10	100	By comparison with $CH_3 + C_2H_3$
$CH_3 + C_6H_5$	$\rightarrow$ SOOTC	6.0×10^{-11}	3	0	Vuitton et al [2012] leads to $k_\infty = k(CH_3 + C_6H_5 -> toluene)$
$CH_3 + C_6H_5$	$\rightarrow C_6H_4 + CH_4$	2.0×10^{-12}	5	0	By comparison with $CH_3 + C_2H_3$
$C_2 + H_2$	$\rightarrow C_2H + H$	$1.77 \times 10^{-10} \times \exp(-1470/T)$	1.6	0.2	Reisler et al. [1980], Pitts et al. [1982]
$C_2 + CH_4$	$\rightarrow C_3H_3 + H$	1.2×10^{-11}	1.8	7	Richardson and Francisco [1994], Canosa et al. [2007], Paramo et al. [2008], Matsugi et al. [2010], Hornet et al. [1995]
$C_2 + C_2H_2$	$\rightarrow C_4H + H$	4.0×10^{-10}	1.6	0	Canosa et al. [2007], Daugey et al. [2008], Paramo et al. [2008]
$C_2 + C_2H_4$	$\rightarrow C_4H_3 + H$	3.0×10^{-10}	1.8	0	Gu et al. [2006], Mebel et al. [2006], Canosa et al. [2007], Paramo et al. [2008]
$C_2 + C_2H_4$	$\rightarrow C_2H_2 + C_2H_2$	1.0×10^{-10}	2	0	Gu et al. [2006], Mebel et al. [2006], Canosa et al. [2007], Paramo et al. [2008]
$C_2 + C_2H_6$	$\rightarrow C_3H_3 + CH_3$	$1.3 \times 10^{-10} \times (T/300)^{-0.94} \times \exp(-44/T)$	1.4	0	Paramo et al. [2008], Canosa et al. [2007]
$C_2 + C_3H_8$	$\rightarrow C_3H_3 + C_2H_5$	$2.2 \times 10^{-10} \times (T/300)^{-1.31} \times \exp(-94/T)$	1.4	0	Paramo et al. [2008], Canosa et al. [2007]
$C_2 + C_4H_{10}$	$\rightarrow C_3H_3 + C_3H_7$	$2.2 \times 10^{-10} \times (T/300)^{-1.31} \times \exp(-94/T)$	1.4	0	By comparison with $C_2 + C_3H_8$
$C_2 + C_6H_6$	$\rightarrow C_8H_5 + H$	5.2×10^{-10}	1.6	0	Reisler et al. [1980]
$C_2H + H_2$	$\rightarrow C_2H_2 + H$	$1.2 \times 10^{-11} \times \exp(-998/T)$	1.6	57	Opansky and Leone [1996]
$C_2H + CH_4$	$\rightarrow C_2H_2 + CH_3$	$1.2 \times 10^{-11} \times \exp(-491/T)$	1.2	12	Opansky and Leone [1996a], Murphy et al. [2003]
$C_2H + C_2H$	$\rightarrow C_2H_2 + C_2$	3.0×10^{-12}	3	100	Tsang and Hampson [1986]
$C_2H + C_2H_2$	$\rightarrow C_4H_2 + H$	1.3×10^{-10}	2	0	Vakhtin et al. [2001], Chastaing et al. [1998]
$C_2H + C_2H_3$	$\rightarrow C_2H_2 + C_2H_2$	1.6×10^{-12}	3	100	Tsang and Hampson [1986]
$C_2H + C_2H_3$	$\rightarrow C_4H_3 + H$	3.0×10^{-11}	3	100	Tsang and Hampson [1986]
$C_2H + C_2H_4$	$\rightarrow C_4H_4 + H$	1.4×10^{-10}	1.7	0	Vakhtin et al. [2001], Chastaing et al. [1998]
$C_2H + C_2H_5$	$\rightarrow C_2H_4 + C_2H_2$	3.0×10^{-12}	3	100	Tsang and Hampson [1986]
$C_2H + C_2H_5$	$\rightarrow C_3H_3 + CH_3$	3.0×10^{-11}	3	100	Tsang and Hampson [1986]
$C_2H + C_2H_6$	$\rightarrow C_2H_5 + C_2H_2$	$5.1 \times 10^{-11} \times \exp(-76/T)$	1.5	20	Murphy et al. [2003]
$C_2H + C_3$	$\rightarrow C_5 + H$	3.0×10^{-10}	3	0	Considering no barrier for this reaction
$C_2H + c{-}C_3H_2$	$\rightarrow C_5H_2 + H$	3.0×10^{-10}	3	0	Considering no barrier for this reaction
$C_2H + t{-}C_3H_2$	$\rightarrow C_5H_2 + H$	3.0×10^{-10}	3	0	Considering no barrier for this reaction
$C_2H + l{-}C_3H_2$	$\rightarrow C_5H_2 + H$	3.0×10^{-10}	3	0	Considering no barrier for this reaction
$C_2H + CH_3C_2H$	$\rightarrow C_5H_4 + H$	$2.1 \times 10^{-10} \times (T/300)^{-0.3}$	1.6	0	Carty et al. [2001]
$C_2H + CH_2CCH_2$	$\rightarrow C_5H_4 + H$	$2.04 \times 10^{-10} \times (T/300)^{-0.4}$	1.8	0	Carty et al. [2001]
$C_2H + C_3H_5$	$\rightarrow CH_2CCH_2 + C_2H_2$	1.2×10^{-11}	3	100	Tsang [1991]
$C_2H + C_3H_6$	$\rightarrow C_4H_4 + CH_3$	2.0×10^{-10}	1.3	0	Vakhtin et al. [2001], Chastaing et al. [1998], Woon and Park [2009]
$C_2H + C_3H_7$	$\rightarrow C_2H_5 + C_3H_3$	2.0×10^{-11}	2	100	Tsang [1988]

Reactions		Rate coefficients	$F(300\ K)$	g	References
$C_2H + C_3H_7$	$\rightarrow C_2H_2 + C_3H_6$	1.0×10^{-11}	3	100	Tsang [1988]
$C_2H + C_3H_8$	$\rightarrow C_3H_7 + C_2H_2$	$9.8 \times 10^{-11} \times \exp(-71/T)$	1.9	80	Murphy et al. [2003]
$C_2H + C_4H$	$\rightarrow C_6H + H$	3.0×10^{-12}	10	100	Considering no barrier for this reaction
$C_2H + C_4H_2$	$\rightarrow C_6H_2 + H$	$2.54 \times 10^{-10} \times (T/300)^{-0.31}$	2	0	Rennes [2013]
$C_2H + C_4H_3$	$\rightarrow C_4H_2 + C_2H_2$	1.6×10^{-12}	10	100	By comparison with $C_2H + C_2H_3$
$C_2H + C_4H_3$	$\rightarrow C_6H_3 + H$	3.0×10^{-11}	10	100	By comparison with $C_2H + C_2H_3$
$C_2H + C_4H_4$	$\rightarrow C_6H_4 + H$	2.0×10^{-10}	2	0	By comparison with $C_2H + C_3H_4$
$C_2H + C_4H_6$	$\rightarrow C_6H_6 + H$	2.0×10^{-10}	2	0	By comparison with $C_2H + C_3H_6$
$C_2H + C_4H_8$	$\rightarrow C_6H_8 + H$	2.1×10^{-10}	1.5	0	Nizamov and Leone [2004]
$C_2H + C_4H_{10}$	$\rightarrow C_4H_9 + C_2H_2$	1.23×10^{-10}	1.31	0	Murphy et al. [2003]
$C_2H + C_6H_2$	$\rightarrow C_8H_2 + H$	1.3×10^{-10}	10	100	By comparison with $C_2H + C_2H_2$
$C_2H + C_6H_4$	$\rightarrow C_8H_4 + H$	4.0×10^{-10}	2	0	By comparison with $C_2H + C_6H_6$
$C_2H + C_6H_6$	$\rightarrow C_6H_5C_2H + H$	$3.28 \times 10^{-10} \times (T/300)^{-0.18}$	1.5	30	Goulay and Leone [2006]
$C_2H + C_8H_2$	$\rightarrow$ SOOTC	1.3×10^{-10}	10	100	By comparison with $C_2H + C_2H_2$
$C_2H_3 + H_2$	$\rightarrow C_2H_4 + H$	$3.45 \times 10^{-14} \times (T/300)^{2.56} \times \exp(-2529/T)$	3	600	Knyazev et al. [1996a], Callear and Smith [1986]
$C_2H_3 + CH_4$	$\rightarrow C_2H_4 + CH_3$	$2.13 \times 10^{-14} \times (T/300)^{4.02} \times \exp(-2750/T)$	3	600	Tsang and Hampson [1986], Liu et al. [2002], this work
$C_2H_3 + C_2H_2$	$\rightarrow C_4H_5$	$k_0 = 5.3 \times 10^{-29} \times (T/300)^{-5.84} \times \exp(-2000/T)$	10	200	Wang and Frenklach [1994], Knyazev et al. [1996b], Callear and Smith [1986]
		$k_\infty = 2.0 \times 10^{-12} \times \exp(-2700/T)$	4	200	
		$k_r = 0$	1	0	
$C_2H_3 + C_2H_2$	$\rightarrow C_4H_4 + H$	$k = k_\infty - k_{\text{adduct}}$	0	0	
$C_2H_3 + C_2H_3$	$\rightarrow C_2H_4 + C_2H_2$	3.5×10^{-11}	1.6	0	Laufer and Fahr [2004]
$C_2H_3 + C_2H_3$	$\rightarrow C_4H_6$	$k_0 = 1.0 \times 10^{-26}$	10	0	k_0 from our semi empirical model Hébrard et al. [2013] taking into account the bimolecular exit channel, k_∞ from Laufer from Fahr [2004]
		$k_\infty = 9.5 \times 10^{-11}$	1.4	0	
		$k_r = 0$	1	0	
$C_2H_3 + C_2H_3$	$\rightarrow C_4H_5 + H$	$k = k_\infty - k_{\text{adduct}}$	0	0	
$C_2H_3 + C_2H_4$	$\rightarrow C_4H_6 + H$	$7.0 \times 10^{-14} \times (T/300)^2 \times \exp(-1430/T)$	2	100	Ismail et al. [2007]. Addition channel leading to methylallyl is negligible for Titan's atmospheric conditions
$C_2H_3 + C_2H_5$	$\rightarrow C_2H_4 + C_2H_4$	1.8×10^{-11}	3	100	Tsang and Hampson [1986]
$C_2H_3 + C_2H_5$	$\rightarrow C_2H_6 + C_2H_2$	9.8×10^{-12}	3	100	Tsang and Hampson [1986]
$C_2H_3 + C_2H_5$	$\rightarrow C_4H_8$	$k_0 = 1.0 \times 10^{-30}$	10	0	Laufer and Fahr [2004], Fahr et al. [2007]
		$k_\infty = 6.5 \times 10^{-11}$	1.4	0	
		$k_r = 0$	1	0	
$C_2H_3 + C_2H_5$	$\rightarrow C_3H_5 + CH_3$	$k = k_\infty - k_{\text{adduct}}$	0	0	
$C_2H_3 + C_2H_6$	$\rightarrow C_2H_4 + C_2H_5$	$1.46 \times 10^{-13} \times (T/300)^{3.3} \times \exp(-5280/T)$	3	600	Tsang and Hampson [1986]
$C_2H_3 + c{-}C_3H_2$	$\rightarrow C_5H_4 + H$	3.0×10^{-11}	3	0	Considering no barrier for this reaction
$C_2H_3 + CH_3C_2H$	$\rightarrow C_5H_6 + H$	$3.31 \times 10^{-12} \times \exp(-2520/T)$	10	100	By comparison with $C_2H_3 + C_2H_2$ Tsang [1989]
$C_2H_3 + CH_2CCH_2$	$\rightarrow C_5H_6 + H$	$3.31 \times 10^{-12} \times \exp(-2520/T)$	10	100	By comparison with $C_2H_3 + C_2H_2$ Tsang [1989]
$C_2H_3 + C_3H_5$	$\rightarrow C_3H_6 + C_2H_2$	8.0×10^{-12}	3	100	Tsang [1991]
$C_2H_3 + C_3H_5$	$\rightarrow C_2H_4 + CH_3C_2H$	4.0×10^{-12}	3	100	Tsang [1991]
$C_2H_3 + C_3H_5$	$\rightarrow C_5H_6 + H + H$	8.0×10^{-11}	2	100	Tsang [1991]
$C_2H_3 + C_3H_5$	$\rightarrow C_2H_4 + CH_2CCH_2$	2.0×10^{-12}	3	100	Tsang [1991]
$C_2H_3 + C_3H_6$	$\rightarrow C_3H_5 + C_2H_4$	$1.72 \times 10^{-15} \times (T/300)^{3.5} \times \exp(-2360/T)$	10	100	Tsang [1991]
$C_2H_3 + C_3H_6$	$\rightarrow C_4H_6 + CH_3$	$1.2 \times 10^{-12} \times \exp(-2520/T)$	3	100	Tsang [1991]
$C_2H_3 + C_3H_6$	$\rightarrow C_5H_8 + H$	$1.2 \times 10^{-12} \times \exp(-3240/T)$	3	100	Tsang [1991]
$C_2H_3 + C_3H_7$	$\rightarrow C_3H_6 + C_2H_4$	2.0×10^{-12}	3	100	Tsang [1988]
$C_2H_3 + C_3H_7$	$\rightarrow C_3H_8 + C_2H_2$	2.0×10^{-12}	3	100	Tsang [1988]
$C_2H_3 + C_3H_7$	$\rightarrow C_5H_{10}$	$k_0 = 1.13 \times 10^{-25} \times (T/300)^{-3.75} \times \exp(-494/T)$	10	100	By comparison with $CH_3 + CH_3$
		$k_\infty = 1.6 \times 10^{-11}$	2.5	100	
		$k_r = 0$	30	0	
$C_2H_3 + C_3H_8$	$\rightarrow C_3H_7 + C_2H_4$	$1.46 \times 10^{-13} \times (T/300)^{3.3} \times \exp(-5280/T)$	3	600	Tsang [1988]
$C_2H_3 + C_4H$	$\rightarrow C_4H_2 + C_2H_2$	1.6×10^{-12}	10	100	By comparison with $C_2H + C_2H_3$
$C_2H_3 + C_4H$	$\rightarrow C_6H_3 + H$	3.0×10^{-11}	10	100	By comparison with $C_2H + C_2H_3$
$C_2H_3 + C_4H_2$	$\rightarrow C_6H_4 + H$	$1.2 \times 10^{-11} \times \exp(-1400/T)$	4	300	M06/aug-cc-pVTZ + TST calculations (This work)
$C_2H_3 + C_4H_3$	$\rightarrow C_4H_4 + C_2H_2$	2.0×10^{-11}	2	100	By comparison with $C_2H_3 + C_2H_3$
$C_2H_3 + C_4H_3$	$\rightarrow C_4H_2 + C_2H_4$	2.0×10^{-11}	2	100	By comparison with $C_2H_3 + C_2H_3$
$C_2H_3 + C_4H_3$	$\rightarrow C_6H_5 + H$	8.0×10^{-11}	3	0	adapted from Duran et al [1988]
$C_2H_3 + C_4H_5$	$\rightarrow C_6H_6 + H_2$	$9.94 \times 10^{-20} \times (T/300)^{7.07} \times \exp(1820/T)$	2	100	Westmoreland et al. [1989]
$C_2H_5 + H_2$	$\rightarrow C_2H_6 + H$	$4.23 \times 10^{-15} \times (T/300)^{3.6} \times \exp(-4250/T)$	5	100	Tsang and Hampson [1986]
$C_2H_5 + CH_4$	$\rightarrow C_2H_6 + CH_3$	$2.57 \times 10^{-15} \times (T/300)^{4.14} \times \exp(-6320/T)$	2	100	Tsang and Hampson [1986]
$C_2H_5 + C_2H_2$	$\rightarrow C_2H_6 + C_2H$	$4.5 \times 10^{-13} \times \exp(-11800/T)$	5	100	Tsang and Hampson [1986]
$C_2H_5 + C_2H_2$	$\rightarrow C_4H_7$	$k_0 = 3.3 \times 10^{-30} \times \exp(-740/T)$	10	100	By comparison with $H + C_2H_2$
		$k_\infty = 5.6 \times 10^{-14} \times \exp(-3520/T)$	2	100	
		$k_r = 0$	30	0	

Reactions		Rate coefficients	$F(300\ K)$	g	References
$C_2H_5 + C_2H_4$	$\rightarrow C_2H_6 + C_2H_3$	$5.67 \times 10^{-14} \times (T/300)^{3.13} \times \exp(-9060/T)$	5	100	Tsang and Hampson [1986]
$C_2H_5 + C_2H_4$	$\rightarrow C_4H_9$	$k_0 = 1.39 \times 10^{-29} \times \exp(-562/T)$	10	100	By comparison with $H + C_2H_4$
		$k_\infty = 1.8 \times 10^{-13} \times \exp(-3670/T)$	2	100	
		$k_r = 0$	30	0	
$C_2H_5 + C_2H_5$	$\rightarrow C_2H_6 + C_2H_4$	2.4×10^{-12}	2	0	Baulch et al. [1992]
$C_2H_5 + C_2H_5$	$\rightarrow C_4H_{10}$	$k_0 = 6.4 \times 10^{-20} \times (T/300)^{-3.5}$	10	0	k_0 from our semi empirical model Hébrard
		$k_\infty = 2.0 \times 10^{-11}$	1.4	0	[2012], k_∞ from Shafir et al. [2003]
		$k_r = 2.0 \times 10^{-11}$	1.4	0	
$C_2H_5 + c{-}C_3H_2$	$\rightarrow C_5H_6 + H$	1.0×10^{-12}	10	0	Value at 150-190K considering a small barrier
$C_2H_5 + c{-}C_3H_2$	$\rightarrow C_4H_4 + CH_3$	1.0×10^{-12}	10	0	Value at 150-190K considering a small barrier
$C_2H_5 + c{-}C_3H_2$	$\rightarrow C_3H_3 + C_2H_4$	1.0×10^{-12}	10	0	Value at 150-190K considering a small barrier
$C_2H_5 + t{-}C_3H_2$	$\rightarrow C_5H_6 + H$	1.0×10^{-11}	10	0	Value at 150-190K considering a very small barrier
$C_2H_5 + t{-}C_3H_2$	$\rightarrow C_4H_4 + CH_3$	1.0×10^{-11}	10	0	Value at 150-190K considering a very small barrier
$C_2H_5 + t{-}C_3H_2$	$\rightarrow C_3H_3 + C_2H_4$	1.0×10^{-11}	10	0	Value at 150-190K considering a very small barrier
$C_2H_5 + l{-}C_3H_2$	$\rightarrow C_5H_6 + H$	1.0×10^{-11}	10	0	Value at 150-190K considering a very small barrier
$C_2H_5 + l{-}C_3H_2$	$\rightarrow C_4H_4 + CH_3$	1.0×10^{-11}	10	0	Value at 150-190K considering a very small barrier
$C_2H_5 + l{-}C_3H_2$	$\rightarrow C_3H_3 + C_2H_4$	1.0×10^{-11}	10	0	Value at 150-190K considering a very small barrier
$C_2H_5 + CH_3C_2H$	$\rightarrow C_5H_9$	$k_0 = 3.3 \times 10^{-30} \times \exp(-740/T)$	10	100	By comparison with $H + C_2H_2$
		$k_\infty = 5.6 \times 10^{-14} \times \exp(-3520/T)$	10	100	
		$k_r = 0$	30	0	
$C_2H_5 + CH_2CCH_2$	$\rightarrow C_5H_9$	$k_0 = 3.3 \times 10^{-30} \times \exp(-740/T)$	10	100	By comparison with $H + C_2H_2$
		$k_\infty = 5.6 \times 10^{-14} \times \exp(-3520/T)$	10	100	
		$k_r = 0$	30	0	
$C_2H_5 + C_3H_5$	$\rightarrow CH_2CCH_2 + C_2H_6$	$1.6 \times 10^{-12} \times \exp(66/T)$	2	100	Tsang [1991]
$C_2H_5 + C_3H_5$	$\rightarrow C_3H_6 + C_2H_4$	$4.3 \times 10^{-12} \times \exp(66/T)$	2	100	Tsang [1991]
$C_2H_5 + C_3H_5$	$\rightarrow C_5H_{10}$	$k_0 = 1.13 \times 10^{-25} \times (T/300)^{-3.75} \times \exp(-494/T)$	10	100	By comparison with $CH_3 + CH_3$
		$k_\infty = 3.33 \times 10^{-13} \times \exp(66/T)$	2	100	
		$k_r = 0$	30	0	
$C_2H_5 + C_3H_6$	$\rightarrow C_3H_5 + C_2H_6$	$1.73 \times 10^{-15} \times (T/300)^{3.5} \times \exp(-3340/T)$	3	100	Tsang [1991]
$C_2H_5 + C_3H_6$	$\rightarrow C_5H_{11}$	$k_0 = 1.39 \times 10^{-29} \times \exp(-562/T)$	10	100	By comparison with $H + C_2H_4$
		$k_\infty = 1.7 \times 10^{-13} \times \exp(-3620/T)$	2	100	
		$k_r = 0$	30	0	
$C_2H_5 + C_3H_7$	$\rightarrow C_3H_8 + C_2H_4$	1.91×10^{-12}	2	0	Tsang and Hampson [1988]
$C_2H_5 + C_3H_7$	$\rightarrow C_3H_6 + C_2H_6$	2.41×10^{-12}	2	0	Tsang and Hampson [1988]
$C_2H_5 + C_3H_7$	$\rightarrow C_5H_{12}$	$k_0 = 2.0 \times 10^{-17} \times (T/300)^{-3.5}$	10	0	Tsang and Hampson [1988], Klippenstein et al. [2006]
		$k_\infty = 3.3 \times 10^{-11}$	1.6	0	
		$k_r = 3.3 \times 10^{-11}$	16	0	
$C_2H_5 + C_3H_8$	$\rightarrow C_3H_7 + C_2H_6$	$1.65 \times 10^{-15} \times (T/300)^{3.65} \times \exp(-4600/T)$	2.5	100	Tsang [1988]
$C_2H_5 + C_4H$	$\rightarrow C_2H_4 + C_4H_2$	3.0×10^{-12}	10	100	By comparison with $C_2H + C_2H_5$
$C_2H_5 + C_4H$	$\rightarrow C_5H_3 + CH_3$	3.0×10^{-11}	10	100	By comparison with $C_2H + C_2H_5$
$C_2H_5 + C_4H_2$	$\rightarrow C_6H_7$	$k_0 = 3.3 \times 10^{-30} \times \exp(-740/T)$	10	100	By comparison with $H + C_2H_2$
		$k_\infty = 5.6 \times 10^{-14} \times \exp(-3520/T)$	10	100	
		$k_r = 0$	30	0	
$C_2H_5 + C_4H_3$	$\rightarrow C_4H_4 + C_2H_4$	1.8×10^{-11}	10	100	By comparison with $C_2H_3 + C_2H_5$
$C_2H_5 + C_4H_3$	$\rightarrow C_4H_2 + C_2H_6$	9.8×10^{-12}	10	100	By comparison with $C_2H_3 + C_2H_5$
$C_2H_5 + C_4H_3$	$\rightarrow C_6H_8$	$k_0 = 1.13 \times 10^{-25} \times (T/300)^{-3.75} \times \exp(-494/T)$	10	100	k_0 by comparison with $CH_3 + CH_3$, k_∞ by comparison with $C_2H_3 + C_2H_5$
		$k_\infty = 2.5 \times 10^{-11}$	10	100	
		$k_r = 0$	30	0	
$c{-}C_3H + H_2$	$\rightarrow c{-}C_3H_2 + H$	$6.86 \times 10^{-14} \times (T/300)^{2.74} \times \exp(-4740/T)$	10	1000	By comparison with $CH_3 + H_2$ ($c{-}C_3H$ is close to sp3 radical)
$l{-}C_3H + H_2$	$\rightarrow c{-}C_3H_2 + H$	$1.39 \times 10^{-13} \times (T/300)^{2.38} \times \exp(-7150/T)$	10	1000	by comparison with $C_3H_5 + H_2$
$l{-}C_3H + H_2$	$\rightarrow l{-}C_3H_2 + H$	$1.39 \times 10^{-13} \times (T/300)^{2.38} \times \exp(-7150/T)$	10	1000	by comparison with $C_3H_5 + H_2$
$l{-}C_3H + H_2$	$\rightarrow t{-}C_3H_2 + H$	$1.39 \times 10^{-13} \times (T/300)^{2.38} \times \exp(-7150/T)$	10	1000	by comparison with $C_3H_5 + H_2$
$l{-}C_3H + C_2H_4$	$\rightarrow C_5H_4 + H$	1.0×10^{-10}	4	0	DFT (M06-2X/cc-pVTZ) calculations, Georgievskii and Klippenstein [2005], Jamal and Mebel [2010], Goulay et al. [2011]
$t{-}C_3H_2 + H_2$	$\rightarrow C_3H_3 + H$	$8.0 \times 10^{-12} \times \exp(-4500/T)$	10	1000	By comparison with $^3CH_2 + H_2$
$C_3H_3 + H_2$	$\rightarrow CH_3C_2H + H$	$1.42 \times 10^{-13} \times (T/300)^{2.38} \times \exp(-9560/T)$	10	100	By comparison with C_2H_5, $CH_3 + H_2$, C_3H_3 is an sp^3 radical and has a low reactivity with closed-shell molecules, Knyazev and Slagle [2002], Faravelli [2000]
$C_3H_3 + H_2$	$\rightarrow CH_2CCH_2 + H$	$1.42 \times 10^{-13} \times (T/300)^{2.38} \times \exp(-9560/T)$	10	100	By comparison with C_2H_5, $CH_3 + H_2$, C_3H_3 is an sp^3 radical and has a low reactivity with closed-shell molecules, Knyazev and Slagle [2002], Faravelli [2000]

Reactions		Rate coefficients	$F(300\ K)$	g	References
$C_3H_3 + CH_4$	$\rightarrow CH_3C_2H + CH_3$	$1.74 \times 10^{-14} \times (T/300)^{3.4} \times \exp(-11700/T)$	10	100	By comparison with C_2H_5, $CH_3 + CH_4$, C_3H_3 is an sp^3 radical and has a low reactivity with closed-shell molecules, Knyazev and Slagle [2002], Faravelli [2000]
$C_3H_3 + CH_4$	$\rightarrow CH_2CCH_2 + CH_3$	$1.74 \times 10^{-14} \times (T/300)^{3.4} \times \exp(-11700/T)$	10	100	By comparison with C_2H_5, $CH_3 + CH_4$, C_3H_3 is an sp^3 radical and has a low reactivity with closed-shell molecules, Knyazev and Slagle [2002], Faravelli [2000]
$C_3H_3 + C_2H_2$	$\rightarrow C_5H_5$	$k_0 = 3.3 \times 10^{-30} \times \exp(-740/T)$	10	100	By comparison with $H + C_2H_2$
		$k_\infty = 5.3 \times 10^{-14} \times \exp(-3500/T)$	10	100	
		$k_r = 0$	30	0	
$C_3H_3 + C_2H_4$	$\rightarrow C_5H_6 + H$	$1.0 \times 10^{-14} \times \exp(-5780/T)$	10	100	By comparison with $C_3H_3 + C_2H_2$, C_3H_4, Knyazev and Slagle [2002], Faravelli [2000]
$C_3H_3 + C_2H_6$	$\rightarrow CH_3C_2H + C_2H_5$	$5.83 \times 10^{-14} \times (T/300)^{3.3} \times \exp(-9990/T)$	10	100	By comparison with C_2H_5, $CH_3 + C_2H_6$, C_3H_3 is an sp^3 radical and has a low reactivity with closed-shell molecules, Knyazev and Slagle [2002], Faravelli [2000]
$C_3H_3 + C_2H_6$	$\rightarrow CH_2CCH_2 + C_2H_5$	$5.83 \times 10^{-14} \times (T/300)^{3.3} \times \exp(-9990/T)$	10	100	By comparison with C_2H_5, $CH_3 + C_2H_6$, C_3H_3 is an sp^3 radical and has a low reactivity with closed-shell molecules, Knyazev and Slagle [2002], Faravelli [2000]
$C_3H_3 + C_3H_3$	$\rightarrow C_6H_6$	$k_0 = 1.0 \times 10^{-17} \times (T/300)^{-2.54} \times \exp(-122/T)$	10	0	k_0 by comparison with $H + C_6H_5$ (Vuitton et al. [2012], k_∞ Georgievskii et al. [2007]
		$k_\infty = 1.5 \times 10^{-11} \times (T/300)^{0.101} \times \exp(295/T)$	2	0	
		$k_r = 1.5 \times 10^{-11} \times (T/300)^{0.101} \times \exp(295/T)$	100	0	
$C_3H_3 + C_3H_5$	$\rightarrow C_6H_8$	$k_0 = 1.0 \times 10^{-17} \times (T/300)^{-2.54} \times \exp(-122/T)$	10	0	k_0 by comparison with $H + C_6H_5$ (Vuitton et al. [2012], k_∞ Georgievskii et al. [2007]
		$k_\infty = 1.1 \times 10^{-11} \times (T/300)^{-0.166} \times \exp(312/T)$	2	0	
		$k_r = 1.1 \times 10^{-11} \times (T/300)^{-0.166} \times \exp(312/T)$	100	0	
$C_3H_3 + C_3H_6$	$\rightarrow C_6H_8 + H$	$1.0 \times 10^{-14} \times \exp(-5780/T)$	10	100	By comparison with $C_3H_3 + C_2H_2$, C_3H_4, Knyazev and Slagle [2002], Faravelli [2000]
$C_3H_3 + C_3H_8$	$\rightarrow CH_3C_2H + C_3H_7$	$5.83 \times 10^{-14} \times (T/300)^{3.3} \times \exp(-9990/T)$	10	100	By comparison with C_2H_5, $CH_3 + C_2H_6$, C_3H_3 is an sp^3 radical and has a low reactivity with closed-shell molecules, Knyazev and Slagle [2002], Faravelli [2000]
$C_3H_3 + C_3H_8$	$\rightarrow CH_2CCH_2 + C_3H_7$	$5.83 \times 10^{-14} \times (T/300)^{3.3} \times \exp(-9990/T)$	10	100	By comparison with C_2H_5, $CH_3 + C_2H_6$, C_3H_3 is an sp^3 radical and has a low reactivity with closed-shell molecules, Knyazev and Slagle [2002], Faravelli [2000]
$C_3H_3 + C_4H_2$	$\rightarrow C_7H_5$	$k_0 = 3.3 \times 10^{-30} \times \exp(-740/T)$	10	100	By comparison with $H + C_2H_2$
		$k_\infty = 5.3 \times 10^{-14} \times \exp(-3500/T)$	10	100	
		$k_r = 0$	30	0	
$C_3H_5 + H_2$	$\rightarrow C_3H_6 + H$	$1.42 \times 10^{-13} \times (T/300)^{2.38} \times \exp(-9560/T)$	5	100	Tsang [1991]
$C_3H_5 + CH_4$	$\rightarrow C_3H_6 + CH_3$	$1.74 \times 10^{-14} \times (T/300)^{3.4} \times \exp(-11700/T)$	3	100	Tsang [1991]
$C_3H_5 + C_2H_2$	$\rightarrow C_5H_7$	$k_0 = 3.3 \times 10^{-30} \times \exp(-740/T)$	10	100	k_0 by comparison with $H + C_2H_2$, k_∞ from
		$k_\infty = 5.3 \times 10^{-14} \times \exp(-3500/T)$	10	100	Tsang [1991]
		$k_r = 0$	30	0	
$C_3H_5 + C_2H_4$	$\rightarrow C_5H_8 + H$	$1.0 \times 10^{-14} \times \exp(-5780/T)$	10	100	Tsang [1991]
$C_3H_5 + C_2H_6$	$\rightarrow C_3H_6 + C_2H_5$	$5.83 \times 10^{-14} \times (T/300)^{3.3} \times \exp(-9990/T)$	5	100	Tsang [1991]
$C_3H_5 + CH_3C_2H$	$\rightarrow C_6H_9$	$k_0 = 3.3 \times 10^{-30} \times \exp(-740/T)$	10	100	k_0 by comparison with $H + C_2H_2$, k_∞ by
		$k_\infty = 5.3 \times 10^{-14} \times \exp(-3500/T)$	10	100	comparison with $C_3H_5 + C_3H_5$
		$k_r = 0$	30	0	
$C_3H_5 + CH_2CCH_2$	$\rightarrow C_6H_9$	$k_0 = 3.3 \times 10^{-30} \times \exp(-740/T)$	10	100	k_0 by comparison with $H + C_2H_2$, k_∞ by
		$k_\infty = 5.3 \times 10^{-14} \times \exp(-3500/T)$	10	100	comparison with $C_3H_5 + C_3H_5$
		$k_r = 0$	30	0	
$C_3H_5 + C_3H_5$	$\rightarrow C_3H_6 + CH_2CCH_2$	$1.4 \times 10^{-13} \times \exp(132/T)$	2.5	100	Tsang [1991]
$C_3H_5 + C_3H_5$	$\rightarrow C_6H_{10}$	$k_0 = 1.13 \times 10^{-25} \times (T/300)^{-3.75} \times \exp(-494/T)$	10	100	k_0 by comparison with $CH_3 + CH_3$, k_∞ from Baulch et al. [1994]
		$k_\infty = 1.7 \times 10^{-11} \times \exp(132/T)$	2	100	
		$k_r = 0$	30	0	
$C_3H_5 + C_3H_6$	$\rightarrow C_6H_{10} + H$	$1.0 \times 10^{-14} \times \exp(-5780/T)$	10	100	Tsang [1991]
$C_3H_5 + C_3H_7$	$\rightarrow C_3H_6 + C_3H_6$	$2.4 \times 10^{-12} \times \exp(66/T)$	3	100	Tsang [1991]
$C_3H_5 + C_3H_7$	$\rightarrow CH_2CCH_2 + C_3H_8$	$1.2 \times 10^{-12} \times \exp(66/T)$	3	100	Tsang [1991]
$C_3H_5 + C_3H_7$	$\rightarrow C_6H_{12}$	$k_0 = 1.13 \times 10^{-25} \times (T/300)^{-3.75} \times \exp(-494/T)$	10	100	k_0 by comparison with $CH_3 + CH_3$, k_∞ from Tsang [1991]
		$k_\infty = 3.4 \times 10^{-11} \times \exp(66/T)$	2	100	
		$k_r = 0$	30	0	
$C_3H_5 + C_3H_8$	$\rightarrow C_3H_6 + C_3H_7$	$5.83 \times 10^{-14} \times (T/300)^{3.3} \times \exp(-9990/T)$	5	100	Tsang [1991]
$C_3H_5 + C_4H$	$\rightarrow CH_2CCH_2 + C_4H_2$	1.2×10^{-11}	10	100	By comparison with $C_3H_5 + C_2H$
$C_3H_5 + C_4H_2$	$\rightarrow C_7H_7$	$k_0 = 3.3 \times 10^{-30} \times \exp(-740/T)$	10	100	k_0 by comparison with $H + C_2H_2$, k_∞ by
		$k_\infty = 5.3 \times 10^{-14} \times \exp(-3500/T)$	10	100	comparison with $C_3H_5 + C_3H_5$
		$k_r = 0$	30	0	
$C_3H_5 + C_4H_3$	$\rightarrow C_4H_4 + CH_2CCH_2$	2.0×10^{-12}	10	100	By comparison with $C_3H_5 + C_2H_3$
$C_3H_5 + C_4H_3$	$\rightarrow C_4H_2 + C_3H_6$	8.0×10^{-12}	10	100	By comparison with $C_3H_5 + C_2H_3$
$C_3H_7 + H_2$	$\rightarrow C_3H_8 + H$	$3.25 \times 10^{-14} \times (T/300)^{2.84} \times \exp(-4600/T)$	1.5	100	Tsang [1988]

Reactions		Rate coefficients	$F(300\ K)$	g	References
$C_3H_7 + CH_4$	$\rightarrow C_3H_8 + CH_3$	$3.63 \times 10^{-16} \times (T/300)^{4.02} \times \exp(-5470/T)$	2	100	Tsang [1988]
$C_3H_7 + C_2H_2$	$\rightarrow C_2H_4 + C_3H_5$	$1.2 \times 10^{-12} \times \exp(-4530/T)$	3	100	Tsang [1988]
$C_3H_7 + C_2H_4$	$\rightarrow C_3H_8 + C_2H_3$	$5.67 \times 10^{-14} \times (T/300)^{3.13} \times \exp(-9060/T)$	10	100	By comparison with $C_2H_5 + C_2H_4$
$C_3H_7 + C_2H_4$	$\rightarrow C_5H_{11}$	$k_0 = 1.39 \times 10^{-29} \times \exp(-562/T)$	10	100	k_0 by comparison with $H + C_2H_4$, k_∞ from
		$k_\infty = 7.5 \times 10^{-14} \times \exp(-3470/T)$	2	100	Baulch et al. [1994]
		$k_r = 0$	30	0	
$C_3H_7 + C_2H_6$	$\rightarrow C_3H_8 + C_2H_5$	$1.22 \times 10^{-15} \times (T/300)^{3.82} \times \exp(-4550/T)$	3	100	Tsang [1988]
$C_3H_7 + CH_3C_2H$	$\rightarrow C_6H_{11}$	$k_0 = 3.3 \times 10^{-30} \times \exp(-740/T)$	10	100	k_0 by comparison with $H + C_2H_2$, k_∞ by
		$k_\infty = 1.2 \times 10^{-12} \times \exp(-4530/T)$	10	100	comparison with $C_3H_7 + CH_4$
		$k_r = 0$	30	0	
$C_3H_7 + CH_2CCH_2$	$\rightarrow C_6H_{11}$	$k_0 = 3.3 \times 10^{-30} \times \exp(-740/T)$	10	100	k_0 by comparison with $H + C_2H_2$, k_∞ by
		$k_\infty = 1.2 \times 10^{-12} \times \exp(-4530/T)$	10	100	comparison with $C_3H_7 + CH_4$
		$k_r = 0$	30	0	
$C_3H_7 + C_3H_6$	$\rightarrow C_3H_8 + C_3H_5$	$1.73 \times 10^{-15} \times (T/300)^{3.5} \times \exp(-3340/T)$	3	100	Tsang [1991]
$C_3H_7 + C_3H_6$	$\rightarrow C_6H_{13}$	$k_0 = 1.39 \times 10^{-29} \times \exp(-562/T)$	10	100	k_0 by comparison with $H + C_2H_4$, k_∞ from
		$k_\infty = 7.5 \times 10^{-14} \times \exp(-3470/T)$	2	100	Baulch et al. [1994]
		$k_r = 0$	30	0	
$C_3H_7 + C_3H_7$	$\rightarrow C_3H_8 + C_3H_6$	2.8×10^{-12}	1.5	100	Tsang [1988]
$C_3H_7 + C_3H_7$	$\rightarrow C_6H_{14}$	$k_0 = 9.77 \times 10^{-22} \times (T/300)^{-6.39} \times \exp(-301/T)$	10	100	k_0 by comparison with $C_2H_5 + C_2H_5$, k_∞ from Tsang [1988]
		$k_\infty = 1.7 \times 10^{-11}$	1.5	100	
		$k_r = 0$	30	0	
$C_3H_7 + C_4H$	$\rightarrow C_2H_5 + C_5H_3$	2.0×10^{-11}	10	100	By comparison with $C_3H_7 + C_2H$
$C_3H_7 + C_4H$	$\rightarrow C_4H_2 + C_3H_6$	1.0×10^{-11}	10	100	By comparison with $C_3H_7 + C_2H$
$C_3H_7 + C_4H_2$	$\rightarrow C_7H_9$	$k_0 = 3.3 \times 10^{-30} \times \exp(-740/T)$	10	100	k_0 by comparison with $H + C_2H_2$. k_∞ by
		$k_\infty = 5.3 \times 10^{-14} \times \exp(-3500/T)$	10	100	comparison with $C_3H_5 + C_2H_2$
		$k_r = 0$	30	0	
$C_3H_7 + C_4H_3$	$\rightarrow C_4H_4 + C_3H_6$	2.0×10^{-12}	10	100	By comparison with $C_3H_7 + C_2H_3$
$C_3H_7 + C_4H_3$	$\rightarrow C_4H_2 + C_3H_8$	2.0×10^{-12}	10	100	By comparison with $C_3H_7 + C_2H_3$
$C_3H_7 + C_4H_3$	$\rightarrow C_7H_{10}$	$k_0 = 1.13 \times 10^{-25} \times (T/300)^{-3.75} \times \exp(-494/T)$	10	100	k_0 by comparison with $CH_3 + CH_3$, k_∞ by comparison with $C_2H_3 + C_3H_7$
		$k_\infty = 1.6 \times 10^{-11}$	10	100	
		$k_r = 0$	30	0	
$C_4 + C_2H_2$	$\rightarrow C_6H + H$	9×10^{-11}	2	0	By comparison with $^3C_2 + C_2H_2$, Loison [2014]
$C_4 + C_2H_4$	$\rightarrow C_4H_2 + C_2H_2$	2.0×10^{-11}	2	0	By comparison with $^3C_2 + C_2H_4$, Loison [2014]
$C_4 + C_2H_4$	$\rightarrow C_6H_3 + H$	8.0×10^{-11}	2	0	By comparison with $^3C_2 + C_2H_4$, Loison [2014]
$C_4H + H_2$	$\rightarrow C_4H_2 + H$	$1.2 \times 10^{-11} \times \exp(-998/T)$	10	100	By comparison with $C_2H + H_2$
$C_4H + CH_4$	$\rightarrow C_4H_2 + CH_3$	$1.6 \times 10^{-11} \times \exp(-610/T)$	1.1	0	Berteloite et al. [2010a]
$C_4H + C_2H_2$	$\rightarrow C_6H_2 + H$	$1.82 \times 10^{-10} \times (T/300)^{-1.06} \times \exp(-65.8/T)$	1.21	0	Berteloite et al. [2010b]
$C_4H + C_2H_4$	$\rightarrow C_6H_4 + H$	$1.95 \times 10^{-10} \times (T/300)^{-0.4} \times \exp(9.4/T)$	1.21	0	Berteloite et al. [2008]
$C_4H + C_2H_6$	$\rightarrow C_4H_2 + C_2H_5$	$2.87 \times 10^{-11} \times (T/300)^{-1.24} \times \exp(-25.6/T)$	1.2	0	Berteloite et al. [2010a]
$C_4H + CH_3C_2H$	$\rightarrow C_6H_2 + CH_3$	$3.2 \times 10^{-10} \times (T/300)^{-0.82} \times \exp(-47.5/T)$	1.12	0	Berteloite et al. [2010b]
$C_4H + CH_2CCH_2$	$\rightarrow C_7H_4 + H$	1.3×10^{-10}	10	100	Berteloite et al. [2010b]
$C_4H + C_3H_6$	$\rightarrow C_4H_3 + CH_3C_2H$	2.0×10^{-11}	10	100	By comparison with $C_2H + C_3H_6$, see also Berteloite et al. [2010b]
$C_4H + C_3H_6$	$\rightarrow C_6H_6 + CH$	2.0×10^{-11}	10	100	By comparison with $C_2H + C_3H_6$, see also Berteloite et al. [2010b]
$C_4H + C_3H_6$	$\rightarrow C_7H_6 + H$	$1.6 \times 10^{-11} \times \exp(-4.04/T)$	10	100	By comparison with $C_2H + C_3H_6$, see also Berteloite et al. [2010b]
$C_4H + C_3H_8$	$\rightarrow C_4H_2 + C_3H_7$	$1.05 \times 10^{-10} \times (T/300)^{-1.35} \times \exp(-56.3/T)$	1.22	0	Berteloite et al. [2008]
$C_4H + C_4H$	$\rightarrow C_8H + H$	3.0×10^{-12}	10	100	By comparison with $C_2H + C_2H$
$C_4H + C_4H_2$	$\rightarrow C_8H_2 + H$	1.3×10^{-10}	10	100	By comparison with $C_4H + C_2H_2$
$C_4H + C_4H_3$	$\rightarrow C_4H_2 + C_4H_2$	1.6×10^{-12}	10	100	By comparison with $C_2H + C_2H_3$
$C_4H + C_4H_3$	$\rightarrow C_8H_3 + H$	3.0×10^{-11}	10	100	By comparison with $C_2H + C_2H_3$
$C_4H + C_6H_2$	$\rightarrow$ SOOTC	1.3×10^{-10}	10	100	By comparison with $C_4H + C_2H_2$
$C_4H + C_8H_2$	$\rightarrow$ SOOTC	1.3×10^{-10}	10	100	By comparison with $C_4H + C_2H_2$
C_4H_2X	$\rightarrow C_4H_2$	$1.0 \times 10^{+01}$	10	100	Vuitton et al. [2003]
$C_4H_2X + H_2$	$\rightarrow C_4H_2 + H_2$	1.4×10^{-15}	3	100	Zwier and Allen [1996]
$C_4H_2X + CH_4$	$\rightarrow C_4H_2 + CH_4$	1.4×10^{-15}	3	100	Zwier and Allen [1996]
$C_4H_2X + C_2H_2$	$\rightarrow C_6H_2 + H_2$	1.75×10^{-13}	3	100	Zwier and Allen [1996]
$C_4H_2X + C_2H_2$	$\rightarrow C_6H_2 + H + H$	1.75×10^{-13}	3	100	Zwier and Allen [1996]
$C_4H_2X + C_2H_4$	$\rightarrow C_6H_5 + H$	9.8×10^{-14}	3	100	Zwier and Allen [1996]
$C_4H_2X + C_2H_4$	$\rightarrow C_6H_4 + H_2$	3.69×10^{-13}	3	100	Zwier and Allen [1996]
$C_4H_2X + CH_3C_2H$	$\rightarrow C_7H_4 + H_2$	1.59×10^{-13}	3	100	Zwier and Allen [1996]
$C_4H_2X + CH_3C_2H$	$\rightarrow C_6H_2 + CH_3 + H$	2.31×10^{-13}	3	100	Zwier and Allen [1996]
$C_4H_2X + CH_3C_2H$	$\rightarrow C_5H_4 + C_2H_2$	2.46×10^{-13}	3	100	Zwier and Allen [1996]
$C_4H_2X + CH_3C_2H$	$\rightarrow C_5H_3 + C_2H_3$	8.68×10^{-13}	3	100	Zwier and Allen [1996]

Reactions		Rate coefficients	$F(300\ K)$	g	References
$C_4H_2X + C_3H_6$	$\rightarrow C_7H_6 + H_2$	1.63×10^{-13}	3	100	Zwier and Allen [1996]
$C_4H_2X + C_3H_6$	$\rightarrow C_6H_4 + CH_3 + H$	3.76×10^{-13}	3	100	Zwier and Allen [1996]
$C_4H_2X + C_3H_6$	$\rightarrow C_5H_6 + C_2H_2$	2.29×10^{-13}	3	100	Zwier and Allen [1996]
$C_4H_2X + C_3H_6$	$\rightarrow C_5H_5 + C_2H_3$	4.9×10^{-13}	3	100	Zwier and Allen [1996]
$C_4H_2X + C_4H_2$	$\rightarrow C_8H_2 + H + H$	2.57×10^{-13}	3	100	Zwier and Allen [1996]
$C_4H_2X + C_4H_2$	$\rightarrow C_8H_2 + H_2$	2.57×10^{-13}	3	100	Zwier and Allen [1996]
$C_4H_2X + C_4H_2$	$\rightarrow C_6H_2 + C_2H_2$	8.17×10^{-13}	3	100	Zwier and Allen [1996]
$C_4H_2X + C_4H_2$	$\rightarrow C_8H_3 + H$	1.0×10^{-12}	3	100	Zwier and Allen [1996]
$C_4H_2X + C_4H_6$	$\rightarrow C_6H_6 + C_2H_2$	8.8×10^{-13}	3	100	Zwier and Allen [1996]
$C_4H_2X + N_2$	$\rightarrow C_4H_2 + N_2$	1.4×10^{-15}	3	100	Zwier and Allen [1996]
$C_4H_3 + H_2$	$\rightarrow C_4H_4 + H$	$3.31 \times 10^{-14} \times (T/300)^{2.56} \times \exp(-2562/T)$	10	1000	By comparison with $C_2H_3 + H_2$
$C_4H_3 + CH_4$	$\rightarrow C_4H_4 + CH_3$	$2.13 \times 10^{-14} \times (T/300)^{4.02} \times \exp(-2750/T)$	10	1000	By comparison with $C_2H_3 + CH_4$
$C_4H_3 + C_2H_2$	$\rightarrow C_6H_5$	$k_0 = 2.55 \times 10^{-22} \times (T/300)^{-12.8} \times \exp(-5890/T)$	2	100	Wang and Frenklach [1994], Wang and Frenklach [1997], Westmoreland et al. [1989]
		$k_\infty = 4.09 \times 10^{-16} \times (T/300)^{0.47} \times \exp(-3020/T)$	2	100	
		$k_r = 0$	30	0	
$C_4H_3 + C_4H_3$	$\rightarrow C_4H_4 + C_4H_2$	3.5×10^{-11}	10	100	By comparison with $C_2H_3 + C_2H_3$ (Fahr et al. [1991], Laufer and Fahr [2004])
$C_4H_3 + C_4H_3$	$\rightarrow C_6H_5C_2H$	$k_0 = 1.13 \times 10^{-25} \times (T/300)^{-3.75} \times \exp(-494/T)$	10	100	k_0 by comparison with $CH_3 + CH_3$, k_∞ by comparison with $C_2H_3 + C_2H_3$
		$k_\infty = 1.2 \times 10^{-10}$	10	100	
		$k_r = 0$	30	0	
$C_4H_5 + H_2$	$\rightarrow C_4H_6 + H$	$4.0 \times 10^{-14} \times (T/300)^2 \times \exp(-2000/T)$	4	600	$6 \times k(C_2H_3 + H_2)$ from Knyazev et al. [1996a], Callear and Smith [1986], Weismann and Benson [1988]
$C_4H_5 + CH_4$	$\rightarrow C_4H_6 + CH_3$	$4.0 \times 10^{-14} \times (T/300)^2 \times \exp(-1600/T)$	4	600	By comparison with $C_2H_3 + CH_4$ and $C_4H_5 + H_2$
$C_4H_5 + C_2H_2$	$\rightarrow C_6H_6 + H$	$1.38 \times 10^{-12} \times (T/300)^{1.47} \times \exp(-2470/T)$	2	100	Westmoreland et al. [1989]
$C_6H + H_2$	$\rightarrow C_6H_2 + H$	$2.18 \times 10^{-12} \times (T/300)^{2.17} \times \exp(-478/T)$	2	100	By comparison with $C_2H + H_2$
$C_6H + CH_4$	$\rightarrow C_6H_2 + CH_3$	$1.2 \times 10^{-11} \times \exp(-491/T)$	10	100	By comparison with C_2H, $C_4H + CH_4$
$C_6H + C_2H_2$	$\rightarrow C_8H_2 + H$	1.3×10^{-10}	10	100	By comparison with C_2H, $C_4H + C_2H_2$
$C_6H + C_2H_6$	$\rightarrow C_6H_2 + C_2H_5$	$5.1 \times 10^{-11} \times \exp(-76/T)$	10	100	By comparison with C_2H, $C_4H + C_2H_6$
$C_6H + C_4H_2$	$\rightarrow$ SOOTC	1.3×10^{-10}	10	100	By comparison with $C_4H + C_4H_2$
$C_6H + C_6H_2$	$\rightarrow$ SOOTC	1.3×10^{-10}	10	100	By comparison with $C_4H + C_4H_2$
$C_6H + C_8H_2$	$\rightarrow$ SOOTC	1.3×10^{-10}	10	100	By comparison with $C_4H + C_4H_2$
$C_6H_5 + H_2$	$\rightarrow C_6H_6 + H$	$9.91 \times 10^{-14} \times (T/300)^{2.43} \times \exp(-3160/T)$	2	100	Mebel et al. [1997]
$C_6H_5 + C_2H_2$	$\rightarrow$ SOOTC + H	$3.25 \times 10^{-12} \times (T/300)^{0.21} \times \exp(-2520/T)$	2	100	Wang and Frenklach [1994]
$C_6H_5 + C_2H_2$	$\rightarrow$ SOOTC	$k_0 = 3.89 \times 10^{-29} \times (T/300)^{-4.08} \times \exp(403/T)$	2	100	Wang and Frenklach [1994]
		$k_\infty = 4.86 \times 10^{-13} \times (T/300)^{1.56} \times \exp(-1910/T)$	2	100	
		$k_r = 0$	30	0	
$C_6H_5 + C_6H_6$	$\rightarrow$ SOOTC + H	$1.35 \times 10^{-12} \times \exp(-2100/T)$	2	150	Park et al. [1999]
$N(^4S) + CH$	$\rightarrow CN + H$	$1.4 \times 10^{-10} \times (T/300)^{4.1}$	3	0	Daranlot et al. [2013]
$N(^4S) + {}^3CH_2$	$\rightarrow HCN + H$	$5.0 \times 10^{-11} \times (T/300)^{0.17}$	3	0	Hébrard et al. [2012]
$N(^4S) + {}^3CH_2$	$\rightarrow HNC + H$	$3.0 \times 10^{-11} \times (T/300)^{0.17}$	3	0	Hébrard et al. [2012]
$N(^4S) + CH_3$	$\rightarrow H_2CN + H$	5.6×10^{-11}	1.6	7	Hébrard et al. [2012]
$N(^4S) + CH_3$	$\rightarrow HCN + H + H$	6.0×10^{-12}	2	7	Hébrard et al. [2012]
$N(^4S) + C_2$	$\rightarrow CN + C$	2.0×10^{-10}	3	0	Capture rate constant Georgievskii and Klippenstein [2005] considering no barrier
$N(^4S) + C_2H$	$\rightarrow C_2N + H$	$2.0 \times 10^{-10} \times (T/300)^{0.17}$	3	0	Hébrard et al. [2012]
$N(^4S) + C_2H$	$\rightarrow HCN + C$	$8.0 \times 10^{-12} \times (T/300)^{0.17}$	3	0	Hébrard et al. [2012]
$N(^4S) + C_2H$	$\rightarrow HNC + C$	$4.0 \times 10^{-12} \times (T/300)^{0.17}$	3	0	Hébrard et al. [2012]
$N(^4S) + C_2H_3$	$\rightarrow CH_2CN + H$	$6.4 \times 10^{-11} \times (T/300)^{0.17}$	2	7	Payne et al. [1996]
$N(^4S) + C_2H_3$	$\rightarrow NH + C_2H_2$	$1.3 \times 10^{-11} \times (T/300)^{0.17}$	2	7	Payne et al. [1996]
$N(^4S) + C_2H_5$	$\rightarrow H_2CN + CH_3$	$6.0 \times 10^{-11} \times (T/300)^{0.17}$	2	7	Stief et al. [1995], Yang et al. [2005]
$N(^4S) + C_2H_5$	$\rightarrow NH + C_2H_4$	$4.0 \times 10^{-11} \times (T/300)^{0.17}$	3	21	Stief et al. [1995], Yang et al. [2005]
$N(^4S) + C_3$	$\rightarrow CN + C_2$	$1.0 \times 10^{-11} \times \exp(-1000/T)$	4	100	KIDA datasheet
$N(^4S) + l\text{-}C_3H$	$\rightarrow CN + C_2H$	$1.0 \times 10^{-10} \times (T/300)^{0.17}$	3	0	Calculs DFT (M06-2X/cc-pVTZ) + Georgievskii and Klippenstein [2005]
$N(^4S) + l\text{-}C_3H$	$\rightarrow C_3N + H$	$1.0 \times 10^{-10} \times (T/300)^{0.17}$	3	0	Calculs DFT (M06-2X/cc-pVTZ) + Georgievskii and Klippenstein [2005]
$N(^4S) + c\text{-}C_3H$	$\rightarrow CN + C_2H$	$1.0 \times 10^{-10} \times (T/300)^{0.17}$	3	0	Calculs DFT (M06-2X/cc-pVTZ) + Georgievskii and Klippenstein [2005]
$N(^4S) + c\text{-}C_3H$	$\rightarrow C_3N + H$	$1.0 \times 10^{-10} \times (T/300)^{0.17}$	3	0	Calculs DFT (M06-2X/cc-pVTZ) + Georgievskii and Klippenstein [2005]
$N(^4S) + t\text{-}C_3H_2$	$\rightarrow HC_3N + H$	4.0×10^{-11}	3	0	By comparison with $N + {}^3CH_2$
$N(^4S) + C_3H_3$	$\rightarrow H_2C_3N + H$	5.0×10^{-11}	4	0	Calculs DFT (M06-2X/cc-pVTZ) + Georgievskii and Klippenstein [2005]
$N(^4S) + C_3H_5$	$\rightarrow C_2H_3CN + H_2$	$3.2 \times 10^{-11} \times (T/300)^{0.17}$	3	0	By comparison with $N + C_2H_3$
$N(^4S) + C_3H_5$	$\rightarrow HCN + C_2H_4$	$3.2 \times 10^{-11} \times (T/300)^{0.17}$	3	0	By comparison with $N + C_2H_3$

Reactions		Rate coefficients	$F(300\ K)$	g	References
$N(^4S) + C_3H_5$	$\rightarrow NH + CH_2CCH_2$	$1.3 \times 10^{-11} \times (T/300)^{0.17}$	2	7	By comparison with $N + C_2H_3$
$N(^4S) + C_3H_7$	$\rightarrow H_2CN + C_2H_5$	1.0×10^{-10}	4	0	By comparison with $N + C_2H_5$
$N(^4S) + C_4H$	$\rightarrow C_4N + H$	$7.0 \times 10^{-11} \times (T/300)^{0.17}$	3	0	By comparison with $N + C_2H$
$N(^4S) + C_4H$	$\rightarrow CN + l\text{-}C_3H$	$1.0 \times 10^{-11} \times (T/300)^{0.17}$	3	0	By comparison with $N + C_2H$
$N(^4S) + C_4H$	$\rightarrow HC_3N + C$	$7.0 \times 10^{-11} \times (T/300)^{0.17}$	3	0	By comparison with $N + C_2H$
$N(^4S) + C_4H_3$	$\rightarrow CH_2C_3N + H$	6.0×10^{-11}	4	0	By comparison with $N + C_2H_3$
$N(^4S) + C_4H_3$	$\rightarrow NH + C_4H_2$	1.0×10^{-11}	4	0	By comparison with $N + C_2H_3$
$N(^4S) + C_4H_9$	$\rightarrow H_2CN + C_3H_7$	$6.0 \times 10^{-11} \times (T/300)^{0.17}$	2	7	By comparison with $N + C_2H_5$
$N(^4S) + C_4H_9$	$\rightarrow NH + C_4H_8$	$4.0 \times 10^{-11} \times (T/300)^{0.17}$	3	21	By comparison with $N + C_2H_5$
$N(^4S) + N(^4S)$	$\rightarrow N_2$	$k_0 = 4.1 \times 10^{-34}$	2.5	100	k_0 from Pravilov et al. [2001], k_∞ from
		$k_\infty = 1.0 \times 10^{-10}$	2	100	capture rate theory
		$k_r = 0$	30	0	
$N(^4S) + NH$	$\rightarrow N_2 + H$	$2.5 \times 10^{-11} \times (T/300)^{0.17}$	1.6	0	Hack et al. [1994], Caridade et al. [2005], Franckcombe and Nyman [2007], Georgievskii and Klippenstein [2005]
$N(^4S) + NH_2$	$\rightarrow N_2 + H + H$	$1.2 \times 10^{-10} \times (T/300)^{0.17}$	3	21	Whyte and Phillips [1983], Whyte and Phillips [1984], Dransfled and Wagner [1987]
$N(^4S) + CN$	$\rightarrow C + N_2$	$9 \times 10^{-11} \times (T/300)^{0.42}$	1.4	0	Daranlot et al. [2012]
$N(^4S) + H_2CN$	$\rightarrow N_2 + {}^3CH_2$	4.0×10^{-11}	2	0	Hébrard et al. [2012]
$N(^4S) + H_2CN$	$\rightarrow HCN + NH$	5.0×10^{-12}	2	0	Hébrard et al. [2012]
$N(^4S) + C_2N$	$\rightarrow CN + CN$	1.0×10^{-10}	3	0	Whyte and Phillips [1983], Daranlot et al. [2012]
$N(^4S) + CHCN$	$\rightarrow HCN + CN$	$1.4 \times 10^{-11} \times (T/300)^{0.17}$	4	21	By comparison with $N + {}^3CH_2$
$N(^4S) + CHCN$	$\rightarrow HNC + CN$	$6.0 \times 10^{-12} \times (T/300)^{0.17}$	4	21	By comparison with $N + {}^3CH_2$
$N(^4S) + CHCN$	$\rightarrow C_2N_2 + H$	$4.0 \times 10^{-11} \times (T/300)^{0.17}$	4	21	By comparison with $N + {}^3CH_2$
$N(^4S) + CH_2CN$	$\rightarrow H_2CN + CN$	2.0×10^{-11}	3	0	By comparison with $N + CH_3$, C_2H_5
$N(^4S) + CH_2CN$	$\rightarrow HC_2N_2 + H$	2.0×10^{-11}	3	0	By comparison with $N + CH_3$, C_2H_5
$N(^4S) + C_4N$	$\rightarrow C_3N + CN$	9×10^{-11}	3	0	Capture rate constant, Georgievskii and Klippenstein [2005] considering no barrier
$N(^4S) + HC_4N$	$\rightarrow C_4N_2 + H$	4.0×10^{-11}	3	0	By comparison with $N + {}^3CH_2$
$N(^4S) + HC_4N$	$\rightarrow C_3N + HCN$	2.0×10^{-11}	3	0	By comparison with $N + {}^3CH_2$
$N(^4S) + CH_2C_3N$	$\rightarrow HC_3N + HCN$	4.0×10^{-11}	3	0	By comparison with $N + CH_3$
$N(^4S) + CN_2$	$\rightarrow CN + N_2$	$6.0 \times 10^{-11} \times (T/300)^{0.17}$	3	21	Capture rate constant, Georgievskii and Klippenstein [2005] considering no barrier
$N(^2D)$	$\rightarrow N(^4S)$	2.3×10^{-05}	2	100	Okabe et al. [1978]
$N(^2D) + H_2$	$\rightarrow NH + H$	$4.2 \times 10^{-11} \times \exp(-880/T)$	1.6	7	Herron [1999]
$N(^2D) + CH_4$	$\rightarrow NH + CH_3$	$1.3 \times 10^{-11} \times \exp(-755/T)$	1.6	7	Herron [1999], Takayanagi and Kurosaki [1999], Takayanagi et al. [1999], Balucani et al. [2009], Ouk et al. [2011]
$N(^2D) + CH_4$	$\rightarrow CH_2NH + H$	$3.5 \times 10^{-11} \times \exp(-755/T)$	1.6	7	Herron [1999], Takayanagi and Kurosaki [1999], Takayanagi et al. [1999], Balucani et al. [2009], Ouk et al. [2011]
$N(^2D) + C_2H_2$	$\rightarrow CHCN + H$	$1.6 \times 10^{-10} \times \exp(-270/T)$	1.4	0	Takayanagi et al. [1998], Herron [1999]
$N(^2D) + C_2H_4$	$\rightarrow CH_2NCH + H$	$1.7 \times 10^{-10} \times \exp(-503/T)$	2	200	Takayanagi et al. [1998], Sato et al. [1999], Balucani et al. [2000a], Balucani et al. [2000b], Lee et al. [2011], Balucani et al. [2012]
$N(^2D) + C_2H_4$	$\rightarrow cCH_2NCH + H$	$6.0 \times 10^{-11} \times \exp(-503/T)$	2	200	Takayanagi et al. [1998], Sato et al. [1999], Balucani et al. [2000a], Balucani et al. [2000b], Lee et al. [2011], Balucani et al. [2012]
$N(^2D) + C_2H_6$	$\rightarrow CH_2NH + CH_3$	1.9×10^{-11}	1.6	7	Herron [1999], Balucani et al. [2010]
$N(^2D) + C_3$	$\rightarrow CN + C_2$	$2.3 \times 10^{-10} \times \exp(-503/T)$	3	0	By comparison with $N(^4S) + C_2H_4$
$N(^2D) + c\text{-}C_3H_2$	$\rightarrow HC_3N + H$	$1.6 \times 10^{-10} \times \exp(-270/T)$	3	0	By comparison with $N(^4S) + C_2H_2$
$N(^2D) + l\text{-}C_3H_2$	$\rightarrow HC_3N + H$	$1.6 \times 10^{-10} \times \exp(-270/T)$	3	0	By comparison with $N(^4S) + C_2H_2$
$N(^2D) + t\text{-}C_3H_2$	$\rightarrow HC_3N + H$	$1.6 \times 10^{-10} \times \exp(-270/T)$	3	0	By comparison with $N(^4S) + C_2H_2$
$N(^2D) + CH_3C_2H$	$\rightarrow CHCN + CH_3$	$8.0 \times 10^{-11} \times \exp(-270/T)$	3	0	By comparison with $N(^4S) + C_2H_2$
$N(^2D) + CH_3C_2H$	$\rightarrow C_2H_3CN + H$	$8.0 \times 10^{-11} \times \exp(-270/T)$	3	0	By comparison with $N(^4S) + C_2H_2$
$N(^2D) + CH_2CCH_2$	$\rightarrow C_2H_3CN + H$	$2.3 \times 10^{-10} \times \exp(-503/T)$	1.4	0	By comparison with $N(^4S) + C_2H_4$
$N(^2D) + C_3H_6$	$\rightarrow SOOTN$	$2.3 \times 10^{-10} \times \exp(-503/T)$	3	0	By comparison with $N(^4S) + C_2H_4$
$N(^2D) + C_3H_8$	$\rightarrow CH_2NH + C_2H_5$	3.0×10^{-11}	3	0	By comparison with $N(^4S) + C_2H_6$
$N(^2D) + C_4H_2$	$\rightarrow HCN + c\text{-}C_3H$	$4.0 \times 10^{-11} \times \exp(-270/T)$	3	0	By comparison with $N(^4S) + C_2H_2$
$N(^2D) + C_4H_2$	$\rightarrow HCN + l\text{-}C_3H$	$4.0 \times 10^{-11} \times \exp(-270/T)$	3	0	By comparison with $N(^4S) + C_2H_2$
$N(^2D) + C_4H_2$	$\rightarrow HC_4N + H$	$8.0 \times 10^{-11} \times \exp(-270/T)$	3	0	By comparison with $N(^4S) + C_2H_2$
$N(^2D) + C_4H_4$	$\rightarrow SOOTN$	$1.6 \times 10^{-10} \times \exp(-270/T)$	3	0	By comparison with $N(^4S) + C_2H_2$
$N(^2D) + C_4H_6$	$\rightarrow C_4H_4NH + H$	$1.6 \times 10^{-10} \times \exp(-270/T)$	3	0	By comparison with $N(^4S) + C_2H_2$
$N(^2D) + C_4H_8$	$\rightarrow C_4H_6NH + H$	$2.3 \times 10^{-10} \times \exp(-503/T)$	3	0	By comparison with $N(^4S) + C_2H_4$
$N(^2D) + C_4H_{10}$	$\rightarrow CH_2NH + C_3H_7$	3.0×10^{-11}	3	0	By comparison with $N(^4S) + C_2H_6$
$N(^2D) + C_6H_4$	$\rightarrow C_5H_3CN + H$	$2.3 \times 10^{-10} \times \exp(-503/T)$	1.4	0	By comparison with $N(^4S) + C_2H_4$
$N(^2D) + Ar$	$\rightarrow N(^4S) + Ar$	1.0×10^{-16}	2	100	Lin and Kaufman [1971]
$N(^2D) + N_2$	$\rightarrow N(^4S) + N_2$	$1.0 \times 10^{-13} \times \exp(-520/T)$	2	42	Herron [1999]
$N(^2D) + NH_3$	$\rightarrow N_2H_2 + H$	5.0×10^{-11}	2	21	Herron [1999]
$N(^2D) + HCN$	$\rightarrow CH + N_2$	5.0×10^{-11}	3	0	Hébrard et al. [2012]

Reactions		Rate coefficients	$F(300\ K)$	g	References
$N(^2D) + HNC$	$\rightarrow CN_2 + H$	2.0×10^{-11}	3	0	Hébrard et al. [2012]
$N(^2D) + HNC$	$\rightarrow CH + N_2$	2.0×10^{-11}	3	0	Hébrard et al. [2012]
$N(^2D) + CH_2NH$	$\rightarrow H_2CNN + H$	$1.0 \times 10^{-10} \times \exp(-503/T)$	2	100	Estimated by comparison with $N(^2D) + C_2H_4$ et $N(^2D) + NH_3$ (Takayanagi et al. [1998], Sato et al. [1999], Balucani et al. [2000a], Balucani et al. [2000b], Lee et al. [2011])
$N(^2D) + CH_2NH$	$\rightarrow HNCNH + H$	$1.0 \times 10^{-10} \times \exp(-503/T)$	2	100	Estimated by comparison with $N(^2D) + C_2H_4$ et $N(^2D) + NH_3$ (Takayanagi et al. [1998], Sato et al. [1999], Balucani et al. [2000a], Balucani et al. [2000b], Lee et al. [2011])
$N(^2D) + CH_3NH_2$	$\rightarrow CH_3NNH + H$	2.0×10^{-11}	4	0	By comparison with $N(^2D) + C_2H_6$
$N(^2D) + CH_3NH_2$	$\rightarrow HNCHNH_2 + H$	3.0×10^{-11}	4	0	By comparison with $N(^2D) + NH_3$
$N(^2D) + CH_3CN$	$\rightarrow CH_2CN + NH$	$1.3 \times 10^{-11} \times \exp(-755/T)$	4	100	By comparison with $N(^2D) + CH_4$
$N(^2D) + CH_3CN$	$\rightarrow HNCHCN + H$	$3.5 \times 10^{-11} \times \exp(-755/T)$	4	100	By comparison with $N(^2D) + CH_4$
$N(^2D) + CH_3CN$	$\rightarrow N_2 + C_2H_3$	5.0×10^{-11}	4	0	By comparison with $N(^2D) + HCN$
$N(^2D) + cCH_2NCH$	$\rightarrow N_2 + C_2H_3$	$2.3 \times 10^{-10} \times \exp(-503/T)$	3	100	By comparison with $N(^2D) + C_2H_4$
$N(^2D) + HC_3N$	$\rightarrow N_2 + c{-}C_3H$	1.5×10^{-11}	4	100	By comparison with $N(^2D) + HCN$, C_2H_2
$N(^2D) + HC_3N$	$\rightarrow N_2 + l{-}C_3H$	1.5×10^{-11}	4	100	By comparison with $N(^2D) + HCN$, C_2H_2
$N(^2D) + HC_3N$	$\rightarrow C_2N + HCN$	3.0×10^{-11}	4	100	By comparison with $N(^2D) + HCN$, C_2H_2
$N(^2D) + HC_5N$	$\rightarrow N_2 + C_5H$	3.0×10^{-11}	4	100	By comparison with $N(^2D) + HCN$, C_2H_2
$N(^2D) + HC_5N$	$\rightarrow C_4N + HCN$	3.0×10^{-11}	4	100	By comparison with $N(^2D) + HCN$, C_2H_2
$N(^2D) + C_2H_3CN$	$\rightarrow HNCCHCN + H$	$2.3 \times 10^{-10} \times \exp(-503/T)$	3	0	By comparison with $N(^2D) + C_2H_4$
$N(^2D) + C_2H_3CN$	$\rightarrow N_2 + C_3H_3$	4.0×10^{-11}	4	0	By comparison with $N(^2D) + HCN$
$N(^2D) + C_2H_5CN$	$\rightarrow CH_2NH + CH_2CN$	1.9×10^{-11}	4	100	By comparison with $N(^2D) + C_2H_6$
$N(^2D) + C_2H_5CN$	$\rightarrow C_3H_5 + N_2$	4.0×10^{-11}	4	100	By comparison with $N(^2D) + HCN$
$N(^2D) + CH_3C_3N$	$\rightarrow SOOTN$	3.0×10^{-11}	4	100	By comparison with $N(^2D) + HCN$, C_2H_2
$N(^2D) + C_2N_2$	$\rightarrow C_2N + N_2$	3.0×10^{-11}	4	100	By comparison with $N(^2D) + HCN$, C_2H_4
$N(^2D) + C_4N_2$	$\rightarrow C_4N + N_2$	3.0×10^{-11}	4	100	By comparison with $N(^2D) + HCN$, C_2H_4
$NH + H$	$\rightarrow N(^4S) + H_2$	$2.2 \times 10^{-12} \times (T/300)^{1.55} \times \exp(-103/T)$	2	7	Adam et al. [2005]
$NH + CH$	$\rightarrow HCN + H$	5.0×10^{-11}	3	0	Takahashi and Takayanagi [2007], Georgievskii and Klippenstein [2005]
$NH + CH$	$\rightarrow HNC + H$	5.0×10^{-11}	3	0	Takahashi and Takayanagi [2007], Georgievskii and Klippenstein [2005]
$NH + {}^3CH_2$	$\rightarrow H_2CN + H$	3.0×10^{-11}	3	21	Capture rate constant, Georgievskii and Klippenstein [2005] considering no barrier and branching ratio deduced from H_2CNH decomposition, Nguyen et al. [1996], Zhou and Schlegel [2009], Georgievskii and Klippenstein [2005]
$NH + {}^3CH_2$	$\rightarrow HCN + H + H$	3.0×10^{-11}	3	21	Capture rate constant, Georgievskii and Klippenstein [2005] considering no barrier and branching ratio deduced from H_2CNH decomposition, Nguyen et al. [1996], Zhou and Schlegel [2009], Georgievskii and Klippenstein [2005]
$NH + {}^3CH_2$	$\rightarrow HNC + H_2$	5.0×10^{-12}	4	21	Capture rate constant, Georgievskii and Klippenstein [2005] considering no barrier and branching ratio deduced from H_2CNH decomposition, Nguyen et al. [1996], Zhou and Schlegel [2009], Georgievskii and Klippenstein [2005]
$NH + CH_3$	$\rightarrow CH_2NH + H$	$1.3 \times 10^{-10} \times (T/300)^{0.17}$	2	100	Redondo et al. [2006], Georgievskii and Klippenstein [2005]
$NH + C_2$	$\rightarrow HNC + C$	1.0×10^{-10}	3	0	Takahashi and Takayanagi [2007], Georgievskii and Klippenstein [2005]
$NH + C_2H$	$\rightarrow CHCN + H$	1.0×10^{-10}	3	7	Takahashi et al. [1998], Georgievskii and Klippenstein [2005]
$NH + C_2H_2$	$\rightarrow CH_2CN + H$	$8.3 \times 10^{-10} \times \exp(-7096/T)$	3	100	Rohrig and Wagner [1994a], Rohrig and Wagner [1994b], Feng et al. [2007]. Likely experimental artefact in Mullen and Smith [2005]
$NH + C_2H_3$	$\rightarrow CH_3CN + H$	1.0×10^{-10}	4	21	Lee et al. [2011], Georgievskii and Klippenstein [2005]
$NH + C_2H_3$	$\rightarrow HNC + CH_3$	1.0×10^{-11}	6	21	Lee et al. [2011], Georgievskii and Klippenstein [2005]
$NH + C_2H_3$	$\rightarrow NH_2 + C_2H_2$	1.0×10^{-11}	4	100	Lee et al. [2011], Georgievskii and Klippenstein [2005]
$NH + C_2H_4$	$\rightarrow H_2CN + CH_3$	$3.0 \times 10^{-12} \times \exp(-6735/T)$	3	100	Yang et al. [2005]. Likely experimental artefact in Mullen and Smith [2005]
$NH + C_2H_5$	$\rightarrow NH_2 + C_2H_4$	1.0×10^{-11}	4	100	By comparison with $NH + CH_3$
$NH + C_2H_5$	$\rightarrow CH_3CHNH + H$	$6.0 \times 10^{-11} \times (T/300)^{0.17}$	3	21	By comparison with $NH + CH_3$
$NH + c{-}C_3H_2$	$\rightarrow H_2C_3N + H$	1.0×10^{-11}	10	100	Value in the 150-190 K range

Reactions		Rate coefficients	$F(300\ K)$	g	References
$NH + C_3H_3$	$\rightarrow C_2H_3CN + H$	1.0×10^{-10}	4	0	Capture rate constant, Georgievskii and Klippenstein [2005] as there is no barrier at DFT (M06-2X/cc-pVTZ) and MP2/cc-pVTZ level.
$NH + NH$	$\rightarrow N_2 + H + H$	2.0×10^{-10}	3	7	Mertens et al. [1989], Xu et al. [1997]
$NH + NH_2$	$\rightarrow N_2H_2 + H$	$1.0 \times 10^{-10} \times (T/300)^{0.17}$	3	21	Dransfeld et al. [1984], Bahng and Macdonald [2009]
$NH + CN$	$\rightarrow CN_2 + H$	1.0×10^{-10}	2	100	Georgievskii and Klippenstein [2005], Berman et al. [2005]
$NH + CN$	$\rightarrow N_2 + CH$	1.0×10^{-10}	2	100	Georgievskii and Klippenstein [2005], Berman et al. [2005]
$NH + H_2CN$	$\rightarrow NH_2 + HCN$	2.0×10^{-11}	4	21	Capture rate constant, Georgievskii and Klippenstein [2005] as there is no barrier at DFT (M06-2X/cc-pVTZ) level.
$NH + H_2CN$	$\rightarrow H_2CNN + H$	2.0×10^{-11}	4	0	Capture rate constant, Georgievskii and Klippenstein [2005] as there is no barrier at DFT (M06-2X/cc-pVTZ) level.
$NH_2 + H$	$\rightarrow NH_3$	$k_0 = 1.0 \times 10^{-33}$	10	100	k_0 from Schofield et al. [1973], k_∞ from
		$k_\infty = 3.5 \times 10^{-12}$	2	100	Pagsberg et al. [1979]
		$k_r = 0$	30	0	
$NH_2 + H_2$	$\rightarrow NH_3 + H$	$2.09 \times 10^{-12} \times \exp(-4280/T)$	12	100	Demissy and Lesclaux [1980]
$NH_2 + H$	$\rightarrow NH + H_2$	$2.0 \times 10^{-11} \times \exp(-2400/T)$	2	100	Linder et al. [1995], Bahng and Macdonald [2009]
$NH_2 + C$	$\rightarrow HCN + H$	$3.0 \times 10^{-11} \times (T/300)^{-0.2} \times \exp(6/T)$	3	0	Talbi [1999], Herbst et al. [2000]
$NH_2 + C$	$\rightarrow HNC + H$	$3.0 \times 10^{-11} \times (T/300)^{-0.2} \times \exp(6/T)$	3	0	Talbi [1999], Herbst et al. [2000]
$NH_2 + CH_3$	$\rightarrow CH_3NH_2$	$k_0 = 1.8 \times 10^{-27} \times (T/300)^{-3.85}$	2	7	Jodkowski et al. [1995], Xu et al. [1999]
		$k_\infty = 1.3 \times 10^{-10} \times (T/300)^{0.42}$	2	7	
		$k_r = 0$	30	0	
$NH_2 + CH_4$	$\rightarrow NH_3 + CH_3$	$3.99 \times 10^{-14} \times (T/300)^{3.59} \times \exp(-4540/T)$	5	200	Mebel and Lin [1999]
$NH_2 + C_2H_2$	$\rightarrow NH_3 + C_2H$	$1.11 \times 10^{-13} \times \exp(-1850/T)$	5	250	Bosco et al. [1984]
$NH_2 + C_2H_3$	$\rightarrow NH_3 + C_2H_2$	2.0×10^{-11}	10	21	By comparison with $NH_2 + H_2CN$ and $CH_3 + C_2H_3$
$NH_2 + C_2H_3$	$\rightarrow C_2H_3NH + H$	8.0×10^{-11}	3	0	By comparison with $NH_2 + H_2CN$ and $CH_3 + C_2H_3$
$NH_2 + C_2H_4$	$\rightarrow NH_3 + C_2H_3$	$3.42 \times 10^{-14} \times \exp(-1320/T)$	1.1	100	Bosco et al. [1984]
$NH_2 + C_2H_5$	$\rightarrow NH_3 + C_2H_4$	1.0×10^{-11}	10	21	By comparison with $NH_2 + H_2CN$ and $NH_2 + CH_3$
$NH_2 + C_2H_5$	$\rightarrow CH_3NH + CH_3$	6.0×10^{-11}	3	0	By comparison with $NH_2 + H_2CN$ and $NH_2 + CH_3$
$NH_2 + C_2H_6$	$\rightarrow NH_3 + C_2H_5$	$6.14 \times 10^{-13} \times \exp(-3600/T)$	2	100	Lesclaux and Demissy [1978]
$NH_2 + NH_2$	$\rightarrow N_2H_4$	$k_0 = 5.7 \times 10^{-29}$	2	100	Fagerström et al. [1995], Bahnd and
		$k_\infty = 8.0 \times 10^{-11}$	1.6	100	Macdonald [2008], Stothard et al. [1995],
		$k_r = 0$	30	0	Klippenstein et al. [2009], Altiney and Macdonald [2012], Asatryan et al. [2012]
$NH_2 + N_2H_2$	$\rightarrow NH_3 + N_2H$	$1.62 \times 10^{-15} \times (T/300)^{4.05} \times \exp(-810/T)$	2	100	Linder et al. [1996]
$NH_2 + N_2H_4$	$\rightarrow N_2H_3 + NH_3$	$2.0 \times 10^{-11} \times \exp(-1100/T)$	2	100	von Gehring at al [1971], Li and Zhang [2006]
$NH_2 + H_2CN$	$\rightarrow HCN + NH_3$	$5.4 \times 10^{-11} \times (T/300)^{-1.1} \times \exp(-60/T)$	3	0	Yelle et al. [2010]
$NH_2 + H_2CN$	$\rightarrow H_2CNNH_2$	$k_0 = 1.0 \times 10^{-28} \times (T/300)^{-3.5}$	10	0	Yelle et al. [2010]
		$k_\infty = 1.0 \times 10^{-10}$	3	0	
		$k_r = 0$	30	0	
$NH_3 + H$	$\rightarrow NH_2 + H_2$	$4.23 \times 10^{-14} \times (T/300)^{3.93} \times \exp(-4060/T)$	5	100	Espinosa-Garcia et al. [1994]
$NH_3 + CH$	$\rightarrow CH_2NH + H$	$1.69 \times 10^{-10} \times (T/300)^{-0.56} \times \exp(-28/T)$	1.6	0	Zabarnick et al. [1989a], Bocherel et al. [1996], Blitz et al. [2012]
$NH_3 + CH_3$	$\rightarrow NH_2 + CH_4$	$5.1 \times 10^{-14} \times (T/300)^{2.86} \times \exp(-7340/T)$	2	100	Yu et al. [1998]
$NH_3 + C_2H$	$\rightarrow NH_2 + C_2H_2$	$2.9 \times 10^{-11} \times (T/300)^{-0.9}$	1.4	0	Nizamov et al. [2004]
$N_2H + H$	$\rightarrow N_2 + H_2$	$1.0 \times 10^{-10} \times (T/300)^{0.17}$	2	100	Glarborg et al. [1995], Georgievskii and Klippenstein [2005]
$N_2H_2 + H$	$\rightarrow N_2H + H_2$	$4.58 \times 10^{-13} \times (T/300)^{2.63} \times \exp(-115/T)$	2	100	Linder et al. [1996]
$N_2H_3 + H$	$\rightarrow NH_2 + NH_2$	$8.0 \times 10^{-11} \times \exp(-1000/T)$	2	100	Gehring et al. [1971], Konnov and de Ruyck [2001]
$N_2H_3 + H$	$\rightarrow N_2H_2 + H_2$	1.7×10^{-11}	3	21	Gehring et al. [1971], Konnov and de Ruyck [2001]
$N_2H_3 + N_2H_3$	$\rightarrow N_2H_4 + N_2 + H_2$	6.0×10^{-11}	2	100	Atreya et al. [1986]
$N_2H_4 + H$	$\rightarrow N_2H_3 + H_2$	$9.86 \times 10^{-12} \times \exp(-1200/T)$	1.2	100	Stief and Payne [1976]
$N_2H_4 + CH_3$	$\rightarrow N_2H_3 + CH_4$	$1.66 \times 10^{-13} \times \exp(-2520/T)$	2	100	Gray and Thynne [1965]
$CN + H$	$\rightarrow HCN$	$k_0 = 8.52 \times 10^{-30} \times (T/300)^{-2.2} \times \exp(-567/T)$	10	100	Tsang et al. [1992]
		$k_\infty = 1.73 \times 10^{-10} \times (T/300)^{-0.5}$	10	100	
		$k_r = 0$	30	0	
$CN + H_2$	$\rightarrow HCN + H$	$4.12 \times 10^{-13} \times (T/300)^{2.87} \times \exp(-820/T)$	1.6	50	Sun et al. [1990]
$CN + CH$	$\rightarrow C_2N + H$	$1.0 \times 10^{-10} \times (T/300)^{-0.17}$	3	0	Mebel and Kaiser [2002], Takahashi and Takayanagi [2006], Georgievskii and Klippenstein [2005]

Reactions		Rate coefficients	$F(300\ K)$	g	References
CN + CH	→ HCN + C	$1.0 \times 10^{-10} \times (T/300)^{-0.17}$	3	0	Mebel and Kaiser [2002], Takahashi and Takayanagi [2006], Georgievskii and Klippenstein [2005]
CN + $^3CH_2$	→ HCN + CH	5.0×10^{-11}	3	0	Takahashi et al. [1998], Du et al. [2005], Osamura and Petrie [2004], Georgievskii and Klippenstein [2005]
CN + $^3CH_2$	→ CHCN + H	5.0×10^{-11}	3	0	Takahashi et al. [1998], Du et al. [2005], Osamura and Petrie [2004], Georgievskii and Klippenstein [2005]
CN + $^3CH_2$	→ C_2N + H_2	5.0×10^{-11}	3	0	Takahashi et al. [1998], Du et al. [2005], Osamura and Petrie [2004], Georgievskii and Klippenstein [2005]
CN + CH_3	→ CH_2CN + H	1.0×10^{-10}	3	21	Yang et al. [2005], Georgievskii and Klippenstein [2005]
CN + CH_4	→ HCN + CH_3	$6.2 \times 10^{-12} \times \exp(-721/T)$	1.6	0	Sims et al. [1993], Yang et al. [1993], Huang et al. [2008]
CN + C_2H_2	→ HC_3N + H	$2.72 \times 10^{-10} \times (T/300)^{-0.52} \times \exp(-19/T)$	1.4	0	Sims et al. [1993], Gannon et al. [2007]
CN + C_2H_4	→ C_2H_3CN + H	$2.67 \times 10^{-10} \times (T/300)^{-0.69} \times \exp(-31/T)$	1.4	0	Sims et al. [1993], Gannon et al. [2007]
CN + C_2H_6	→ HCN + C_2H_5	$2.08 \times 10^{-11} \times (T/300)^{0.22} \times \exp(58/T)$	1.4	0	Sims et al. [1993]
CN + c−C_3H_2	→ HC_4N + H	2.0×10^{-10}	4	0	Wang et al. [2006], Georgievskii and Klippenstein [2005]
CN + l−C_3H_2	→ HC_4N + H	2.0×10^{-10}	4	0	Wang et al. [2006], Georgievskii and Klippenstein [2005]
CN + t−C_3H_2	→ HC_4N + H	2.0×10^{-10}	4	0	Wang et al. [2006], Georgievskii and Klippenstein [2005]
CN + CH_3C_2H	→ HC_3N + CH_3	1.0×10^{-10}	1.6	7	By comparison with CN + C_2H_2
CN + CH_3C_2H	→ CH_3C_3N + H	1.0×10^{-10}	1.6	7	By comparison with CN + C_2H_2
CN + CH_2CCH_2	→ HC_3N + CH_3	1.0×10^{-10}	1.6	7	By comparison with CN + C_2H_2 and C_2H_4
CN + CH_2CCH_2	→ CH_3C_3N + H	1.0×10^{-10}	1.6	7	By comparison with CN + C_2H_2 and C_2H_4
CN + C_3H_6	→ C_3H_5CN + H	1.5×10^{-10}	1.6	7	Sims et al. [1993]
CN + C_3H_6	→ C_2H_3CN + CH_3	1.5×10^{-10}	1.6	7	Sims et al. [1993]
CN + C_3H_8	→ HCN + C_3H_7	$2.14 \times 10^{-11} \times (T/300)^{1.19} \times \exp(378/T)$	1.4	0	Yang et al. [1992]
CN + C_4H_2	→ HC_5N + H	4.0×10^{-10}	1.6	0	Seki [1996]
CN + C_4H_4	→ C_4H_3CN + H	2.0×10^{-10}	2	0	By comparison with CN + C_2H_4
CN + C_4H_6	→ SOOTN	$2.57 \times 10^{-10} \times \exp(169/T)$	1.6	40	Butterfield et al. [1993]
CN + C_4H_8	→ C_2H_3CN + C_2H_5	1.5×10^{-10}	2	0	By comparison with CN + C3H6
CN + C_4H_{10}	→ HCN + C_4H_9	$2.14 \times 10^{-11} \times (T/300)^{1.19} \times \exp(378/T)$	1.4	0	By comparison with CN + C_3H_8
CN + C_6H_6	→ C_6H_5CN + H	2.8×10^{-10}	1.6	0	Bullock and Cooper [1971]
CN + NH_3	→ HCN + NH_2	$2.77 \times 10^{-11} \times (T/300)^{-1.14}$	1.4	0	Meads et al. [1993], Sims et al. [1994], Blitz et al. [2009], Talbi and Smith [2009]
CN + CN	→ C_2N_2	$k_0 = 3.22 \times 10^{-29} \times (T/300)^{-2.61}$	3	100	Tsang et al. [1992]
		$k_\infty = 9.4 \times 10^{-12}$	3	100	
		$k_r = 0$	30	0	
CN + HCN	→ C_2N_2 + H	$4.3 \times 10^{-13} \times (T/300)^{1.71} \times \exp(-770/T)$	1.4	60	Yang et al. [1992a]
CN + HNC	→ C_2N_2 + H	2.0×10^{-10}	4	0	Petrie and Osamura [2004], Georgievskii and Klippenstein [2005]
CN + CH_2NH	→ NCCHNH + H	5.0×10^{-11}	4	0	By comparison with CN + C_2H_4
CN + CH_2NH	→ H_2CNCN + H	5.0×10^{-11}	4	0	By comparison with CN + C_2H_4
CN + CH_3NH_2	→ CH_3NH + HCN	8.0×10^{-11}	3	0	By comparison with CN + NH_3, C_2H_6
CN + CH_3CN	→ C_2N_2 + CH_3	$4.0 \times 10^{-11} \times \exp(-1190/T)$	1.6	71	Zabarnick [1989]
CN + CH_3CN	→ CH_2CN + HCN	$2.46 \times 10^{-11} \times \exp(-1190/T)$	1.6	71	Zabarnick [1989]
CN + cCH_2NCH	→ SOOTN	3.0×10^{-11}	10	100	By comparison with CN + C_2H_4
CN + C_2H_3CN	→ $C_4N_2H_2$ + H	$3.02 \times 10^{-11} \times \exp(103/T)$	1.6	50	Butterfield et al. [1993]
CN + C_2H_5CN	→ C_2H_4CN + HCN	$2.08 \times 10^{-11} \times (T/300)^{0.22} \times \exp(58/T)$	3	100	By comparison with CN + C_2H_6
CN + C_3N	→ C_4N_2	$k_0 = 3.22 \times 10^{-29} \times (T/300)^{-2.61}$	10	100	By comparison with CN + CN
		$k_\infty = 9.4 \times 10^{-12}$	10	100	
		$k_r = 0$	30	0	
CN + HC_3N	→ C_4N_2 + H	$1.79 \times 10^{-11} \times (T/300)^{-0.67}$	1.6	0	Cheikh Sid Ely [2013]
CN + HC_5N	→ C_6N_2 + H	$3.0 \times 10^{-11} \times (T/300)^{-0.7}$	2	0	By comparison with CN + HC_3N
CN + C_4N_2	→ SOOTN	$k_0 = 1.0 \times 10^{-26}$	10	0	k_0 by comparison with CH_3 + CH_3, k_∞ from
		$k_\infty = 3.0 \times 10^{-11}$	3	0	CN + HC_3N
		$k_r = 0$	30	0	
HCN + H	→ H_2CN	$k_0 = 1.0 \times 10^{-34}$	30	100	DFT (M06-2X/cc-pVTZ)/RRKM calculations
		$k_\infty = 9.8 \times 10^{-12} \times \exp(-2076/T)$	4	100	(this work), see also Sumathi and Nguyen
		$k_r = 0$	30	0	[1998], Jiang and Guo [2013]
HCN + CH	→ CHCN + H	$1.4 \times 10^{-10} \times (T/300)^{-0.17}$	2	21	Zabarnick et al. [1991], Du and Zhang [2006], Osamura and Petrie [2004]
HCN + CH	→ C_2N + H_2	$1.4 \times 10^{-10} \times (T/300)^{-0.17}$	2	21	Zabarnick et al. [1991], Du and Zhang [2006], Osamura and Petrie [2004]
HCN + $^3CH_2$	→ CH_2CN + H	$1.5 \times 10^{-12} \times \exp(-3330/T)$	2	100	By comparison with $^3CH_2$ + alkynes
HCN + C_2	→ C_3N + H	$2.0 \times 10^{-10} \times (T/300)^{0.17}$	3	0	Silva et al. [2009], Georgievskii and Klippenstein [2005]

Reactions		Rate coefficients	$F(300\ K)$	g	References
HCN + C_2H	$\rightarrow HC_3N$ + H	$5.3 \times 10^{-12} \times \exp(-769/T)$	1.4	0	Fukuzawa and Osamura [1997], Hoobler and Leone [1997]
HCN + C_2H_3	$\rightarrow C_2H_3CN$ + H	$1.0 \times 10^{-12} \times \exp(-2300/T)$	10	400	DFT (M06-2X/cc-pVTZ) + TST calculations, This work
HCN + C_4H	$\rightarrow HC_5N$ + H	$5.3 \times 10^{-12} \times \exp(-769/T)$	1.4	0	By comparison with C_2H + HCN
HCN + C_3N	$\rightarrow C_4N_2$ + H	1.0×10^{-11}	10	100	Petrie [2004]
HNC + H	$\rightarrow$ HCN + H	$3.0 \times 10^{-11} \times \exp(-800/T)$	10	100	Talbi and Ellinger [1996], Sumathi and Nguyen [1998], Petrie [2002], Hébrard et al. [2012]
HNC + C	$\rightarrow$ HCN + C	1.6×10^{-10}	3	0	Bergeat and loison, submitted
HNC + C	$\rightarrow C_2N$ + H	4.0×10^{-11}	3	0	Bergeat and loison, submitted
HNC + CH	$\rightarrow$ CHCN + H	$1.4 \times 10^{-10} \times (T/300)^{-0.17}$	3	21	Hébrard et al. [2012]
HNC + CH	$\rightarrow C_2N + H_2$	$1.4 \times 10^{-10} \times (T/300)^{-0.17}$	3	21	Hébrard et al. [2012]
HNC + C_2	$\rightarrow C_3N$ + H	2.0×10^{-10}	4	0	Hébrard et al. [2012]
HNC + C_2H	$\rightarrow HC_3N$ + H	2.0×10^{-10}	3	0	Fukuzawa and Osamura [1997], Petrie [2002], Georgievskii and Klippenstein [2005]
HNC + C_2H_3	$\rightarrow C_2H_3CN$ + H	$1.0 \times 10^{-12} \times \exp(-1800/T)$	10	400	DFT (M06-2X/cc-pVTZ) + TST calculations, This work
HNC + C_3N	$\rightarrow C_4N_2$ + H	2.0×10^{-10}	4	0	Petrie and Osamura [2004], Georgievskii and Klippenstein [2005]
H_2CN + H	$\rightarrow$ HCN + H_2	6.0×10^{-11}	2	14	Hébrard et al. [2012]
H_2CN + C	$\rightarrow C_2N + H_2$	3.0×10^{-11}	4	0	Capture rate constant, Georgievskii and Klippenstein [2005] considering no barrier
H_2CN + C	$\rightarrow$ HCN + CH	3.0×10^{-11}	4	0	Capture rate constant, Georgievskii and Klippenstein [2005] considering no barrier
H_2CN + C	$\rightarrow$ CHCN + H	3.0×10^{-11}	4	0	Capture rate constant, Georgievskii and Klippenstein [2005] considering no barrier
H_2CN + H	$\rightarrow CH_2NH$	$k_0 = 1.0 \times 10^{-29}$	10	0	Hébrard et al [2012]
		$k_\infty = 6.0 \times 10^{-11}$	2	0	
		$k_r = 0$	1	0	
H_2CN + H	$\rightarrow$ HNC + H_2	$k = 0.2 \times (k_\infty - k_{\text{adduct}})$	0	0	
H_2CN + CH_3	$\rightarrow CH_4$ + HCN	3.0×10^{-11}	3	0	By comparison with H_2CN + H_2CN (Pang et al. [2009]) and NH_2 + H_2CN (Yelle et al. [2010])
H_2CN + CH_3	$\rightarrow CH_2NCH_3$	$k_0 = 5.7 \times 10^{-27} \times (T/300)^{-3.5}$	10	0	By comparison with H_2CN + H_2CN (Pang et
		$k_\infty = 6.0 \times 10^{-11}$	3	0	al 2009) and NH_2 + H_2CN (Yelle et al. [2010])
		$k_r = 5.0 \times 10^{-14} \times (T/300)^{-1.5}$	10	0	
H_2CN + H_2CN	$\rightarrow CH_2NH$ + HCN	7.0×10^{-12}	1.6	100	Calculs DFT + Pang et al. [2009]
CH_2NH + H	$\rightarrow H_2CN + H_2$	$1.6 \times 10^{-11} \times \exp(-2600/T)$	3	21	DFT (M06-2X/cc-pVTZ) + TST calculations, This work
CH_2NH + H	$\rightarrow CH_3NH$	$k_0 = 4 \times 10^{-29} \times (T/300)^{-1.51} \times \exp(-72.9/T)$	3	100	By comparison with H + C_2H_4
		$k_\infty = 6.07 \times 10^{-13} \times (T/300)^{5.31} \times \exp(174/T)$	3	100	
		$k_r = 0$	30	0	
CH_2NH + C	$\rightarrow$ HCN + $^3CH_2$	1.0×10^{-10}	2	0	Capture rate constant, Georgievskii and Klippenstein [2005] considering no barrier, branching ratio deduced from N + C_2H_3 study of Feng et al. [2007]
CH_2NH + C	$\rightarrow CH_2CN$ + H	1.0×10^{-10}	2	0	Capture rate constant, Georgievskii and Klippenstein [2005] considering no barrier, branching ratio deduced from N + C_2H_3 study of Feng et al. [2007]
CH_2NH + CH	$\rightarrow CH_3CN$ + H	2.0×10^{-10}	2	0	Capture rate constant, Georgievskii and Klippenstein [2005] considering no barrier, branching ratio deduced from N + C_2H_3 study of Lee et al. [2011]
CH_2NH + $^1CH_2$	$\rightarrow H_2CN + CH_3$	3.0×10^{-10}	2	0	Capture rate constant, Georgievskii and Klippenstein [2005] considering no barrier, branching ratio deduced from N + C_2H_3 study of Yang et al. [2005]
CH_2NH + C_2H	$\rightarrow C_2H_3CN$ + H	1.4×10^{-10}	2	0	By comparison with C_2H + C_2H_4
CH_3NH + H	$\rightarrow CH_2NH + H_2$	3.0×10^{-12}	3	0	By comparison with H + C_2H_5
CH_3NH + H	$\rightarrow CH_3NH_2$	$k_0 = 2.0 \times 10^{-29} \times (T/300)^{1.5}$	3	0	By comparison with H + C_2H_5 taking into
		$k_\infty = 1.07 \times 10^{-10}$	3	0	account the bimolecular exit channel
		$k_r = 0$	1	0	
CH_3NH + H	$\rightarrow CH_3$ + NH_2	$k = k_\infty - k_{\text{adduct}}$	0	0	
CH_3NH + CH_3	$\rightarrow CH_2NH + CH_4$	1.91×10^{-12}	5	100	By comparison with CH_3 + C_2H_5
CH_3NH + CH_3	$\rightarrow CH_3NHCH_3$	$k_0 = 4 \times 10^{-24} \times (T/300)^{-4.47} \times \exp(-95/T)$	42	10	By comparison with CH_3 + C_2H_5
		$k_\infty = 8.8 \times 10^{-11} \times (T/300)^{-0.61} \times \exp(-34.8/T)$	3	0	
		$k_r = 0$	30	0	
CH_3NH_2 + CH	$\rightarrow C_2H_3NH_2$ + H	2.0×10^{-10}	2	0	By comparison with CH + NH_3
CH_3NH_2 + CH_3	$\rightarrow CH_3NH + CH_4$	$5.89 \times 10^{-15} \times \exp(-2870/T)$	1.66	100	Gray and Thynne [1965]
CH_3NH_2 + C_2H	$\rightarrow CH_3NH + C_2H_2$	$3.0 \times 10^{-11} \times (T/300)^{-0.9}$	2	0	By comparison with C_2H + NH_3
HNCNH + H	$\rightarrow NH_2$ + HCN	$6.0 \times 10^{-16} \times \exp(-1920/T)$	10	100	DFT (M06-2X/cc-pVTZ) + TST calculations, This work

Reactions		Rate coefficients	$F(300\ K)$	g	References
$C_2N + H$	$\rightarrow HCN + C$	$2.0 \times 10^{-10} \times (T/300)^{0.17}$	4	0	Mebel and Kaiser [2002], Takahashi and Takayanagi [2006], Georgievskii and Klippenstein [2005]
$C_2N + C$	$\rightarrow CN + C_2$	3.0×10^{-11}	4	0	Loison [2014]
$C_2N + C$	$\rightarrow N(^4S) + C_3$	1.0×10^{-11}	4	0	Loison [2014]
$C_2N + CH_3$	$\rightarrow H_2C_3N + H$	6.0×10^{-11}	3	21	Osamura and Petrie [2004], Georgievskii and Klippenstein [2005], Klippenstein et al. [2006]
$C_2N + CH_4$	$\rightarrow C_2H_3CN + H$	$7.0 \times 10^{-12} \times \exp(-1400/T)$	2	100	Zhu et al. [2003b], Osamura and Petrie [2004]
$C_2N + C_2H_2$	$\rightarrow HC_4N + H$	1.0×10^{-10}	3	0	Zhu et al. [2003a], Wang et al. [2006], Georgievskii and Klippenstein [2005]
$C_2N + C_2H_4$	$\rightarrow CH_3C_3N + H$	1.0×10^{-10}	3	0	Zhu et al. [2003a], Wang et al. [2006], Georgievskii and Klippenstein [2005]
$CHCN + H$	$\rightarrow C_2N + H_2$	6.0×10^{-11}	6	0	Takayanagi et al. [1998], Osamura and Petrie [2004], Georgievskii and Klippenstein [2005]
$CHCN + CH_3$	$\rightarrow C_2H_3CN + H$	3.0×10^{-11}	3	21	Osamura and Petrie [2004], Georgievskii and Klippenstein [2005], Klippenstein et al. [2006]
$CHCN + CHCN$	$\rightarrow C_4N_2 + H_2$	1.0×10^{-11}	3	0	Capture rate constant, Georgievskii and Klippenstein [2005] considering no barrier
$CHCN + CHCN$	$\rightarrow HC_4N_2 + H$	3.0×10^{-11}	3	0	Capture rate constant, Georgievskii and Klippenstein [2005] considering no barrier
$CH_2CN + H$	$\rightarrow CH_3CN$	$k_0 = 1.1 \times 10^{-25} \times (T/300)^{-1.8}$	10	0	k_0 from our semi empirical model Hébrard et
		$k_\infty = 2.0 \times 10^{-10}$	3	0	al. [2013], k_∞ by comparison with $H + C_2H_5$
		$k_r = 0$	30	0	(Hanning-Lee and Pilling [1992], Harding and Klippenstein [1998])
$CH_2CN + C$	$\rightarrow HC_3N + H$	1.0×10^{-10}	4	0	Capture rate constant, Georgievskii and Klippenstein [2005] considering no barrier
$CH_2CN + CH_3$	$\rightarrow C_2H_5CN$	$k_0 = 2.0 \times 10^{-23} \times (T/300)^{-3.5}$	10	0	k_0 from our semi empirical model Hébrard et
		$k_\infty = 6.0 \times 10^{-11}$	3	0	al. [2013], k_∞ from $CH_3 + CH_3$
		$k_r = 0$	30	0	
$CH_2CN + C_2H_3$	$\rightarrow CH_3CN + C_2H_2$	3.0×10^{-11}	3	0	By comparison with $C_2H_5 + C_2H_3$
$CH_2CN + C_2H_3$	$\rightarrow CHCN + C_2H_4$	1.0×10^{-12}	3	0	By comparison with $C_2H_5 + C_2H_3$
$CH_2CN + C_2H_3$	$\rightarrow SOOTN$	$k_0 = 6.0 \times 10^{-20} \times (T/300)^{-3.5}$	10	0	k_0 from our semi empirical model Hébrard et
		$k_\infty = 8 \times 10^{-11}$	2	0	al. [2013], k_∞ from capture rate theory
		$k_r = 0$	30	0	
$CH_2CN + C_2H_5$	$\rightarrow CH_3CN + C_2H_4$	2.0×10^{-12}	2	0	By comparison with $C_2H_5 + C_2H_5$
$CH_2CN + C_2H_5$	$\rightarrow SOOTN$	8.0×10^{-11}	3	0	Addition channel always in the high pressure limit using our semi empirical model Hébrard [2012]
$CH_2CN + C_3H_7$	$\rightarrow SOOTN$	6.0×10^{-11}	2	0	Addition channel always in the high pressure limit using our semi empirical model Hébrard [2012]
$CH_3CN + H$	$\rightarrow CH_2CN + H_2$	$1.66 \times 10^{-13} \times \exp(-1500/T)$	2	100	Jamieson et al. [1970]
$CH_3CN + CH$	$\rightarrow C_2H_3CN + H$	2.0×10^{-10}	2	0	By comparison with $CH + CH_4$ (Loison et al. [2006], Canosa et al. [1997] and $CH + HCN$).
$CH_3CN + C_2H$	$\rightarrow CH_2CN + C_2H_2$	$1.8 \times 10^{-11} \times \exp(-766/T)$	1.47	50	Nizamov and Leone [2004]
$CH_3CN + C_2H_3$	$\rightarrow C_2H_3CN + CH_3$	$1.0 \times 10^{-12} \times \exp(-2200/T)$	10	400	DFT (M06-2X/cc-pVTZ) + TST calculations, this work
$CH_2NCH + H$	$\rightarrow HCN + CH_3$	5.0×10^{-11}	3	100	Close to capture rate constant as Balucani et al. [2012] and Lee et al. [2011] found no barrier in the entrance valley
$CH_2NCH + CH_3$	$\rightarrow HCN + C_2H_5$	2.0×10^{-11}	3	100	By comparison wit $H + CH_2NCH$
$cCH_2NCH + H$	$\rightarrow CH_2NCH + H$	$7.0 \times 10^{-11} \times \exp(-1600/T)$	3	100	Estimated from ab-initio calculations from Balucani et al. [2012], Lee et al. [2011]
$cCH_2NCH + H$	$\rightarrow CH_3CN + H$	$3.0 \times 10^{-11} \times \exp(-1600/T)$	3	100	Estimated from ab-initio calculations from Balucani et al. [2012], Lee et al. [2011]
$cCH_2NCH + C_2H$	$\rightarrow SOOTN$	2.0×10^{-10}	3	100	By comparison with $C_2H + C_2H_4$
$CH_2NCH_3 + H$	$\rightarrow CH_2NH + CH_3$	$1.7 \times 10^{-11} \times \exp(-1200/T)$	3	400	By comparison with $H + CH_2NH$
$C_3N + H$	$\rightarrow HC_3N$	$k_0 = 1.86 \times 10^{-25} \times (T/300)^{-1.8}$	10	0	k_0 from our semi empirical model Hébrard et
		$k_\infty = 2.0 \times 10^{-10}$	3	0	al. [2013], k_∞ from capture rate theory
		$k_r = 4.5 \times 10^{-14} \times (T/300)^{-1.5}$	30	0	
$C_3N + H_2$	$\rightarrow HC_3N + H$	$4.0 \times 10^{-11} \times \exp(-1000/T)$	2	100	Clarke and Ferris [1995b]
$C_3N + C$	$\rightarrow CN + C_3$	2.4×10^{-10}	3	0	Loison [2014]
$C_3N + CH_3$	$\rightarrow CH_2C_3N + H$	6.0×10^{-11}	3	100	Capture rate constant, Georgievskii and Klippenstein [2005] considering no barrier
$C_3N + CH_4$	$\rightarrow HC_3N + CH_3$	3.0×10^{-11}	1.6	0	New results from Rennes Team
$C_3N + C_2H_2$	$\rightarrow HC_5N + H$	2.0×10^{-10}	3	0	By comparison with $C_2H + C_2H_2$ and $CN + C_2H_2$
$C_3N + C_2H_4$	$\rightarrow C_2H_3C_3N + H$	2.0×10^{-10}	3	0	By comparison with $C_2H + C_2H_2$ and $CN + C_2H_2$
$C_3N + C_2H_6$	$\rightarrow HC_3N + C_2H_5$	2.0×10^{-10}	2	0	Clarke and Ferris [1995b]
$C_3N + HC_3N$	$\rightarrow C_6N_2 + H$	1.0×10^{-10}	2	0	By comparison with $C_3N + C_2H_2$
$HC_3N + H$	$\rightarrow H_2C_3N$	$k_0 = 6.0 \times 10^{-28} \times (T/300)^{-2.93} \times \exp(-176/T)$	30	0	k_0 from preliminary DFT/RRKM calculations
		$k_\infty = 1.1 \times 10^{-12} \times \exp(-500/T)$	1.4	14	(this work), k_∞ from Parker et al. [2004]
		$k_r = 0$	30	0	

Reactions		Rate coefficients	$F(300\ K)$	g	References
$HC_3N + C$	$\rightarrow C_4N + H$	1.0×10^{-10}	2	0	Li et al. [2006], Georgievskii and Klippenstein [2005]
$HC_3N + CH$	$\rightarrow HC_4N + H$	2.0×10^{-10}	2	0	By comparison with CH + HCN and CH + C_3H_4
$HC_3N + C_2H$	$\rightarrow HC_5N + H$	$3.6 \times 10^{-11} \times (T/300)^{-1.04}$	1.6	0	New results from Rennes Team
$HC_3N + C_2H_3$	$\rightarrow C_2H_3C_3N + H$	$1.0 \times 10^{-12} \times \exp(-1200/T)$	10	300	DFT (M06-2X/cc-pVTZ) + TST calculations, This work
$H_2C_3N + H$	$\rightarrow HC_3N + H_2$	1.0×10^{-11}	3	0	By comparison with H + C_2H_3
$H_2C_3N + H$	$\rightarrow C_2H_3CN$	$k_0 = 1.1 \times 10^{-25}$	100	0	k_0 from our semi empirical model Hébrard et al. [2013] taking into account the bimolecular
		$k_\infty = 1.2 \times 10^{-10}$	4	0	exit channel, k_∞ from capture rate theory, see
		$k_r = 0$	1	0	also Derecskei-Kovacs and North [1999], Homayoon et al. [2011], Blank et al. [1998]
$H_2C_3N + H$	$\rightarrow HCN + C_2H_2$	$k = 0.8 \times (k_\infty - k_{\text{adduct}})$	0	0	
$H_2C_3N + H$	$\rightarrow HC_3N + H_2$	$k = 0.2 \times (k_\infty - k_{\text{adduct}})$	0	0	
$H_2C_3N + CH_3$	$\rightarrow HC_3N + CH_4$	4.0×10^{-12}	3	0	By comparison with $CH_3 + C_2H_3$
$H_2C_3N + CH_3$	$\rightarrow C_3H_5CN$	$k_0 = 1.0 \times 10^{-25}$	10	0	By comparison with $CH_3 + C_2H_3$
		$k_\infty = 6.0 \times 10^{-11}$	2	0	
		$k_r = 0$	1	0	
$H_2C_3N + CH_3$	$\rightarrow H_4C_4N + H$	$k = k_\infty - k_{\text{adduct}}$	0	0	
$H_2C_3N + C_2H_3$	$\rightarrow HC_3N + C_2H_4$	1.0×10^{-11}	3	0	By comparison with $C_2H_3 + C_2H_3$
$H_2C_3N + C_2H_3$	$\rightarrow C_2H_3CN + C_2H_2$	1.0×10^{-11}	3	0	By comparison with $C_2H_3 + C_2H_3$
$H_2C_3N + C_2H_3$	$\rightarrow SOOTN$	8.0×10^{-11}	2	0	Association channel always in the high pressure limit from our semi empirical model Hébrard [2012]
$H_2C_3N + C_2H_5$	$\rightarrow C_2H_3CN + C_2H_4$	1.0×10^{-11}	3	0	By comparison with $C_2H_3 + C_2H_5$
$H_2C_3N + C_2H_5$	$\rightarrow SOOTN$	6.0×10^{-11}	2	0	Association channel always in the high pressure limit from our semi empirical model Hébrard [2012]
$H_2C_3N + C_3H_7$	$\rightarrow SOOTN$	6.0×10^{-11}	2	0	Association channel always in the high pressure limit from our semi empirical model Hébrard [2012]
$C_2H_3CN + H$	$\rightarrow C_2H_4CN$	$k_0 = 4 \times 10^{-28} \times (T/300)^{-1.51} \times \exp(-72.9/T)$	100	0	$k_0 = 10 \times k_0(H + C_2H_4)$ Vuitton et al. [2012],
		$k_\infty = 6.07 \times 10^{-13} \times (T/300)^{5.31} \times \exp(174/T)$	4	0	$k_\infty = k_\infty(H + C_2H_4)$ Vuitton et al [2012]
		$k_r = 5.6 \times 10^{-13} \times (T/300)^{2.75} \times \exp(-50.3/T)$	30	0	
$C_2H_3CN + C$	$\rightarrow CH_2C_3N + H$	2.0×10^{-10}	2	0	Su et al. [2005], Goergievskii and Klippenstein [2005]
$C_2H_3CN + CH$	$\rightarrow HC_3N + CH_3$	2.0×10^{-10}	2	0	By comparison with CH + C_2H_4
$C_2H_3CN + C_2H$	$\rightarrow C_4H_3CN + H$	1.4×10^{-10}	3	0	By comparison with C_2H + C_2H_4
$C_2H_4CN + H$	$\rightarrow C_2H_3CN + H_2$	3.0×10^{-12}	2	0	By comparison with H + C_2H_5, C_3H_7
$C_2H_4CN + H$	$\rightarrow C_2H_5CN$	$k_0 = 1.0 \times 10^{-26} \times (T/300)^{-1.5}$	100	0	By comparison with H + C_2H_5
		$k_\infty = 1.07 \times 10^{-10}$	1.6	0	
		$k_r = 0$	1	0	
$C_2H_4CN + H$	$\rightarrow CH_2CN + CH_3$	$k = k_\infty - k_{\text{adduct}}$	0	0	
$C_2H_4CN + CH_3$	$\rightarrow C_2H_3CN + CH_4$	4.0×10^{-12}	3	0	By comparison with $CH_3 + C_2H_5$, C_3H_7
$C_2H_4CN + CH_3$	$\rightarrow C_3H_7CN$	$k_0 = 1.0 \times 10^{-19} \times (T/300)^{-3.5}$	10	0	By comparison with $CH_3 + C_3H_7$
		$k_\infty = 3.0 \times 10^{-11}$	3	0	
		$k_r = 6.0 \times 10^{-11}$	3	0	
$C_2H_4CN + C_2H_3$	$\rightarrow C_2H_3CN + C_2H_4$	4.0×10^{-12}	3	0	By comparison with $C_2H_3 + C_2H_5$, C_3H_7
$C_2H_4CN + C_2H_3$	$\rightarrow C_2H_5CN + C_2H_2$	8.0×10^{-12}	3	0	By comparison with $C_2H_3 + C_2H_5$, C_3H_7
$C_2H_4CN + C_2H_3$	$\rightarrow SOOTN$	8.0×10^{-11}	2	0	By comparison with $C_2H_3 + C_2H_5$, C_3H_7
$C_2H_4CN + C_2H_5$	$\rightarrow C_2H_5CN + C_2H_4$	4.0×10^{-12}	3	0	By comparison with $C_2H_5 + C_2H_5$, C_3H_7
$C_2H_4CN + C_2H_5$	$\rightarrow SOOTN$	8.0×10^{-11}	2	0	By comparison with $C_2H_5 + C_2H_5$, C_3H_7
$C_2H_4CN + C_3H_7$	$\rightarrow SOOTN$	6.0×10^{-11}	2	0	By comparison with $C_3H_7 + C_2H_5$, C_3H_7
$C_2H_5CN + C$	$\rightarrow H_4C_4N + H$	2.0×10^{-10}	2	0	By comparison with C + HCN, CH + CH_3CN
$C_2H_5CN + CH$	$\rightarrow CH_2CN + C_2H_4$	1.2×10^{-10}	2	0	By comparison with CH + C_2H_6, HCN
$C_2H_5CN + CH$	$\rightarrow C_2H_3CN + CH_3$	8.0×10^{-11}	2	0	By comparison with CH + C_2H_6, HCN
$C_2H_5CN + C_2H$	$\rightarrow C_2H_4CN + C_2H_2$	3.5×10^{-11}	3	0	By comparison with C_2H + C_2H_6, HCN
$C_2H_5CN + C_2H$	$\rightarrow HC_3N + C_2H_5$	$1.0 \times 10^{-11} \times \exp(-600/T)$	3	100	By comparison with C_2H + C_2H_6, HCN
$C_2H_5CN + C_2H_3$	$\rightarrow C_2H_3CN + C_2H_5$	$1.0 \times 10^{-12} \times \exp(-2000/T)$	10	400	By comparison with C_2H_3 + HCN
$C_4N + CH_3$	$\rightarrow H_2C_5N + H$	3.0×10^{-11}	3	0	Close to capture rate constant, Georgievskii and Klippenstein [2005] considering no barrier
$HC_4N + H$	$\rightarrow CH_2C_3N$	$k_0 = 1.6 \times 10^{-22} \times (T/300)^{-1.8}$	10	0	k_0 from our semi empirical model Hébrard et
		$k_\infty = 2.0 \times 10^{-10}$	3	0	al. [2013], k_∞ from capture rate theory
		$k_r = 6.0 \times 10^{-12} \times (T/300)^{-1.5}$	30	0	
$HC_4N + CH_3$	$\rightarrow C_4H_3CN + H$	3.0×10^{-11}	3	0	By comparison with $^3CH_2 + CH_3$
$CH_2C_3N + H$	$\rightarrow HC_4N + H_2$	2.0×10^{-12}	4	0	By comparison with H + C_2H_5
$CH_2C_3N + H$	$\rightarrow CH_3C_3N$	$k_0 = 1.0 \times 10^{-21} \times (T/300)^{-1.8}$	30	0	k_0 from our semi empirical model Hébrard et
		$k_\infty = 1.0 \times 10^{-10}$	4	0	al. [2013], k_∞ from capture rate theory
		$k_r = 1.0 \times 10^{-11} \times (T/300)^{-1.5}$	100	0	
$CH_2C_3N + CH_3$	$\rightarrow HC_4N + CH_4$	1.0×10^{-12}	3	0	By comparison with $CH_3 + C_2H_5$

Reactions		Rate coefficients	$F(300\ K)$	g	References
$CH_2C_3N + CH_3$	$\rightarrow C_2H_5C_3N$	$k_0 = 6.0 \times 10^{-20} \times (T/300)^{-3.5}$	10	0	k_0 from our semi empirical model Hébrard et
		$k_\infty = 6.0 \times 10^{-11}$	2	0	al. [2013], k_∞ from capture rate theory
		$k_r = 6.0 \times 10^{-11}$	2	0	
$CH_3C_3N + H$	$\rightarrow H_4C_4N$	$k_0 = 3.0\times10^{-26}\times(T/300)^{-2.93}\times\exp(-176/T)$	10	0	By comparison with H + HC_3N
		$k_\infty = 1.1 \times 10^{-12} \times \exp(-500/T)$	10	0	
		$k_r = 0$	30	0	
$CH_3C_3N + C_2H$	$\rightarrow HC_5N + CH_3$	$4.0 \times 10^{-11} \times (T/300)^{-1}$	1.6	0	By comparison with C_2H + HC_3N
$CH_3C_3N + C_2H_3$	$\rightarrow C_2H_3C_3N + CH_3$	$1.0 \times 10^{-12} \times \exp(-1600/T)$	10	400	By comparison with C_2H_3 + HC_3N
$CH_3C_3N + CN$	$\rightarrow C_4N_2 + CH_3$	$1.79 \times 10^{-11} \times (T/300)^{-0.67}$	1.6	0	By comparison with CN + HC_3N
$H_4C_4N + H$	$\rightarrow CH_3C_3N + H_2$	1.0×10^{-11}	3	0	By comparison with H + C_3H_5
$H_4C_4N + H$	$\rightarrow C_3H_5CN$	$k_0 = 2.0 \times 10^{-21} \times (T/300)^{-1.5}$	10	0	By comparison H + H_2C_3N
		$k_\infty = 1.0 \times 10^{-10}$	4	0	
		$k_r = 0$	1	0	
$H_4C_4N + H$	$\rightarrow HCN + CH_3C_2H$	$k = 0.8 \times (k_\infty - k_{\rm adduct})$	0	0	
$H_4C_4N + H$	$\rightarrow CH_3C_3N + H_2$	$k = 0.2 \times (k_\infty - k_{\rm adduct})$	0	0	
$H_4C_4N + CH_3$	$\rightarrow CH_3C_3N + CH_4$	$4.03 \times 10^{-13} \times (T/300)^{-0.32} \times \exp(66/T)$	3	0	By comparison with CH_3 + C_3H_5
$H_4C_4N + CH_3$	$\rightarrow C_4H_7CN$	$k_0 = 1.1 \times 10^{-22} \times (T/300)^{-1.5}$	10	0	By comparison with CH_3 + C_3H_5
		$k_\infty = 7.0\times10^{-11}\times(T/300)^{-0.54}\times\exp(117/T)$	1.6	21	
		$k_r = 3.4 \times 10^{-11} \times (T/300)^{-1.5}$	30	0	
$C_3H_5CN + H$	$\rightarrow C_3H_6CN$	$k_0 = 1.4\times10^{-25}\times(T/300)^{-2.48}\times\exp(-191/T)$	100	0	Similar to H + C_3H_6
		$k_\infty = 7.02\times10^{-12}\times(T/300)^{1.16}\times\exp(-440/T)$	4	0	
		$k_r = 0$	1	0	
$C_3H_6CN + H$	$\rightarrow C_3H_5CN + H_2$	3.0×10^{-12}	2	0	By comparison with H + C_2H_5
$C_3H_6CN + H$	$\rightarrow C_3H_7CN$	$k_0 = 1.0 \times 10^{-24}$	100	0	By comparison with H + C_3H_5, H + C_3H_7
		$k_\infty = 1.0 \times 10^{-10}$	2	0	and H + C_4H_3
		$k_r = 0$	1	0	
$C_3H_6CN + H$	$\rightarrow C_2H_4CN + CH_3$	$k = k_\infty - k_{\rm adduct}$	0	0	
$C_3H_6CN + CH_3$	$\rightarrow$ SOOTN	6.0×10^{-11}	3	0	By comparison with CH_3 + C_2H_5
$C_3H_6CN + CH_3$	$\rightarrow C_3H_5CN + CH_4$	2.0×10^{-12}	3	0	By comparison with CH_3 + C_2H_5
$C_3H_7CN + C_2H$	$\rightarrow C_3H_6CN + C_2H_2$	6.0×10^{-11}	2	0	By comparison with C_2H + C_3H_8
$C_3H_7CN + C_2H_3$	$\rightarrow C_2H_3CN + C_3H_7$	$1.0 \times 10^{-12} \times \exp(-1800/T)$	10	400	By comparison with C_2H_3 + HCN
$C_5N + H_2$	$\rightarrow HC_5N + H$	$4.0 \times 10^{-11} \times \exp(-1000/T)$	10	100	By comparison with $C_3N + H_2$
$C_5N + CH_4$	$\rightarrow HC_5N + CH_3$	4.0×10^{-11}	3	100	By comparison with $C_3N + CH_4$
$C_5N + C_2H_2$	$\rightarrow HC_7N + H$	2.0×10^{-10}	3	0	By comparison with $C_3N + C_2H_2$
$C_5N + C_2H_4$	$\rightarrow C_2H_3C_5N + H$	2.0×10^{-10}	3	0	By comparison with $C_3N + C_2H_4$
$C_5N + C_2H_6$	$\rightarrow HC_5N + C_2H_5$	2.0×10^{-10}	3	100	By comparison with $C_3N + C_2H_6$
$C_5N + HCN$	$\rightarrow C_6N_2 + H$	1.0×10^{-11}	4	100	By comparison with C_3N + HCN
$HC_5N + H$	$\rightarrow H_2C_5N$	$k_0 = 3.0\times10^{-25}\times(T/300)^{-2.93}\times\exp(-176/T)$	30	0	Similar to H + C_4H_2
		$k_\infty = 1.6 \times 10^{-12} \times (T/300)^{5.55} \times \exp(153/T)$	4	0	
		$k_r = 0$	1	0	
$HC_5N + C_2H$	$\rightarrow HC_7N + H$	$3.6 \times 10^{-11} \times (T/300)^{-1.04}$	3	0	By comparison with C_2H + HC_3N
$H_2C_5N + H$	$\rightarrow HC_5N + H_2$	1.0×10^{-11}	4	0	By comparison with H + H_2C_3N
$H_2C_5N + H$	$\rightarrow C_4H_3CN$	$k_0 = 1.0 \times 10^{-23}$	10	0	By comparison H + H_2C_3N
		$k_\infty = 1.2 \times 10^{-10}$	4	0	
		$k_r = 0$	1	0	
$H_2C_5N + H$	$\rightarrow HC_3N + C_2H_2$	$k = 0.5 \times (k_\infty - k_{\rm adduct})$	0	0	
$H_2C_5N + H$	$\rightarrow HC_5N + H_2$	$k = 0.5 \times (k_\infty - k_{\rm adduct})$	0	0	
$C_4H_3CN + H$	$\rightarrow C_4H_4CN$	$k_0 = 1.4\times10^{-25}\times(T/300)^{-2.48}\times\exp(-191/T)$	100	0	Similar to H + C_3H_6
		$k_\infty = 7.02\times10^{-12}\times(T/300)^{1.16}\times\exp(-440/T)$	4	0	
		$k_r = 0$	1	0	
$C_4H_3CN + N(^2D)$	$\rightarrow$ SOOTN	3.0×10^{-11}	4	100	By comparison with $N(^2D)$ + C_2H_2 and
					$N(^2D)$ + HCN
$C_4H_4CN + H$	$\rightarrow C_4H_3CN + H_2$	1.0×10^{-11}	3	0	By comparison with H + C_3H_5
$C_4H_4CN + H$	$\rightarrow C_2H_5C_3N$	$k_0 = 1.0 \times 10^{-24}$	100	0	By comparison with H + C_3H_5, H + C_3H_7
		$k_\infty = 1.0 \times 10^{-10}$	2	0	and H +C_4H_3
		$k_r = 0$	1	0	
$C_4H_4CN + H$	$\rightarrow CH_2C_3N + CH_3$	$k = k_\infty - k_{\rm adduct}$	0	0	
$C_4H_4CN + CH_3$	$\rightarrow C_4H_3CN + CH_4$	1.0×10^{-12}	3	0	By comparison with CH_3 + C_3H_5
$C_4H_4CN + CH_3$	$\rightarrow C_3H_7C_3N$	$k_0 = 1.0 \times 10^{-20} \times (T/300)^{-3.5}$	30	0	k_0 from our semi empirical model Hébrard et
		$k_\infty = 6.0 \times 10^{-11}$	2	0	al. [2013], k_∞ from capture rate theory
		$k_r = 0$	1	0	
$C_2H_5C_3N + N(^2D)$	$\rightarrow$ SOOTN	3.0×10^{-11}	4	100	By comparison with $N(^2D)$ + C_2H_2 and
					$N(^2D)$ + HCN
$C_2H_5C_3N + H$	$\rightarrow$ SOOTN	$k_0 = 6.0\times10^{-26}\times(T/300)^{-2.93}\times\exp(-176/T)$	100	0	$k_0 = 100 \times k_0$(H + HC_3N),
		$k_\infty = 1.1 \times 10^{-12} \times \exp(-500/T)$	10	0	$k_\infty = 0.2 \times k_\infty$(H + HC_3N)
		$k_r = 0$	30	0	
$C_3H_7C_3N + N(^2D)$	$\rightarrow$ SOOTN	3.0×10^{-11}	4	100	By comparison with $N(^2D)$ + C_2H_2 and
					$N(^2D)$ + HCN
$C_3H_7C_3N + H$	$\rightarrow$ SOOTN	$k_0 = 1.8\times10^{-25}\times(T/300)^{-2.93}\times\exp(-176/T)$	100	0	$k_0 = 300 \times k_0$(H + HC_3N),
		$k_\infty = 1.1 \times 10^{-12} \times \exp(-500/T)$	10	0	$k_\infty = 0.6 \times k_\infty$(H + HC_3N)
		$k_r = 0$	30	0	

Reactions		Rate coefficients	$F(300\ K)$	g	References
N_2 + C	$\rightarrow CN_2$	$k_0 = 3.1 \times 10^{-33} \times (T/300)^{-1.5}$	1.8	10	Husain and Kirsch [1971]
		$k_\infty = 1.0 \times 10^{-11}$	10	0	
		$k_r = 0$	30	0	
N_2 + CH	$\rightarrow HCNN$	$k_0 = 1.9 \times 10^{-31} \times (T/300)^{-2.2}$	1.4	0	Brownsword et al. [1996], Le Picard and
		$k_\infty = 1.8 \times 10^{-12} \times (T/300)^{-1.5}$	3	100	Canosa [1998]
		$k_r = 0$	30	0	
CN_2 + H	$\rightarrow CH + N_2$	2.0×10^{-10}	3	7	Moskaleva et al. [2000], Georgievskii and Klippenstein [2005]
HCNN + H	$\rightarrow {}^1CH_2 + N_2$	2.0×10^{-10}	3	0	Tomeczek [2003]
H_2CNN + H	$\rightarrow CH_3 + N_2$	1.6×10^{-11}	4	100	Morris and Niki [1973]
C_2N_2 + H	$\rightarrow HC_2N_2$	$k_0 = 2.0 \times 10^{-31} \times (T/300)^{-1.07} \times \exp(-83.8/T)$	10	0	$k_0 = 0.1 \times k_0(H + C_2H_2)$, $k_\infty = 0.1 \times k_\infty(H + C_2H_2)$ considering the
		$k_\infty = 1.17 \times 10^{-14} \times (T/300)^{8.41} \times \exp(359/T)$	3	0	entrance TS value calculated at the
		$k_r = 0$	30	0	M06-2X/cc-pVTZ level
C_2N_2 + C	$\rightarrow C_3 + N_2$	6.0×10^{-11}	4	0	Whyte and Phillips [1983]
C_2N_2 + CH	$\rightarrow C_2N + HCN$	2.0×10^{-10}	3	0	By comparison with CH + HCN
C_2N_2 + C_2H	$\rightarrow HC_3N + CN$	$5.3 \times 10^{-12} \times \exp(-769/T)$	1.4	0	By comparison with C_2H + HCN
C_4N_2 + H	$\rightarrow HC_4N_2$	$k_0 = 4.3 \times 10^{-28} \times (T/300)^{-1.51} \times \exp(-72.9/T)$	100	0	$k_0 = 10 \times k_0(H + C_2H_4)$, $k_\infty = 0.2 \times k_\infty(H + C_2H_2)$ considering the
		$k_\infty = 2.2 \times 10^{-14} \times (T/300)^{8.41} \times \exp(359/T)$	10	0	entrance TS value calculated at the
		$k_r = 0$	30	0	M06-2X/cc-pVTZ level and the size of the system
C_4N_2 + C	$\rightarrow C_5 + N_2$	6.0×10^{-11}	4	0	By comparison with C + C_2N_2
C_4N_2 + CH	$\rightarrow C_4N + HCN$	2.0×10^{-10}	3	0	By comparison with CH + HC_3N, HCN
C_4N_2 + C_2H	$\rightarrow HC_5N + CN$	$2.1 \times 10^{-10} \times (T/300)^{-0.3}$	1.6	0	By comparison with C_2H + HC_3N
HC_2N_2 + H	$\rightarrow C_2N_2 + H_2$	1.0×10^{-11}	3	0	Evans et al. [1991], Smith et al. [2001], Phillips [1978], Basiuk and Kobayashi [2004]
HC_2N_2 + H	$\rightarrow HCN + HNC$	6.0×10^{-11}	3	0	Evans et al. [1991], Smith et al. [2001], Phillips [1978], Basiuk and Kobayashi [2004]
HC_4N_2 + H	$\rightarrow C_4N_2 + H_2$	1.0×10^{-11}	3	0	By comparison with H + C_2N_2
HC_4N_2 + H	$\rightarrow HC_3N + HNC$	6.0×10^{-11}	3	0	By comparison with H + C_2N_2
$O(^3P)$ + $^1CH_2$	$\rightarrow HCO + H$	1.0×10^{-11}	2	0	Bohland et al. [1984], Vinckier [1979], Tsuboi and Hashimoto [1981] and HCO dissociation Shepler et al. [2007], Wang et al. [1973], Baulch et al. [2005], Zhang et al. [2004b]
$O(^3P)$ + $^1CH_2$	$\rightarrow CO + H + H$	5.0×10^{-11}	1.6	0	
$O(^3P)$ + $^1CH_2$	$\rightarrow CO + H_2$	6.0×10^{-11}	1.6	0	
$O(^3P)$ + $^3CH_2$	$\rightarrow HCO + H$	1.0×10^{-11}	2	0	
$O(^3P)$ + $^3CH_2$	$\rightarrow CO + H + H$	5.0×10^{-11}	1.6	0	
$O(^3P)$ + $^3CH_2$	$\rightarrow CO + H_2$	6.0×10^{-11}	1.6	0	
$O(^3P)$ + CH_3	$\rightarrow CO + H_2 + H$	2.9×10^{-11}	1.4	0	Baulch et al. [2005]
$O(^3P)$ + CH_3	$\rightarrow H_2CO + H$	1.1×10^{-10}	1.4	0	
$O(^3P)$ + C_2H_2	$\rightarrow CO + {}^3CH_2$	$6.6 \times 10^{-12} \times \exp(-1600/T)$	1.4	250	Sander et al. [2011], Baulch et al. [2005]
$O(^3P)$ + C_2H_2	$\rightarrow HCCO + H$	$2.6 \times 10^{-11} \times \exp(-1600/T)$	1.4	250	
$O(^3P)$ + C_2H_3	$\rightarrow CH_3 + CO$	6.0×10^{-11}	2	0	Heinemann et al. [1988], Harding et al. [2005]
$O(^3P)$ + C_2H_3	$\rightarrow OH + C_2H_2$	1.0×10^{-11}	3	0	Heinemann et al. [1988], Harding et al. [2005]
$O(^3P)$ + C_2H_4	$\rightarrow CH_3CO + H$	$3.0 \times 10^{-14} \times (T/300)^{1.88} \times \exp(-92/T)$	1.6	100	Baulch et al. [2005], Fu et al. [2012a], Fu et al. [2012b], Balucani et al. [2012]. Branching ratio values are for 298 K. This reaction has a very small flux in Titan's atmosphere. Second reaction: CH_2CHO.
$O(^3P)$ + C_2H_4	$\rightarrow CH_3CO + H$	$4.8 \times 10^{-13} \times (T/300)^{1.88} \times \exp(-92/T)$	1.6	100	
$O(^3P)$ + C_2H_4	$\rightarrow HCO + CH_3$	$5.0 \times 10^{-13} \times (T/300)^{1.88} \times \exp(-92/T)$	1.6	100	
$O(^3P)$ + C_2H_4	$\rightarrow H_2CO + {}^3CH_2$	$1.0 \times 10^{-13} \times (T/300)^{1.88} \times \exp(-92/T)$	1.6	100	
$O(^3P)$ + C_2H_4	$\rightarrow CH_2CO + H_2$	$3.0 \times 10^{-14} \times (T/300)^{1.88} \times \exp(-92/T)$	1.6	100	
$O(^3P)$ + C_2H_5	$\rightarrow H_2CO + CH_3$	5.0×10^{-11}	2	0	Heinemann et al. [1988], Harding et al. [2005]
$O(^3P)$ + C_2H_5	$\rightarrow CH_3CHO + H$	6.0×10^{-11}	2	0	Heinemann et al. [1988], Harding et al. [2005]
$O(^3P)$ + C_2H_5	$\rightarrow OH + C_2H_4$	3.0×10^{-11}	2	0	Heinemann et al. [1988], Harding et al. [2005]
$O(^3P)$ + C_3	$\rightarrow CO + C_2$	3.0×10^{-11}	4	500	Deduced from ab-initio calculations, Woon [1996], T=150-200K
$O(^3P)$ + C_3H_6	$\rightarrow HCO + C_2H_5$	1.0×10^{-12}	2	0	Sabbah et al. [2007], Savee et al. [2012]
$O(^3P)$ + C_3H_6	$\rightarrow CH_3CO + CH_3$	1.1×10^{-12}	2	0	
$O(^3P)$ + C_3H_6	$\rightarrow SOOTC + H$	1.8×10^{-12}	2	0	
$O(^3P)$ + C_3H_6	$\rightarrow SOOTC + H_2$	6.0×10^{-14}	2	0	
$O(^3P)$ + C_4H_2	$\rightarrow CO + t\text{-}C_3H_2$	$1.31 \times 10^{-11} \times \exp(-678/T)$	1.4	60	Mitchell [1986]
$O(^3P)$ + NH	$\rightarrow NO + H$	6.6×10^{-11}	1.4	100	Adamson et al. [1994], Dransfeld et al. 1985, Li et al. [2013]

Reactions		Rate coefficients	$F(300\ K)$	g	References
$O(^3P) + H_2CN$	$\rightarrow OH + HCN$	4.0×10^{-11}	3	0	rate constant from capture theory, Georgievskii and Klippenstein [2005] considering no barrier in the entrance valley and branching ratio deduced from Fikri et al. [2001], Zhang et al. [2004]
$O(^3P) + H_2CN$	$\rightarrow OH + HNC$	1.0×10^{-11}	3	0	
$O(^3P) + H_2CN$	$\rightarrow HNCO + H$	5.0×10^{-11}	3	0	
$O(^3P) + HCCO$	$\rightarrow H + CO + CO$	1.6×10^{-10}	1.6	0	Baulch et al. [2005]
$O(^3P) + HCCO$	$\rightarrow CH + CO_2$	$4.9 \times 10^{-11} \times \exp(-560/T)$	2	100	
$O(^3P) + HNO$	$\rightarrow OH + NO$	3.8×10^{-11}	1.6	0	Inomata and Washida [1999]
$O(^1D) + H_2$	$\rightarrow OH + H$	1.1×10^{-10}	1.1	100	Sander et al. [2011]
$O(^1D) + CH_4$	$\rightarrow OH + CH_3$	1.05×10^{-10}	1.4	100	Atkinson et al. [2006]
$O(^1D) + CH_4$	$\rightarrow CH_3O + H$	3.5×10^{-11}	1.3	100	
$O(^1D) + CH_4$	$\rightarrow H_2CO + H_2$	7.5×10^{-12}	1.3	100	
$O(^1D) + N_2$	$\rightarrow O(^3P) + N_2$	$2.15 \times 10^{-11} \times \exp(110/T)$	1.1	30	Sander et al. [2011]
$OH + H_2$	$\rightarrow H_2O + H$	$2.8 \times 10^{-12} \times \exp(-1800/T)$	1.05	100	Sander et al. [2011]
$OH + CH_3$	$\rightarrow H_2O + {}^1CH_2$	3.2×10^{-11}	1.4	100	De Avillez Pereira et al. [1997], Jasper et al. [2007], Sangwan et al. [2012]
$OH + CH_3$	$\rightarrow H_2CO + H_2$	8.0×10^{-12}	2	100	De Avillez Pereira et al. [1997], Jasper et al. [2007], Sangwan et al. [2012]
$OH + CH_3$	$\rightarrow CH_3OH$	$k_0 = 2.0 \times 10^{-26} \times (T/300)^{-6} \times \exp(-1000/T)$	2	100	De Avillez Pereira et al. [1997], Jasper et al.
		$k_\infty = 1.2 \times 10^{-10} \times (T/300)^{-0.49}$	1.2	100	[2007b], Sangwan et al. [2012]
		$k_r = 0$	30	0	
$OH + CH_4$	$\rightarrow H_2O + CH_3$	$1.85 \times 10^{-12} \times \exp(-1690/T)$	1.2	100	Atkinson et al. [2006]
$OH + C_2H_2$	$\rightarrow C_2H_2OH$	$k_0 = 5.5 \times 10^{-30}$	1.6	100	Sander et al. [2011]
		$k_\infty = 8.3 \times 10^{-13} \times (T/300)^2$	1.2	50	
		$k_r = 0$	30	0	
$OH + C_2H_4$	$\rightarrow C_2H_4OH$	$k_0 = 1.0 \times 10^{-28} \times (T/300)^{-4.5}$	2	100	Sander et al. [2011]
		$k_\infty = 7.5 \times 10^{-12} \times (T/300)^{-0.85}$	1.2	50	
		$k_r = 0$	30	0	
$OH + N(^4S)$	$\rightarrow NO + H$	4.5×10^{-11}	1.3	0	Daranlot et al. [2011]
$OH + N(^2D)$	$\rightarrow NO + H$	4.5×10^{-11}	2	0	Daranlot et al. [2011]
$OH + CO$	$\rightarrow CO_2 + H$	1.3×10^{-13}	1.4	0	Atkinson et al. [2006]
$OH + CO$	$\rightarrow CO_2 + H$	$k_0 = 3.23 \times 10^{-33} \times (T/300)^1$	1.4	21	Atkinson et al. [2006]
		$k_\infty = 1.0 \times 10^{+90}$	1	0	
		$k_r = 0$	30	0	
$H_2O + CH$	$\rightarrow H_2CO + H$	$2.8 \times 10^{-11} \times (T/300)^{-1.22} \times \exp(-12/T)$	1.2	21	Blitz et al. [1999], Bergeat et al. [2009]
$H_2O + C_2H$	$\rightarrow OH + C_2H_2$	$7.9 \times 10^{-14} \times (T/300)^{3.05} \times \exp(-376/T)$	1.2	100	Carl et al. [2005]
$H_2O + N(^2D)$	$\rightarrow OH + NH$	4.5×10^{-11}	2	100	Umemoto et al. [1998], Herron [1999], Kurosaki and Takayanagi [1999], Umemoto et al. [1999], Casavecchia et al. [2001]
$H_2O + N(^2D)$	$\rightarrow HNO + H$	5.0×10^{-12}	2	100	
$CO + H$	$\rightarrow HCO$	$k_0 = 7.5 \times 10^{-35} \times (T/300)^{0.2}$	1.6	100	k_0 from Baulch et al. [2005], k_∞ from Wagner
		$k_\infty = 1.0 \times 10^{-10} \times \exp(-1000/T)$	3	300	and Bowman [1987], Wang et al. [1973]
		$k_r = 0$	30	0	
$HCO + H$	$\rightarrow CO + H_2$	1.5×10^{-10}	1.4	0	Baulch et al. [2005]
$HCO + CH_3$	$\rightarrow CO + CH_4$	9.3×10^{-11}	1.4	0	Krasnoperov et al. [2005]
$HCO + CH_3$	$\rightarrow CH_3CHO$	$k_0 = 7.0 \times 10^{-26} \times (T/300)^{-3.5}$	10	100	
		$k_\infty = 3.01 \times 10^{-11}$	2	100	k_0 from our semi empirical model Hébrard et al. [2013], k_∞ from Tsang and Herron [1991]
		$k_r = 0$	30	0	
$HCO + N(^4S)$	$\rightarrow CO + NH$	1.0×10^{-10}	3	0	Catpure rate constant considering no barrier in the entrance valley
$H_2CO + H$	$\rightarrow HCO + H_2$	$3.3 \times 10^{-11} \times \exp(-1850/T)$	1.4	200	Klemm [1979]
$H_2CO + C$	$\rightarrow CO + {}^3CH_2$	4.0×10^{-10}	1.8	0	Husain and Ioannou [1999]
$H_2CO + CH$	$\rightarrow CO + CH_3$	$5.0 \times 10^{-11} \times \exp(-260/T)$	2	0	Zabarnick et al. [1988]
$H_2CO + CH$	$\rightarrow CH_2CO + H$	$1.0 \times 10^{-10} \times \exp(-260/T)$	2	0	Zabarnick et al. [1988]
$H_2CO + N(^2D)$	$\rightarrow HNCO + H$	4.0×10^{-11}	4	0	Umemoto et al. [1998], Herron [1999], Kurosaki and Takayanagi [1999], Umemoto et al. [1999], Casavecchia et al. [2001], Homayoon [2014]
$H_2CO + CN$	$\rightarrow HCO + HCN$	$6.7 \times 10^{-11} \times \exp(-412/T)$	1.6	20	Yu et al. [1993], Chang and Wang [1995]
$CH_3O + H$	$\rightarrow H_2CO + H_2$	3.0×10^{-11}	1.6	100	Hoyermann et al. [1981], Dobe et al. [1991], Jasper et al [2007]
$CH_3O + H$	$\rightarrow OH + CH_3$	3.0×10^{-12}	1.6	100	Hoyermann et al. [1981], Dobe et al. [1991], Jasper et al [2007]
$CH_3O + CH_3$	$\rightarrow H_2CO + CH_4$	4.0×10^{-11}	1.6	0	Tsang and Hampson [1986]
$CH_3O + N(^4S)$	$\rightarrow NO + CH_3$	6.0×10^{-11}	3	100	By comparison with N + OH
$CH_3OH + H$	$\rightarrow CH_3O + H_2$	$2.16 \times 10^{-11} \times \exp(-2650/T)$	2	100	Hoyermann et al. [1981]
$CH_3OH + CH$	$\rightarrow H_2CO + CH_3$	1.3×10^{-10}	1.8	100	Johnson et al. [2000]
$CH_3OH + CH$	$\rightarrow OH + C_2H_4$	1.3×10^{-10}	1.8	100	Johnson et al. [2000]
$CH_3OH + C_2H$	$\rightarrow CH_3O + C_2H_2$	5.0×10^{-12}	3	100	Tsang 1987, Carl et al. [2005], Murphy et al. [2003]
$CH_3OH + N(^2D)$	$\rightarrow OH + CH_2NH$	1.0×10^{-11}	4	0	By comparison with $N(^2D) + C_2H_6$ and $N(^2D) + H_2O$

Reactions		Rate coefficients	$F(300\ K)$	g	References
$CH_3OH + N(^2D)$	$\rightarrow HNO + CH_3$	1.0×10^{-11}	4	0	By comparison with $N(^2D) + C_2H_6$ and $N(^2D) + H_2O$
$CH_3OH + CN$	$\rightarrow CH_3O + HCN$	1.2×10^{-10}	1.4	100	Sayah et al. [1988]
$CH_3CO + H$	$\rightarrow HCO + CH_3$	4.0×10^{-11}	2	100	Bartels et al. [1991], Ohmori et al. [1990]
$CH_3CO + H$	$\rightarrow CH_2CO + H_2$	2.0×10^{-11}	2	100	Bartels et al. [1991], Ohmori et al. [1990]
$HCCO + H$	$\rightarrow {}^3CH_2 + CO$	1.7×10^{-10}	1.6	0	Glass et al. [2000], Baulch et al. [2005]
$HCCO + CH_3$	$\rightarrow C_2H_4 + CO$	1.0×10^{-10}	3	0	By comparison with H + HCCO
$HCCO + N(^4S)$	$\rightarrow HCN + CO$	1.0×10^{-10}	3	0	By comparison with N + $^3CH_2$
$CH_3CHO + H$	$\rightarrow CH_3CO + H_2$	$2.23 \times 10^{-11} \times \exp(-1660/T)$	1.4	200	Baulch et al. [2005]
$CH_3CHO + C$	$\rightarrow C_2H_2 + H_2 + CO$	3.0×10^{-10}	1.8	0	Husain and Ioannou [1999]. Various products possible.
$CH_3CHO + CH$	$\rightarrow C_2H_2 + H_2 + CO + H$	2.0×10^{-10}	3	0	Capture rate constant considering no barrier. CH_2CHCHO likely to be produced but giving finally CO.
$CH_3CHO + N(^2D)$	$\rightarrow HNCO + CH_3$	4.0×10^{-11}	4	0	By comparison with $N(^2D) + C_2H_4$
$C_2H_2OH + H$	$\rightarrow HCO + CH_3$	6.0×10^{-11}	3	100	Nguyen et al. [2005], Horowitz and Calvert [1982], Bartels et al. [1982]
$C_2H_2OH + H$	$\rightarrow CH_3CO + H$	1.0×10^{-11}	3	100	Nguyen et al. [2005], Horowitz and Calvert [1982], Bartels et al. [1982]
$C_2H_2OH + H$	$\rightarrow CO + CH_4$	1.0×10^{-11}	3	100	Nguyen et al. [2005], Horowitz and Calvert [1982], Bartels et al. [1982]
$C_2H_4OH + H$	$\rightarrow H_2O + C_2H_4$	2.0×10^{-11}	3	100	Bartels et al. [1982], Park et al. [2002]
$C_2H_4OH + H$	$\rightarrow CH_3O + CH_3$	5.0×10^{-11}	3	100	Bartels et al. [1982], Park et al. [2002]
$C_2H_4OH + H$	$\rightarrow OH + C_2H_5$	1.0×10^{-11}	3	100	Bartels et al. [1982], Park et al. [2002]
$CO_2 + CH$	$\rightarrow CO + CO + H$	$5.71 \times 10^{-12} \times \exp(-345/T)$	1.4	50	Berman et al. [1982]
$CO_2 + N(^2D)$	$\rightarrow CO + NO$	$1.0 \times 10^{-11} \times \exp(-1000/T)$	1.6	300	Herron [1999]
$NO + H$	$\rightarrow HNO$	$k_0 = 1.34 \times 10^{-31} \times (T/300)^{-1.32} \times \exp(-370/T)$	2	0	Tsang and Herron [1991]
		$k_\infty = 2.44 \times 10^{-10} \times (T/300)^{-0.41}$	1.6	0	
		$k_r = 0$	30	0	
$NO + C$	$\rightarrow CN + O(^3P)$	$7.0 \times 10^{-11} \times (T/300)^{-0.16}$	1.4	0	Geppert et al. [2000], Bergeat et al. [1999], Andersson et al. [2003]
$NO + C$	$\rightarrow CO + N(^4S)$	$8.0 \times 10^{-11} \times (T/300)^{-0.16}$	1.4	0	Geppert et al. [2000], Bergeat et al. [1999], Andersson et al. [2003]
$NO + CH$	$\rightarrow HCN + O(^3P)$	$1.0 \times 10^{-10} \times (T/300)^{-0.13}$	2	7	Bocherel et al. [1996], Bergeat et al. [1998], Marchand et al. [1997]
$NO + CH$	$\rightarrow NCO + H$	$3.0 \times 10^{-11} \times (T/300)^{-0.13}$	2	7	Bocherel et al. [1996], Bergeat et al. [1998], Marchand et al. [1997]
$NO + CH$	$\rightarrow CO + NH$	$3.0 \times 10^{-11} \times (T/300)^{-0.13}$	2	7	Bocherel et al. [1996], Bergeat et al. [1998], Marchand et al. [1997]
$NO + CH$	$\rightarrow OH + CN$	$1.0 \times 10^{-11} \times (T/300)^{-0.13}$	2	7	Bocherel et al. [1996], Bergeat et al. [1998], Marchand et al. [1997]
$NO + {}^3CH_2$	$\rightarrow HNCO + H$	$2.1 \times 10^{-12} \times \exp(554/T)$	1.2	0	Vinckier and Debruyn [1979], Seidler et al. [1989], Darwin et al. [1989] + Fikri et al. [2001], Zhang et al. [2004a]
$NO + {}^3CH_2$	$\rightarrow CO + NH_2$	$3.0 \times 10^{-13} \times \exp(554/T)$	2	0	Vinckier and Debruyn [1979], Seidler et al. [1989], Darwin et al. [1989] + Fikri et al. [2001], Zhang et al. [2004a]
$NO + CH_3$	$\rightarrow CH_3NO$	$k_0 = 1.1 \times 10^{-29} \times (T/300)^{-3.5}$	2	0	Kaiser [1993], Jodkowski et al. [1993], Baulch
		$k_\infty = 1.1 \times 10^{-11} \times (T/300)^{0.6}$	1.6	0	et al. [2005]
		$k_r = 0$	30	0	
$NO + N(^4S)$	$\rightarrow O(^3P) + N_2$	4.0×10^{-11}	1.3	0	Bergeat et al. [2009a]
$NO + N(^2D)$	$\rightarrow O(^3P) + N_2$	6.0×10^{-11}	1.6	100	Herron [1999]
$NO + NH$	$\rightarrow N_2O + H$	$2.9 \times 10^{-11} \times (T/300)^{-0.3} \times \exp(77/T)$	1.6	0	Mullen and Smith [2005], Baulch et al. [2005], Okada et al. [1994], Durant [1994]
$NO + NH$	$\rightarrow OH + N_2$	$1.2 \times 10^{-11} \times (T/300)^{-0.3} \times \exp(77/T)$	1.6	0	Mullen and Smith [2005], Baulch et al. [2005], Okada et al. [1994], Durant [1994]
$HNO + H$	$\rightarrow NO + H_2$	$3.1 \times 10^{-11} \times \exp(-500/T)$	2	200	Tsang and Herron [1991], Nguyen et al. [2004]
$HNO + C$	$\rightarrow NO + CH$	3.8×10^{-11}	3	0	By comparison with O + HNO
$HNO + C$	$\rightarrow NCO + H$	3.0×10^{-11}	3	0	
$HNO + C$	$\rightarrow HNC + O(^3P)$	3.0×10^{-11}	3	0	
$HNO + C$	$\rightarrow CO + NH$	3.0×10^{-11}	3	0	
$HNO + CH$	$\rightarrow NO + {}^3CH_2$	3.8×10^{-11}	3	100	Capture rate constant considering no barrier
$HNO + CH$	$\rightarrow HNCO + H$	1.0×10^{-10}	3	100	Capture rate constant considering no barrier
$HNO + N(^2D)$	$\rightarrow NO + NH$	5.0×10^{-11}	2	100	By comparison with $N(^2D) + H_2O$, NH_3
$NCO + H$	$\rightarrow CO + NH$	3.0×10^{-11}	2	100	Becker et al. [2000], Louge and Hanson [1984], Klippenstein and Harding [2009]
$NCO + N(^4S)$	$\rightarrow CO + N_2$	5.5×10^{-11}	2	100	Brownsword [1997]
$HNCO + C$	$\rightarrow HCN + CO$	1.0×10^{-10}	3	100	By comparison with C + alkynes and C + alkenes
$HNCO + C$	$\rightarrow HNC + CO$	1.0×10^{-10}	3	100	By comparison with C + alkynes and C + alkenes
$HNCO + CH$	$\rightarrow CO + H_2CN$	1.0×10^{-10}	3	100	By comparison with CH + alkynes and CH + alkenes

Reactions		Rate coefficients	$F(300\ K)$	g	References
HNCO + CH	$\rightarrow$ CO + HCN + H	1.0×10^{-10}	3	100	By comparison with CH + alkynes and CH + alkenes
HNCO + $N(^2D)$	$\rightarrow$ CO + N_2 + H	5.0×10^{-11}	3	100	By comparison with $N(^2D)$ + NH_3
HNCO + CN	$\rightarrow$ NCO + HCN	3.0×10^{-11}	3	100	By comparison with CN + C_2H_6 and CN + NH_3
CH_3NO + H	$\rightarrow$ HNO + CH_3	$1.39 \times 10^{-11} \times (T/300)^{0.84} \times \exp(120/T)$	2	100	Choi and Lin [2005]
N_2O + C	$\rightarrow$ CO + N_2	$1.5 \times 10^{-11} \times \exp(-300/T)$	1.4	100	Husain and Young [1975], Dorthe et al. [1991]
N_2O + C	$\rightarrow$ NO + CN	$1.5 \times 10^{-11} \times \exp(-300/T)$	1.4	100	Husain and Young [1975], Dorthe et al. [1991]
N_2O + CH	$\rightarrow$ CO + N_2 + H	$1.5 \times 10^{-11} \times \exp(257/T)$	1.2	10	Becker et al. [1993], Zabarnick et al. [1989b]
N_2O + CH	$\rightarrow$ NO + HCN	$1.5 \times 10^{-11} \times \exp(257/T)$	1.2	10	Becker et al. [1993], Zabarnick et al. [1989b]
N_2O + $N(^2D)$	$\rightarrow$ N_2 + NO	$1.5 \times 10^{-11} \times \exp(-570/T)$	1.6	70	Herron [1999]

References

Adam, L., Hack, W., McBane, G. C., Zhu, H., Qu, Z.-W., Schinke, R., 2007. Exploring Renner-Teller induced quenching in the reaction $H(^2S)$ + $NH(a^1\Delta)$: A combined experimental and theoretical study. J. Chem. Phys. 126 (3), 034304.

Adamson, J., DeSain, J., Curl, R., Glass, G., 1997. Reaction of cyanomethylene with nitric oxide and oxygen at 298 K: HCCN + NO, O_2. J. Phys. Chem. A 101 (5), 864–870.

Adamson, J. D., Farhat, S. K., Morter, C. L., Glass, G. P., Curl, R. F., Phillips, L. F., 1994. The reaction of NH_2 with O. J. Phys. Chem. 98 (22), 5665–5669.

Adriani, A., Dinelli, B. M., López-Puertas, M., García-Comas, M., Moriconi, M. L., D'Aversa, E., Funke, B., Coradini, A., Aug. 2011. Distribution of HCN in Titan's upper atmosphere from Cassini/VIMS observations at 3 μm. Icarus 214, 584–595.

Altinay, G., Macdonald, R. G., 2012. Determination of the rate constant for the $NH_2(X^2B_1)$ + $NH_2(X^2B_1)$ recombination reaction with collision partners He, Ne, Ar, and N_2 at low pressures and 296 K. Part 1. J. Phys. Chem. A 116 (5), 1353–1367.

Andersson, S., Markovic, N., Nyman, G., 2003. Computational Studies of the Kinetics of the C + NO and O + CN Reactions. J. Phys. Chem. A 107 (28), 5439–5447.

Anicich, V. G., 2003. An index of the literature for bimolecular gas phase cation-molecule reaction kinetics. JPL Publication 03-19, 1–1194.

Asatryan, R., Bozzelli, J. W., Silva, G. d., Swinnen, S., Nguyen, M. T., 2010. Formation and decomposition of chemically activated and stabilized hydrazine. J. PHys. Chem. A 114 (21), 6235–6249.

Ashfold, M. N. R., Fullstone, M. A., Hancock, G., Ketley, G. W., 1981. Singlet methylene kinetics: Direct measurements of removal rates of $\tilde{a}^1A_1$ and $\tilde{b}^1B_1$ CH_2 and CD_2. Chem. Phys. 55 (2), 245–257.

Atkinson, R., Baulch, D. L., Cox, R. A., Crowley, J. N., Hampson, R. F., Haynes, R. G., Jenkin, M. E., Rossi, M. J., Troe, J., 2004. Evaluated kinetic and photochemical data for atmospheric chemistry: Volume I - Gas phase reactions of O_x, HO_x, NO_x and SO_x species. Atmos. Chem. Phys. 4 (6), 1461–1738.

Atkinson, R., Baulch, D. L., Cox, R. A., Hampson, R. F., Kerr, J. A., Rossi, M. J., Troe, J., 2006. Evaluated kinetic and photochemical data for atmospheric chemistry: Volume II - Gaz phase reactions of organic species. Atmos. Chem. Phys. 6 (11), 3625–4055.

Atreya, S., 1986. Atmospheres and ionospheres of the outer planets and their satellites. Springer-Verlag.

Bahng, M.-K., Macdonald, R. G., 2008. Determination of the rate constant for the $NH_2(X^2B_1)$ + $NH_2(X^2B_1)$ reaction at low pressure and 293 K. J. Phys. Chem. A 112 (51), 13432–13443.

Bahng, M.-K., Macdonald, R. G., 2009. Determination of the rate constants for the radicalradical reactions $NH_2(\tilde{X}^2B_1)$ + $NH(\tilde{X}^3\Sigma)$ and $NH_2(\tilde{X}^2B_1)$ + $H(^2S)$ at 293 K. J. Phys. Chem. A 113 (11), 2415–2423.

Balucani, N., Alagia, M., Cartechini, L., Casavecchia, P., Volpi, G. G., Sato, K., Takayanagi, T., Kurosaki, Y., 2000a. Cyanomethylene formation from the reaction of excited nitrogen atoms with acetylene: A crossed beam and ab initio study. J. Am. Chem. Soc. 122 (18), 4443–4450.

Balucani, N., Bergeat, A., Cartechini, L., Volpi, G., Casavecchia, P., Skouteris, D., Rosi, M., 2009. Combined crossed molecular beam and theoretical studies of the $N(^2D)$ + CH_4 reaction and implications for atmospheric models of Titan. J. Chem. Phys. A 113 (42), 11138–11152.

Balucani, N., Cartechini, L., Alagia, M., Casavecchia, P., Volpi, G. G., 2000b. Observation of nitrogen-bearing organic molecules from reactions of nitrogen atoms with hydrocarbons: A crossed beam Study of $N(^2D)$ + ethylene. J. Phys. Chem. A 104 (24), 5655–5659.

Balucani, N., Leonori, F., Casavecchia, P., 2012. Crossed molecular beam studies of bimolecular reactions of relevance in combustion. Energy 43 (1), 47–54.

Balucani, N., Leonori, F., Petrucci, R., Stazi, M., Skouteris, D., Rosi, M., Casavecchia, P., 2010. Formation of nitriles and imines in the atmosphere of Titan: Combined crossed-beam and theoretical studies on the reaction dynamics of excited nitrogen atoms $N(^2D)$ with ethane. Faraday Discuss. 147, 189–216.

Barger, T., Wodtke, A. M., Bowman, J. M., 2003. Radiative relaxation and isomeric branching of highly excited H/C/N: The importance of delocalized vibrational states. Astrophys. J. 587 (2 I), 841–846.

Bartels, M., Edelbuttel-Einhaus, J., Hoyermann, K., 1991. The detection of CH_3CO, C_2H_5, and CH_3CHO by rempi/mass spectrometry and the application to the study of the reactions H + CH_3CO and O + CH_3CO. Symp. Int. Combust. Proc. 23 (1), 131–138.

Bartels, M., Hoyermann, K., Sievert, R., 1982. Elementary reactions in the oxidation of ethylene: The reaction of OH radicals with ethylene and the reaction of C_2H_4OH radicals with H atoms. Symp. Int. Combust. Proc. 19, 61–72.

Barth, E. L., Toon, O. B., Mar. 2003. Microphysical modeling of ethane ice clouds in titan's atmosphere. Icarus 162, 94–113.

Basiuk, V. A., Kobayashi, K., 2004. DFT study of HCN and N≡C−C=N reactions with hydrogen species. Int. J. Quantum Chem. 99 (2), 91–101.

Baulch, D., Cobos, C., Cox, R., Esser, C., Frank, P., Just, T., Kerr, J., Pilling, M., Troe, J., Walker, R., Warnatz, J., 1992. Evaluated kinetic data for combustion modeling. J. Phys. Chem. Ref. Data 21 (3), 411–734.

Baulch, D. L., Bowman, C. T., Cobos, C. J., Cox, R. A., Just, T., Kerr, J. A., Pilling, M. J., Stocker, D., Troe, J., Tsang, W., Walker, R. W., Warnatz, J., 2005. Evaluated kinetic data for combustion modeling: Supplement II. J. Phys. Chem. Ref. Data 34 (3), 757–1397.

Baulch, D. L., Cobos, C. J., Cox, R. A., Frank, P., Hayman, G., Just, T., Kerr, J. A., Murrells, T., Pilling, M. J., Troe, J., Walker, R. W., Warnatz, J., 1994. Evaluated kinetic data for combustion modelling: Supplement I. J. Phys. Chem. Ref. Data 23, 847–1034.

Becker, K., Kurtenbach, R., Schmidt, F., Wiesen, P., 2000. Kinetics of the NCO radical reacting with atoms and selected molecules. Combust. Flame 120 (4), 570–577.

Becker, K. H., Engelhardt, B., Geiger, H., Kurtenbach, R., Weisen, P., 1993. Temperature dependence of the reactions of CH radicals with NO, NH_3 and N_2O in the range 200-1300 K. Chem. Phys. Lett. 210 (1-3), 135–140.

Bergeat, A., Calvo, T., Daugey, N., Loison, J.-C., Dorthe, G., 1998. Product branching ratios of the CH + NO reaction. J. Phys. Chem. A 102 (42), 8124–8130.

Bergeat, A., Calvo, T., Dorthe, G., Loison, J.-C., 1999. Fast-flow study of the C + NO and C + O_2 reactions. Chem. Phys. Lett. 308 (1), 7–12.

Bergeat, A., Hickson, K. M., Daugey, N., Caubet, P., Costes, M., 2009. A low temperature investigation of the N(^{4}S) + NO reaction. Phys. Chem. Chem. Phys. 11 (37), 8149–8155.

Bergeat, A., Loison, J.-C., 2001. Reaction of carbon atoms, C($_2$P^2^{3}P) with C_2H_2, C_2H_4 and C_6H_6 : Overall rate constant and relative atomic hydrogen production. Phys. Chem. Chem. Phys. 3 (11), 2038–2042.

Berman, M., Fleming, J., Harvey, A., Lin, M., 1982a. Temperature dependence of CH radical reactions with O_2, NO, CO and CO_2. Symp. Int. Combust. Proc. 19 (1), 73–79.

Berman, M., Fleming, J., Harvey, A., Lin, M., 1982b. Temperature dependence of the reactions of CH radicals with unsaturated hydrocarbons. Chem. Phys. 73 (1-2), 27–33.

Berman, M. R., Tsuchiya, T., Gregusova, A., Perera, S. A., Bartlett, R. J., 2007. HNNC radical and its role in the CH + N_2 reaction. J. Phys. Chem A. 111 (29), 6894–6899.

Berteloite, C., Le Picard, S. D., Balucani, N., Canosa, A., Sims, I. R., 2010a. Low temperature rate coefficients for reactions of the butadiynyl radical, C_4H, with various hydrocarbons. Part I: reactions with alkanes (CH_4, C_2H_6, C_3H_8, C_4H_{10}) . Phys. Chem. Chem. Phys. 12 (15), 3666–3676.

Berteloite, C., Le Picard, S. D., Balucani, N., Canosa, A., Sims, I. R., 2010b. Low temperature rate coefficients for reactions of the butadiynyl radical, C_4H, with various hydrocarbons. Part II: reactions with alkenes (ethylene, propene, 1-butene), dienes (allene, 1,3-butadiene) and alkynes (acetylene, propyne and 1-butyne). Phys. Chem. Chem. Phys. 12 (15), 3677–3689.

Berteloite, C., Le Picard, S. D., Birza, P., Gazeau, M.-C., Canosa, A., Bnilan, Y., Sims, I. R., 2008. Low temperature (39298 K) kinetics study of the reactions of the C_4H radical with various hydrocarbons observed in Titan's atmosphere. Icarus 194 (2), 746–757.

Bettinger, H. F., Schleyer, P. V. R., Schaefer Iii, H. F., Schreiner, P. R., Kaiser, R. I., Lee, Y. T., 2000. Reaction of benzene with a ground state carbon atom, C(^3P_j). J. Chem. Phys. 113 (10), 4250–4264.

Blank, D. A., Suits, A. G., Lee, Y. T., North, S. W., Hall, G. E., 1998. Photodissociation of acrylonitrile at 193 nm: A photofragment translational spectroscopy study using synchrotron radiation for product photoionization. J. Chem. Phys. 108 (14), 5784–5794.

Blitz, M. A., Pesa, M., Pilling, M. J., Seakins, P. W., 1999. Reaction of CH with H_2O: Temperature dependence and isotope effect. J. Phys. Chem. A 103 (29), 5699–5704.

Blitz, M. A., Seakins, P. W., Smith, I. W. M., 2009. An experimental confirmation of the products of the reaction between CN radicals and NH_3. Phys. Chem. Chem. Phys. 11 (46), 10824–10826.

Blitz, M. A., Talbi, D., Seakins, P. W., Smith, I. W. M., 2012. Rate constants and branching ratios for the reaction of CH radicals with NH_3: A combined experimental and theoretical study. J. Phys. Chem. A 116 (24), 5877–5885.

Bocherel, P., Herbert, L. B., Rowe, B. R., Sims, I. R., Smith, I. W. M., Travers, D., 1996. Ultralow-temperature kinetics of CH($X^2\Pi$) reactions: Rate coefficients for reactions with O_2 and NO (T = 13-708 K), and with NH_3 (T = 23-295 K). J. Phys. Chem 100 (8), 3063–3069.

Böhland, T., Temps, F., Wagner, H. G., 1984. Direct investigation of the reaction $CH_2(X^2B_1)$ + O(^{3}P) with the LMR. Ber. Bunsenges. Phys. Chem. 88 (12), 1222–1228.

Böhland, T., Temps, F., Wagner, H. G., 1985. The contributions of intersystem crossing and reaction in the removal of $CH_2(\tilde{a}^1A_1)$ by hydrocarbons studied with the LMR. Ber. Bunsenges. Phys. Chem. 89 (9), 1013–1018.

Böhland, T., Temps, F., Wagner, H. G., 1987. A direct study of the reactions of methylene($\tilde{X}^3B_1$) radicals with hydrogen and deuterium atoms. J. Phys. Chem. 91 (5), 1205–1209.

Bosco, S., Nava, D., Brobst, W., Stief, L., 1984. Temperature and pressure-dependence of the absolute rate-constant for the reactions of NH_2 radicals with acetylene and ethylene. J. Chem. Phys. 81 (8), 3505–3511.

Boullart, W., Devriendt, T., Borms, R., Peeters, J., 1996. Identification of the sequence CH($^2\Pi$) + C_2H_2 → C_3H_2 + H (and C_3H + H_2) followed by C_3H_2 + O → C_2H + HCO (or H + CO) as C_2H source in C_2H_2/O/H atomic flames. J. Phys. Chem. 100 (3), 998–1007.

Boullart, W., Peeters, J., 1992. Product distributions of the C_2H_2 + H and HCCO (ketenyl) + H reactions. Rate constant of CH($\tilde{X}^3B_1$) + H. J. Phys. Chem. 96 (24), 9810–9816.

Bouwman, J., Goulay, F., Leone, S. R., Wilson, K. R., 2012. Bimolecular rate constant and product branching ratio measurements for the reaction of C_2H with ethene and propene at 79 K. J. Phys. Chem. A 116 (15), 3907–3917.

Brouard, M., Macpherson, M. T., Pilling, M. J., 1989. Experimental and RRKM modeling study of the methyl + hydrogen atom and deuterium atom reactions. J. Phys. Chem. 93 (10), 4047–4059.

Brownsword, R., Hancock, G., Heard, D., 1997. Kinetics of the N + NCO reaction at 298 K. J. Chem. Soc. Faraday Trans. 93, 2473–2475.

Brownsword, R. A., Herbert, L. B., Smith, I. W. M., Stewart, D. W. A., 1996. Pressure and temperature dependence of the rate constants for the association reactions of CH radicals with CO and N_2 between 202 and 584 K. J. Chem. Soc. Faraday Trans. 92, 1087–1094.

Bullock, G., Cooper, R., 1971. Reactions of cyanogen radicals with hydrocarbons. Trans. Faraday Soc. 67, 3258.

Busfield, W., Lee, R., Merigold, D., 1973. Gas phase equilibrium between acetaldehyde and paraldehyde, thermodynamic values for the trimerisation of acetaldehyde and the polymerisability of paraldehyde. Journal of the Chemical Society, Faraday Transactions 1: Physical Chemistry in Condensed Phases 69, 936–940.

Butler, J., Fleming, J., Goss, L., Lin, M., 1981. Kinetics of CH radical reactions with selected molecules at room temperature. Chem. Phys. 56 (3), 355–365.

Butterfield, M. T., Yu, T., Lin, M. C., 1993. Kinetics of CN reactions with allene, butadiene, propylene and acrylonitrile. Chem. Phys. 169 (1), 129–134.

Callear, A. B., Smith, G. B., 1986. Recurring chains following addition of atomic hydrogen to acetylene. J. Phys. Chem. 90 (14), 3229–3237.

Camilleri, P., Marshall, R., Purnell, J., 1974. Reaction of hydrogen atoms with ethane. J. Chem. Soc. Faraday Trans. 1 70, 1434–1444.

Canosa, A., Paramo, A., Le Picard, S. D., Sims, I. R., 2007. An experimental study of the reaction kinetics of $C_2(X^1\Sigma_g^+)$ with hydrocarbons (CH_4, C_2H_2, C_2H_4, C_2H_6 and C_3H_8) over the temperature range 24-300 K: Implications for the atmospheres of Titan and the Giant Planets. Icarus 187 (2), 558–568.

Canosa, A., Sims, I., Travers, D., Smith, I., Rowe, B., 1997. Reactions of the methylidine radical with CH_4, C_2H_2, C_2H_4, C_2H_6 and but-1-ene studied between 23 and 295 K with a CRESU apparatus. Astron. Astrophys. 323 (2), 644–651.

Caridade, P. J. S. B., Rodrigues, S. P. J., Sousa, F., Varandas, A. J. C., 2005. Unimolecular and bimolecular calculations for HN_2. J. Phys. Chem. A 109 (10), 2356–2363.

Carl, S. A., Nguyen, H. M. T., Elsamra, R. M. I., Nguyen, M. T., Peeters, J., 2005. Pulsed laser photolysis and quantum chemical-statistical rate study of the reaction of the ethynyl radical with water vapor. J. Chem. Phys. 122 (11), 114307.

Carty, D., Le Page, V., Sims, I. R., Smith, I. W. M., 2001. Low temperature rate coefficients for the reactions of CN and C_2H radicals with allene (CH_2=C=CH_2) and methyl acetylene ($CH_3C{\equiv}CH$). Chem. Phys. Lett. 344 (3-4), 310–316.

Casavecchia, P., Balucani, N., Cartechini, L., Capozza, G., Bergeat, A., Volpi, G. G., 2001. Crossed beam studies of elementary reactions of N and C atoms and CN radicals of importance in combustion. Faraday Discuss. 119, 27–49.

Chang, A. H. H., Mebel, A. M., Yang, X. M., Lin, S. H., Lee, Y. T., 1998a. Ab initio calculations of potential energy surface and rate constants for ethylene photodissociation at 193 and 157 nm. Chem. Phys. Lett. 287 (3-4), 301–306.

Chang, A. H. H., Mebel, A. M., Yang, X. M., Lin, S. H., Lee, Y. T., 1998b. Ab initio/RRKM approach toward the understanding of ethylene photodissociation. J. Chem. Phys. 109 (7), 2748–2761.

Chang, Y.-W., Wang, N. S., 1995. Rates of the reactions CN + H_2CO and NCO + H_2CO in the temperature range 294-769 K. Chem. Phys. 200 (3), 431–437.

Chastaing, D., James, P., Sims, I., Smith, I., 1998. Neutral-neutral reactions at the temperatures of interstellar clouds: Rate coefficients for reactions of C_2H radicals with O_2, C_2H_2, C_2H_4 and C_3H_6 down to 15 K. Faraday Discuss. 109, 169–181.

Chastaing, D., James, P., Sims, I., Smith, I., 1999. Neutral-neutral reactions at the temperatures of interstellar clouds: Rate coefficients for reactions of atomic carbon, C(^{3}P), with O_2, C_2H_2, C_2H_4 and C_3H_6 down to 15 K. Phys. Chem. Chem. Phys. 1 (9), 2247–2256.

Chastaing, D., Picard, S. D. L., Sims, I. R., Smith, I. W. M., 2001. Rate coefficients for the reactions of C(^3P_J) atoms with C_2H_2, C_2H_4, CH_3CCH and H_2CCCH_2 at temperatures down to 15 K. Astron. Astrophys. 365 (2), 241–247.

Cheikh Sid Ely, S., Morales, S. B., Guillemin, J.-C., Klippenstein, S. J., Sims, I. R., 2013. Low temperature rate coefficients for the reaction CN + HC_3N. J. Phys. Chem. A 117 (46), 12155–12164.

Choi, Y. M., Lin, M. C., 2005. Kinetics and mechanisms for reactions of HNO with CH_3 and C_6H_5 studied by quantum-chemical and statistical-theory calculations. Int. J. Chem. Kinet. 37 (5), 261–274.

Clarke, D. W., Ferris, J. P., 1995. Photodissociation of cyanoacetylene: Application to the atmospheric chemistry of Titan. Icarus 115 (1), 119–125.

Cody, R. J., Payne, W. A., Thorn, R. P., Nesbitt, F. L., Iannone, M. A., Tardy, D. C., Stief, L. J., 2002. Rate constant for the recombination reaction CH_3 + CH_3 → C_2H_6 at T = 298 and 202 K. J. Phys. Chem. A 106 (25), 6060–6067.

Cody, R. J., Romani, P. N., Nesbitt, F. L., Iannone, M. A., Tardy, D. C., Stief, L. J., 2003. Rate constant for the reaction CH_3 + CH_3 → C_2H_6 at T = 155 K and model calculation of the CH_3 abundance in the atmospheres of Saturn and Neptune. J. Geophys. Res. - Planet. 108 (E11), 5119.

Costes, M., Halvick, P., Hickson, K. M., Daugey, N., Naulin, C., 2009. Non-threshold, threshold, and nonadiabatic behavior of the key interstellar C + C_2H_2 reaction. Astrophys. J. 703 (2), 1179–1187.

Cottini, V., Nixon, C. A., Jennings, D. E., Anderson, C. M., Gorius, N., Bjoraker, G. L., Coustenis, A., Teanby, N. A., Achterberg, R. K., Bézard, B., de Kok, R., Lellouch, E., Irwin, P. G. J., Flasar, F. M., Bampasidis, G., Aug. 2012. Water vapor in Titan's stratosphere from Cassini CIRS far-infrared spectra. Icarus 220, 855–862.

Cotton, E. C., Francisco, J. S., Klemperer, W., 2013. Computational study of the linear proton bound ion-molecule complexes of $HCNH^+$ with HCN and HNC. J. Chem. Phys. 139 (1), 014304.

Courtin, R., Swinyard, B. M., Moreno, R., Fulton, T., Lellouch, E., Rengel, M., Hartogh, P., Dec. 2011. First results of Herschel-SPIRE observations of Titan. Astronomy and Astrophysics 536, L2.

Coustenis, A., Bezard, B., May 1995. Titan's atmosphere from Voyager infrared observations. 4: Latitudinal variations of temperature and composition. Icarus 115, 126–140.

Coustenis, A., Bezard, B., Gautier, D., Marten, A., Samuelson, R., Jan. 1991. Titan's atmosphere from Voyager infrared observations. III - Vertical contributions of hydrocarbons and nitriles near Titan's north pole. Icarus 89, 152–167.

Cremer, D., Kraka, E., Joo, H., Stearns, J. A., Zwier, T. S., 2006. Exploration of the potential energy surface of C_4H_4 for rearrangement and decomposition reactions of vinylacetylene: A computational study. Part I. Phys. Chem. Chem. Phys. 8 (45), 5304–5316.

Crespin, A., Lebonnois, S., Vinatier, S., Bézard, B., Coustenis, A., Teanby, N. A., Achterberg, R. K., Rannou, P., Hourdin, F., Oct. 2008. Diagnostics of Titan's stratospheric dynamics using Cassini/CIRS data and the 2-dimensional IPSL circulation model. Icarus 197, 556–571.

Crider, P. E., Castiglioni, L., Kautzman, K. E., Neumark, D. M., 2009. Photodissociation of the propargyl and propynyl (C_3D_3) radicals at 248 and 193 nm. J. Chem. Phys. 130 (4), 044310.

Cui, J., Yelle, R. V., Vuitton, V., Waite, J. H., Kasprzak, W. T., Gell, D. A., Niemann, H. B., Müller-Wodarg, I. C. F., Borggren, N., Fletcher, G. G., Patrick, E. L., Raaen, E., Magee, B. A., Apr. 2009. Analysis of Titan's neutral upper atmosphere from Cassini Ion Neutral Mass Spectrometer measurements. Icarus 200, 581–615.

Daranlot, J., Hincelin, U., Bergeat, A., Costes, M., Loison, J.-C., Wakelam, V., Hickson, K., 2012. Elemental nitrogen partitioning in dense interstellar clouds. Proc. Natl. Acad. Sci. U. S. A. 109 (26), 1023310238.

Daranlot, J., Hu, X., Xie, C., Loison, J.-C., Caubet, P., Costes, M., Wakelam, V., Xie, D., Guo, H., Hickson, K. M., 2013. Low temperature rate constants for the $N(^4S)$ + $CH(X^2\Pi_r)$ reaction. Implications for N_2 formation cycles in dense interstellar clouds. Phys. Chem. Chem. Phys. 15 (33), 13888–13896.

Daranlot, J., Jorfi, M., Xie, C., Bergeat, A., Costes, M., Caubet, P., Xie, D., Guo, H., Honvault, P., Hickson, K. M., 2011. Revealing atom-radical reactivity at low temperature through the N + OH reaction. Science 334 (6062), 1538–1541.

Darwin, D. C., Young, A. T., Johnston, H. S., Moore, C. B., 1989. Rate constants for triplet methylene ($\tilde{X}^3B_1$) removal by oxygen, nitric oxide and acetylene from infrared diode laser flash kinetic spectroscopy. J. Phys. Chem. 93 (3), 1074–1078.

Daugey, N., Caubet, P., Bergeat, A., Costes, M., Hickson, K. M., 2008. Reaction kinetics to low temperatures. Dicarbon + acetylene, methylacetylene, allene and propene from 77 $\leq$ T $\leq$ 296 K. Phys. Chem. Chem. Phys. 10 (5), 729–737.

Daugey, N., Caubet, P., Retail, B., Costes, M., Bergeat, A., Dorthe, G., 2005. Kinetic measurements on methylidyne radical reactions with several hydrocarbons at low temperatures. Phys. Chem. Chem. Phys. 7 (15), 2921–2927.

Davis, S. G., Law, C. K., Wang, H., 1999. Propyne pyrolysis in a flow reactor: An experimental, RRKM, and detailed kinetic modeling study. J. Phys. Chem. A 103 (30), 5889–5899.

De Avillez Pereira, R., Baulch, D. L., Pilling, M. J., Robertson, S. H., Zeng, G., 1997. Temperature and pressure dependence of the multichannel rate coefficients for the CH_3 + OH system. J. Phys. Chem. A 101 (50), 9681–9693.

de Kok, R., Irwin, P. G. J., Teanby, N. A., Oct. 2008. Condensation in Titan's stratosphere during polar winter. Icarus 197, 572–578.

de Kok, R., Irwin, P. G. J., Teanby, N. A., Lellouch, E., Bézard, B., Vinatier, S., Nixon, C. A., Fletcher, L., Howett, C., Calcutt, S. B., Bowles, N. E., Flasar, F. M., Taylor, F. W., Feb. 2007. Oxygen compounds in Titan's stratosphere as observed by Cassini CIRS. Icarus 186, 354–363.

Dean, A. J., Hanson, R. K., 1992. CH and C-atom time histories in dilute hydrocarbon pyrolysis: Measurements and kinetics calculations. Int. J. Chem. Kinet 24 (6), 517–532.

Demissy, M., Lesclaux, R., 1980. Kinetics of hydrogen abstraction by NH_2 radicals from alkanes in the gas-phase - A flash-photolysis laser resonance-absorption study. J. Am. Chem. Soc. 102 (9), 2897–2902.

Deng, W.-Q., Han, K.-L., Zhan, J.-P., He, G.-Z., 1998. Ab initio and RRKM calculations of o-benzyne pyrolysis. Chem. Phys. Lett. 288 (1), 33–36.

Derecskei-Kovacs, A., North, S. W., 1999. The unimolecular dissociation of vinylcyanide: A theoretical investigation of a complex multichannel reaction. J. Chem. Phys. 110 (6), 2862–2871.

Dobe, S., Berces, T., Szilagyi, I., 1991. Kinetics of the reaction between methoxyl radicals and hydrogen atoms. J. Chem. Soc., Faraday Trans. 87, 2331–2336.

Dobrijevic, M., Carrasco, N., Hébrard, E., Pernot, P., Nov. 2008. Epistemic bimodality and kinetic hypersensitivity in photochemical models of Titan's atmosphere. Planetary and Space Science 56, 1630–1643.

Dobrijevic, M., Hébrard, E., Loison, J. C., Hickson, K. M., Jan. 2014. Coupling of oxygen, nitrogen, and hydrocarbon species in the photochemistry of Titan's atmosphere. Icarus 228, 324–346.

Dorthe, G., Caubet, P., Vias, T., Barrre, B., Marchais, J., 1991. Fast flow studies of atomic carbon kinetics at room temperature. J. Phys. Chem. 95 (13), 5109–5116.

Dransfeld, P., Hack, W., Kurzke, H., Temps, F., Wagner, H. G., 1985. Direct studies of elementary reactions of NH_2-radicals in the gas phase. Symp. Int. Combust. Proc. 20 (1), 655–663.

Dransfeld, P., Wagner, H., 1987. Investigation of the gas phase reaction N + NH_2 → N_2 + 2H at room temperature. Z. Phys. Chem. 153 (1-2), 89–97.

Du, B., Zhang, W., 2006. Ab initio MO study of potential energy surface of NH_2 with CN reaction. Int. J. Quantum Chem. 106 (8), 1827–1843.

Du, B., Zhang, W., Feng, C., Zhou, Z., 2005. Ab initio quantum chemical studies of reaction mechanism for triplet CH_2 with CN radical. J. Mol. Struct. - THEOCHEM 713 (1-3), 71–78.

Dunning Jr, T. H., 1989. Gaussian basis sets for use in correlated molecular calculations. I. The atoms boron through neon and hydrogen. J. Chem. Phys. 90 (2), 1007–1023.

Duran, R. P., Amorebieta, V. T., Colussi, A. J., 1988. Is the homogeneous thermal dimerization of acetylene a free-radical chain reaction? Kinetic and thermochemical analysis. J. Phys. Chem. 92 (3), 636–640.

Durant, J. L., 1994. Product branching fractions in the reaction of NH (ND) ($^3\Sigma_-$) with nitric oxide. J. Phys. Chem. 98 (2), 518–521.

Dutuit, O., Carrasco, N., Thissen, R., Vuitton, V., Alcaraz, C., Pernot, P., Balucani, N., Casavecchia, P., Canosa, A., Le Picard, S., Loison, J.-C., Herman, Z., Zabka, J., Ascenzi, D., Tosi, P., Franceschi, P., Price, S. D., Lavvas, P., 2013. Critical review of N, N^+, N_2^+, N^{++}, and N_2^{++} main production processes and reactions of relevance to Titan's atmosphere. Astrophys. J. Suppl. Ser. 204 (2), 20.

Eden, S., Limã-Vieira, P., Kendall, P., Mason, N. J., Hoffmann, S. V., Spyrou, S. M., 2003. High resolution photo-absorption studies of acrylonitrile, C_2H_3CN, and acetonitrile, CH_3CN. Eur. Phys. J. D 26 (2), 201–210.

Edvardsson, D., Baltzer, P., Karlsson, L., Wannberg, B., Holland, D. M. P., Shaw, D. A., Rennie, E. E., 1999. A photoabsorption, photodissociation and photoelectron spectroscopy study of NH_3 and ND_3. J. Phys. B 32 (11), 2583.

Espinosa-Garcia, J., Corchado, J., 1994. Variational transition-state theory calculation using the direct dynamics method - NH_3 + H → NH_2 + H_2 reaction. J. Chem. Phys. 101 (2), 1333–1342.

Evans, R. A., Lorencak, P., Ha, T. K., Wentrup, C., 1991. HCN dimers: iminoacetonitrile and N-cyanomethanimine. J. Am. Chem. Soc. 113 (19), 7261–7276.

Fagerstrom, K., Jodkowski, J. T., Lund, A., Ratajczak, E., 1995. Kinetics of the self-reaction and the reaction with OH of the amidogen radical. Chem. Phys. Lett. 236 (1-2), 103–110.

Fahr, A., Halpern, J. B., Tardy, D. C., 2007. Calculational and experimental investigations of the pressure effects on radical-radical cross combination ceactions: C_2H_5 + C_2H_3. J. Phys. Chem. A 111 (29), 6600–6609.

Fahr, A., Laufer, A., Klein, R., Braun, W., 1991. Reaction rate determinations of vinyl radical reactions with vinyl, methyl, and hydrogen atoms. J. Phys. Chem. 95 (8), 3218–3224.

Fahr, A., Laufer, A., Tardy, D., 1999. Pressure effect on CH_3 and C_2H_3 cross-radical reactions. J. Phys. Chem. A 103 (42), 8433–8439.

Fahr, A., Laufer, A. H., 1992. The 1,1-elimination of hydrogen cyanide and formation of triplet vinylidene from the photolysis of acrylonitrile. J. Phys. Chem. 96 (11), 4217–4219.

Fahr, A., Nayak, A., 2000. Kinetics and products of propargyl (C_3H_3) radical self-reactions and propargyl-methyl cross-combination reactions. Int. J. Chem. Kinet. 32 (2), 118–124.

Faravelli, T., Goldaniga, A., Zappella, L., Ranzi, E., Dagaut, P., Cathonnet, M., 2000. An experimental and kinetic modeling study of propyne and allene oxidation. Proc. Combust. Inst. 28 (2), 2601–2608.

Feng, W., Hershberger, J. F., 2007. Kinetics of the O + HCNO Reaction. J. Phys. Chem. A 111 (42), 10654–10659.

Fikri, M., Meyer, S., Roggenbuck, J., Temps, F., 2001. An experimental and theoretical study of the product distribution of the reaction CH_2 ($\tilde{X}^3B_1$) + NO. Faraday Discuss. 119, 223–242.

Flasar, F. M., Achterberg, R. K., Conrath, B. J., Gierasch, P. J., Kunde, V. G., Nixon, C. A., Bjoraker, G. L., Jennings, D. E., Romani, P. N., Simon-Miller, A. A., Bézard, B., Coustenis, A., Irwin, P. G. J., Teanby, N. A., Brasunas, J., Pearl, J. C., Segura, M. E., Carlson, R. C., Mamoutkine, A., Schinder, P. J., Barucci, A., Courtin, R., Fouchet, T., Gautier, D., Lellouch, E., Marten, A., Prangé, R., Vinatier, S., Strobel, D. F., Calcutt, S. B., Read, P. L., Taylor, F. W., Bowles, N., Samuelson, R. E., Orton, G. S., Spilker, L. J., Owen, T. C., Spencer, J. R., Showalter, M. R., Ferrari, C., Abbas, M. M., Raulin, F., Edgington, S., Ade, P., Wishnow, E. H., May 2005. Titan's Atmospheric Temperatures, Winds, and Composition. Science 308, 975–978.

Fleming, J., Fujimoto, G., Lin, M., Harvey, A., 1980. Applications of multiphoton dissociation and laser induced fluorescence to combustion: Reactions of CH radicals with unsaturated hydrocarbons. In: Corcoran, V. J. (Ed.), Proc. Int. Conf. Lasers79. STS Press, McLean, VA, pp. 246–250.

Fournier, M., Guillemin, J., Sims, I., 2014. Low temperature kinetics of C_3N radical reactions. In preparation.

Frankcombe, T. J., Nyman, G., 2007. Adiabatic capture theory applied to N + NH → N_2 + H at low temperature. J. Phys. Chem. A 111 (50), 13163–13167.

Fray, N., Schmitt, B., Dec. 2009. Sublimation of ices of astrophysical interest: A bibliographic review. Planetary and Space Science 57, 2053–2080.

Frost, R., Green, D., Osborn, M., Smith, I., 1986. Time-resolved vibrational chemiluminescence: Rate constants for the reactions of F atoms with H_2O and HCN, and for the relaxation of HF (v = 1) by H_2O and HCN. Int. J. Chem. Kinet. 18 (8), 885–898.

Fu, B., Han, Y.-C., Bowman, J. M., Angelucci, L., Balucani, N., Leonori, F., Casavecchia, P., 2012a. Intersystem crossing and dynamics in O(^{3}P) + C_2H_4 multichannel reaction: Experiment validates theory. P. Natl. A. Sci. 109 (25), 9733–9738.

Fu, B., Han, Y.-C., Bowman, J. M., Leonori, F., Balucani, N., Angelucci, L., Occhiogrosso, A., Petrucci, R., Casavecchia, P., 2012b. Experimental and theoretical studies of the O(^{3}P) + C_2H_4 reaction dynamics: Collision energy dependence of branching ratios and extent of intersystem crossing. J. Chem. Phys. 137 (22), 22A532.

Fukuzawa, K., Osamura, Y., 1997. Molecular orbital study of neutral-neutral reactions concerning HC_3N formation in interstellar space. Astrophys. J. 489 (1), 113–121.

Fulle, D., Hippler, H., 1997. The temperature and pressure dependence of the reaction CH + H_2 ↔ CH_3 ↔ CH_2 + H. J. Chem. Phys. 106 (21), 8691–8698.

Galland, N., Caralp, F., Hannachi, Y., Bergeat, A., Loison, J.-C., 2003. Experimental and theoretical studies of the methylidyne CH($X^2\Pi$) radical reaction with ethane (C_2H_6): Overall rate constant and product channels. J. Phys. Chem. A 107 (28), 5419–5426.

Gandini, A., Hackett, P. A., 1978. The photochemistry of acrylonitrile vapour at 213.9 nm. Can. J. Chem. 56 (15), 2096–2098.

Gannon, K., Blitz, M., Kovacs, T., Pilling, M., Seakins, P., 2010a. State resolved measurements of a $^1CH_2$ removal confirm predictions of the gateway model for electronic quenching. J. Chem. Phys. 132 (2), 024302.

Gannon, K., Blitz, M., Liang, C., Pilling, M., Seakins, P., Glowacki, D., 2010b. Temperature dependent kinetics and H atom yields from reactions of $^1CH_2$ with acetylene, ethene, and propene. J. Phys. Chem. A 114 (35), 9413–9424.

Gannon, K., Blitz, M., Liang, C.-H., Pilling, M., Seakins, P., Glowacki, D., Harvey, J., 2010c. An experimental and theoretical investigation of the competition between chemical reaction and relaxation for the reactions of $^1CH_2$ with acetylene and ethene: implications for the chemistry of the giant planets. Faraday Discuss. 147, 1–16.

Gannon, K., Blitz, M., Pilling, M., Seakins, P., Klippenstein, S., Harding, L., 2008. Kinetics and product branching ratio of the reaction of $^1CH_2$ with H_2 and D_2. J. Phys. Chem A. 112 (39), 9575–9583.

Gannon, K., Glowacki, D., Blitz, M., Hughes, K., Pilling, M., Seakins, P., 2007. H atom yields from the reactions of CN radicals with C_2H_2, C_2H_4, C_3H_6, trans-2-C_4H_8, and iso-C_4H_8. J. Phys. Chem. A 111 (29), 6679–6692.

Gans, B., Boy-Pronne, S., Broquier, M., Delsaut, M., Douin, S., Fellows, C. E., Halvick, P., Loison, J. C., Lucchese, R. R., Gauyacq, D., 2011. Photolysis of methane revisited at 121.6 nm and at 118.2 nm: Quantum yields of the primary products, measured by mass spectrometry. Phys. Chem. Chem. Phys. 13 (18), 8140–8152.

Geballe, T. R., Kim, S. J., Noll, K. S., Griffith, C. A., Jan. 2003. High-Resolution 3 Micron Spectroscopy of Molecules in the Mesosphere and Troposphere of Titan. The Astrophysical Journal 583, L39–L42.

Georgievskii, Y., Klippenstein, S. J., 2005. Long-range transition state theory. J. Chem. Phys. 122 (19), 194103–17.

Georgievskii, Y., Miller, J. A., Klippenstein, S. J., 2007. Association rate constants for reactions between resonance-stabilized radicals: C_3H_3 + C_3H_3, C_3H_3 + C_3H_5, and C_3H_5 + C_3H_5. Phys. Chem. Chem. Phys. 9 (31), 4259–4268.

Geppert, W. D., Reignier, D., Stoecklin, T., Naulin, C., Costes, M., Chastaing, D., Le Picard, S. D., Sims, I. R., Smith, I. W. M., 2000. Comparison of the cross-sections and thermal rate constants for the reactions of C(^3P_J) atoms with O_2 and NO. Phys. Chem. Chem. Phys. 2 (13), 2873–2881.

Ghibaudi, E., Colussi, A. J., 1988. Kinetics and thermochemistry of the equilibrium 2 C_2H_2 ↔ C_4H_4: direct evidence against a chain mechanism. J. Phys. Chem. 92 (20), 5839–5842.

Gladstone, G. R., Allen, M., Yung, Y. L., 1996. Hydrocarbon photochemistry in the upper atmosphere of Jupiter. Icarus 119 (1), 1–52.

Glarborg, P., Dam-Johansen, K., Miller, J. A., 1995. The reaction of ammonia with nitrogen dioxide in a flow reactor: Implications for the NH_2 + NO_2 reaction. Int. J. Chem. Kin. 27 (12), 1207–1220.

Glass, G. P., Kumaran, S. S., Michael, J. V., 2000. Photolysis of ketene at 193 nm and the rate constant for H + HCCO at 297 K. J. Phys. Chem. A 104 (36), 8360–8367.

Golden, D. M., 2012. The reaction OH + C_2H_4: An example of rotational channel switching. J. Phys. Chem. A 116 (17), 4259–4266.

Gosavi, R. K., Safarik, I., Strausz, O. P., 1985. Molecular orbital studies of carbyne reactions: addition and insertion reaction paths for the CH($\tilde{X}^2\Pi$) + C_2H_4($\tilde{X}\,^1A_g$) reaction. Can. J. Chem. 63 (7), 1689–1693.

Goulay, F., Leone, S., 2006. Low-temperature rate coefficients for the reaction of ethynyl radical (C_2H) with benzene. J. Phys. Chem. A 110 (5), 1875–1880.

Goulay, F., Soorkia, S., Meloni, G., Osborn, D. L., Taatjes, C. A., Leone, S. R., 2011. Detection of pentatetraene by reaction of the ethynyl radical (C_2H) with allene (CH_2=C=CH_2) at room temperature. Phys. Chem. Chem. Phys. 13 (46), 20820–20827.

Goulay, F., Trevitt, A. J., Meloni, G., Selby, T. M., Osborn, D. L., Taatjes, C. A., Vereecken, L., Leone, S. R., 2009. Cyclic versus linear isomers produced by reaction of the methylidyne radical (CH) with small unsaturated hydrocarbons. J. Am. Chem. Soc. 131 (3), 993–1005.

Gray, P., Thynne, J., 1964. Arrhenius parameters for elementary combustion reactions: H-atom abstraction from N-H bonds. Proc. Combust. Inst. 10 (1), 435–44.

Gronoff, G., Mertens, C., Lilensten, J., Desorgher, L., Flückiger, E., Velinov, P., May 2011. Ionization processes in the atmosphere of Titan. III. Ionization by high-Z nuclei cosmic rays. Astronomy and Astrophysics 529, A143.

Gronoff, G., Simon Wedlund, C., Mertens, C. J., Lillis, R. J., Apr. 2012. Computing uncertainties in ionosphere-airglow models: I. Electron flux and species production uncertainties for Mars. Journal of Geophysical Research (Space Physics) 117, 4306.

Gu, X., Guo, Y., Zhang, F., Mebel, A. M., Kaiser, R. I., 2006. Reaction dynamics of carbon-bearing radicals in circumstellar envelopes of carbon stars. Faraday Disc. 133, 245–275.

Guo, J., Eng, R., Carrington, T., Filseth, S. V., 2000. Photodissociation of HCN at 157 nm: Energy disposal in the CN($A^2\Pi$) fragment. J. Chem. Phys. 112 (20), 8904–8909.

Gurwell, M. A., Nov. 2004. Submillimeter Observations of Titan: Global Measures of Stratospheric Temperature, CO, HCN, HC_3N, and the Isotopic Ratios $^{12}C/^{13}C$ and $^{14}N/^{15}N$. The Astrophysical Journal 616, L7–L10.

Hack, W., Wagner, H., Zaspypkin, A., 1994. Elementary reactions of NH($a^1\Delta$) and NH($X^3\Sigma$) with N, O and NO. Ber. Bunsenges. Phys. Chem. 98 (2), 156–164.

Haider, N., Husain, D., 1993a. Absolute rate data for the reactions of ground-state atomic carbon, C[$^2p^2(^3P_J)$], with alkenes investigated by time-resolved atomic resonance absorption spectroscopy in the vacuum ultraviolet. J. Chem. Soc. Faraday Trans. 89, 7–14.

Haider, N., Husain, D., 1993b. The collisional behaviour of ground state atomic carbon, C($_2p^2(^3P_j)$), with ethylene and acetylene investigated by time-resolved atomic resonance absorption spectroscopy in the vacuum ultraviolet. J. Photochem. Photobiol. A 70 (2), 119–124.

Halonen, L., Deeley, C. M., Mills, I. M., 1986. Intensities in the ν_7, ν_8, and ν_9 bands of CH_2NH and the harmonic force field of methyleneimine. J. Chem. Phys. 85 (2), 692–696.

Halpern, J. A., Miller, G. E., Okabe, H., Nottingham, W., 1988. The UV photochemistry of cyanoacetylene. J. Photochem. Photobiol. A 42 (1), 63–72.

Hanning-Lee, M. A., Pilling, M. J., 1992. Kinetics of the reaction between H atoms and allyl radicals. Int. J. Chem. Kinet. 24 (3), 271–278.

Harding, L., Guadagnini, R., Schatz, G., 1993. Theoretical-studies of the reactions H + CH → C + H_2 and C + H_2 → CH_2 using an abinitio global ground-state potential surface for CH_2. J. Phys. Chem. 97 (21), 5472–5481.

Harding, L., Klippenstein, S., Georgievskii, Y., 2007. On the combination reactions of hydrogen atoms with resonance-stabilized hydrocarbon radicals. J. Phys. Chem. A 111 (19), 3789–3801.

Harding, L. B., Klippenstein, S. J., 1998. A theoretical analysis of the reaction of H with C_2H_5. Symp. Int. Combust. Proc. 27 (1), 151–157.

Harding, L. B., Klippenstein, S. J., Georgievskii, Y., 2005. Reactions of oxygen atoms with hydrocarbon radicals: a priori kinetic predictions for the CH_3 + O, C_2H_5 + O, and C_2H_3 + O reactions. P. Combust. Inst. 30 (1), 985–993.

Harris, G. W., Pitts, J. J. N., 1982. Absolute rate constants and temperature dependencies for the gas phase reactions of H atoms with propene and the butenes in the temperature range 298 to 445 K. J. Chem. Phys. 77 (8), 3994–3997.

Hébrard, E., Dobrijevic, M., Bénilan, Y., Raulin, F., 2006. Photochemical kinetics uncertainties in modeling Titan's atmosphere: a review. J. Photochem. Photobiol. C - Photochem. Rev. 7, 211–230.

Hébrard, E., Dobrijevic, M., Bénilan, Y., Raulin, F., 2007. Photochemical kinetics uncertainties in modeling Titan's atmosphere: First consequences. Planet. Space Sci. 55, 1470–1489.

Hébrard, E., Dobrijevic, M., Loison, J., Bergeat, A., Hickson, K., F., C., 2013. Photochemistry of C_3H_p hydrocarbons in Titan's stratosphere revisited. Astronomy and Astrophysics.

Hébrard, E., Dobrijevic, M., Loison, J. C., Bergeat, A., Hickson, K. M., May 2012. Neutral production of hydrogen isocyanide (HNC) and hydrogen cyanide (HCN) in Titan's upper atmosphere. Astronomy and Astrophysics 541, A21.

Hébrard, E., Dobrijevic, M., Pernot, P., Carrasco, N., Bergeat, A., Hickson, K. M., Canosa, A., Le Picard, S. D., Sims, I. R., 2009. How Measurements of Rate Coefficients at Low Temperature Increase the Predictivity of Photochemical Models of Titan's Atmosphere. Journal of Physical Chemistry 113 (42), 11227–11237.

Heinemann, P., Hofmann-Sievert, R., Hoyermann, K., 1988. Direct study of the reactions of vinyl radicals with hydrogen and oxygen atoms. Symp. Int. Combust. Proc. 21 (1), 865.

Herbst, E., Terzieva, R., Talbi, D., 2000. Calculations on the rates, mechanisms, and interstellar importance of the reactions between C and NH_2 and between N and CH_2. Mon. Not. Roy. Astron. Soc. 311 (4), 869–876.

Herron, J. T., 1999. Evaluated chemical kinetics data for reactions of N(^{2}D), N(^{2}P), and $N_2(A^3\Sigma_u^+)$ in the gas phase. J. Phys. Chem. Ref. Data 28 (5), 1453–1483.

Herzberg, G., 1957. Molecular spectra and molecular structures. Vol. III. D. Van Nostrand Company, New York.

Homayoon, Z., Bowman, J. M., 2014. A global potential energy surface describing the N(^{2}D) + H_2O reaction and a quasiclassical trajectory study of the reaction to NH + OH. J. Phys. Chem. A 118 (3), 545–553.

Homayoon, Z., Vazquez, S. A., Rodriguez-Fernandez, R., Martinez-Nunez, E., 2011. Ab initio and RRKM study of the HCN/HNC elimination channels from vinyl cyanide. J. Phys. Chem. A 115 (6), 979–985.

Hoobler, R., Leone, S., 1997. Rate coefficients for reactions of ethynyl radical (C_2H) with HCN and CH_3CN: implications for the formation of complex nitriles on titan. J. Geophys. Res. - Planet. 102 (E12), 28717 – 28723.

Horner, D. A., Curtiss, L. A., Gruen, D. M., 1995. A theoretical study of the energetics of insertion of dicarbon (C_2) and vinylidene into methane C−H bonds. Chem. Phys. Lett. 233 (3), 243–248.

Horowitz, A., Calvert, J. G., 1982. Wavelength dependence of the primary processes in acetaldehyde photolysis. J. Phys. Chem. 86 (16), 3105–3114.

Hörst, S. M., Vuitton, V., Yelle, R. V., Oct. 2008. Origin of oxygen species in Titan's atmosphere. Journal of Geophysical Research (Planets) 113, 10006.

Hourdin, F., Lebonnois, S., Luz, D., Rannou, P., Dec. 2004. Titan's stratospheric composition driven by condensation and dynamics. Journal of Geophysical Research (Planets) 109 (E18), 12005.

Hoyermann, K., Loftfield, N. S., Sievert, R., Wagner, H. G., 1981. Mechanism and rates of the reactions of CH_3O and CH_2OH radicals with H atoms. Symp. Int. Combust. Proc. 18 (1), 831–842.

Huang, C., Li, W., Estillore, A. D., Suits, A. G., 2008. Dynamics of CN + alkane reactions by crossed-beam DC slice imaging. J. Chem. Phys. 129 (7), 074301.

Hubin-Franskin, M. J., Delwiche, J., Giuliani, A., Ska, M. P., Motte-Tollet, F., Walker, I. C., Mason, N. J., Gingell, J. M., Jones, N. C., 2002. Electronic excitation and optical cross sections of methylamine and ethylamine in the UV-VUV spectral region. J. Chem. Phys. 116 (21), 9261–9268.

Hunter, E. P. L., Lias, S. G., 1998. Evaluated gas phase basicities and proton affinities of molecules: An update. J. Phys. Chem. Ref. Data 27 (3), 413–656.

Husain, D., Ioannou, A. X., 1997. Reactions of atomic carbon, $C[_2p^2(^3P_J)]$, with dienes and diynes investigated by time-resolved atomic resonance absorption spectroscopy in the vacuum ultraviolet. J. Chem. Soc. Faraday Trans. 93, 3625–3629.

Husain, D., Ioannou, A. X., 1999. Collisional removal of atomic carbon, $C[2p^2(^3P_J)]$, by aldehydes and ketones, investigated by time-resolved atomic resonance absorption spectroscopy in the vacuum ultra-violet. J. Photochem. Photobiol. A 129 (1-2), 1–7.

Husain, D., Kirsch, L., 1971. Reactions of atomic carbon by kinetic absorption spectroscopy in vacuum ultraviolet. Trans. Faraday Soc. 67 (583), 2025–2035.

Husain, D., Young, A. N., 1975. Kinetic investigation of ground state carbon atoms, $C(2^3P_J)$. J. Chem. Soc. Faraday Trans. 2 71, 525–531.

Inomata, S., Washida, N., 1999. Rate constants for the reactions of NH_2 and HNO with atomic oxygen at temperatures between 242 and 473 K. J. Phys. Chem. A 103 (26), 5023–5031.

Irle, S., Morokuma, K., 2000. A molecular orbital study on H and H_2 elimination pathways from methane, ethane, and propan. J. Chem. Phys. 113 (15), 6139–6148.

Ismail, H., Goldsmith, C. F., Abel, P. R., Howe, P.-T., Fahr, A., Halpern, J. B., Jusinski, L. E., Georgievskii, Y., Taatjes, C. A., Green, W. H., 2007. Pressure and temperature dependence of the reaction of vinyl radical with ethylene. J. Phys. Chem. A 111 (29), 6843–6851.

Jamal, A., Mebel, A. M., 2010. An ab initio/RRKM study of the reaction mechanism and product branching ratios of the reactions of ethynyl radical with allene and methylacetylene. Phys. Chem. Chem. Phys. 12 (11), 2606–2618.

Jamieson, J. W. S., Brown, G. R., Tanner, J. S., 1970. The reaction of atomic hydrogen with methyl cyanide. Can. J. Chem. 48 (23), 3619–3622.

Jasper, A. W., Klippenstein, S. J., Harding, L. B., 2007a. Secondary kinetics of methanol decomposition: Theoretical rate coefficients for $^3CH_2$ + OH, $^3CH_2$ + $^3CH_2$, and $^3CH_2$ + CH_3. J. Phys. Chem. A 111 (35), 8699–8707.

Jasper, A. W., Klippenstein, S. J., Harding, L. B., Ruscic, B., 2007b. Kinetics of the reaction of methyl radical with hydroxyl radical and methanol decomposition. J. Phys. Chem. A 111 (19), 3932–3950.

Jiang, B., Guo, H., 2013. Competition between abstraction and exchange channels in H + HCN reaction: Full-dimensional quantum dynamics. J. Chem. Phys. 139 (22), 224310.

Jodkowski, J. T., Ratajczak, E., E.; Sillesen, A., Pagsberg, P., 1993. Kinetics of the addition reaction of methyl radicals with nitric oxide studied by pulse radiolysis combined with infrared diode laser spectroscopy. Chem. Phys. Lett. 203, 490–496.

Jodkowski, J. T., Ratajczak, E., Fagerstrom, K., Lund, A., Stothard, N. D., Humpfer, R., Grotheer, H.-H., 1995. Kinetics of the cross reaction between amidogen and methyl radicals. Chem. Phys. Lett. 240 (1-3), 63–71.

Johnson, D. G., Blitz, M., Seakins, P. W., 2000. The reaction of methylidene (CH) with methanol isotopomers. Phys. Chem. Chem. Phys. 2, 2549–2553.

Kaiser, E. W., 1993. Pressure dependence of the rate constants for the reactions methyl + oxygen and methyl + nitric oxide from 3 to 104 torr. J. Phys. Chem 97 (45), 11681–11688.

Kanda, K., Nagata, T., Ibuki, T., 1999. Photodissociation of some simple nitriles in the extreme vacuum ultraviolet region. Chem. Phys. 243 (1-2), 89–96.

Keil, D., Lynch, K., Cowfer, J., Michael, J., 1976. An investigation of nonequilibrium kinetic isotope effects in chemically activated vinyl radicals. Int. J. Chem. Kinet. 8 (6), 825–857.

Kerr, J., Parsonage, M., 1972. Evaluated kinetic data on gas phase addition reactions. Reactions of atoms and radicals with alkenes, alkynes and aromatic compound. Butterworths, London.

Khanna, R. K., Sep. 2005. Condensed species in Titan's atmosphere: Identification of crystalline propionitrile (C $_2$H $_5$CN, CH $_3$CH $_2$C tbnd N) based on laboratory infrared data. Icarus 177, 116–121.

Khlifi, M., Paillous, P., Bruston, P., Guillemin, J. C., Bnilan, Y., Daoudi, A., Raulin, F., 1997. Gas infrared spectra, assignments, and absolute IR band intensities of C_4N_2 in the 250-3500 cm^{-1} region: implications for Titan's stratosphere. Spectrochim. Acta A 53 (5), 707–712.

Kiefer, J., von Drasek, W., 1990. The mechanism of the homogeneous pyrolysis of acetylene. Int. J. Chem. Kin. 22 (7), 747–786.

Kiefer, J. H., Mitchell, K. I., 1988. Molecular dissociation of vinylacetylene and its implications for acetylene pyrolysis. Energ. Fuels 2 (4), 458–461.

Kim, S. J., Geballe, T. R., Noll, K. S., Courtin, R., Feb. 2005. Clouds, haze, and CH_4, CH_3D, HCN, and C_2H_2 in the atmosphere of Titan probed via 3 μm spectroscopy. Icarus 173, 522–532.

Kinsman, A., Roscoe, J., 1994. A kinetic-analysis of the photolysis of mixtures of acetone and propylene. Int. J. Chem. Kin. 26 (1), 191–200.

Klemm, R. B., 1979. Absolute rate parameters for the reactions of formaldehyde with O atoms and H atoms over the temperature range 250-500 K. J. Chem. Phys. 71 (5), 1987–1993.

Klippenstein, J., Georgievskii, Y., Harding, L. B., 2006. Predictive theory for the association kinetics of two alkyl radicals. Phys. Chem. Chem. Phys. 8 (10), 1133–1147.

Klippenstein, S. J., Harding, L. B., 1999. A theoretical study of the kinetics of C_2H_3 + H. Phys. Chem. Chem. Phys. 1 (6), 989–997.

Klippenstein, S. J., Harding, L. B., 2009. Kinetics of the H + NCO reaction. Proc. Combust. Inst. 32 (1), 149–155.

Knyazev, V., Slagle, I., 2002. Kinetics of the reaction between propargyl radical and acetylene. J. Phys. Chem. A 106 (23), 5613 – 5617.

Knyazev, V. D., Bencsura, A., Stoliarov, S. I., Slagle, I. R., 1996a. Kinetics of the C_2H_3 + H_2 ↔ H + C_2H_4 and CH_3 + H_2 ↔ H + CH_4 reactions. J. Phys. Chem. 100 (27), 11346–11354.

Knyazev, V. D., Slagle, I. R., 2001. Kinetics of the reactions of allyl and propargyl radicals with CH_3. J. Phys. Chem. A 105 (13), 3196–3204.

Knyazev, V. D., Stoliarov, S. I., Slagle, I. R., 1996b. Kinetics of the reaction of vinyl radicals with acetylene. Symp. (Int.) Comb. 26 (1), 513–519.

Konnov, A. A., De Ruyck, J., 2001. Temperature-dependent rate constant for the reaction NNH + O → NH + NO. Combust. Flame 125 (4), 1258–1264.

Koskinen, T. T., Yelle, R. V., Snowden, D. S., Lavvas, P., Sandel, B. R., Capalbo, F. J., Benilan, Y., West, R. A., Dec. 2011. The mesosphere and lower thermosphere of Titan revealed by Cassini/UVIS stellar occultations. Icarus 216, 507–534.

Kovacs, T., Blitz, M. A., Seakins, P. W., 2010. H-atom yields from the photolysis of acetylene and from the reaction of C_2H with H_2, C_2H_2, and C_2H_4. J. Phys. Chem. A 114 (14), 4735–4741.

Krasnoperov, L. N., Chesnokov, E. N., Stark, H., Ravishankara, A. R., 2005. Elementary reactions of formyl (HCO) radical studied by laser photolysis transient absorption spectroscopy. Proceedings of the Combustion Institute 30 (1), 935–943.

Krasnopolsky, V. A., May 2009. A photochemical model of Titan's atmosphere and ionosphere. Icarus 201, 226–256.

Krasnopolsky, V. A., Dec. 2012. Titan's photochemical model: Further update, oxygen species, and comparison with Triton and Pluto. Planetary and Space Science 73, 318–326.

Kurosaki, Y., Takayanagi, T., 1999. Ab initio molecular orbital study of the N(^{2}D) + H_2O reaction. J. Phys. Chem. A 103 (3), 436–442.

Kyogoku, T., Watanabe, T., Tsunashima, S., Sato, S., 1983. Arrhenius parameters for the reactions of hydrogen and deuterium atoms with four butenes. Bull. Chem. Soc. Jpn. 56 (1), 19–21.

Langford, A. O., Petek, H., Moore, C. B., 1983. Collisional removal of $^1CH_2$: Absolute rate constants for atomic and molecular collisional partners at 295 K. J. Chem. Phys. 78 (11), 6650–6659.

Lara, L. M., Lellouch, E., López-Moreno, J. J., Rodrigo, R., Oct. 1996. Vertical distribution of Titan's atmospheric neutral constituents. Journal of Geophysical Research 101, 23261–23283.

Laufer, A. H., 1983. Quenching of triplet vinylidene radicals by helium. Chem. Phys. Lett. 94 (2), 240–242.

Laufer, A. H., Fahr, A., 2004. Reactions and kinetics of unsaturated C_2 hydrocarbon radicals. Chem. Rev. 104 (6), 2813–2832.

Läuter, A., Lee, K. S., Jung, K. H., Vatsa, R. K., Mittal, J. P., Volpp, H. R., 2002. Absolute primary H atom quantum yield measurements in the 193.3 and 121.6 nm photodissociation of acetylene. Chem. Phys. Lett. 358 (3-4), 314–319.

Lavvas, P., Galand, M., Yelle, R. V., Heays, A. N., Lewis, B. R., Lewis, G. R., Coates, A. J., May 2011. Energy deposition and primary chemical products in Titan's upper atmosphere. Icarus 213, 233–251.

Lavvas, P. P., Coustenis, A., Vardavas, I. M., 2008. Coupling photochemistry with haze formation in Titan's atmosphere, Part I: Model description. Planet. Space Sci. 56 (1), 27–66.

Lavvas, P. P., Coustenis, A., Vardavas, I. M., Jan. 2008a. Coupling photochemistry with haze formation in Titan's atmosphere, Part I: Model description. Planet. Space Sci. 56, 27–66.

Lavvas, P. P., Coustenis, A., Vardavas, I. M., Jan. 2008b. Coupling photochemistry with haze formation in Titan's atmosphere, Part II: Results and validation with Cassini/Huygens data. Planet. Space Sci. 56, 67–99.

Le Picard, S., Canosa, A., 1998. Measurement of the rate constant for the association reaction CH + N_2 at 53 K and its relevance to Triton's atmosphere. Geophys. Res. Lett. 25 (4), 485–488.

Lebonnois, S., Toublanc, D., Hourdin, F., Rannou, P., Aug. 2001. Seasonal Variations of Titan's Atmospheric Composition. Icarus 152, 384–406.

Lee, L., 1980. CN($A^2\Pi_i \rightarrow X^2\Sigma^+$) and CN($B^2\Sigma^+ \rightarrow X^2\Sigma^+$) yields from HCN photodissociation. J. Chem. Phys. 72 (12), 6414–6421.

Lee, S., Samuels, D. A., Hoobler, R. J., Leone, S. R., 2000. Direct measurements of rate coefficients for the reaction of ethynyl radical (C_2H) with C_2H_2 at 90 and 120 K using a pulsed Laval nozzle apparatus. J. Geophys. Res. - Planet. 105 (E6), 15085–15090.

Lee, S.-H., Chin, C.-H., Chen, W.-K., Huang, W.-J., Hsieh, C.-C., 2011. Exploring the dynamics of reactionN(^{2}D) + C_2H_4 with crossed molecular-beam experiments and quantum-chemical calculations. Phys. Chem. Chem. Phys. 13 (18), 8515–8525.

Lee, S.-H., Lee, Y. T., Yang, X., 2004. Dynamics of photodissociation of ethylene and its isotopomers at 157 nm: Branching ratios and kinetic-energy distributions. J. Chem. Phys. 120 (23), 10983–10991.

Lee, S.-H., Lee, Y.-Y., Lee, Y. T., Yang, X., 2003. Photodissociation dynamics of propene at 157.6 nm: Kinetic energy distributions and branching ratios. J. Chem. Phys. 119 (2), 827–838.

Lellouch, E., Romani, P. N., Rosenqvist, J., Mar. 1994. The vertical Distribution and Origin of HCN in Neptune's Atmosphere. Icarus 108, 112–136.

Lesclaux, R., Demissy, M., 1978. Kinetics of gas-phase reactions of NH_2 radicals with alkane and alkyl radicals. J. Photochem. 9 (2-3), 110–112.

Li, A., Xie, C., Xie, D., Guo, H., 2013. State-to-state quantum dynamics of the $O(^3P)$ + $NH(X^3\Sigma^-)$ reaction on the three lowest-lying electronic states of HNO/HON. J. Chem. Phys. 138 (2), 024308.

Li, H. Y., Geng, C.-Y., Huang, X. R., Zhan, J.-H., Sun, C. C., 2006a. F/Cl + C_2H_2 reactions: Are the addition and hydrogen abstraction direct processes? Chem. Phys. 331 (1), 42–54.

Li, J.-L., Geng, C.-Y., Huang, X.-R., Sun, C.-C., 2006b. A barrier-free atomic radical-molecule reaction: F + propene. J. Chem. Theory Comput. 2 (6), 1551–1564.

Li, Q. S., Zhang, X., 2006. Direct dynamics study on the hydrogen abstraction reactions N_2H_4 + R → N_2H_3 + RH (R=NH_2,CH_3). J. Chem. Phys. 125 (6), 064304.

Liang, M.-C., Yung, Y. L., Shemansky, D. E., 2007. Photolytically generated aerosols in the mesosphere and thermosphere of Titan. Astrophys. J. Lett. 661 (2), L199.

Lide, D., Kehiaian, H., 1994. CRC Handbook of Thermophysical and Thermochemical Data. CRC Press, Boca Raton, FL.

Lin, C., Kaufman, F., 1971. Reactions of metastable nitrogen atoms. J. Chem. Phys. 55 (8), 3760–3770.

Linder, D. P., Duan, X., Page, M., 1995. Ab initio variational transition state theory calculations for the H + NH_2 ⇔ H_2 + NH hydrogen abstraction reaction on the triplet potential energy surface. J. Phys. Chem. 99 (29), 11458–11463.

Linder, D. P., Duan, X., Page, M., 1996. Thermal rate constants for R + N_2H_2 → RH + N_2H (R=H, OH, NH_2) determined from multireference configuration interaction and variational transition state theory calculations. J. Chem. Phys. 104 (16), 6298–6307.

Liu, G.-x., Li, Z.-s., Xiao, J.-f., Liu, J.-y., Fu, Q., Huang, X.-r., Sun, C.-c., Tang, A.-c., 2002. Calculations of the rate constants for the hydrogen abstraction reactions C_2H_3 + CH_4 →C_2H_4 + CH_3 and C_2H_3 + C_2H_6 → C_2H_4 + C_2H_5. ChemPhysChem 3 (7), 625–629.

Loison, J.-C., Bergeat, A., 2004. Reaction of carbon atoms, $C(_2p^{23}P)$ with C_3H_4 (allene and methylacetylene), C_3H_6 (propylene) and C_4H_8 (trans-butene): Overall rate constants and atomic hydrogen branching ratios. Phys. Chem. Chem. Phys. 6 (23), 5396–5401.

Loison, J.-C., Bergeat, A., 2009. Rate constants and the H atom branching ratio of the reactions of the methylidyne $CH(X^2\Pi)$ radical with C_2H_2, C_2H_4, C_3H_4, (methylacetylene and allene), C_3H_6,(propene) and C_4H_8, (trans-butene). Phys. Chem. Chem. Phys. 11 (4), 655–664.

Loison, J. C., Bergeat, A., Caralp, F., Hannachi, Y., 2006. Rate constants and H atom branching ratios of the gas-phase reactions of methylidyne CH radical with a series of alkanes. J. Phys. Chem. A 110 (50), 13500–13506.

Loison, J.-C., Wakelam, V., Hickson, K. M., Bergeat, A., Mereau, R., 2014. The gas-phase chemistry of carbon chains in dark cloud chemical models. Mon. Not. Roy. Astron. Soc. 437 (1), 930–945.

Louge, M., Hanson, R., 1984. High temperature kinetics of NCO. Combust. Flame 58 (3), 291–300.

Luo, C., Du, W.-N., Duan, X.-M., Li, Z.-S., 2008. A theoretical study of the photodissociation mechanism of cyanoacetylene in its lowest singlet and triplet excited states. Astrophys. J. 687 (1), 726.

Madden, L. K., Moskaleva, L. V., Kristyan, S., Lin, M. C., 1997. Ab initio MO study of the unimolecular decomposition of the phenyl radical. J. Phys. Chem. A 101 (36), 6790–6797.

Magee, B. A., Waite, J. H., Mandt, K. E., Westlake, J., Bell, J., Gell, D. A., Dec. 2009. INMS-derived composition of Titan's upper atmosphere: Analysis methods and model comparison. Planet. Space Sci. 57, 1895–1916.

Maki, A. G., Mellau, G. C., 2001. High-temperature infrared emission measurements on HNC. J. Mol. Spectrosc. 206 (1), 47–52.

Maksyutenko, P., Zhang, F., Gu, X., Kaiser, R. I., 2010. A crossed molecular beam study on the reaction of methylidyne radicals $[CH(X^2\Pi)]$ with acetylene $[C_2H_2(X^1\Sigma_g^+)]$-competing C_3H_2 + H and C_3H + H_2 channels. Phys. Chem. Chem. Phys. 13 (1), 240–252.

Marchand, N., Jimeno, P., Rayez, J.-C., Liotard, D., 1997. Theoretical study of the reaction $CH(X^2P)$ + NO (X^2P). I. Determination of some reaction paths in the lowest triplet potential energy surface. J. Phys. Chem. A 101 (34), 6077–6091.

Marten, A., Hidayat, T., Biraud, Y., Moreno, R., Aug. 2002. New Millimeter Heterodyne Observations of Titan: Vertical Distributions of Nitriles HCN, HC $_3$N, CH $_3$CN, and the Isotopic Ratio ^{15}N/ ^{14}N in Its Atmosphere. Icarus 158, 532–544.

Martinotti, F. F., Welch, M. J., Wolf, A. P., 1968. The reactivity of thermal carbon atoms in the gaz phase. Chem. Commun. 3, 115–116.

Matsugi, A., Suma, K., Miyoshi, A., 2010. Rate constants and kinetic isotope effects on the reaction of $C_2(X^1\Sigma_g^+)$ with CH_4 and CD_4. J. Phys. Chem. A 114 (13), 4580–4585.

McElcheran, D. E., Wijnen, M. H. J., Steacie, E. W. R., 1958. The photolysis of methyl cyanide at 184.9 nm. Can. J. Chem. 36 (2), 321–329.

McKee, K., Blitz, M. A., Hughes, K. J., Pilling, M. J., Qian, H.-B., Taylor, A., Seakins, P. W., 2003. H atoms branching ratio from the reactions of CH with C_2H_2, C_2H_4, C_2H_6 and neo-C_5H_{12}. J. Phys. Chem. 107 (30), 5710–5716.

McKee, K. W., Blitz, M. A., Cleary, P. A., Glowacki, D. R., Pilling, M. J., Seakins, P. W., Wang, L., 2007. Experimental and master equation study of the kinetics of OH + C_2H_2: Temperature dependence of the limiting high pressure and pressure dependent rate coefficients. J. Phys. Chem. A 111 (19), 4043–4055.

Meads, R., Maclagan, R., Phillips, L., 1993. Kinetics, energetics, and dynamics of the reactions of CN with NH_3 and ND_3. J. Phys. Chem. 97 (13), 3257–3265.

Mebel, A., Lin, M., 1999. Prediction of absolute rate constants for the reactions of NH_2 with alkanes from ab initio G2M/TST calculation. J. Phys. Chem. A 103 (13), 2088–2096.

Mebel, A. M., Kaiser, R. I., 2002. An ab initio study on the formation of interstellar tricarbon isomers l−C_3($X^1\Sigma_g^+$) and c−C_3(X^3A_2'). Chem. Phys. Lett. 360 (1-2), 139–143.

Mebel, A. M., Kislov, V. V., Kaiser, R. I., 2006. Potential energy surface and product branching ratios for the reaction of dicarbon, C_2($X^1\Sigma_g^+$), with methylacetylene, CH_3CCH(X^1A_1): An ab initio/RRKM study. J. Phys. Chem. A 110 (7), 2421–2433.

Mebel, A. M., Lin, M. C., Yu, T., Morokuma, K., 1997. Theoretical study of potential energy surface and thermal rate constants for the C_6H_5 + H_2 and C_6H_6 + H reactions. J. Phys. Chem. A 101 (17), 3189–3196.

Mendes, M., Buhr, H., Berg, M., Froese, M., Grieser, M., Heber, O., Jordon-Thaden, B., Krantz, C., Novotny, O., Novotny, O., Orlov, D., Petrignani, A., Rappaport, M. L., Repnow, R., Schwalm, D., Shornikov, A., Sttzel, J., Zajfman, D., Wolf, A., 2012. Cold electron reactions producing the energetic isomer of hydrogen cyanide in interstellar clouds. Astrophys. J. 746 (1), L8.

Mertens, J. D., Chang, A. Y., Hanson, R. K., Bowman, C. T., 1989. Reaction kinetics of NH in the shock tube pyrolysis of HNCO. Int. J. Chem. Kin. 21 (11), 1049–1067.

Michael, J. V., Osborne, D. T., Suess, G. N., 1973. Reaction H + C_2H_4 : Investigation into the effects of pressure, stoichiometry, and the nature of the third body species. J. Chem. Phys. 58 (7), 2800–2806.

Miller, J. A., Klippenstein, S. J., 2004. The H + C_2H_2 (+ M) ↔ C_2H_3 (+ M) and H + C_2H_2 (+ M) ↔ C_2H_5 (+ M) reactions: Electronic structure, variational transition-state theory, and solutions to a two-dimensional master equation. Phys. Chem. Chem. Phys. 6 (6), 1192–1202.

Miller, J. A., Senosiain, J. P., Klippenstein, S. J., Georgievskii, Y., 2008. Reactions over multiple, interconnected potential wells: Unimolecular and bimolecular reactions on a C_3H_5 potential. J. Phys. Chem. A 112 (39), 9429–9438.

Mitchell, M., Nava, D., Stief, L., 1986. Rate constant for the reaction of O(^{3}P) with diacetylene from 210 to 423 K. J. Chem. Phys. 85 (6), 3300.

Monks, P., Romani, P., Nesbitt, F., Scanlon, M., Stief, L., 1993. The kinetics of the formation of nitrile compounds in the atmospheres of Titan and Neptune. J. Geophys. Res. - Planet. 98 (E9), 17115–17122.

Monks, P. S., Nesbitt, F. L., Payne, W. A., Scanlon, M., Stief, L. J., Shallcross, D. E., 1995. Absolute rate constant and product branching ratios for the reaction between H and C_2H_3 at T = 213 and 298 K. J. Phys. Chem. 99 (47), 17151–17159.

Moreno, R., Lellouch, E., Lara, L. M., Courtin, R., Bockelée-Morvan, D., Hartogh, P., Rengel, M., Biver, N., Banaszkiewicz, M., González, A., Dec. 2011. First detection of hydrogen isocyanide (HNC) in Titan's atmosphere. Astronomy and Astrophysics 536, L12.

Moreno, R., Lellouch, E., Lara, L. M., Feuchtgruber, H., Rengel, M., Hartogh, P., Courtin, R., Nov. 2012. The abundance, vertical distribution and origin of H_2O in Titan's atmosphere: Herschel observations and photochemical modelling. Icarus 221, 753–767.

Moriyama, M., Tsutsui, Y., Honma, K., 1998. Vacuum ultraviolet photodissociation dynamics of acetonitrile. J. Chem. Phys. 108 (15), 6215–6221.

Morris, E.D., J., Niki, H., 1973. Reaction of methyl radicals with atomic oxygen. Int. J. Chem. Kinet. 5 (5), 47–53.

Moses, J., Fouchet, T., Bézard, B., Gladstone, G., Lellouch, E., Feuchtgruber, H., 2005. Photochemistry and diffusion in Jupiter's stratosphere: Constraints from ISO observations and comparisons with other giant planets. J. Geophys. Res. - Planet. 110 (E8), E08001.

Moskaleva, L. V., Xia, W. S., Lin, M. C., 2000. The CH + N_2 reaction over the ground electronic doublet potential energy surface: a detailed transition state search. Chem. Phys. Lett. 331 (2-4), 269–277.

Mu, X., Lu, I. C., Lee, S.-H., Wang, X., Yang, X., 2004. Photodissociation dynamics of 1,2-butadiene at 157 nm. J. Chem. Phys. 121 (10), 4684–4690.

Mullen, C., Smith, M. A., 2005. Low temperature NH($X^3\Sigma^-$) radical reactions with NO, saturated, and unsaturated hydrocarbons studied in a pulsed supersonic laval nozzle flow reactor between 53 and 188 K. J. Phys. Chem. A 109 (7), 1391–1399.

Murphy, J., Vakhtin, A., Leone, S., 2003. Laboratory kinetics of C_2H radical reactions with ethane, propane, and n-butane at T = 96-296 K: Implications for Titan. Icarus 163 (1), 175–181.

Nava, D. F., Mitchell, M. B., Stief, L. J., 1986. The reaction H + C_4H_2: Absolute rate constant measurement and implication for atmospheric modeling of Titan. J. Geophys. Res. - Space Phys. 91 (A4), 4585–4589.

Nesbitt, F. L., Monks, P. S., Scanlon, M., Stief, L. J., 1994. Absolute rate constants for the reactions of F(^{2}P) with C_2H_2 and C_2H_4 at T = 298 K. J. Phys. Chem. 98 (16), 4307–4311.

Nesbitt, F. L., Thorn, R. P., Payne, W. A., Tardy, D. C., 1999. Absolute rate constant and product branching fractions for the reaction between F and C_2H_4 at T = 202-298 K. J. Phys. Chem. A 103 (23), 4470–4479.

Newby, J. J., Stearns, J. A., Liu, C.-P., Zwier, T. S., 2007. Photochemical and discharge-driven pathways to aromatic products from 1,3-Bbutadiene. J. Phys. Chem. A 111 (43), 10914–10927.

Nguyen, H., Zhang, S., Peeters, J., Truong, T., Nguyen, M., 2004. Direct ab initio dynamics studies of the reactions of HNO with H and OH radicals. Chem. Phys. Lett. 388 (1-3), 94–99.

Nguyen, M. T., Sengupta, D., Ha, T., 1996. Another look at the decomposition of methyl azide and methanimine : How is HCN formed? J. Phys. Chem. 100 (16), 6499–6503.

Nguyen, T. L., Mebel, A. M., Kaiser, R. I., 2001a. A theoretical investigation of the triplet carbon atom C(^{3}P) + vinyl radical C_2H_3(^{2}A,) reaction and thermochemistry of C_3H_n (n = 1-4) species. J. Phys. Chem. A 105 (13), 3284–3299.

Nguyen, T. L., Mebel, A. M., Lin, S. H., Kaiser, R. I., 2001b. Product branching ratios of the C(^{3}P) + C_2H_3(^{2}A,) and CH($^2\Pi$) + C_2H_2($^1\Sigma_g^+$) reactions and photodissociation of H_2CCCH($^2B_1$) at 193 and 242 nm: An ab initio/RRKM Study. J. Phys. Chem. A 105 (51), 11549–11559.

Nguyen, T. L., Vereecken, L., Hou, X. J., Nguyen, M. T., Peeters, J., 2005. Potential energy surfaces, product distributions and thermal rate coefficients of the reaction of O(^{3}P) with C_2H_4(X^1A_g): A comprehensive theoretical study. J. Phys. Chem. A 109 (33), 7489–7499.

Nixon, C. A., Jennings, D. E., Bézard, B., Vinatier, S., Teanby, N. A., Sung, K., Ansty, T. M., Irwin, P. G. J., Gorius, N., Cottini, V., Coustenis, A., Flasar, F. M., Oct. 2013. Detection of Propene in Titan's Stratosphere. The Astrophysical Journal Letters 776, L14.

Nizamov, B., Leone, S., 2004a. Kinetics of C_2H reactions with hydrocarbons and nitriles in the 104-296 K temperature range. J. Phys. Chem. A 108 (10), 1746–1752.

Nizamov, B., Leone, S. R., 2004b. Rate coefficients and kinetic isotope effect for the C_2H reactions with NH_3 and ND_3 in the 104-294 K temperature range. J. Phys. Chem. A 108 (17), 3766–3771.

North, S. W., Hall, G. E., 1996. The radical photodissociation channel of acrylonitrile. Chem. Phys. Lett. 263 (1-2), 148–153.

Ohmori, K., Miyoshi, A., Matsui, H., Washida, N., 1990. Studies on the reaction of acetaldehyde and acetyl radicals with atomic hydrogen. J. Phys. Chem. 94 (8), 3253–3255.

Oka, K., Cvetanovic, R., 1979. Determination of rates of hydrogen atom reactions with alkenes at 298 K by a double modulation technique. Can. J. Chem. 57 (7), 777–784.

Okabe, H., 1978. Photochemistry of small molecules. Wiley Interscience. Wiley.

Okabe, H., 1983. Photochemistry of acetylene at 1849 Å. The Journal of Chemical Physics 78 (3), 1312–1317.

Okada, S., Tezaki, A., Miyoshi, A., Matsui, H., 1994. Product branching fractions in the reactions of NH($a^1\Delta$) and NH($X^3\Sigma^-$]) with NO. J. Chem. Phys. 101 (11), 9582–9588.

Opansky, B. J., Leone, S. R., 1996. Rate coefficients of C_2H with C_2H_4, C_2H_6, and H_2 from 150-359 K. J. Phys. Chem. 100 (51), 19904–19910.

Osamura, Y., Petrie, S., 2004. NCCN and NCCCCN formation in Titan's atmosphere : 1. Competing reactions of precursor HCCN($^3A_{\prime\prime}$) with H(^{2}S) and CH_3(^{2}A,). J. Phys. Chem. A 108 (16), 3615–3622.

Ouk, C. M., Zvereva-Loete, N., Bussery-Honvault, B., 2011. Towards a converged barrier height for the entrance channel transition state of the N(^{2}D) + CH4 reaction and its implication for the chemistry in Titan's atmosphere. Chem. Phys. Lett. 515 (1-3), 13–18.

Pagsberg, P. B., Eriksen, J., Christensen, H. C., 1979. Pulse radiolysis of gaseous ammonia-oxygen mixtures. J. Phys. Chem. 83 (5), 582–590.

Pang, J. L., Xie, H. B., Zhang, S. W., Ding, Y. H., Tang, A. Q., 2009. Gaseous reaction mechanism between two H_2CN radicals. Phys. Chem. Chem. Phys. 11 (21), 4326–4334.

Paramo, A., Canosa, A., Le Picard, S. D., Sims, I. R., 2008. Rate coefficients for the reactions of C_2($a^3\Pi_u$) and C_2($X^1\Sigma_g^+$) with various hydrocarbons (CH_4, C_2H_2, C_2H_4, C_2H_6, and C_3H_8): A gas-phase experimental study over the temperature range 24-300 K. J. Phys. Chem. A 112 (39), 9591–9600.

Park, J., Burova, S., Rodgers, A. S., Lin, M. C., 1999. Experimental and theoretical studies of the C_6H_5 + C_6H_6 reaction. J. Phys. Chem. A 103 (45), 9036–9041.

Park, J., Zhu, R. S., Lin, M. C., 2002. Thermal decomposition of ethanol. I. *Ab Initio molecular orbital/Rice-Ramsperger-Kassel-Marcus prediction of rate constant and product branching ratios.* J. Chem. Phys. 117 (7), 3224–3231.

Parker, J. K., Payne, W. A., Cody, R. J., Stief, L. J., 2004. Kinetics of the reaction of atomic hydrogen with cyanoacetylene from T = 200 to 298 K. J. Phys. Chem. A 108 (11), 1938–1945.

Payne, W. A., Monks, P. S., Nesbitt, F. L., Stief, L. J., 1996. The reaction between N(^{4}S) and C_2H_3: Rate constant and primary reaction channels. J. Chem. Phys. 104 (24), 9808–9815.

Payne, W. A., Stief, L. J., 1976. Absolute rate constant for the reaction of atomic hydrogen with acetylene over an extended pressure and temperature range. J. Chem. Phys. 64 (3), 1150–1155.

Petrie, S., 2002. Reactivity of HNC with small hydrocarbon radicals. J. Phys. Chem. A 106 (46), 11181–11189.

Petrie, S., Osamura, Y., 2004. NCCN and NCCCCN formation in Titan's atmosphere: 2. HNC as a viable precursor. J. Phys. Chem. A 108 (16), 3623–3631.

Phillips, L. F., 1978. Reaction of H with C_2N_2 at pressures near 1 Torr. Int. J. Chem. Kinet. 10 (8), 899–904.

Pimentel, A. S., Payne, W. A., Nesbitt, F. L., Cody, R. J., Stief, L. J., 2004. Rate constant for the reaction H + C_2H_5 at T = 150-295 K. J. Phys. Chem. A 108 (35), 7204–7210.

Pitts, W. M., Pasternack, L., McDonald, J. R., 1982. Temperature dependence of the C_2($X^1\Sigma_g^+$) reaction with H_2 and CH_4 and C_2($X^1\Sigma_g^+$ and a $^3\Pi_u$ equilibrated states) with O_2. Chem. Phys. 68 (3), 417–422.

Plessis, S., Carrasco, N., Dobrijevic, M., Pernot, P., May 2012. Production of neutral species in Titan's ionosphere through dissociative recombination of ions. Icarus 219, 254–266.

Prozument, K., Shaver, R. G., Ciuba, M. A., Muenter, J. S., Park, G. B., Stanton, J. F., Guo, H., Wong, B. M., Perry, D. S., Field, R. W., 2013. A new approach toward transition state spectroscopy. Faraday Disc. 163, 33–57.

Rannou, P., Lebonnois, S., Hourdin, F., Luz, D., 2005. Titan atmosphere database. Advances in Space Research 36, 2194–2198.

Redondo, P., Pauzat, F., Ellinger, Y., 2006. Theoretical survey of the NH + CH_3 potential energy surface in relation to Titan atmospheric chemistry. Planet. Space Sci. 54 (2), 181–187.

Reisler, H., Mangir, M. S., Wittig, C., 1980. Kinetics of free radicals generated by IR laser photolysis. IV. Intersystem crossings and reactions of $C_2(X^1\Sigma_g^+)$ and $C_2(a^3\Pi_u)$ in the gaseous phase. J. Chem. Phys. 73 (5), 2280–2286.

Rianda, R., Frueholz, R. P., Kuppermann, A., 1984. Singlet → triplet transitions in C≡N containing molecules by electron impact. J. Chem. Phys. 80 (9), 4035–4043.

Richardson, S. L., Francisco, J. S., 1994. A computational study of the reaction of C_2 with CH_4. Mol. Phys. 83 (5), 1041–1044.

Röhrig, M., Wagner, H. G., 1994a. A kinetic study about the reactions of $NH(X^3\Sigma^-)$ with hydrocarbons. Part 2: Ethene, propene, and 2,3-dimethyl-2-butene. Ber. Bunsen-Ges. Phys. Chem. 98 (6), 864–868.

Röhrig, M., Wagner, H. G., 1994b. The reactions of $NH(X^3\Sigma^-)$ with the water gas components CO_2, H_2O, and H_2. Symp. Int. Combust. Proc. 25 (1), 975–981.

Sabbah, H., Biennier, L., Sims, I. R., Georgievskii, Y., Klippenstein, S. J., Smith, I. W. M., 2007. Understanding reactivity at very low temperatures: The reactions of oxygen atoms with alkenes. Science 317 (5834), 102–105.

Samuelson, R. E., Mayo, L. A., Knuckles, M. A., Khanna, R. J., Aug. 1997. C $_4$N $_2$ ice in Titan's north polar stratosphere. Planet. Space Sci. 45, 941–948.

Sander, S. P., Abbatt, J., Barker, J. R., Burkholder, J. B., Friedl, R. R., Golden, D. M., Huie, R. E., Kolb, C. E., Kurylo, M. J., Moortgat, G. K., Orkin, V. L., Wine, P. H., 2011. Chemical Kinetics and Photochemical Data for Use in Atmospheric Studies, Evaluation Number 17. JPL Publication 10-6.

Sangwan, M., Chesnokov, E. N., Krasnoperov, L. N., 2012. Reaction CH_3 + OH Studied over the 294-714 K temperature and 1-100 bar pressure ranges. J. Phys. Chem. A 116 (34), 8661–8670.

Sato, K., Misawa, K., Kobayashi, Y., Matsui, M., Tsunashima, S., Kurosaki, Y., Takayanagi, T., 1999. Measurements of thermal rate constants for the reactions of $N(^2D-^2P)$ with C_2H_4 and C_2D_4 between 225 and 292 K. J. Phys. Chem. 103 (43), 8650–8656.

Satyapal, S., Bersohn, R., 1991. Photodissociation of acetylene at 193.3 nm. J. Phys. Chem. 95 (21), 8004–8006.

Savee, J. D., Welz, O., Taatjes, C. A., Osborn, D. L., 2012. New mechanistic insights to the O(^{3}P) + propene reaction from multiplexed photoionization mass spectrometry. Phys. Chem. Chem. Phys. 14, 10410–10423.

Sayah, N., Li, X., Caballero, J. F., Jackson, W. M., 1988. Laser induced fluorescence studies of CN reactions with alkanes, alkenes and substituted aliphatic species. J. Photochem. Photobiol. A 45 (2), 177–194.

Scherzer, K., Claus, P., Karwath, M., 1985. Untersuchungen zur Kinetik und zum Mechanismus der Addition von Methylradicalen an Vinylacetylen. Z. Phys. Chem. 266 (2), 321–328.

Schofield, K., 1973. Evaluated chemical kinetic rate constants for various gas phase reactions. J. Phys. Chem. Ref. Data 2, 25–84.

Schwanebeck, W., Warnatz, J., 1975. Reaktionen des Butadiins. I. Die reaktion mit Wasserstoffatomen. Ber. Bunsenges. Phys. Chem. 79 (6), 530–535.

Schwell, M., Jochims, H.-W., Baumgrtel, H., Leach, S., 2008. VUV photophysics of acetonitrile: Fragmentation, fluorescence and ionization in the 7-22eV region. Chem. Phys. 344 (1-2), 164–175.

Seakins, P. W., Robertson, S. H., Pilling, M. J., Slagle, I. R., Gmurczyk, G. W., Bencsura, A., Gutman, D., Tsang, W., 1993. Kinetics of the unimolecular decomposition of iso-C_3H_7: Weak collision effects in helium, argon, and nitrogen. J. Phys. Chem. 97 (17), 4450–4458.

Seidler, V., Temps, F., Wagner, H. G., Wolf, M., 1989. Kinetics of the reactions of methylene ($\tilde{X}^3B_1$)-radicals with NO and NO_2. J. Phys. Chem. 93 (3), 1070–1073.

Seki, K., He, M., Liu, R., Okabe, H., 1996. Photochemistry of cyanoacetylene at 193.3 nm. J. Phys. Chem. 100 (13), 5349–5353.

Seki, K., Nakashima, N., Nishi, N., Kinoshita, M., 1986. Photochemistry of acetylene at 193 nm: Two pathways for diacetylene formation. J. Chem. Phys. 85 (1), 274–279.

Seki, K., Okabe, H., 1993. Photochemistry of acetylene at 193.3 nm. J. Phys. Chem. 97 (20), 5284–5290.

Sekine, Y., Imanaka, H., Matsui, T., Khare, B. N., Bakes, E. L. O., McKay, C. P., Sugita, S., 2008a. The role of organic haze in Titan's atmospheric chemistry: I. Laboratory investigation on heterogeneous reaction of atomic hydrogen with Titan tholin. Icarus 194 (1), 186–200.

Sekine, Y., Lebonnois, S., Imanaka, H., Matsui, T., Bakes, E. L. O., McKay, C. P., Khare, B. N., Sugita, S., 2008b. The role of organic haze in Titan's atmospheric chemistry: II. Effect of heterogeneous reaction to the hydrogen budget and chemical composition of the atmosphere. Icarus 194 (1), 201–211.

Semaniak, J., Minaev, B. F., Derkatch, A. M., Hellberg, F., Neau, A., Rosn, S., Thomas, R., Larsson, M., Danared, H., Paal, A., Af Ugglas, M., 2001. Dissociative recombination of $HCNH^+$: Absolute cross-sections and branching ratios. Astrophys. J. Suppl. Ser. 135 (2), 275–283.

Shafir, E. V., Slagle, I. R., Knyazev, V. D., 2003. Kinetics of the self-reaction of C_2H_5 radicals. J. Phys. Chem. A 107 (35), 6804–6813.

Shemansky, D. E., Stewart, A. I. F., West, R. A., Esposito, L. W., Hallett, J. T., Liu, X., May 2005. The Cassini UVIS stellar probe of the Titan atmosphere. Science 308, 978–982.

Shen, D., Pritchard, H., 1991. On the dynamics of free-radical disproportionation reactions. Theor. Chim. Acta 78 (4), 241–246.

Shepler, B. C., Yang, B. H., Kumar, T. J. D., Stancil, P. C., Bowman, J. M., Balakrishnan, N., Zhang, P., Bodo, E., Dalgarno, A., 2007. Low energy H + CO scattering revisited. Astron. Astrophys. 475 (2), L15–L18.

Shin, K. S., Michael, J. V., 1991. Rate constants (296-1700 K) for the reactions ethynyl radical + acetylene → C_4H_2 + H and C_2D + C_2D_2 → C_4D_2 + D. J. Phys. Chem. 95 (15), 5864–5869.

Silva, R., Gichuhi, W. K., Kislov, V. V., Landera, A., Mebel, A. M., Suits, A. G., 2009. UV photodissociation of cyanoacetylene: A combined ion imaging and theoretical investigation. J. Phys. Chem. A 113 (42), 11182–11186.

Sims, I. R., Queffelec, J. L., Travers, D., Rowe, B. R., Herbert, L. B., Karthauser, J., Smith, I. W. M., 1993. Rate constants for the reactions of CN with hydrocarbons at low and ultra-low temperatures. Chem. Phys. Lett. 211 (4-5), 461–468.

Slack, M. W., 1976. Kinetics and thermodynamics of the CN molecule. III. Shock tube measurement of CNdissociation rates. J. Chem. Phys. 64 (1), 228–236.

Slagle, I. R., Gutman, D., Davies, J. W., Pilling, M. J., 1988. Study of the recombination reaction methyl + methyl → ethane. 1. Experiment. J. Phys. Chem. 92 (9), 2455–2462.

Smith, G. P., 2003. Rate theory of methyl recombination at the low temperatures and pressures of planetary atmospheres. Chem. Phys. Lett. 376 (3-4), 381–388.

Smith, I. W. M., Talbi, D., Herbst, E., 2001. The production of HCN dimer and more complex oligomers in dense interstellar clouds. Astron. Astrophys. 369 (2), 611–615.

Stewart, P., Smith, G., Golden, D., 1989. The pressure and temperature dependence of methane decomposition. Int. J. Chem. Kinet. 21 (10), 923–945.

Stief, L. J., DeCarlo, V. J., Mataloni, R. J., 1965. Vacuum-ultraviolet photolysis of acetylene. J. Chem. Phys. 42 (9), 3113–3121.

Stief, L. J., Nesbitt, F. L., Payne, W. A., Kuo, S. C., Tao, W., Klemm, R. B., 1995. Rate constant and reaction channels for the reaction of atomic nitrogen with the ethyl radical. J. Chem. Phys. 102 (13), 5309–5316.

Stief, L. J., Payne, W. A., Klemm, R. B., 1975. A flasch photolysis–resonance fluorescence study of the formation of O(^{1}D) in the photolysis of water and the reaction of O(^{1}D) with H_2, Ar, and He. J. Chem. Phys. 62 (10), 4000–4008.

Stoliarov, S. I., Knyazev, V. D., Slagle, I. R., 2000. Experimental study of the reaction between vinyl and methyl radicals in the gas phase. Temperature and pressure dependence of overall rate constants and product yields. J. Phys. Chem. A 104 (43), 9687–9697.

Stothard, N., Humpfer, R., Grotheer, H. H., 1995. The multichannel reaction NH_2 + NH_2 at ambient temperature and low pressures. Chem. Phys. Lett. 240 (5-6), 474–480.

Stranges, D., O'Keeffe, P., Scotti, G., Santo, R. D., Houston, P. L., 2008. Competing sigmatropic shift rearrangements in excited allyl radicals. J. Chem. Phys. 128 (15), 151101–151104.

Sumathi, R., Nguyen, M. T., 1998. A theoretical study of the CH_2N system: Reactions in both lowest lying doublet and quartet states. J. Phys. Chem. A 102 (41), 8013–8020.

Sun, Q., Yang, D. L., Wang, N. S., Bowman, J. M., Lin, M. C., 1990. Experimental and reduced dimensionality quantum rate coefficients for H_2 (D_2) + CN → H(D)CN + H(D). J. Chem. Phys. 93 (7), 4730–4739.

Takahashi, K., Takayanagi, T., 2006. Theoretical study on HNC($^1\Sigma$) production from the $C_2(X^1\Sigma_g^+)$ + NH($X^3\Sigma^-$ reaction. Chem. Phys. Lett. 429 (4-6), 399–404.

Takahashi, K., Takayanagi, T., 2007. Production of HNC from the CH($X^2\Pi$)+NH($X^3\Sigma^-$) reaction: Direct dynamics study. J. Mol. Struct. - THEOCHEM 817 (1-3), 153–160.

Takayanagi, T., Kurosaki, Y., 1999. Direct ab initio classical trajectory calculations for the N(^{2}D) + CH_4 insertion reaction. J. Mol. Struct. - THEOCHEM 492 (1-3), 151–158.

Takayanagi, T., Kurosaki, Y., Misawa, K., Sugiura, M., Kobayashi, Y., Sato, K., Tsunashima, S., 1998. Measurements of thermal rate constants and theoretical calculations for the N(^{2}D^{2}P) + C_2H_2 and C_2D_2 reactions. J. Phys. Chem. A 102 (31), 6251–6258.

Takayanagi, T., Kurosaki, Y., Sato, K., Misawa, K., Kobayashi, Y., Tsunashima, S., 1999. Kinetic studies on the N(^{2}D^{2}P) + CH_4 and CD_4 reactions: The role of nonadiabatic transitions on thermal rate constants. J. Phys. Chem. A 103 (2), 250–255.

Talbi, D., 1999. An extensive ab-initio study of the C + NH_2 and N + CH_2 reactions in relation to the HCN/HNC space abundance ratios. Chem. Phys. Lett. 313 (3-4), 626–632.

Talbi, D., Ellinger, Y., 1996. Isomerization versus hydrogen exchange reaction in the HNC ↔ HCNconversion. Chem. Phys. Lett. 263 (3-4), 385–392.

Talbi, D., Smith, I. W. M., 2009. A theoretical analysis of the reaction between CN radicals and NH_3. Phys. Chem. Chem. Phys. 11 (38), 8477–8483.

Teanby, N. A., de Kok, R., Irwin, P. G. J., Osprey, S., Vinatier, S., Gierasch, P. J., Read, P. L., Flasar, F. M., Conrath, B. J., Achterberg, R. K., Bézard, B., Nixon, C. A., Calcutt, S. B., Dec. 2008. Titan's winter polar vortex structure revealed by chemical tracers. Journal of Geophysical Research (Planets) 113 (E12), 12003.

Teanby, N. A., Irwin, P. G. J., de Kok, R., Jolly, A., Bézard, B., Nixon, C. A., Calcutt, S. B., Aug. 2009. Titan's stratospheric C $_2$N $_2$, C $_3$H $_4$, and C $_4$H $_2$ abundances from Cassini/CIRS far-infrared spectra. Icarus 202, 620–631.

Teanby, N. A., Irwin, P. G. J., de Kok, R., Nixon, C. A., 2010. Mapping Titan's HCN in the far infra-red: implications for photochemistry. Faraday Discussions 147, 51.

Teanby, N. A., Irwin, P. G. J., de Kok, R., Nixon, C. A., Coustenis, A., Bézard, B., Calcutt, S. B., Bowles, N. E., Flasar, F. M., Fletcher, L., Howett, C., Taylor, F. W., Mar. 2006. Latitudinal variations of HCN, HC $_3$N, and C $_2$N $_2$ in Titan's stratosphere derived from Cassini CIRS data. Icarus 181, 243–255.

Teanby, N. A., Irwin, P. G. J., de Kok, R., Vinatier, S., Bézard, B., Nixon, C. A., Flasar, F. M., Calcutt, S. B., Bowles, N. E., Fletcher, L., Howett, C., Taylor, F. W., Feb. 2007. Vertical profiles of HCN, HC $_3$N, and C $_2$H $_2$ in Titan's atmosphere derived from Cassini/CIRS data. Icarus 186, 364–384.

Teanby, N. A., Irwin, P. G. J., Nixon, C. A., Courtin, R., Swinyard, B. M., Moreno, R., Lellouch, E., Rengel, M., Hartogh, P., Jan. 2013. Constraints on Titan's middle atmosphere ammonia abundance from Herschel/SPIRE sub-millimetre spectra. Planet. Space Sci. 75, 136–147.

Teslja, A., Nizamov, B., Dagdigian, P. J., 2004. The electronic spectrum of methyleneimine. J. Phys. Chem. A 108 (20), 4433–4439.

Thiesemann, H., Clifford, E. P., Taatjes, C. A., Klippenstein, S. J., 2001. Temperature dependence and deuterium kinetic isotope effects in the CH (CD) + C_2H_4 (C_2D_4) reaction between 295 and 726 K. J. Phys. Chem. A 105 (22), 5393–5401.

Thiesemann, H., MacNamara, J., Taatjes, C., 1997. Deuterium kinetic isotope effect and temperature dependence in the reactions of CH[$^2\Pi$] with methane and acetylene. J. Phys. Chem. A 101 (10), 1881–1886.

Thorn, R. P., Payne, W. A., Chillier, X. D. F., Stief, L. J., Nesbitt, F. L., Tardy, D. C., 2000. Rate constant and RRKM product study for the reaction between CH_3 and C_2H_3 at T = 298 K. Int. J. Chem. Kinet. 32 (5), 304–316.

Tomeczek, J., Gradon, B., 2003. The role of N_2O and NNH in the formation of NO via HCN in hydrocarbon flames. Combust. Flame 133 (3), 311–322.

Toon, O. B., McKay, C. P., Griffith, C. A., Turco, R. P., Jan. 1992. A physical model of Titan's aerosols. Icarus 95, 24–53.

Tsang, W., 1987. Chemical kinetic database for combustion chemistry. 2. Methanol. J. Phys. Chem. Ref. Data 16 (3), 471–508.

Tsang, W., 1988. Chemical kinetic database for combustion chemistry. Part 3. Propane. J. Phys. Chem. Ref. Data 17 (2), 887–952.

Tsang, W., 1990. Chemical kinetic database for combustion chemistry Part 4. Isobutane. J. Phys. Chem. Ref. Data 19 (1), 1–68.

Tsang, W., 1991. Chemical kinetic database for combustion chemistry. Part 5. Propene. J. Phys. Chem. Ref. Data 20 (2), 221–273.

Tsang, W., 1992. Chemical kineticdata base for propellant combustion. II. Reactions involving CN, NCO, and HNCO. J. Phys. Chem. Ref. Data 21 (4), 753–791.

Tsang, W., Hampson, R., 1986. Chemical kinetic database for combustion chemistry. 1. Methane and related-compounds. J. Phys. Chem. Ref. Data 15 (3), 1087–1279.

Tsang, W., Herron, J., 1991. Chemical kinetic database for propellant combustion. I. Reactions involving NO, NO_2, HNO, HNO_2, HCN and N_2O. J. Phys. Chem. Ref. Data 20 (4), 609 – 663.

Tsuboi, T., Hashimoto, K., 1981. Shock tube study on homogeneous thermal oxidation of methanol. Combust. Flame 42, 61–76.

Umemoto, H., Asai, T., Hashimoto, H., Nakae, T., 1999. Reactions of N(^{2}D) with H_2O and D_2O; Identification of the two exit channels, NH(ND) + OH(OD) and H(D) + HNO(DNO). J. Phys. Chem. A 103 (6), 700–704.

Umemoto, H., Hachiya, N., Matsunaga, E., Suda, A., Kawasaki, M., 1998. Rate constants for the deactivation of N(^{2}D) by simple hydride and deuteride molecules. Chem. Phys. Lett. 296 (1-2), 203–207.

Vakhtin, A. B., Heard, D. E., Smith, I. W. M., Leone, S. R., 2001a. Kinetics of C_2H radical reactions with ethene, propene and 1-butene measured in a pulsed Laval nozzle apparatus at T=103 and 296 K. Chem. Phys. Lett. 348 (1-2), 21–26.

Vakhtin, A. B., Heard, D. E., Smith, I. W. M., Leone, S. R., 2001b. Kinetics of reactions of C_2H radical with acetylene, O_2, methylacetylene, and allene in a pulsed Laval nozzle apparatus at T=103 K. Chem. Phys. Lett. 344 (3-4), 317–324.

Vakhtin, A. B., Lee, S., Smith, I. W. M., Leone, S. R., 2001c. Low-temperature kinetics of reactions of the OH radical with propene and 1-butene studied by a pulsed Laval nozzle apparatus combined with laser-induced fluorescence. J. Phys. Chem. A 105 (33), 7889–7895.

Vervack, R. J., Sandel, B. R., Strobel, D. F., Jul. 2004. New perspectives on Titan's upper atmosphere from a reanalysis of the Voyager 1 UVS solar occultations. Icarus 170, 91–112.

Vinatier, S., Bézard, B., Nixon, C. A., Nov. 2007. The Titan ^{14}N/ ^{15}N and ^{12}C/ ^{13}C isotopic ratios in HCN from Cassini/CIRS. Icarus 191, 712–721.

Vinatier, S., Bézard, B., Nixon, C. A., Mamoutkine, A., Carlson, R. C., Jennings, D. E., Guandique, E. A., Teanby, N. A., Bjoraker, G. L., Michael Flasar, F., Kunde, V. G., Feb. 2010. Analysis of Cassini/CIRS limb spectra of Titan acquired during the nominal mission. I. Hydrocarbons, nitriles and CO $_2$ vertical mixing ratio profiles. Icarus 205, 559–570.

Vinckier, C., 1979. Determination of the rate constant of the reaction CH + O $\rightarrow$ CHO^+ + e^- at 295 K. J. Phys. Chem. 83 (9), 1234–1235.

Vinckier, C., Debruyn, W., 1979. Temperature dependence of the reactions of methylene with oxygen atoms, oxygen, and nitric oxide. J. Phys. Chem. 83 (16), 2057–2062.

von Gehring, M., Hoyermann, K., Wagner, H., Wolfrum, J., 1971. Die Reaktion von Atomarem Wasserstoff mit Hydrazin. Ber. Bunsen-Ges. Phys. Chem. 75 (12), 1287–1294.

Vuitton, V., Lavvas, P., Yelle, R. V., Galand, M., Wellbrock, A., Lewis, G. R., Coates, A. J., Wahlund, J.-E., Nov. 2009. Negative ion chemistry in Titan's upper atmosphere. Planet. Space Sci. 57, 1558–1572.

Vuitton, V., Yelle, R. V., Anicich (Retired), V. G., Aug. 2006. The Nitrogen Chemistry of Titan's Upper Atmosphere Revealed. The Astrophysical Journal Letters 647, L175–L178.

Vuitton, V., Yelle, R. V., Lavvas, P., Klippenstein, S. J., 2012. Rapid association reactions at low pressure: Impact on the formation of hydrocarbons on Titan. Astrophys. J. 744 (1), 11.

Vuitton, V., Yelle, R. V., McEwan, M. J., Nov. 2007. Ion chemistry and N-containing molecules in Titan's upper atmosphere. Icarus 191, 722–742.

Wagner, A. F., Bowman, J. M., 1987. The addition and dissociation reaction atomic hydrogen + carbon monoxide $\rightleftarrows$ oxomethyl. 1. Theoretical RRKM studies. J. Phys. Chem. 91 (20), 5314–5324.

Waite, J. H., Bell, J., Lorenz, R., Achterberg, R., Flasar, F. M., Sep. 2013. A model of variability in Titan's atmospheric structure. Planet. Space Sci. 86, 45–56.

Wakelam, V., Herbst, E., Loison, J.-C., Smith, I. W. M., Chandrasekaran, V., Pavone, B., Adams, N. G., Bacchus-Montabonel, M.-C., Bergeat, A., Béroff, K., Bierbaum, V. M., Chabot, M., Dalgarno, A., van Dishoeck, E. F., Faure, A., Geppert, W. D., Gerlich, D., Galli, D., Hébrard, E., Hersant, F., Hickson, K. M., Honvault, P., Klippenstein, S. J., Le Picard, S., Nyman, G., Pernot, P., Schlemmer, S., Selsis, F., Sims, I. R., Talbi, D., Tennyson, J., Troe, J., Wester, R., Wiesenfeld, L., Mar. 2012. A KInetic Database for Astrochemistry (KIDA). The Astrophysical Journal Supplement 199, 21.

Wang, B., Fockenberg, C., 2001. Direct measurement of the rate constant for the $CH_2(\tilde{X}^3B_1)$ + CH_3 reaction at 300 K. J. Phys. Chem. A 105 (37), 8449 – 8455.

Wang, H., Frenklach, M., 1994. Calculations of rate coefficients for the chemically activated reactions of acetylene with vinylic and aromatic radicals. J. Phys. Chem. 98 (44), 11465–11489.

Wang, H., Frenklach, M., 1997. A detailed kinetic modeling study of aromatics formation in laminar premixed acetylene and ethylene flames. Combust. Flame 110 (1-2), 173–221.

Wang, H. Y., Eyre, J. A., Dorfman, L. M., 1973. Activation energy for the gas phase reaction of hydrogen atoms with carbon monoxide. J. Chem. Phys. 59 (9), 5199–5200.

Wang, J., Ding, Y.-h., Sun, C.-c., 2006. Cyanomethylidyne: A reactive carbyne radical. ChemPhysChem 7 (3), 710–722.

Wang, Z.-X., Huang, M.-B., 1998. Insertion of methylidyne into the C−H bond of ethylene. Chem. Phys. Lett. 291 (3-4), 381–386.

Weissman, M. A., Benson, S. W., 1988. Rate parameters for the reactions of vinyl and butadienyl radicals with hydrogen and acetylene. J. Phys. Chem. 92 (14), 4080–4084.

West, G. A., Berry, M. J., 1974. CN photodissociation and predissociation chemical lasers: Molecular electronic and vibrational laser emissions. J. Chem. Phys. 61 (11), 4700–4716.

Westmoreland, P. R., Dean, A. M., Howard, J. B., Longwell, J. P., 1989. Forming benzene in flames by chemically activated isomerization. J. Phys. Chem. 93 (25), 8171–8180.

Whyte, A. R., Phillips, L. F., 1983. Rates of reaction of NH_2 with N, NO and NO_2. Chem. Phys. Lett. 102 (5), 451–454.

Whyte, A. R., Phillips, L. F., 1984. Products of reaction of nitrogen atoms with NH_2. J. Phys. Chem. 88 (23), 5670–5673.

Whytock, D. A., Payne, W. A., Stief, L. J., 1976. Rate of the reaction of atomic hydrogen with propyne over an extended pressure and temperature range. J. Chem. Phys. 65 (1), 191–195.

Wilhelm, M. J., Nikow, M., Letendre, L., Dai, H.-L., 2009. Photodissociation of vinyl cyanide at 193 nm: Nascent product distributions of the molecular elimination channels. J. Chem. Phys. 130 (4), 044307–12.

Wilson, A. V., Parker, D. S. N., Zhang, F., Kaiser, R. I., 2012. Crossed beam study of the atom-radical reaction of ground state carbon atoms ($C(^3P)$) with the vinyl radical ($C_2H_3(X^2A')$). Phys. Chem. Chem. Phys. 14 (2), 477–481.

Wilson, E., Atreya, S., 2004. Current state of modeling the photochemistry of titan's mutually dependent atmosphere and ionosphere. J. Geophys. Res. - Planets 109 (E6), E06002.

Woon, D., Herbst, E., 1996. On the stability of interstellar carbon clusters: The rate of the reaction between C_3 and O. Astrophys. J. 465, 795–799.

Woon, D. E., Park, J.-Y., 2009. Modeling chemical growth processes in Titan's atmosphere 2. Theoretical study of reactions between C_2H and ethene, propene, 1-butene, 2-butene, isobutene, trimethylethene, and tetramethylethene. Icarus 202 (2), 642–655.

Xu, Z.-F., Fang, D.-C., Fu, X.-Y., 1997. Ab initio study on the reaction NH + NH → NH_2 + N. Chem. Phys. Lett. 275 (3-4), 386–391.

Xu, Z.-F., Li, S.-M., Yu, Y.-X., Li, Z.-S., Sun, C.-C., 1999. Theoretical studies on the reaction path dynamics and variational transition-state theory rate constants of the hydrogen-abstraction reactions of the $NH(X^3\Sigma^-)$ radical with methane and ethane. J. Phys. Chem. A 103 (25), 4910–4917.

Yang, D. L., Yu, T., Lin, M. C., Melius, C. F., 1992a. CN radical reactions with hydrogen cyanide and cyanogen: Comparison of theory and experiment. J. Chem. Phys. 97 (1), 222–226.

Yang, D. L., Yu, T., Lin, M. C., Melius, C. F., 1993. The reaction of CN with CH_4 and CD_4: an experimental and theoretical study. Chem. Phys. 177 (1), 271–280.

Yang, D. L., Yu, T., Wang, N. S., Lin, M. C., 1992b. Temperature dependence of cyanogen radical reactions with selected alkanes: CN reactivities towards primary, secondary and tertiary C−H bonds. Chem. Phys. 160 (2), 307–315.

Yang, Y., Zhang, W., Pei, S., Shao, H., Huang, W., Gao, X., 2005. Theoretical study on the mechanism of the $N(^4S)$ + C_2H_5 reaction. J. Mol. Struct. - THEOCHEM 725 (1-3), 133–138.

Yelle, R. V., Cui, J., Müller-Wodarg, I. C. F., Oct. 2008. Methane escape from Titan's atmosphere. Journal of Geophysical Research (Planets) 113 (E12), 10003.

Yelle, R. V., Griffith, C. A., Nov. 2003. HCN fluorescence on Titan. Icarus 166, 107–115.

Yelle, R. V., Vuitton, V., Lavvas, P., Klippenstein, S. J., Smith, M. A., Horst, S. M., Cui, J., 2010. Formation of NH_3 and CH_2NH in Titan's upper atmosphere. Faraday Discuss. 147, 31–49.

Yu, T., Yang, D., Lin, M., 1993. Kinetics of CN radical reactions with formaldehyde and 1,3,5-trioxane. Int. J. Chem. Kinet. 25 (12), 1053–1064.

Yu, Y., Li, S., Xu, Z., Li, Z., Sun, C., 1998. An ab initio study on the reaction NH_2 + CH_4 → NH_3 + CH_3. Chem. Phys. Lett. 296 (1-2), 131–136.

Zabarnick, S., 1989. Kinetics of CN($X^2\Sigma^+$) radical reactions with HCN, BrCN and CH_3CN. Chem. Phys. 134 (1), 185–191.

Zabarnick, S., Fleming, J., Lin, M., 1988. Temperature dependence of CH radical reactions with H_2O and CH_2O. Symp. Int. Combust. Proc. 21 (1), 713–719.

Zabarnick, S., Fleming, J., Lin, M., 1989a. Kinetics of CH radical reactions with N_2O, SO_2, OCS, CS_2, and SF_6. Int. J. Chem. Kinet. 21 (9), 765–774.

Zabarnick, S., Fleming, J. W., Lin, M. C., 1989b. Kinetics of methylidyne ($CHX^2\Pi$) radical reactions with ammonia and methylamines. Chem. Phys. 132 (3), 407–411.

Zabarnick, S., Fleming, J. W., Lin, M. C., 1991. Direct measurement of rate constants for the reactions of CH and CD with HCN and DCN. Chem. Phys. 150 (1), 109–115.

Zhang, W., Du, B., Feng, C., 2004a. Theoretical investigation of reaction mechanism for $CH_2(\tilde{X}^3B_1)$ with NO radical. J. Mol. Struct. - THEOCHEM 679 (1-2), 121–125.

Zhang, X., Zou, S., Harding, L. B., Bowman, J. M., 2004b. A global ab initio potential energy surface for formaldehyde. J. Phys. Chem. A 108 (41), 8980–8986.

Zhao, Y., Truhlar, D. G., 2008. Exploring the limit of accuracy of the global hybrid meta density functional for main-group thermochemistry, kinetics, and noncovalent interactions. J. Chem. Theory Comput. 4 (11), 1849–1868.

Zhou, J., Schlegel, H. B., 2009. Ab initio classical trajectory study of the dissociation of neutral and positively charged methanimine (CH_2NH^{n+} n = 0-2). J. Phys. Chem. A 113 (37), 9958–9964.

Zhu, L., Talukda, R., Burkholder, J., Ravishankara, A., 2008. Rate Coefficients for the OH + Acetaldehyde (CH_3CHO) Reaction Between 204 and 373 K. International Journal of Chemical Kinetics 40, 635–646.

Zhu, Z., Ji, M., Zhang, S. W., Chen, Y., 2003a. Temperature-dependent kinetics of the reactions of the CCN ($X2^\Pi$) radical with C_2H_2 and C_2H_4. http://oasys2.confex.com/acs/235nm/techprogram/P1157562.HTM.

Zhu, Z., Zhang, Z., Huang, C., Pei, L., Chen, C., Chen, Y., 2003b. Kinetics of CCN radical reactions with a series of normal alkanes. J. Phys. Chem. A. 107 (48), 10288–10291.

Zwier, T. S., Allen, M., 1996. Metastable diacetylene reactions as routes to large hydrocarbons in Titan's atmosphere. Icarus 123 (2), 578–583.